Seismic Evaluation of Traditional Timber Structures in Taiwan

Tsai, Pin-Hui

Award date:
2009

Awarding institution:
University of Bath

SEISMIC EVALUATION OF TRADITIONAL TIMBER STRUCTURES IN TAIWAN

Pin-Hui Tsai

A Thesis Submitted for the Degree of Doctor of Philosophy

University of Bath

Department of Architecture and Civil Engineering

June 2009

Table of Contents

Acknowledgements

I would like to thank everyone who helped and assisted me during my doctoral study, especially my supervisor, Dr D. F. D'Ayala, for her expert guidance.

This thesis is jointly dedicated to my husband, Pierfrancesco, and my parents, who are always beside me with great patience, and love and support me unconditionally.

Abstract

Taiwan is located in a highly seismic zone and the historical “Dieh-Dou” timber buildings, constructed without following any code or standard, are prone to collapse under earthquake. These buildings are unique and represent the culture, heritage and art of Taiwan, therefore need to be preserved while minimizing unnecessary intervention that could damage their authenticity.

This research comprises a thorough investigation on the parameters influencing the seismic vulnerability of the Dieh-Dou timber frames in Taiwan, and propose a methodology of assessment and a strategy for strengthening validated through experimental testing and numerical analysis.

After review existing literature and post-earthquake surveys, the failure modes of the buildings are identified, showing that the dislocation of the elements of the frame from the joints is the primary source of damage. An experimental investigation is carried out comprising both rotational and translational tests on full scale joint specimens which, together with a parametric study undertaken with an appropriate FE simulation, demonstrates how both the rotational and translational stiffness of the joints play a key role in defining the behaviour of these structures.

Lateral force, response spectrum, and step-by-step pushover analyses are performed and compared with the post-earthquake survey of two Dieh-Dou buildings seriously affected by the 1999 Chi-Chi earthquake. The results show that the proposed FE modelling can successfully be employed to assess the vulnerability of the frames.

Based on a damage level approach, an assessment methodology is suggested that would allow to optimisation of the strengthening strategy, permitting protection these precious structures from future earthquakes while avoiding unnecessary interventions.

Chapter 1
Introduction

1.1 Background and Motivation

The historic timber buildings known as “Dieh-Dou” represent the traditional architecture, culture, heritage and art of Taiwan. Dieh-Dou buildings are unique because of their peculiar construction, with the joints made of several small stacked pieces of timber to form the Dou-Gon joint set. Also, as they are generally temples for ceremonial purposes, their elements are thoroughly painted and decorated by famous traditional artists.

Taiwan is located in a highly seismic area, and it is regularly affected by destructive earthquakes. Traditional timber frame buildings, and particularly Dieh-Dou buildings, were severely damaged and in some cases destroyed, by the 1999 Chi-Chi earthquake. The ones that have survived need to be repaired and protected from future damage. An efficient assessment method should be established that is able to identify the weak parts of the structure and provide advice for strengthening strategies. The Taiwanese document “Cultural Heritage Preservation Law” (1982) and international conservation chapters state that historic buildings have to be protected in such a way to preserve their originality and authenticity. Considering the heritage value of these structures and the preciousness of their elements, it is essential to minimize unnecessary interventions.

Academic research on architectural and construction aspects of Dieh-Dou buildings is available, but relatively few studies regarding Dieh-Dou timber structural analysis have been carried out to date. Therefore, fundamental research is needed to understand the structural behaviour of these unique structures properly and serve the conservation purpose.

1.2 Methodology

Previous studies reveal that finite element methods can be successfully employed to analyse historic timber buildings, and this is particularly true for complex indeterminate structures like Dieh-Dou frames where load transfer path between elements in not straightforward. However, the joint stiffness can govern the behaviour of timber frames, and it is necessary to simulate them properly in a numerical model. Formulas proposed by other researchers to predict rotational stiffness of beam to column timber joints exist, but no value is available for the peculiar Dou-Gon joints present in the Dieh-Dou buildings.

Post-earthquake survey shows that elements of Dieh-Dou timber frames are likely to pull out, so both rotational and translational stiffness should be considered. Hence, testing of full scale specimens of Dou-Gon joints, including cyclic test, forms part of this research, performed to obtain rotational stiffness and moment capacity under different levels of vertical constant loads, and translational stiffness and pull out capacity. The results from the experimental campaign are directly implemented in a FE model.

A parametric study is undertaken to highlight the importance of the rotational and translational stiffness on the behaviour of the Dieh-Dou frames. Based on the provisions of the Taiwanese code and the Eurocode, three different earthquake analysis methods (lateral force, step by step pushover and response spectrum) are performed to assess the vulnerability of existing Dieh-Dou frames. The results of the numerical model are verified and validated against the post-earthquake survey of the reference buildings and, in general, of the buildings damaged by the 1999 Chi-Chi earthquake. Finally, a strengthening strategy is suggested that would help to protect these valuable structures from future earthquakes.

1.3 Research Objectives

The Dieh-Dou buildings were built by carpenters without any codes or standards, and are particularly prone to damage or collapse under earthquake. An entire Dieh-Dou building consists in timber frames, roof, and masonry walls. The aim of this thesis is to focus on the preservation of these timber frames, which represent an

invaluable architectural heritage of Taiwan, by providing a methodology to assess their vulnerability under seismic actions.

Based on the comparison between the results of a proper numerical model and the post earthquake survey, an assessment strategy can be set. Although it is important to enhance the structural capacity, redundant interventions on strengthening, repair or replacement may lead to loss of originality and authenticity of the heritage value. Following the evaluation method, vulnerable parts of the structure can be identified and only strictly necessary strengthening works should be undertaken. Through this procedure, safety and authenticity of Dieh-Dou buildings can be maintained according to best practice in conservation engineering.

1.4 Outline of dissertation

This dissertation includes eight Chapters. Chapter 1 is a brief description of background, methodology and objective of this research. Chapter 2 illustrates the construction details of Dieh-Dou buildings, the importance and cultural value of these historic building and the generic issues related to conservation. Through reviewing existing literature and post earthquake surveys, failure modes and assessment methodologies are discussed in Chapter 3.

Chapter 4 concentrates on the full scale Dou-Gon joint tests, where rotational and translational stiffness and moment and pull out capacities of the joints are measured. A proper FE model of Dieh-Dou frame that includes semi-rigid joint behaviour is set up in Chapter 5, together with a parametric study on the joint stiffness.

Chapter 6 deals with the assessment methodology and validates the model against two reference Dieh-Dou buildings damaged by the 1999 Chi-Chi earthquake. The strengthening strategy is discussed in Chapter 7, while Chapter 8 includes the conclusions and recommendations for future work.

Chapter 2

Architecture and Conservation Issues

2.1 Introduction

The island of Taiwan is located South-East of mainland China, north of Philippines (Fig. 2.1.1) and is populated by indigenous people and Hans (a race of Chinese people). In the early 17th century, the Spanish and Dutch arrived to Taiwan and occupied the island partially as a basis for their commerce. From the middle of the 17th century until 1895, the island belonged to the Chinese Empire. Large number of Chinese people originally from South-East of the mainland moved to Taiwan, they brought with them some aspects of the Chinese culture such as craftsmanship and architecture. From 1895 until the end of Second World War (1945), before becoming an independent and democratic country, Taiwan was a colony of Japan.

Figure 2.1.1 Location of Fujian and Taiwan
(http://en.wikipedia.org/wiki/File:China_Fujian.svg)

In 1936, during the Japanese colonial period, Fujishima Gaijiro (professor of architecture) surveyed and classified Taiwanese architecture into three categories: indigenous style, Chinese style and western style (Fujishima and Chan, 1999); this classification reflects the historical background and development of Taiwan.

Fu (2005) pointed out that before the middle of 19th century Taiwanese architecture was basically Minnan in style. The Minnan originated in Southern Fujian, a province of China where the majority of Taiwanese immigrated from (Fig. 2.1.1). Then, from the middle of the 19th century foreign trade and western missionaries arrived to Taiwan bringing western architectural knowledge; the combination of Taiwanese and western architectures is marked as Minnan-Western Eclectic style. Minnan and Minnan-Western Eclectic styles were named the "traditional architecture" by architectural historians. Minnan style architecture is based on the Minnan culture and reveals its link with this culture in several aspects, like the functionality of space, living philosophy, ornaments, and art.

The Minnan style traditional architecture in Taiwan was strongly influenced by Chinese architecture. Guo (1999) classified the mainland Chinese vernacular dwelling timber frame construction into Chuandou, which means "inserting pieces", and Tailiang, which means "lifting beam" framework.

Generally speaking, in Chuandou (also written as Chuan-Dou) structures, most columns extend from the roof to the ground, and the frame is created by these columns and the tie-beams that connect them. In the Tailiang system, fewer full length columns are used; instead, two pillars (short columns) sit on the tie-beam which goes on two full length columns and an additional beam crosses them, to create the first layer. Another pair of pillars sit on the latter cross beam and the same layout is repeated until the last single pillar reaches the ridge height.

The Taiwanese traditional timber architecture, Chuan-Dou and Dieh-Dou, has developed from these two Chinese styles. The Taiwanese Chuan-Dou (Fig. 2.1.2) is very similar to the Chinese counterpart. The Dieh-Dou (Fig. 2.1.3) system shares similar structural concepts with the Chinese Tailiang system: the Dou-Gon joint sets are equivalent to the pillars in the Tailiang system, and they are placed on the tie beams to support the roof weight and create larger spans. However, the Dou-Gon

joint sets of Dieh-Dou frames, formed by several pieces of timbers stacked together, a modified shape of pillars, are the unique feature of Taiwanese timber structures.

Figure 2.1.2 Chuan-Dou building in Taiwan (Chen 2008)

Figure 2.1.3 Dieh-Dou building in Taiwan
(Source: Taichung City Cultural Affair Bureau)

In general, Dieh-Dou buildings were used as religious and family temples or houses for the wealthy families, because this stacking of pieces of timber on the beams allowed to create larger spans useful for ceremony purposes,while; the Chuan-Dou building were used for ordinary houses.

Apart from this distinctive structural feature, the architectonic, sculptural and painting decorations on the structure elements of Dieh-Dou frames (Fig. 2.1.3) are valuable art. The Dieh-Dou buildings not only represent architecture, but also an art display of the Taiwanese culture. Hence the importance of properly recording and preserving them in the best possible way for future generations. Therefore, in order to establish an evaluation method for Dieh-Dou buildings to prevent structural damage and destruction of the heritage value, in future earthquake but also by improper strengthening techniques, it is necessary to better understand their construction features.

2.2 Construction of Dieh-Dou buildings

2.2.1 Architecture compound and its buildings

A Taiwanese temple compound consists of several buildings forming an enclosure which may include *front hall, yard, corridor, main hall* and *terrace*, see Fig.2.2.1. The *front hall* is the element that delimitates the space from outside to the inside of the building. Next to the *front hall* is the *yard*, which is surrounded by the *front hall, main hall* and *corridors*. The *main hall* is used for the main temple activity, i.e. to place the carved statues (in the case of religious temples) or the pedigree of a family (in the ancestral temples). The *terrace* is used for common rooms and storage rooms. In these traditional building sites, buildings are independently connected with separated *corridors* and in this way different size of *yards* are created. Figure 2.2.1 shows a temple compound formed by two buildings. In some cases, one temple compound may include three or more buildings, with *front hall, main hall and back hall*. Contrary to western architecture the frames are oriented parallel to the main entrance axis to the compound and they are usually non-symmetrical.

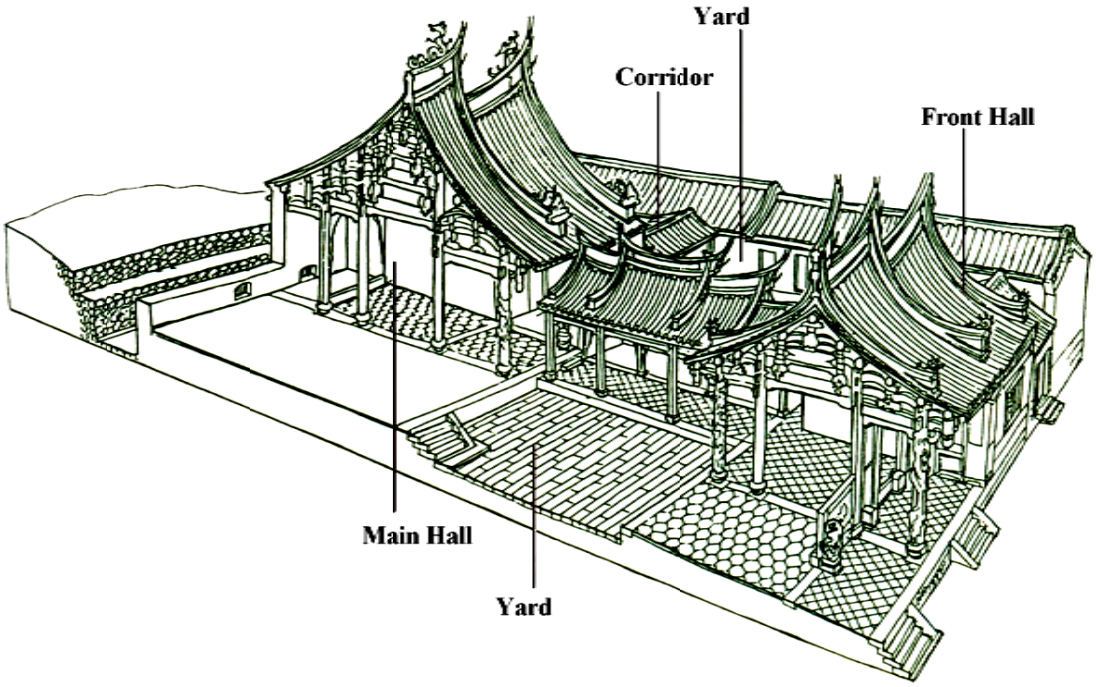

Figure 2.2.1 One temple compound (Lee, 2003)

Huang et al. (2003) surveyed 37 Dieh-Dou buildings from 24 temple compounds across Taiwan. Only 5 have a roof with two slopes, while the remaining 32 buildings have one slope only on each side of the roof, Fig. 2.2.2. The latter case, representing the great majority of cases, will be discussed in detail in the following and will be the object of the structural analysis and experimental work presented in the following chapters.

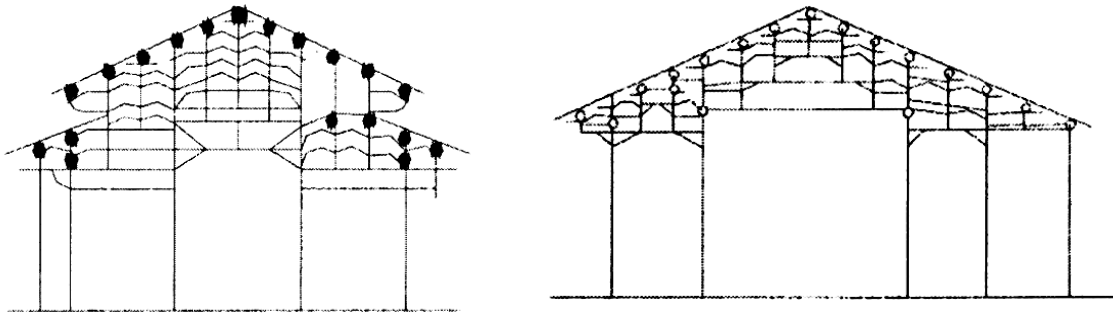

Roof with two slopes Roof with one slope

Figure 2.2.2 Different roof layout in Dieh-Dou buildings (Huang, et al, 2003)

Each building of an architectural compound consists of two parallel timber plane frames, with the same layout supporting a system of purlins, which are connected to the two perimeter masonry walls parallel to the frames (Fig. 2.2.3). The weight of the roof is transmitted from the purlins to these two timber frames and to the masonry walls. There is no other bearing structure between the two timber frames; this allows larger inner spaces around the structures but does not help the stability under horizontal loading.

The construction of a Dieh-Dou building is based on plinths, wall, roof and frames. The plinth made by stone, lies above ground and support the timber frame columns (Fig 2.2.3) preventing damage to the timber from flood and humidity. In traditional Taiwanese buildings, the shape, height, type and decoration of the plinth differs among buildings according to the owners' social status (Lin, 1995). The plinth takes the additional role of identifying the importance of the building.

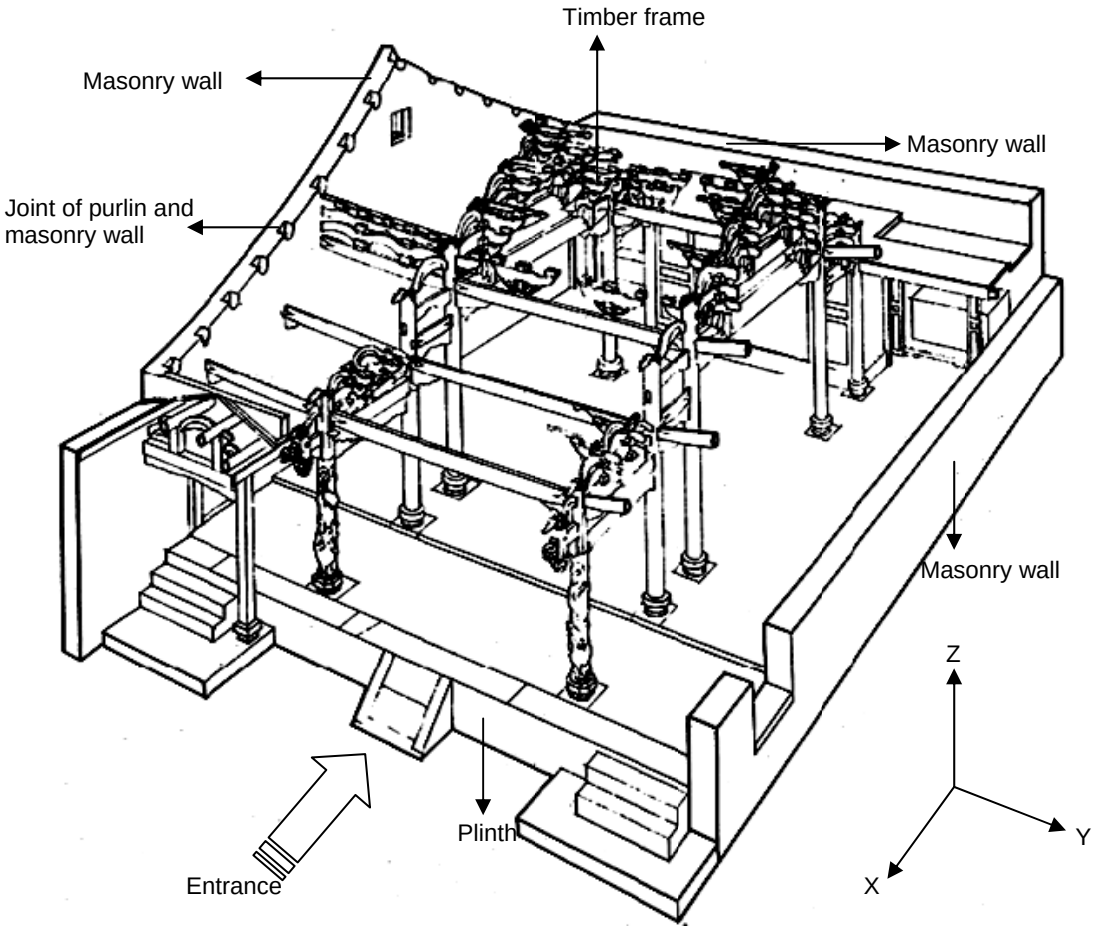

Figure 2.2.3 Typical 3D exploded isometric of a Dieh-Dou building (Lee, 1988)

In Dieh-Dou buildings, the frames are the main structural element while the wall is used for dividing spaces and providing protection from the outdoor environment. Brick masonry is used for the walls of Dieh-Dou buildings. Two of the three masonry walls, which enclose the sides of the building, are parallel to the frames and are connected to the frames through the transverse purlins that support the roof. However, there is no rigid connection between the purlins and the masonry walls (Fig.2.2.3).

In Chinese style based architecture, roofs are usually massive and highly decorated, reflecting the social status of the owners (Lin, 1995). For example, the roofs of government officials often use the swallow-tail style, whilst others have different forms of roof ridges. The configuration of the roof dictates its construction. Figure 2.2.4 illustrates the typical roof layout of a Dieh-Dou building. Purlins are placed on the top of columns and Dieh-Dou joint sets (see Fig.2.2.5); above the purlins, wooden planks form the shape of the roof. Mud mortar is normally used to set the roof tiles on brick tiles over the wooden planks. Finally, the ridges, designed in various styles and carved with symbolic decorations like dragons, plants or other auspicious features, are placed over the wooden planks in the appropriate positions.

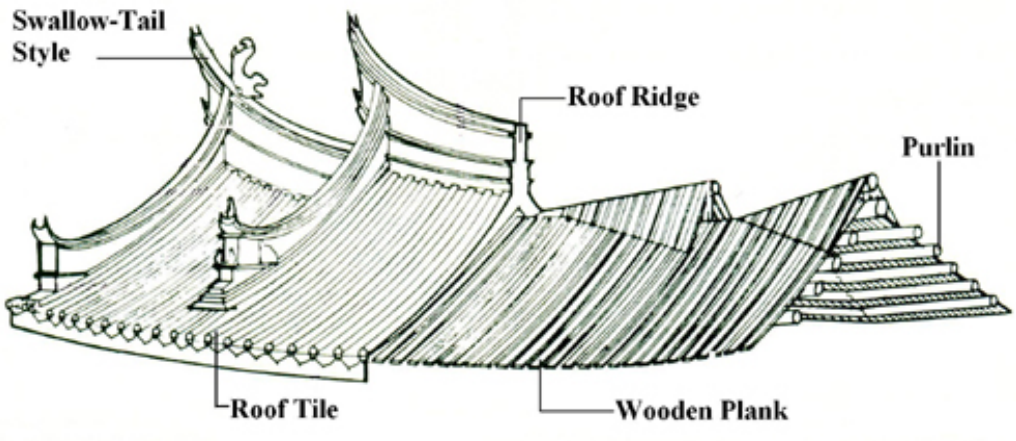

Figure 2.2.4 Roof of Dieh-Dou buildings (Lee, 2003)

This brief introduction of the Dieh-Dou buildings shows that the two timber frames are the main elements to supports the weight of the roof and transmit it to the ground while embodying several unique features representing Taiwanese culture.

Thus, to preserve Dieh-Dou buildings, it is essential to protect Dieh-Dou frames. The description of Dieh-Dou frame is illustrated in the following sections.

2.2.2 Description of the Dieh-Dou timber frames

Timber frame and elements definition

Figure 2.2.5 is a schematic illustration of the various pieces forming a Dieh-Dou timber frame. Skilled carpenters built such buildings without following any code or standard; the name given to each single piece is slightly different and varies from position in the frame and from carpenter to carpenter. Chen (2004) attempted, on the basis of information gathered from five reports, and by interviewing four carpenters, to unify the nomenclature, which is referred to Figure 2.2.5 and explain in Table 2.2.1.

Zone C of the frame (Fig 2.2.5) is the area between the outdoor (or yard) and main space (zone B in Fig 2.2.5), while zone A is the back area of the buildings.

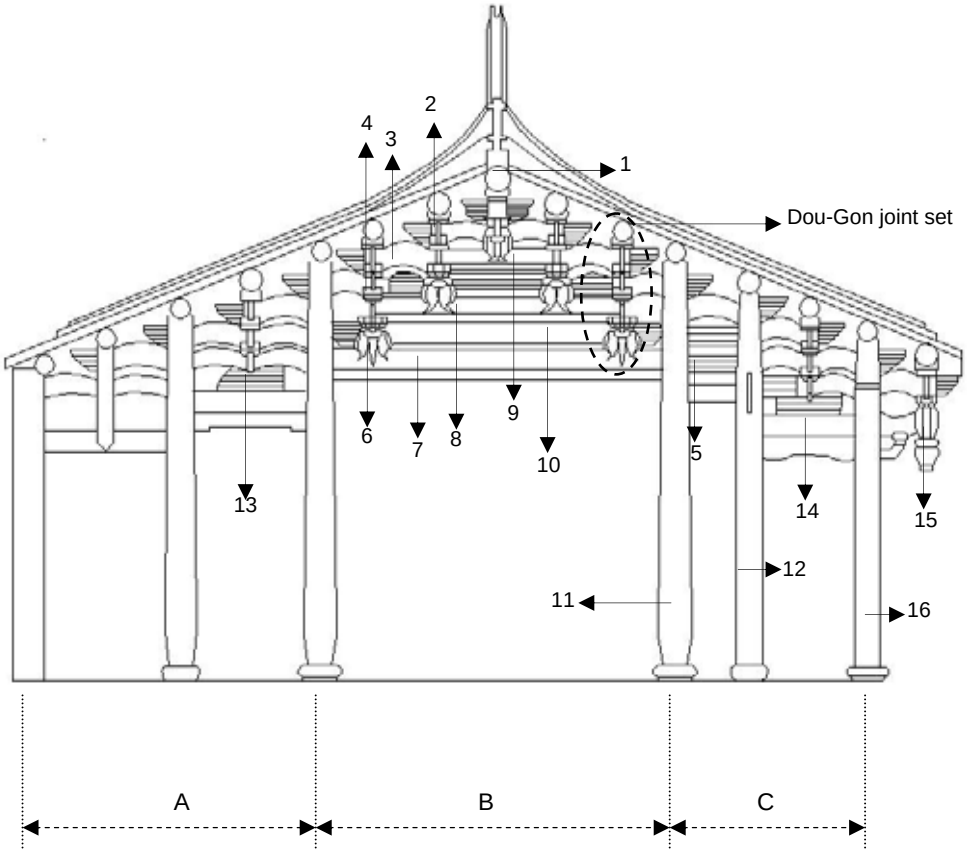

Figure 2.2.5 Schematic illustration of a Dieh-Dou timber frame

Figure 2.2.6 is an exploded diagram of the assembly of zone B, showing beams, columns and the many small components that form the Dou-Gon joint set.

The structure is formed by columns; the total number of columns in the outer and back parts (zones C and A in Fig. 2.2.5) can vary from buildings to buildings. However, the central part of the structure, zone B, is generally very similar among all Dieh-Dou frames.

The central part of the frames, which is the main space of the buildings, is supported by the two columns (No.11 of Fig 2.2.5) and by the first main beam (No.7). Two Dou-Gon joint sets sit above the first main beam. A Dou-Gon joint set consists in Dou, Gon, binding, decorated arc beams and main beams; it will be described in the following section. The second main beam connects with the two Dou-Gon joint sets sitting on the first main beam, while further Dou-Gon joint sets sit on the second main beam and connect with the remaining structural elements. This arrangement repeats until the ridge is reached. In the central part of the frame (zone B), purlins are placed on the top of Dou-Gon joints set and transmit loads to these two internal columns. Fig. 2.2.7 shows a photo of the upper portion of the central zone of the frame.

While the central zones are always similar in the Dieh-Dou frames, zones A and C of Fig. 2.2.5 include variable numbers of columns and beams, but between two columns there can be just beams linked together (element 5) or a Dou-Gon joint set (elements 13 and 14), and in each building there can be a combination of the two with varying number of columns.

The columns are generally connected to the ground by a stone interface element, the podium (Fig 2.2.8), which protects the wood against humidity and spreads the load.

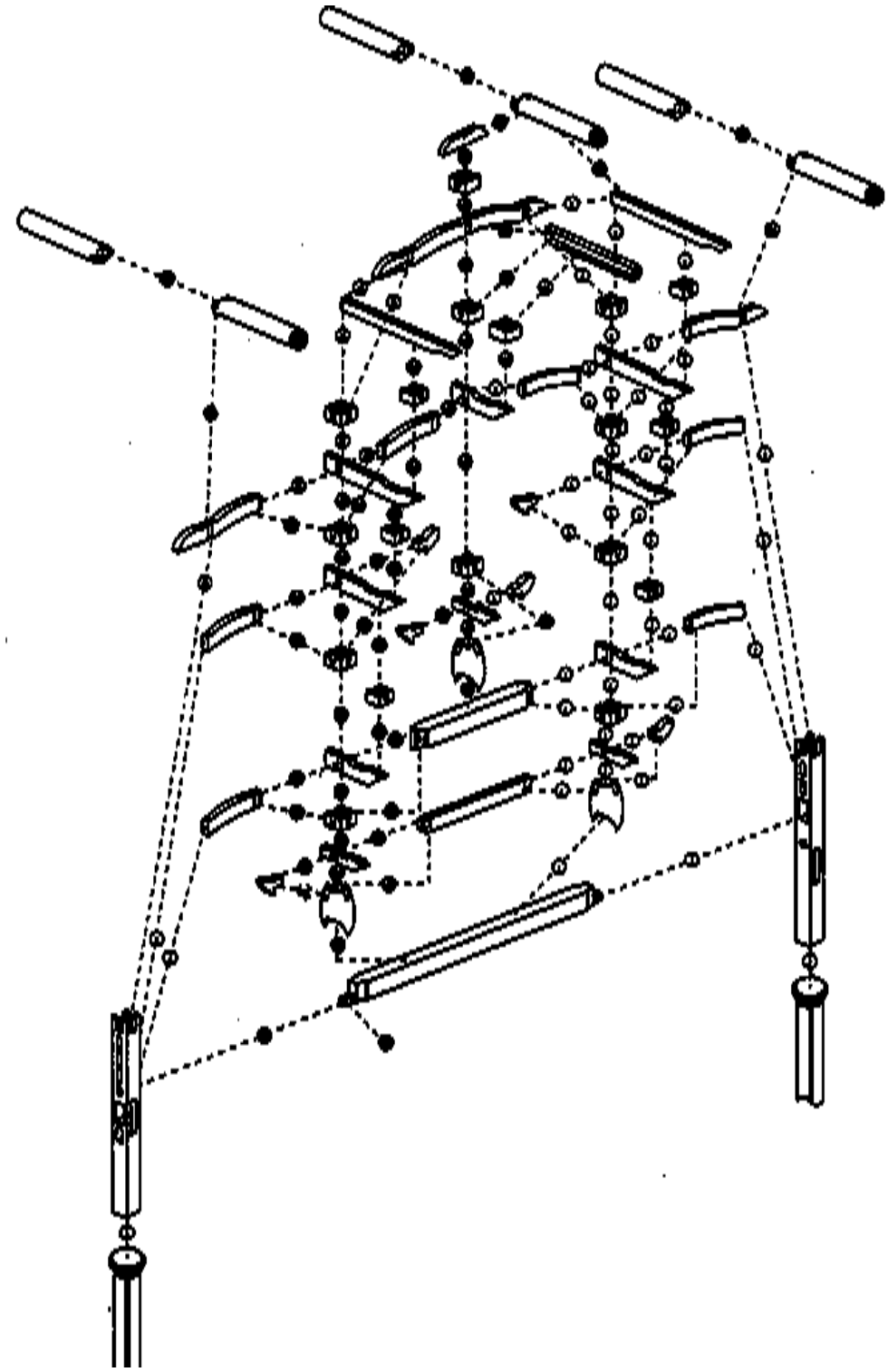

Figure 2.2.6 Exploded diagram of assembly of Dieh-Dou timber frame (Shu, 2000)

Table 2.2.1 Nomenclature of the frame elements

Number	Named by Chen (2004)		Translation and Name used in the dissertation	Description by P. Tsai (2009)
	Original name	Transliteration Sound translation		
1	楹	Inh	**Purlin**	The purlin that connects two frames in the transverse direction.
2	栱	Gon	**Gon**	Bracket. Supports Inh out of plane across the beam and sits on Dou.
3	束仔	Shu-Zai	**Binding Beam**	Arc beam. Links two bracket sets together.
4	斗	Dou	**Dou**	Double notch piece. Keeps Gon, Arc and binding beams together.
5	隨	Sueh	**Decorated carved beam**	Decorated stiffening component, which lies below beams and between column and bracket sets.
6	瓜筒	Gua-Tohn	**Bottom of Dou-Gon joint set**	Bottom of bracket sets. Shaped similar to an egg, hollowed inside. Sits on the main beam.
7	大通	Da-Ton	**First main beam**	First main beam. Cross section is bigger than second and third beam.
8	二通	Hr-Ton	**Second main beam**	Second main beam.
9	三通	San-Ton	**Third main beam**	Third main beam.
10	通隨	Ton-Sueh	**Decorated beam**	Stiffening component below the main beams.
11	點金柱	Dien-Jin-Ju	**Internal column**	Internal column.
12	副點金柱	Fu Dien-Jin-Ju	**External column.**	External column.
13	瓜筒	Gua-Tohn	**Bottom of Dou-Don joint sets**	The bottom of bracket sets. Shaped similar to a ball; it can represent a lucky symbol such as a lion.
14	步通	Bu-Ton	**Corridor beam**	The beam in the corridor.
15	吊筒	Diao-Tohn	**Hanging piece**	Outer piece of building entrance eave. Shaped as a flower.
16	簷柱	Ien-Ju	**Eave column**	The outer column that supports eave.

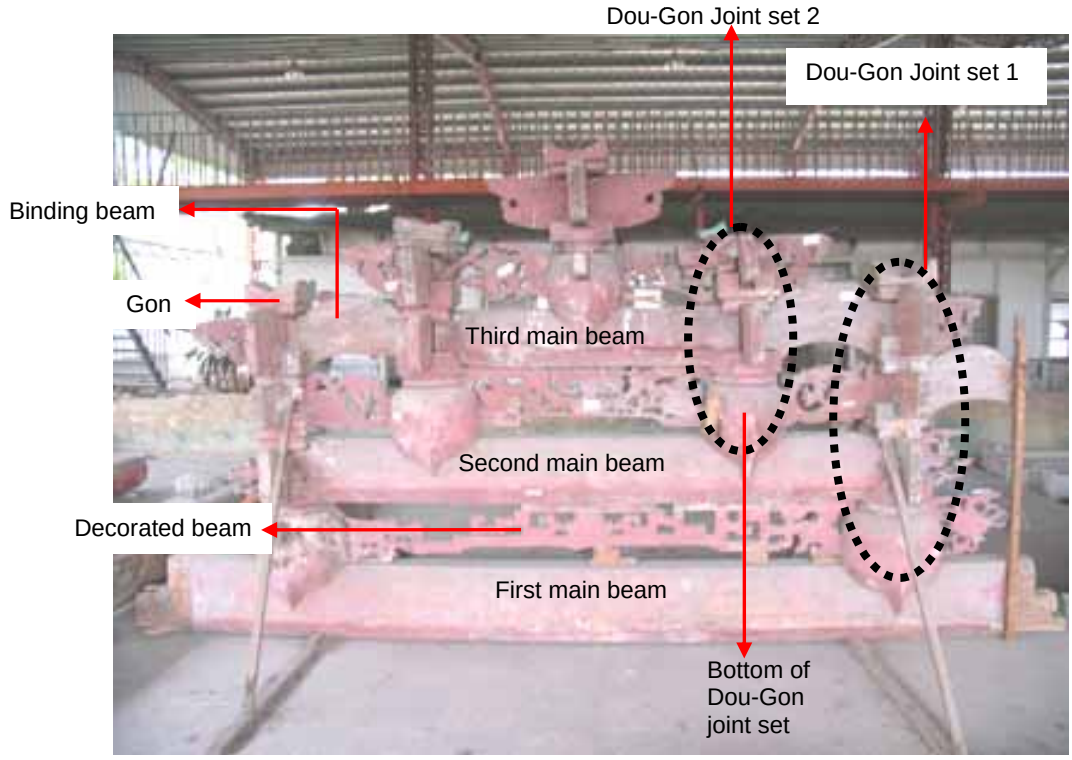

Figure 2.2.7 Upper portion of frame (section B)

Figure 2.2.8 Stone podium (Lin, 1995)

Dou-Gon joint set

Dou-Gon joint sets in Dieh-Dou timber buildings are made by several wood elements (the Dou, the Gon and the beams) stacked together. Lin (1995) pointed out that this construction adds flexibility but may not be very stable. Hence between two Gon, lateral auxiliary elements such as arc beams (in plane), the Gon (out of plane) and the decorated beams (in plane) are incorporated to improve stiffness.

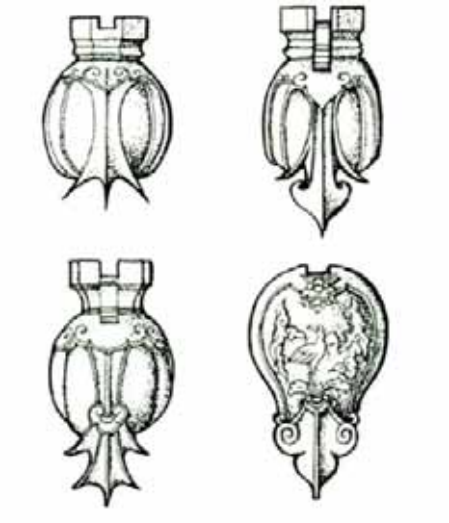

Figure 2.2.9 Bottom of Dou-Gon joint set (Lee, 2003)

Figure 2.2.10 Shape of lucky symbol

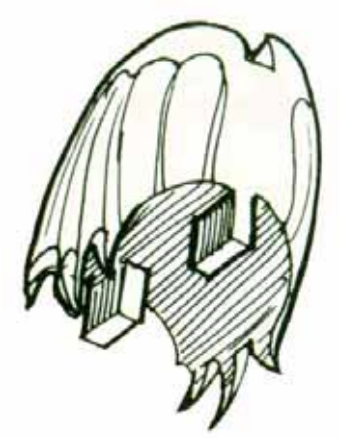

Figure 2.2.11 Tenons of Gua-Ton (Lee, 2003)

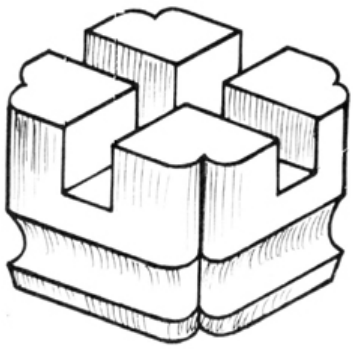

Figure 2.2.12 Dou (Lee, 2003)

Figure 2.2.13 a) detail of Gon beam, b) Gon sitting on Dou

The bottom of a Dou-Gon joint set in zone B (see Fig. 2.2.5) has usually an oval shape and is carved like a papaya (see Fig. 2.2.9). The bottom pieces of the Dou-Gon joint set in the exterior part or back part of the building (zones C and A in Fig 2.2.5) are carved like a lion, tiger or other lucky figure (see Fig. 2.10). The base of these wooden pieces, the Gua-Ton, has two tenons (see Fig. 2.2.11) which are inserted into the main beams; the presence of the tenons and the shape of the Gua-Ton, which embraces the main beam all round, makes this connection rigid in both shear and bending.

At the top of the set there is the Dou, see Fig. 2.2.12, which is a cubic element with a double notch cut, where the in-plane elements (curved, decorated and main beams) and out of plane elements (Gon) are slotted together. The Gon, out-of-plane element, is opportunely carved as a continuous beam to fit the joint (see Fig. 2.2.13) where the in-plane elements (binding beams, main beams, decorated arc beams) are linked. Above these horizontal elements there is another Dou which forms another layer of the Dou-Gon joint set (see Figure 2.2.14).

Figure 2.2.14 One layer of Dou and Gon joint

If two Dou and the in-plane and out-of-plane beam elements are defined as one layer, then one complete Dou-Gon joint set is formed by one or more layers according to their positioning on the timber frame. Dou-Gon joint set 1 in Fig. 2.2.7, which sits on the first main beam, consists of three layers, while Dou-Gon joint set 2 has two layers, one layer less than the set in the lower position.

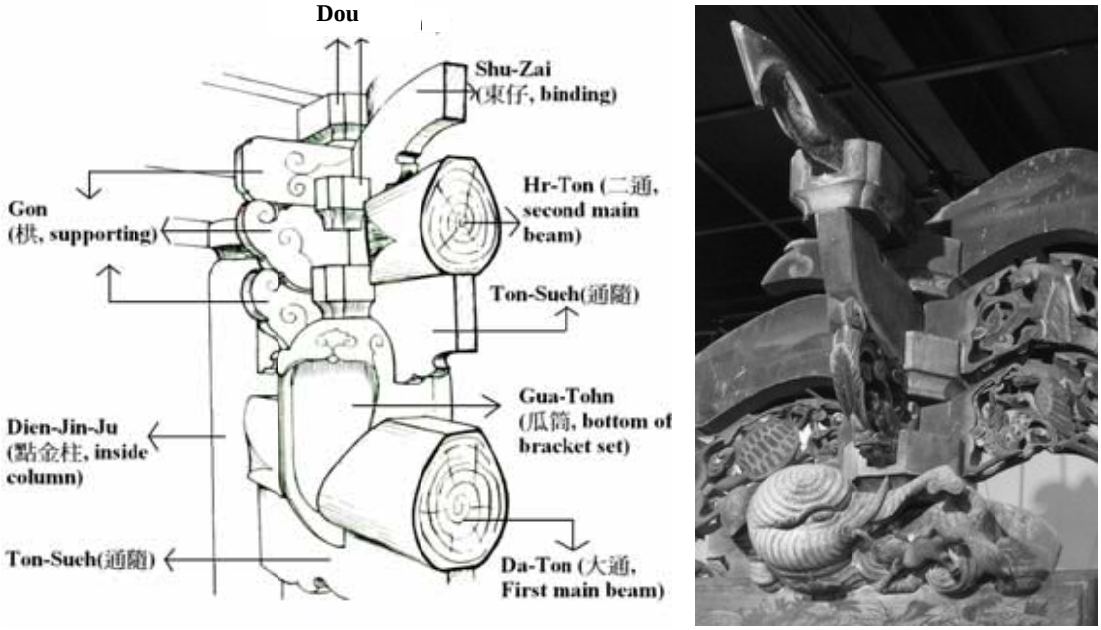

Figure 2.2.15 Dou-Gon joint set (left figure modified from Lee, 2003)

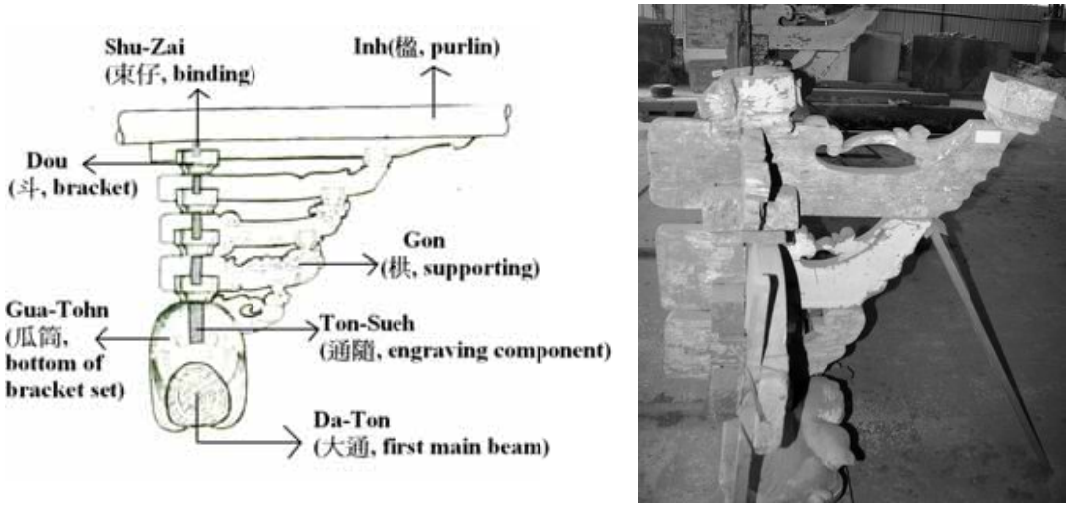

Figure 2.2.16: Out-of-plane section of a Dou-Gon joint set (left figure modified from Lee, 2003)

Figures 2.2.15 and 2.2.16 show a 3-D view of a Dou-Gon joint set. Out-of-plane, Gon (supports) are present in different layers and transfer some of the weight of the roof directly to the bottom of the Dou-Gon. The Dou-Gon joint set, therefore, consists of varying number of layers of Dou and represents the main feature of the Dieh-Dou buildings, rendering the unique character of these building.

2.2.3 Discussion on Dieh-Dou frame classifications

The Dieh-Dou buildings were built in a period when construction standards and codes did not exist in Taiwan. In addition, there is lack of survey on Dieh-Dou buildings around the Country. It is hard to classify them from an engineering point of view, so in order to clarify the general construction of Dieh-Dou buildings, some survey reports are discussed.

Lee (2007) surveyed 33 Dieh-Dou buildings and classified them into two groups, the 'three main beams and five Dou-Gon joint sets (Type 3-5)' and 'two main beams and three Dou-Gon joint sets (Type 2-3)', see Fig. 2.2.17 and Fig. 2.2.18. Lee reported 24 Type 3-5 and 9 Type 2-3 buildings.

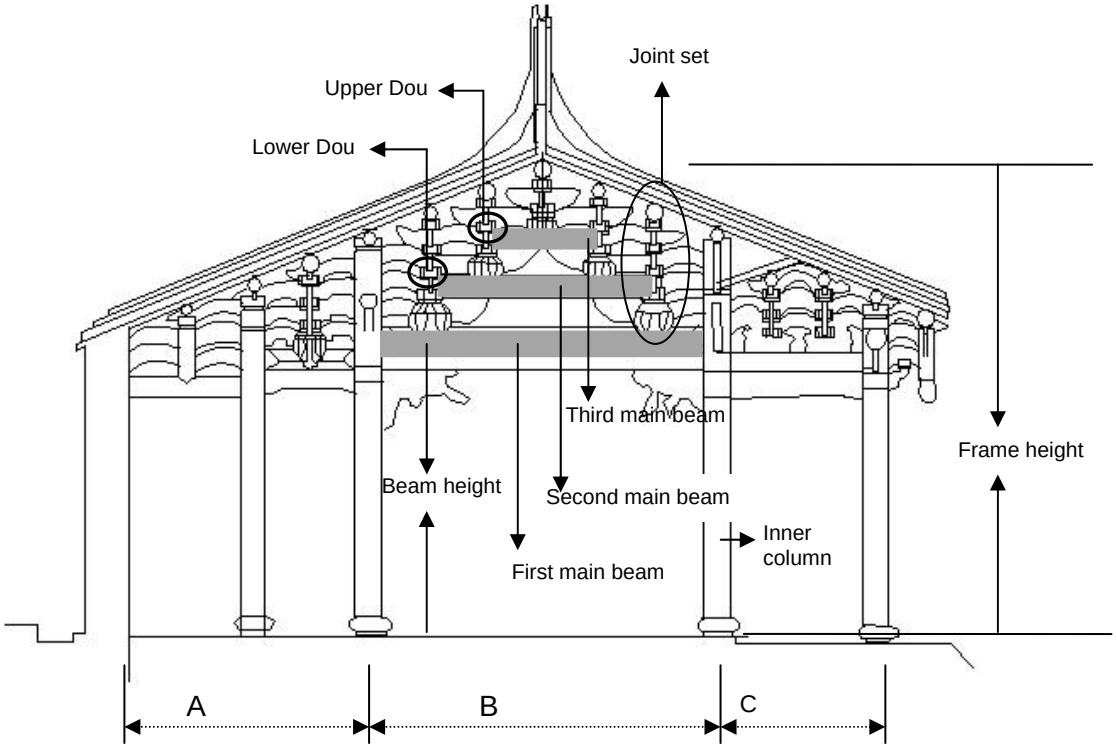

Figure. 2.2.17 Type 3-5 (three main beams and five Dou-Gon joint sets)

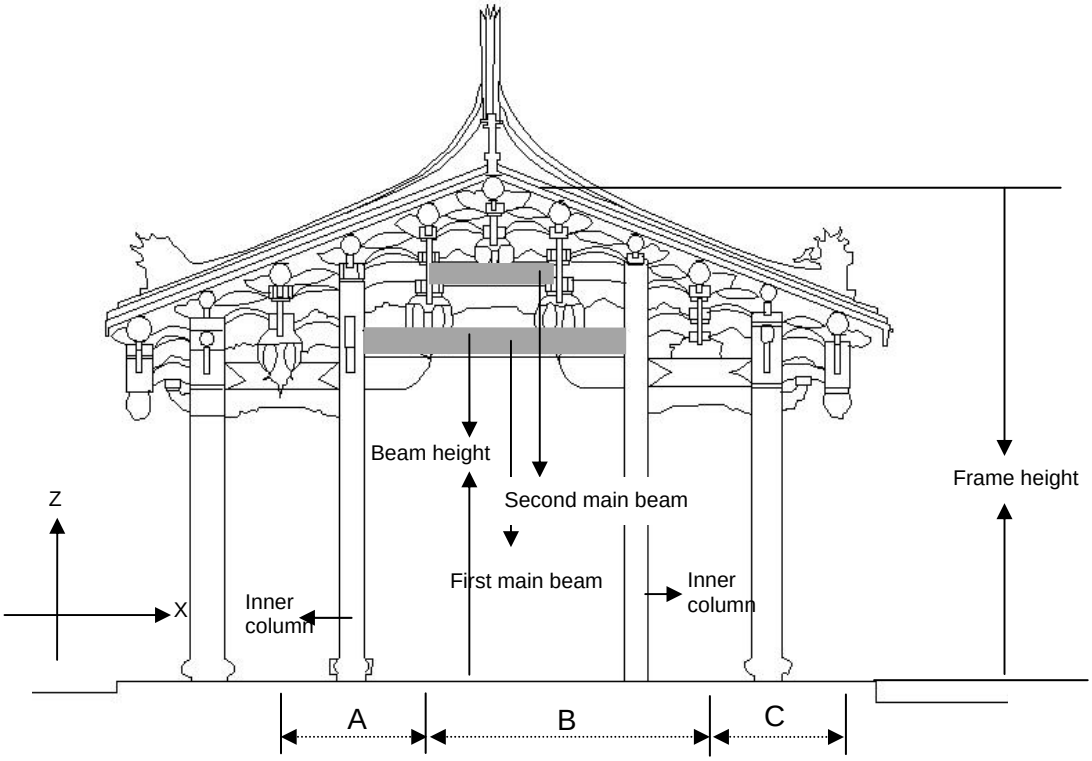

Fig. 2.2.18 Type 2-3 (three main beams and five Dou-Gon joint sets)

In general, Type 3-5 frames are found in the main hall of architectural compound where ceremonies are held, while Type 2-3 frames, which are smaller, are used as entrance halls, see Fig. 2.2.1. Furthermore, elements of the main hall are usually painted and have great heritage value. Therefore, in this project the main attention will be focused on Type 3-5 buildings.

When taking Type 3-5 frames into account, Lee (2007) pointed out that the distance between two purlins is in the range of 60 to 90 cm. The purlins are placed on the top of columns or over a Dou-Gon joint sets, meaning that two columns in the outer parts of the frame (A and C) can be linked with straight beams or with one or more Dou-Gon joint sets in between them (Fig. 2.2.19).

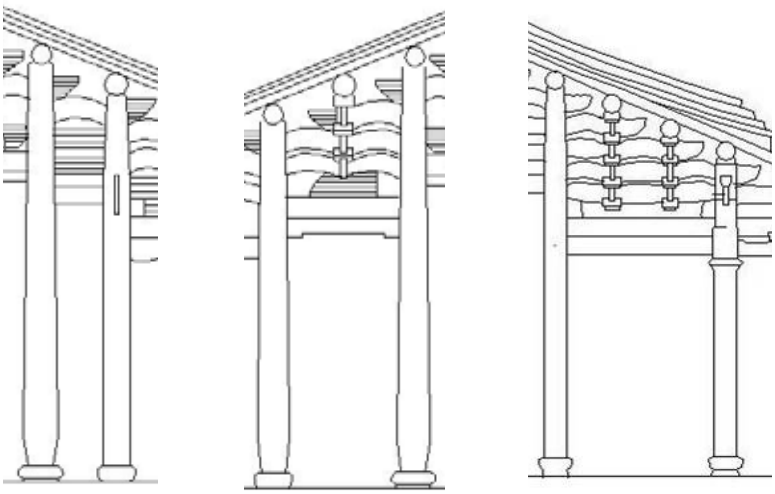

Figure 2.2.19 Elements between two columns of outer part of frame

These arrangements vary between buildings, and it is difficult to classify and distinguish them accurately. However, the central part of the frames (zone B) are all similar in Type 3-5 (three main beams and five Dou-Gon joint sets) frames.

Lee (2007) interviewed carpenters and analysed 33 architectural drawings of Type 3-5 frames, and concluded that the geometry of the central zone (B, Fig. 2.2.17) is in proportion with other dimensions in the Dieh-Dou buildings. For example, the width of the central zone, the height of the first main beam, the beams' length and depth and the column diameters are all in proportion with the total frame height, defined by the height of ridge purlin, see Fig. 2.2.17. The great majority of the buildings have an height comprised between 550 cm to 650 cm, see Fig. 2.2.20. The ratio between the main space length and the first main beam height is in the range of 0.75 to 1, with an average of 0.86, for both types of building. In the 3-5 Type frames, the main space length to frame height ratio is 0.6 to 0.8, and the average ratio between the main beam height to the frame height equals 0.6. The diameter of the inner columns varies between 25 and 35 cm, the depth of first main beams falls between 25 and 35 cm and the depth of the third main beams ranges between 20 and 30 cm.

Although Taiwanese timber buildings originate from China, which is an ancient country and influenced the culture and architecture of most Far East nations, the construction details of Dieh-Dou buildings are different. Being of Taiwanese traditional architecture (Dieh-Dou building) it has its own peculiar characteristics

from a structural point of view, which also developed in response to the environment of Taiwan, an island subject to strong earthquakes.

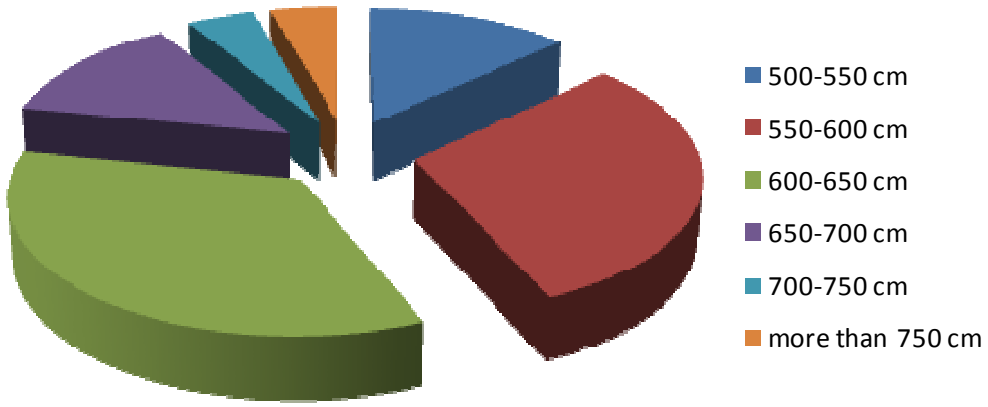

Figure 2.2.20 Height of Type 3-5 frames by Lee (2007)'s survey

2.3 Conservation issues

Architecture is one aspect of culture of humanity; it represents the art, lifestyle and knowledge of a given age. According to Jokileto (1999), the idea of protection of ancient monuments and historic buildings originated in the eighteenth century, but the conservation as a subject starts with the foundation of the International Institute for Conservation of Historic and Artistic Works (IIC) in 1950. Then, in 1965, ICOMOS (International Council of Monument and Sites) was established for archaeological, architectural and planning issues based on the *Venice Charter* (1964) that was promulgated when the Second International Congress of Architecture was held in Venice in 1964. Since then several institutes, such as IIC, ICOM (International Council of Museums), ICOMOS (International Council of Monument and Sites) and ICCROM (International Centre for the Study of the Preservation and Restoration of Culture Property) are devoted to the conservation of historic objects and buildings.

Whether the historic buildings become display monuments or are continuously used in the modern life, it is important that the structure can exist safely and last in to the

future. Thus, the conservation engineering can be defined as one of the ways to approach this goal (D'Ayala & Forsyth, 2007). Structures in modern architecture design are guided by integrated codes and standards, while in the ancient world were built through the knowledge of builders. Furthermore, craftsmanship, paintings, even sculptures are often contained in structural elements of the historic buildings.

The preamble of *Venice Charter* emphasized the "authenticity" of heritage; later, the *Nara Document on Authenticity* (1994) further pointed out that:

> *The understanding of authenticity plays a fundamental role in all scientific studies of the cultural heritage, in conservation and restoration planning…*

These worldwide recognised rules of conservation reflect the importance of authenticity in heritage monument conservation, which any engineering work should obey before further action.

Although the spirit of conservation has been widely spread and maintaining the heritage has become a universally accepted concept, the *Nara Document on Authenticity* emphasises that culture diversities and heritage types should be respected; in other words, the concept of "authenticity" may differ from country to country and culture to culture.

In Taiwan, modern conservation of historic building started to be formally considered in 1982, when the Cultural Heritage Preservation law was established. This law states that historic buildings are to be protected in such a way to preserve their original appearance. Also, historic buildings of cultural value should be listed and information such as location, owner, building construction and material should be recorded carefully; work undertaken should be reported and submitted to the records.

However, even after the law came into force conservation of historic buildings was still considered an issue of minor importance and many historic building were not maintained or repaired properly. In 1999, the Chi-Chi earthquake awakened many to its importance. Several buildings were damaged, including the precious historic

buildings. The vast damage highlighted the importance of protecting culture and history properly.

As Taiwan is located in a highly seismic area, safety issues related to heritage are even more essential. The Taiwanese historic Dieh-Dou buildings are built by timber, but there is lack of laws or regulations of timber conservation in Taiwan. However, ICOMOS (International Council of Monument and Sites) published the *Principle for the Preservation of Historic Timber Structure* (1999), described as:

- *Recognise the importance of timber structures from all periods as part of the cultural heritage of the world;*
- *Take into account the great diversity of historic timber structures;*
- *Take into account the various species and qualities of wood used to build them;*
- *Recognise the vulnerability of structures wholly or partially in timber due to material decay and degradation in varying environmental and climatic conditions, caused by humidity fluctuations, light, fungal and insect attacks, wear and tear, fire and other disasters;*
- *Recognise the increasing scarcity of historic timber structures due to vulnerability, misuse and the loss of skills and knowledge of traditional design and construction technology;*
- *Take into account the great variety of actions and treatments required for the preservation and conservation of these heritage resources;*
- *Note the Venice Charter, the Burra Charter and related UNESCO and ICOMOS doctrine, and seek to apply these general principles to the protection and preservation of historic timber structures.*

The Principles acknowledge the important role of historic timber structures, their vulnerabilities and the targets for their preservation; subsequently, the document states that:

> *The aim of restoration is to conserve the historic structure and its load bearing function and to reveal its cultural values by improving the legibility of its historical integrity.*

In other words, the main target for a successful conservation of the historic timber structures is to take into account both “authenticity” and “safety” at the same time.

D’Ayala and Wang (2006a, 2006b), with reference to the ‘no originality to be changed’ approach of the *Principles for Conservation of Heritage in China* (2004), outlined the limits of application of the concepts of the document to Asian timber structures, concluding that the use of replacement or repair should be considered only when proven necessary by safety considerations or the preservation of the integrity of the structure.

In a Dieh-Dou timber frame, the elements do not only have structural functionality, but also represent art and culture; for example, the bottom pieces of Dou-Gon joint are usually carved as lucky symbols. Besides, one unique feature of Dieh-Dou building is the painting of the structural elements that were usually done by important local artists. Thus, it is essential to analyse the structure properly before a strengthening job is undertaken to prevent replacing or repairing highly valued parts unnecessarily.

The Preservation of Historic Timber Structure (1999) recommends that interventions of preservation and conservation should be preceded by proper studies and assessments; before intervention, an accurate diagnosis of decay and structural failure should be done based on documentary evidence and physical inspection and analysis. These recommendations offer the conceptual basis of how a thorough procedure for the historic Dieh-Dou building conservation could be implemented in order to maintain the “authenticity” and “safety” of the structure.

In order to understand the vulnerability of these structures, in the following chapter the documentary evidence of failures following field survey is presented together with a literature review of relevant research; finally, the procedure for an appropriate Dieh-Dou building assessment is discussed.

Chapter 3

Structural behaviour of Dieh-Dou buildings

3.1 Review of Dieh-Dou structures

3.1.1 Introduction

Historic building conservation is a subject which includes several topics ranging from history to urban design to structural analysis and material science. Even only from an architectural point of view, there are several aspects involved. Ipekoglu (2006) provided a method to evaluate traditional dwellings starting from their exterior and interior architectural characteristics and classified them in different groups offering valuable data for further work in conservation planning. The historian and architecture professions can judge and grade the heritage; however, in practice, for an historic building the most essential goal is to ensure it can be safely used and maintained for future generations, especially if located in zones at high risk of natural disasters.

One Dieh-Dou building is usually formed by two timber frames and three masonry walls, however, considering that timber frames are the main structural elements to transmit roof weight to ground, and also given the fact that Dieh-Dou frames are adorned with precious paintings, the conservation of Dieh-Dou building is focused on Dieh-Dou frame.

In order to understand Dieh-Dou timber frames structural behaviour and establish an accurate and efficient assessment method to improve their performance under earthquake, previous research on Dieh-Dou timber frames and related to historic timber structures is reviewed. Furthermore, post-earthquake surveys of Dieh-Dou are discussed, and their seismic behaviour is deducted from their failure modes.

3.1.2 Research on Dieh-Dou buildings

The research on Dieh-Dou buildings so far includes several aspects; however, only structure, construction and material issues are included in this section.

Material and Non Destructive Testing Techniques (NDT)

Tsai (1997) surveyed and collected timber pieces from traditional buildings which were under construction work. The mechanical characteristics and categories of wood were investigated. Tsai found that 67% of the surveyed specimens were Chinese Cedar, 13% Japanese Cedar, 13% Taiwanese Cypress, and the remaining 7% Taiwanese Cedar.

The elements of Die-Dou buildings are rich with paintings, which increases the difficulty of a non-destructive investigation. Tseng (1997) is one of the earliest researchers who focused on damaged Dieh-Dou buildings. Tseng introduced mechanical instruments to investigate decay of structural components rather than relying upon visual detection by carpenters. Based on the research by Tseng (1997), Chen (2004) applied ultrasonic and drill resistance methods to detect rotten material and proposed approaches to deal with the material decay without destroying existing painting.

Tseng (2007) compared the ultrasonic waves to test defects in new timber material and old elements from historic building sites and found out that ultrasonic waves cannot be successfully applied on Dieh-Dou frames as the timber pieces in situ do not allow a proper positioning of the devices to reflect the waves correctly. Therefore, Tseng concluded that the drill resistance method is much more reliable than ultrasonic method for the characterization of the properties of existing Dieh-Dou buildings.

The Dieh-Dou frames are built of softwood, in a period with codes or standards had not been introduced, and the wood used to build Dieh-Dou frames is not necessarily on the same type. Furthermore, humidity and termites can cause chemical or physical damage of timber. However, in this project, these effects are not considered, as only structural aspects are analysed. Therefore, in the future in-situ

conservation work, non-destructive analysis techniques may be needed to assess decay and combine it with structural analysis.

Construction

Shu (2000) described the full construction sequence of the Dieh-Dou buildings. Dieh-Dou buildings are built by small pieces of wood elements linked by joints; however, the details of joints are difficult to understand by visual observation without removing elements piece by piece. Through construction site dismantling, carpenters interviews and references, Shu (2000) recorded the construction details of frames, roof, wooden members, joints, and how they are connected together and form the structure.

Chang (2004) recorded the dimensions of Dieh-Dou frames, joints and mortise and tenon, observed damage, and classified it as being caused by material natural decay, mechanical effects, or errors in the dismantling process. Song (2004) focused on the material cracks caused by natural decay and discussed the possibility of using epoxy resins to repair.

Lee (2007) gathered construction details of 33 Dieh-Dou buildings from references and sources to analyse the size and proportion of elements, like for example the relationship between column height and diameter. Yang (2008) further concluded the joints and elements dimensions are in proportion between each other after he surveyed three Dieh-Dou buildings and recorded tenon and mortise geometry of the timber joints. Chen (2007) applied a new technology, 3D laser scanning, to draw details of the Dieh-Dou buildings, as the construction is complex and difficult to survey and draw by traditional methods. The results showed that 3D scanning laser ranger technique can be used for a Dieh-Dou building detailed survey.

These details on Dieh-Dou construction are based on surveys. There is still no document listing all the Dieh-Dou building existing in Taiwan, but from the reports discussed above it can be shown that although construction of Dieh-Dou frames is not standard, the geometry of the buildings and dimensions of joints and elements are in proportion and fall in certain ranges.

Structure

Shiao et al. (2003) analysed the timber frames of a Dieh-Dou building by FE software STAAD.Pro. A 3D Dieh-Dou physical model in 1:20 scale was created and tested in the laboratory to compare the natural frequencies with the numerical model. There is no mass participation results included in this report, but was indicated that the first two modes were sufficient to excite the whole structure, while other modes were of minor importance. Table 3.1.1 shows the natural frequencies of these two models. The results between the FE and the scale model are very different. Shiao et al (2003) pointed out this may be due to difficulties in simulating joints properly in a physical model that is too small to represent the full scale structural behaviour of a such complex structure accurately.

Table 3.1.1 Natural frequencies of numerical model and physical model by Shiao et al (2003)

Mode number	Model	Frequency (Hertz)	Direction
1	Numerical model	0.51	Out of plane
	Physical model (1/20)	3.38	Out of plane
2	Numerical model	0.75	In plane
	Physical model (1/20)	3.95	In plane

The Dieh-Dou buildings are constructed by small pieces of timbers, this unique system makes it difficult to understand the load transfer path. Although a FE numerical model can be a good way to simulate and understand this structures, it is necessary to properly account for the joint property, that are an important feature for all timber structures and in particular for Die-Dou buildings.

From the aforementioned previous research where FE models of Dieh-Dou frames were used, it was not possible to accurately validate these models by comparing them with laboratory tests, as full-scale testing of the whole frame was unfeasible and small scale physical models are unlikely to represent the structure (especially the joints) properly.

Therefore, the issue of a proper joint simulation in the FE model and the validation of the model results are the principal challenges in the evaluation process of Dieh-Dou frames. In order to provide more context to these issues, further work related to historic timber structures is reviewed in the following.

3.1.3 Review of evaluation of historic timber buildings

According to D'Ayala & Forsyth (2007), a systematic interest on repair and restoration can be traced back to Renaissance architects, who focused not only on proportion and decoration, but also material and technology. Later, mechanical interpretation and structural repair and prevention were introduced to the historic building conservation. In 1748, a report by Giovanni Poleni on cracks in the dome of St. Peter in Rome was considered as the first application of rational analysis and an engineering method for the damage on existing buildings.

Following the development of science, more accurate engineering methods were applied to buildings; more recently, with the advances in computer industry numerical analyses could be coupled with other evaluation method and provide a useful tool for building engineers, as historic structures are often indeterminate and have several possible load paths.

Morris et al. (1995) illustrated the results of a finite elements analysis on the historic timber roof structure of Westminster Hall in London. Nodes defined the geometry of trusses and frame elements represented the truss members with given dimensions and material properties. The connections were modelled as fixed, released, constrained, or partially released, according to mathematical representation of the physical condition. Then, different conditions of support and loading at the roof were analysed. The results of the Westminster Hall truss shows that to consider the truss subjected to axial forces only may not represent the reality properly. Performing the analysis of the truss with and without the tracery, it was found out that the tracery absorbs and redistributes loads from the surrounding members and was confirmed that the original structure had a higher factor of safety versus collapse than what could be found using the simplified method. In this paper, the contribution of the structural elements could be evaluated simply by changing the condition in the

numerical model, showing that finite element analysis can provide a bridge between historical and technical overview and help the conservation.

Numerical analysis has expanded dramatically in recent decades. However, someone may argue that laboratory base structural performance is necessary to complement it. Fang et al. (2001, I and II) published a series of research papers on Chinese timber structures, where results on laboratory tests and numerical models were compared with in-situ monitoring. An ancient timber tower built in the 14th century, measuring 18.14m of height, 50.6m of length and 10.52m of width, with 36 timber columns was analyzed (see Fig. 3.1.1) after on-site structural microtremors were measured to obtain the natural frequencies of the tower both with and without roof.

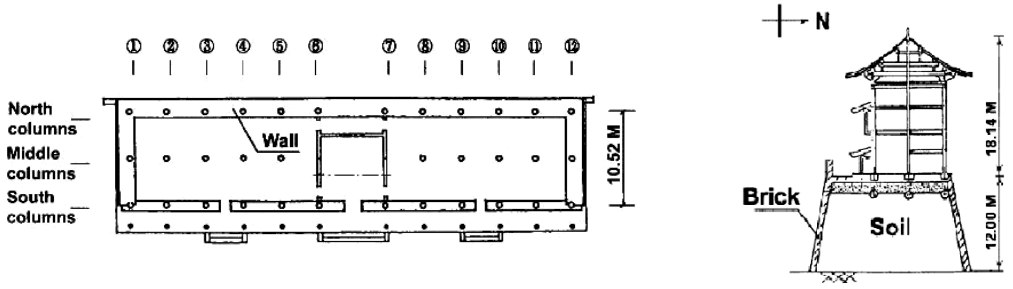

Figure 3.1.1 Plane section of a Chinese timber structure (Fang et al, 2001, I and II)

In the laboratory, two models were built. The first was a partial wooden model at a scale of 1:10, while the second was an integral PMMA (Perspex) model at a scale of 1:30. These two models were tested by multipoint excitation and compared against the result of the full-scale natural frequencies. The results of these three tests indicated that first and second natural frequencies could be matched by the small-scale model testing while the third and the fourth modes were not identified by laboratory testing. In the second part of this project a numerical verification was carried out.

The finite element software SAFATS (Structural Analysis for Ancient Timber Structures) was developed to simulate the tower. A 3D Semi Rigid Connection Element (SRCE, see Fig. 3.1.2) was created to model the stiffness of the corbel

bracket where node i and j are at the same coordinate. The SRCE has no mass and dimension and is assumed that all six degrees of freedom are uncoupled in the matrix for simplicity of analysis. The whole structural model, made with linear frame elements, is shown in Fig. 3.1.3.

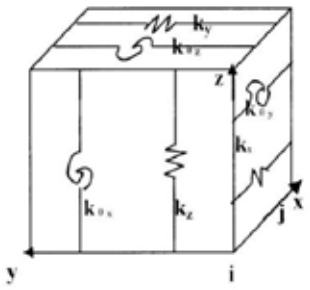

Figure 3.1.2 3D Semi Rigid Connection Element (Fang et al, 2001, I and II)

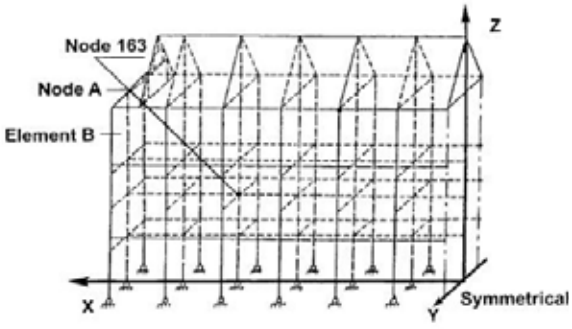

Figure 3.1.3 Whole structural model (Fang et al,2001, I and II)

From on-site tests, the first and second natural frequencies were known, so Equation (3.1.1) below was employed as an objective function by changing the stiffness parameters of the SRCE element until the function approached zero, which meant that the correct first and second natural frequencies of the structure were obtained with the stiffness inserted in the joint model.

$$OBJ = \sqrt{(F_B - F_{BO})^2 + (F_T - F_{TO})^2} \tag{3.1.1}$$

where F_B = first natural frequency obtained by computation; F_{BO} = first natural frequency obtained in the on-site measurement; F_T = second natural frequency obtained by computation; F_{TO} = second natural frequency obtained in the on-site measurement.

Looking at the third and fourth natural frequencies, the result of FEM matched well with on-site recording while the correlation with laboratory testing was poor. This two papers show that this type of Chinese historic building can be analysed accurately by FE model, while the small-scale entire models are often affected by parameters that is difficult to control in laboratory, such as the way in which the excitation is

produced, the joints that cannot be carved in the same way as for a real building and the loss of accuracy of the scaled down connections.

Jaishi et al (2003) modelled three temples in Nepal, which were built multi-tiered with masonry walls and timber roofs. Field tests were performed by ambient vibration methods under wind-induced excitation to extract real properties, which matched with the finite element model results well, proving that the FE modelling could be successfully implemented.

In order to understand the static behaviour of the timber roof structure of the medieval Swedish castle of Glimmingehus, Thelin (2005) developed a computational model in which the undamaged state and different damage types were simulated in a finite element model. The different load cases were imposed over both the undamaged and damaged models; when compared with the in-situ observations, it was revealed that damage could be related to wind load. This paper concluded that FEM analysis can describe the static behaviour of complex historic structures and provide a better dialogue between different professional groups in the conservation project, also giving the opportunity of testing different parameters with little effort.

Therefore, for existing historic structures, which were built before standards were established and whose construction is unknown and complex, numerical approaches using FE can be a quick and reasonably accurate approach to use for assessment.

Timber has been widely used as a building material for a long time. Construction techniques are different from culture to culture and from country to country; also, the characteristics of timber structures differ from other material substantially. In the past, modern analysis regarded timber joints as pin or rigid; however, in recent work, the rotational stiffness of timber joints was defined as semi-rigid (Chang 2006). In Far-East Asian historic timber construction the timber joints are usually connected by tenon and mortise only without additional elements, and it is important to understand how stiff the joint is to represent the behaviour of the structure properly. This section discusses the historic timber frames with modern analytical tools.

King et al. (1996) studied a traditional Chinese timber frame. where the connection of beam to column is of the plug-slot type (see Figure 3.1.4). This joint type is usually used for the connection between main beams and columns in Dieh-Dou buildings. In order to obtain a complete understanding of both undamaged and damaged joint; four types of experiments were performed, one with the original shape and the other three with a 50% volume reduction to simulate termite deterioration, with the size scaled down to 1:3. The experimental results showed that the initial stiffness of these joints ranges from 1.47E+3 to 9.8E+3 Nm/rad.

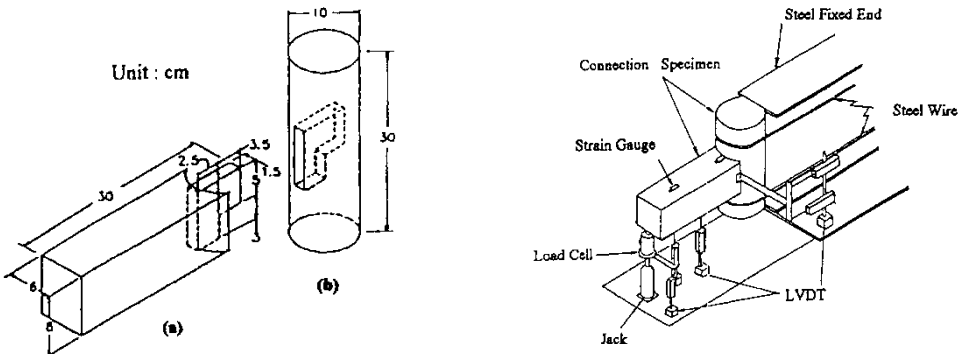

Figure 3.1.4 Joint detail and test device (King et al 1996)

In addition, small scale timber frames (including two columns and one beam) were set to test the P-Δ effect varying the column axial loads, column height and timber joint conditions; The test setting is shown in Figure 3.1.5.

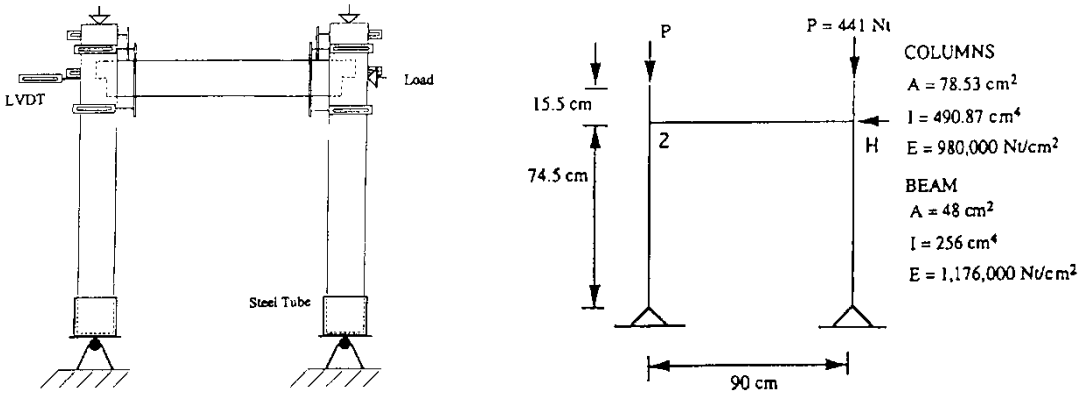

Figure 3.1.5 Frame test device (King et al 1996)

After testing, analyses were performed to compare with tests results. King et al. (1996) concluded that both new and damaged connections have semi-rigid behaviour; besides, the non-linearity of the load-deflection response is due not only to the behaviour of connection but also to the magnitude of the axial load in the column that can cause a decrease of the stiffness of the column.

Parisi and Piazza (2002) investigated the static and dynamic behaviour of old timber connections and identified suitable retrofitting criteria. Tests on joint connections under monotonic and cyclic loads and a test of an assembled roof truss were performed in laboratory. Then a numerical model was created to simulate and analyse the roof truss. The joints of the truss were modelled by spring elements (see Figure 3.1.6) and a dynamic analysis of the whole roof was also performed (see Figure 3.1.7). The results showed that different reinforcement methods affect the whole structural behaviour through their different joint stiffness.

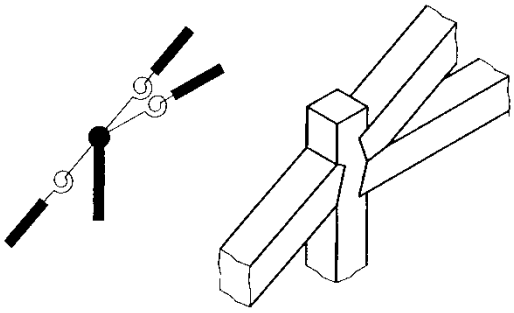

Figure 3.1.6 Spring element to model the truss joint (Parisi & Piazza 2002)

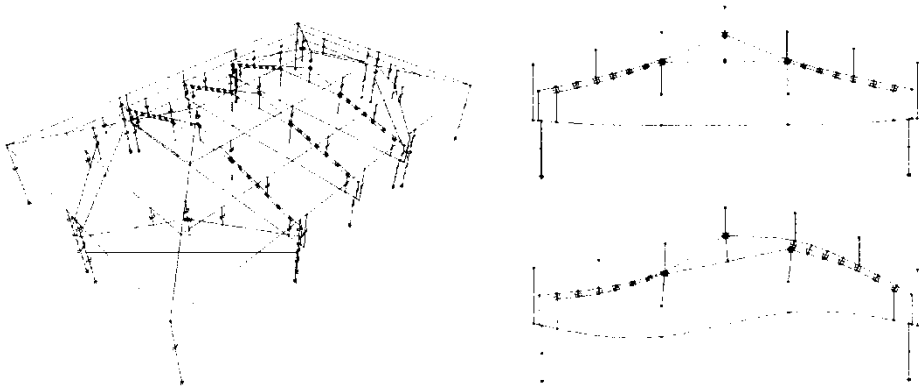

Figure 3.1.7 Complete modelling of the roof (Parisi & Piazza 2002)

The Resho-ji Hondo temple was used as an example for Miyamoto et al. (2004) to analyse. A diagnosis using a limit value of 1/120 radians for the storey drift was proposed to calculate the strength of each floor. FE models with semi-rigid joints were employed and results compared with in-situ measurement on both unstrengthened and strengthened building. The results show that a numerical model employing semi-rigid joints can represent the structural behaviour well and can be used for timber buildings.

Hanazato et al. (2004) chose to analyze a five-storied timber pagoda (Eimyou-in Goju-no-to), designed by a modern carpenter and strengthened by Hanazato et al. (2004) against earthquake. Two types of models were employed to analyse this structure. The first was a 2D nonlinear frame model, in which the joints of beam and column were simulated as semi rigid. This nonlinear model was analysed with a step by step static pushover analysis by applying lateral horizontal forces and the load-displacement relation at every floor. In the second model, a modal and earthquake spectra analysis (using reference earthquakes) with lumped masses applied at the various floors was performed.

These analyses were used to evaluate the structural capacity before and after strengthening, confirming the improvement due to the strengthening. However, the modal analysis showed significant differences in natural frequency, when compared with the in-situ measurements, and the authors suggest that verification of the analysis should be done with records during a large earthquake or heavy typhoon, as it is only in those extreme conditions that more clear responses could be obtained.

Chang (2006) surveyed and tested three types of beam-to-column joints widely used in Taiwanese Chuan-Dou buildings (see Figure 3.1.8). A total of 72 specimens were tested to study these three types of joints, including the mechanical failure, the bending-slip characteristics, initial rotational stiffness, and moment-rotation relation. Models to predict the initial rotational stiffness and moment-rotation curve of each type of joints were proposed. Chang (2006) found that the behaviour of the joints was semi-rigid and proposed formulae as functions of column width, beam width,

Beam depth and modulus of elasticity of timber perpendicular to grain. The formulas proposed by Chang (2006) will be used on the beam to column mortised joint in FE model and discussed in more detail later.

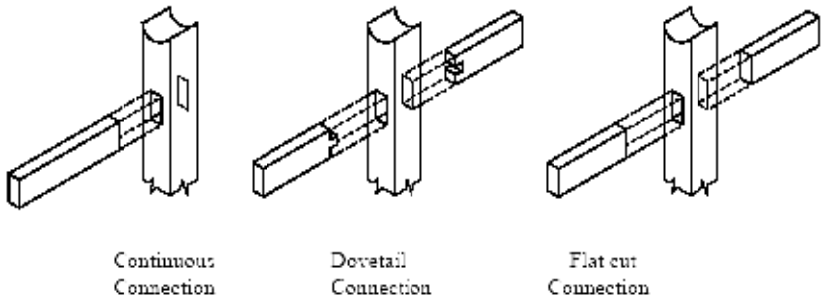

Figure 3.1.8 Three types of beam to column joints (Chang 2006)

3.1.4 Discussions

In the previous research on the issue of historic building conservation, especially on structural evaluation and safety, numerical and reduced scale tests are often used to analyse historic timber structures. Most historic buildings were built before standards and may in some cases be over designed (Morris et al 1995) as well as deficient, as is often the case for earthquake resistant design.

The advantages of a computer simulation for a structure whose characteristics are not well defined is the possibility of parametric studies with corresponding identification of vulnerable areas and avoidance of extensive and expensive experimental work. Through FE model, Morris et al (1995) could soon understand the behaviour and the role of tracery and the truss of St.George's Hall at Windsor could be examined, too. Jaishi et al (2003) and Thelin (2005) revealed FE models can be reliable by comparing with on-site test and failure observations.

The FE model can simulate the overall structural behaviour, and research shows that for timber structures it is very important to simulate the joints properly. For Dieh-Dou frames, joints can be classified into two groups, Dou-Gon joints and beam to column mortised joint. For the latter one, Chang (2006) has provided formulas to predict rotational stiffness, verified by laboratory tests; however, there is lack of information about Dou-Gon joints, and in order to simulate Dieh-Dou frames properly, it is essential to understand the joint behaviour.

Although results of researches showed that timber structural behaviour can be analysed by FE model, it is important to verify the accuracy of modelling. Small scale structure models were used to validate FE models by Fang et al (2001, I and II) and Shiao et al (2003); however, results showed that small scale reductions may affect results excessively and not necessarily match on site test or numerical analysis findings.

In Dieh-Dou buildings, it is difficult to test full scale models and reduced model are not necessarily reliable, as the joints of Dieh-Dou fames are too complex for carpenters to be recreated and simulated properly at reduced scale. The 1999 Chi-Chi earthquake damaged several Dieh-Dou buildings, thus, the failure mode of Dieh-Dou buildings post earthquake can provide valuable evidence on the vulnerability of these structures, and further validate the accuracy of mathematical models. Before discussing the numerical model and analysis methods for Dieh-Dou frames, the failure modes post earthquake are discussed.

3.2 Failure modes post-earthquake

3.2.1 Failure observations after the 1999 Chi-Chi earthquake

Taiwan is located between the Eurasian and Philippine Sea plates where the plate erupted from Philippine Sea pushes towards northwest into the Eurasian Plate: this is the cause of the frequent earthquakes in the island of Taiwan. According to Dong et al. (1999), there are more than 40 mapped active surface faults moving in the north-south direction of the island, parallel to the plate boundary.

On the 21st of September 1999 at 1:47 am, a devastating earthquake of magnitude Mw 7.6~7.7 occurred in central Taiwan, with epicentre located near Chi-Chi Town, Nan-Tou county, 7 kilometres below ground level (see Fig. 3.2.1). The earthquake ruptured for 83 km along the Chelungpu fault (see Fig. 3.2.2) and the western edge of the Central Mountain. Peak ground accelerations of 1.0 g were recorded in the southern end of the earthquake rupture zone (Dong et al, 1999). This strong shock struck in the middle of the night when most people were at home, and caused more than two thousands deaths and one hundred thousands buildings were damaged or collapsed.

After the earthquake, the Architecture and Building Research Institute of the National Ministry of Taiwan established teams of professionals to survey and record 8773 damaged buildings around the earthquake's epicentre. The report "*Survey of 9-21 Chi-Chi earthquake buildings damage*" (Architecture and Building Research Institute, 1999) shows that 42% of buildings were built before 1974, when the first seismic design codes were introduced. Generally, the later the buildings were built, the lesser damage occurred. Unfortunately, all historic buildings were built without proper consideration of their structural behaviour under seismic loading.

Figure 3.2.1 Epicentre of Chi-Chi earthquake
(Dong et al, 1999)

Figure 3.2.2 Chelungpu fault
(photo taken by Tseng)

For the historic buildings, Su (2003) collected post earthquake damage data of 40 traditional temples post earthquake (the structural types were not specified) and classified them into six different levels of damage based on the "*Prediction of classic masonry brick houses damaged under earthquake*" method from Japan. These six levels of damage are: no damage, slight damage, little damage, medium damage, serious damage and collapse. Furthermore, the values of ground acceleration (both North to South and East to West) near these 40 buildings were taken to compare against the different levels of damage. The results indicate that the seriously damaged and collapsed buildings were mostly found in the zones where accelerometers recorded peak ground acceleration of more than 300 gal (980 gal equals 1.0 g, so 300 gal is about 0.3 g). Although the results from Su (2003) focus on masonry walls observation, they are a valuable indication on the severity of damage that may have occurred to timber frames as well.

Huang and Sheu (2001) classified the damage of timber and bamboo buildings by their architectural elements, assuming seven parts form the building: column, purlin, beam, Dou-Gon joints set, mud and timber interior wall, roof and eave part. They stated that the failures of Dieh-Dou building were mainly caused by the weight of the roof compared with the lightness of the lower portion of the building that led to large lateral sway during horizontal earthquake load (Fig. 3.2.3); the tiny joint between wooden column and stone podium would, therefore, be considered as a pin, rather than a restrained base (Fig. 3.2.4).

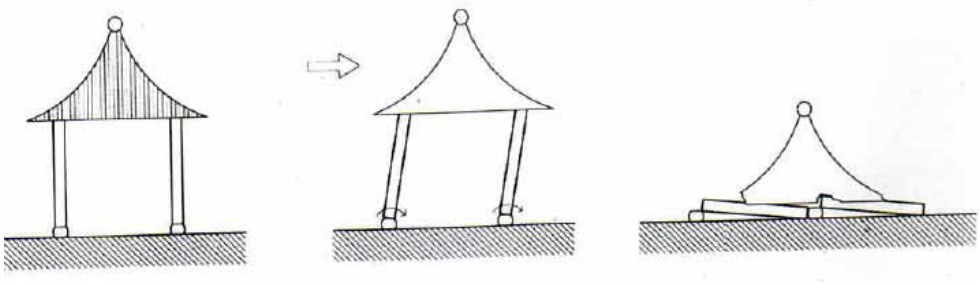

Figure 3.2.3 Collapse of building (Hung et al, 2002)

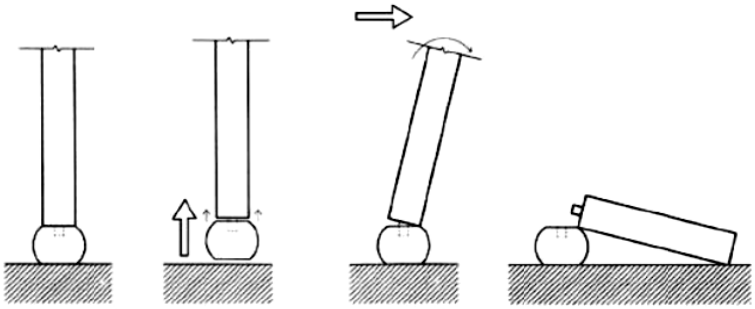

Figure 3.2.4 Failure of column (Hung et al, 2002)

Chang et al. (2002) observed traditional temples after the 1999 Chi-Chi earthquake and drew the conclusion that six types of damage were evident:

1. *Purlins slid and pulled out from the masonry walls*
2. *Wooden columns moved away from the stone podiums*
3. *Corners were damaged between two perpendicularly enclosed masonry walls*
4. *Eave parts were leaning and distorted*
5. *The roof ridge decoration was broken and led to roof damage*
6. *Frame elements pulled out from the vertical members*

Although timber buildings were surveyed and common damage types were recorded, the types of the buildings were not specified, therefore is hard to quantify Dieh-Dou buildings damage based solely on the information provided by Su (2003), Huang and Sheu (2001), and Chang et al. (2002). To understand the vulnerability of Dieh-Dou buildings and evaluate their structural behaviour, it is necessary, firstly, to classify the damage types in detail and also to obtain the percentage of each type occurred, in order to identify the weak parts of Dieh-Dou buildings.

3.2.2 Failure modes classifications

In Taiwan, traditional temples are often built using Dieh-Dou timber frames. In order to focus on the Dieh-Dou structures, an investigation carried out within the present

project identified at least 52 historical architecture compounds built as Dieh-Dou structures over the Chi-Chi earthquake stricken region, however for 29 of them was not possible to gather data about their condition after the event. For the remaining 23 Dieh-Dou compounds, details of damage were collected.

EMS 98 (European Macroseismic Scale 1998) classifies buildings damage under earthquake into 5 grades, which are

- *Grade 1: Negligible to slight damage (no structural damage, slight non-structure damage)*
- *Grade 2: Moderate damage (slight structure damage, moderate non-structural damage)*
- *Grade 3: Substantial to heavy damage (moderate structural damage, heavy non-structural damage)*
- *Grade 4: Very heavy damage (heavy structural damage, very heavy non-structural damage)*
- *Grade 5: Destruction (very heavy structural damage)*

HAZUS-MH MR3 (2003) describes structural damage as “Slight”, “Moderate”, “Extensive” and “Complete”. In these two documents, damage classifications also depend on the structural system. Considering the damage levels on Dieh-Dou building in accordance with the damage classification concepts of EMS 98 (1998) and HAZUS-MH MR3 (2003), five levels of damage on Dieh-Dou buildings can be reasonably considered:

- **Level 1**: No structural damage
- **Level 2**: Elements pulling out from joints and damage of the roof ridge, etc.
- **Level 3**: Eaves rupture, masonry wall cracks, columns rotating or sliding, etc.
- **Level 4**: Overall in plane or out of plane leaning
- **Level 5**: Dieh-Dou frames collapse

Damage levels 2 and 3 are considered still below an immediate safety threat, while damage levels 4 and 5 represent an unsafe building. Based on this damage level

classification, the proportion of each damage type and class for the 23 Dieh-Dou compounds surveyed are shown in Table 3.2.1 and Fig. 3.2 5.

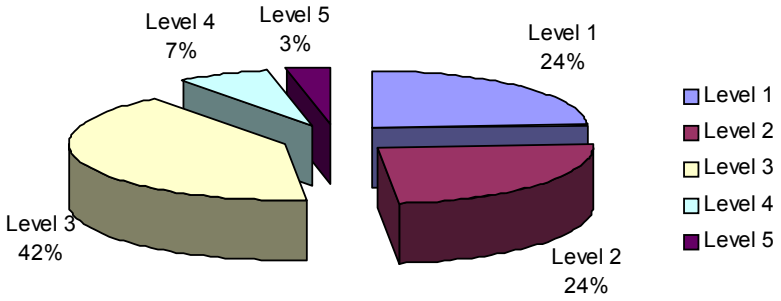

Figure 3.2.5: Level of damage of Dieh-Dou buildings after the 1999 Chi-Chi earthquake

Table 3.2.1 Level of damage of Dieh-Dou buildings after Chi-Chi earthquake according to Tsai Survey

Damage level	Failure mode	%
Level 1	No structural damage	24%
Level 2	Elements pulling out (10%) Damage of the roof decorated ridge (14%)	24%
Level 3	Eaves rupture (7%) Masonry wall cracks (21%) Columns rotation (14%)	42%
Level 4	Dieh-Dou frames with in plane or out of plane leaning	7%
Level 5	Dieh-Dou frames with in plane or out of plane collapse	3%

A more detailed description of the damage types and failure observed during survey and their implications for the structure integrity of the buildings are presented below

Level 2

Dieh-Dou timber frame are formed by several pieces of wooden elements, as described in Chapter 2. The joints are all based on tiny mortise and tenon which under earthquake loading suffer from dislocations, caused either by a pull out or relative rotation between elements.

The Dou-Gon joint set is easily deformed by a horizontal force, but its deformed shape is different to that of a continuous column (see Fig. 3.2.6). On the left of the diagram is shown the deformed shape under a horizontal force of a continuous column, whilst the right side shows the type of deformed shape of a joint set, which can be considered as a stack of small columns. The Dou-Gon joint set of the Guan-Shi temple displayed this kind of deformed shape (see Fig. 3.2.7). Furthermore, the in plane pieces which connect with the Dou-Gon joint sets are likely to pull out because of the horizontal force and the leaning of the bracket set.

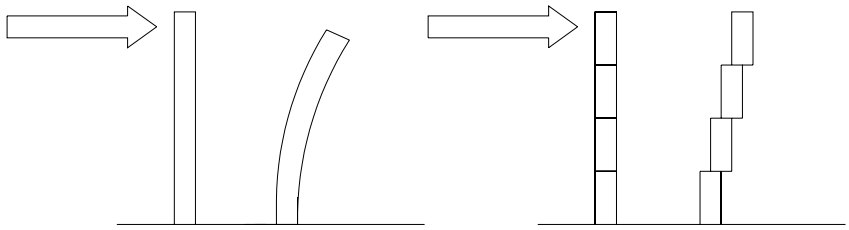

Figure 3.2.6 Deformed shape of continuous column (left) and a bracket set (right) under lateral force

Other joints damaged by the earthquake were the connection between horizontal and vertical structural elements, for example, the joints between column and beams. Fig. 3.2.8 show beams pulled out from columns in the Guan-Shi temple. The photo shows that the joint of beam is a simple straight tenon, weak against lateral force and easily pulled out.

The roof ridges of temples are full of heavy decorations (see Chapter 2), which are placed on the roof and lack strong connections with the main structural elements of the temple; hence under vibration these ridge decorations easily fall down. These failure modes are classified as damage Level 2 in the sense that while each of them

cannot trigger structural failure, if a significant number of elements pull out, the structure global integrity is substantially impaired and collapse can be accelerated. Also, falling pieces of very heavy roof decorations are a threat for human life.

Figure 3.2.7 Deformed Dou-Gon set and elements pull out

Figure 3.2.8 Beams pull out from column

Level 3

Eave rupture, column sliding and masonry wall cracks are classified as damage level 3. Most of the joint failures mentioned in level 2 come from loss of geometry (i.e. elements moving out irreversibly from their original positions). In some situations, however, they can results in material failure caused by excessive normal, bending and shear force on the pairing element (see Fig. 3.2.9). This type of failure has been observed in the eave part of Dieh-Dou building only. The beam elements of the eave are inserted one side into the corridor column, whilst the other side is hanging. Under an earthquake, these cantilever beams can rupture once the moment and shear overcome the material strength, causing localised collapse of this portion of the roof.

Figure 3.2.9 Eave rupture failure

In order to isolate the wooden columns from ground humidity and avoid decay, stone podiums or half stone columns are placed between the columns and the ground. These joints represent a weak point under earthquake loading. The connection of the podium stone and the timber column is tenon (wood) and mortise (stone); Fig. 3.2.10 shows the section of a wooden column and stone podium, which forms the foundation, while Fig. 3.2.11 shows the tenon of a timber column. As can be seen, generally the length of the tenon is small compared to the whole column length; during a strong earthquake with high horizontal and vertical acceleration this tenon is subjected to rotation or even sliding if the shear is higher than the timber tenon capacity, Fig. 3.2.12 shows an example of column rotated.

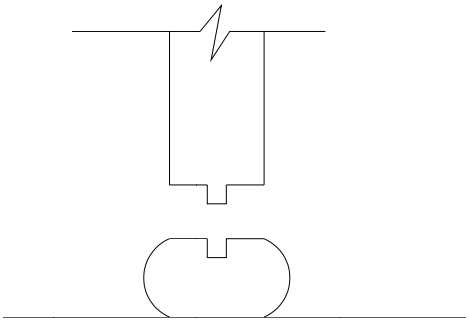

Figure 3.2.10 Connection of column

Figure 3.2.11 Tenon of timber column

Figure 3.2.12 Columns rotated

The remaining failure type in damage level 3, masonry wall cracks, are neglected in the present Dieh-Dou frame failure mode discussion as masonry assessment is not an objective of this study.

Levels 4 and 5

Timber frames are flexible and easily deformed under lateral forces, especially Dieh-Dou frames due to their unstable joint arrangements. In addition, the column ends have tiny tenons to connect with stone podiums, as aforementioned, and this connection cannot provide moment resistance. Thus, the columns can easily rotate. The purlins, which link the frames to the masonry walls, are simply placed on a hole in the wall without any specific connection. These construction details permit Dieh-Dou frames to lean easily in the in-plane direction.

Masonry walls provide little resistance to earthquake load and fail easily during sustained vibration; according to Chang et al (2002) there is only surface friction between purlin and masonry wall to resist relative movement; once the horizontal force is greater than the frictional resistance the purlins can pull out from the masonry. When the masonry wall of Dieh-Dou building falls, this can lead to a total failure of the roof in the secondary spaces, while the main space is still standing (see Fig. 3.2.13). De-Shin temple is an example of this type of failure, see Fig. 3.2.14.

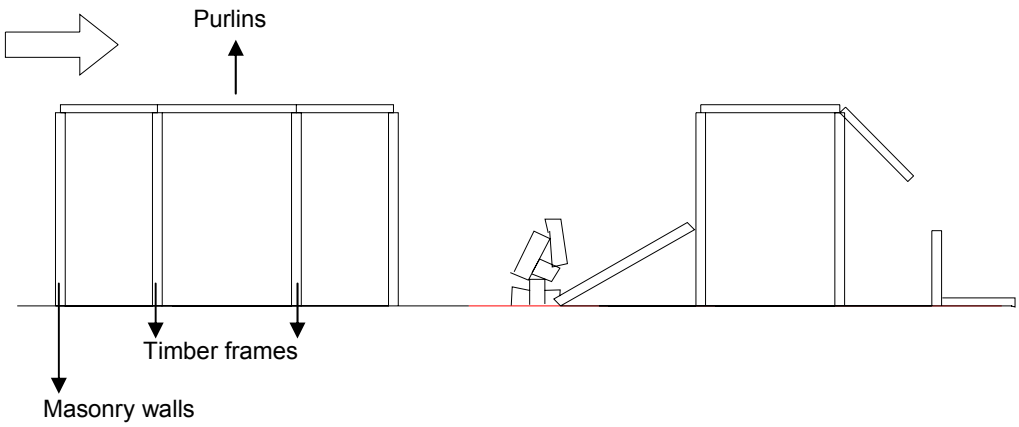

Figure 3.2.13 Failure of purlins under lateral force (out of plane)

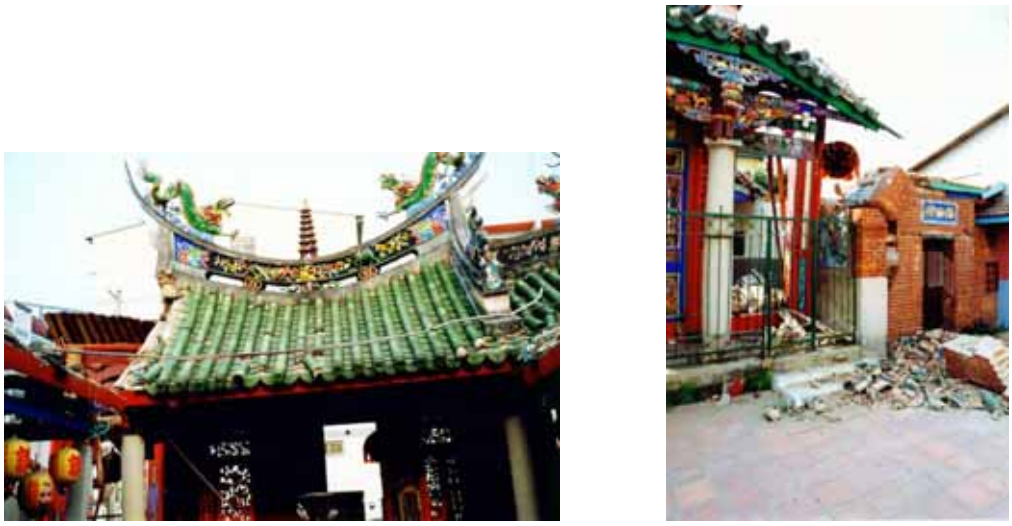

Figure 3.2.14 Failure of the secondary spaces De-Shin temple (photo taken by Tseng)

Once the frames are disconnected from masonry walls, the two frames become vulnerable and easy to rotate and deform. The purlins are placed on the top of the Dou, shaped like a saddle, but without tenon and mortise, see Fig. 3.2.15. Under seismic load, they can also fall down and separate the two frames; in this case, the structure is likely to collapse out-of-plane, as the frames no longer have stabilizing weight from the roof.

Figure 3.2.15 Upper Dou saddle, seating for the purlin

3.2.3 Discussion

The Survey of the 9-21 Chi-Chi earthquake buildings damage indicated that the seriously damaged or collapsed buildings were distributed over a 6 kilometres wide area either side of the Chelungpu fault and that where ground accelerations were higher than 300 gal (0.3g) global failures always occurred. This phenomenon was also confirmed by Su's 2003 survey of the damage of all traditional temples. Although natural disasters like serious earthquakes are difficult to prevent, the improvement of the building structure can reduce injury to human beings and preserve cultural heritage.

From the surveys of Dieh-Dou building after the 1999 Ch-Chi earthquake, the most common local damage modes were found to be the elements pulling out, damage of

the roof decorated ridge, eave ruptures, masonry wall cracks, and sliding columns. The partial or global leaning or collapse are caused by several of these local damages concurring at the same time or by large quantity of same type of local damages, as for instance a large number of elements pulling out.

From the failure modes discussed before, the following conclusions can be drawn:

1. The bottoms of columns can be considered as hinges
2. Horizontal elements are very easily to pull out from joints
3. Several elements may pull out and rotate from their joints, but few fail by material rupture
4. The movement of the frames can be substantial before the frame collapses

These failure modes of Dieh-Dou frame draw a picture of global behaviour of the building, which can be used to verify a numerical model analysis; however, in order to confirm accuracy of the analysis method, a detail of failure on some specific buildings is necessary for further quantification.

3.3 Discussions and proposal to evaluate Dieh-Dou buildings

In the discussion of Dieh-Dou building evaluation, it was concluded that the main challenges for a proper mathematical model were to simulate the joints properly and validate this mathematical model against reality.

Regarding the joint simulation, all previous researches focused on rotational behaviour; however, the survey post earthquake reveals that for Dieh-Dou timber frames, not only rotational but also translational stiffness is important. To analyse Dieh-Dou frames properly, it is necessary to perform pull out tests in addition to rotational tests for the Dou-Gon joints. The beam to column mortised joint stiffness

can be calculated by existing verified formulas, as for example the one proposed by Chang (2006).

The finite element model with proper rotational and translational stiffness can be verified by post earthquake survey of specific buildings and through the damage levels identified in this Chapter.

In the following Chapter, rotational and translational tests are performed on Dou-Gon joints, while Chapter 5 discusses the numerical model employed and Chapter 6 presents the assessment method that is compared with qualitative and quantitative data to validate the analysis.

Chapter 4
Experimental investigation on Dieh-Dou joints

4.1 Introduction

Joints govern the structural behaviour of timber buildings, and their structural behaviour is in reality neither pinned nor fixed. Rotational stiffness is usually considered when undertaking timber joint analysis. However, post earthquake survey shows that, for the peculiarity of Dieh-Dou buildings in which the unique Dou-Gon joint sets support the vertical load of the roof and transfer this load to the columns in the in-plane main frames, horizontal elements can easily be pulled out from the frames under seismic excitation. Hence, in the FE simulation, not only rotational but also finite translational stiffness and capacity of the joint need to be considered.

In this Chapter, a series of rotational and translational tests on full-scale samples of Dou-Gon joints are presented, to help with the characterisation of the joint behaviour for modelling.

4.2 Test specimens

4.2.1 Details and dimensions of the joints

One Dou-Gon joint set of a Dieh-Dou frame can be divided into different layers; one layer is formed by two Dou, in between which two in-plane elements are linked to out of plane elements by dove tail connections as shown in Fig 4.2.1 where an example of a two-layer Dou-Gon joint set is reproduced.

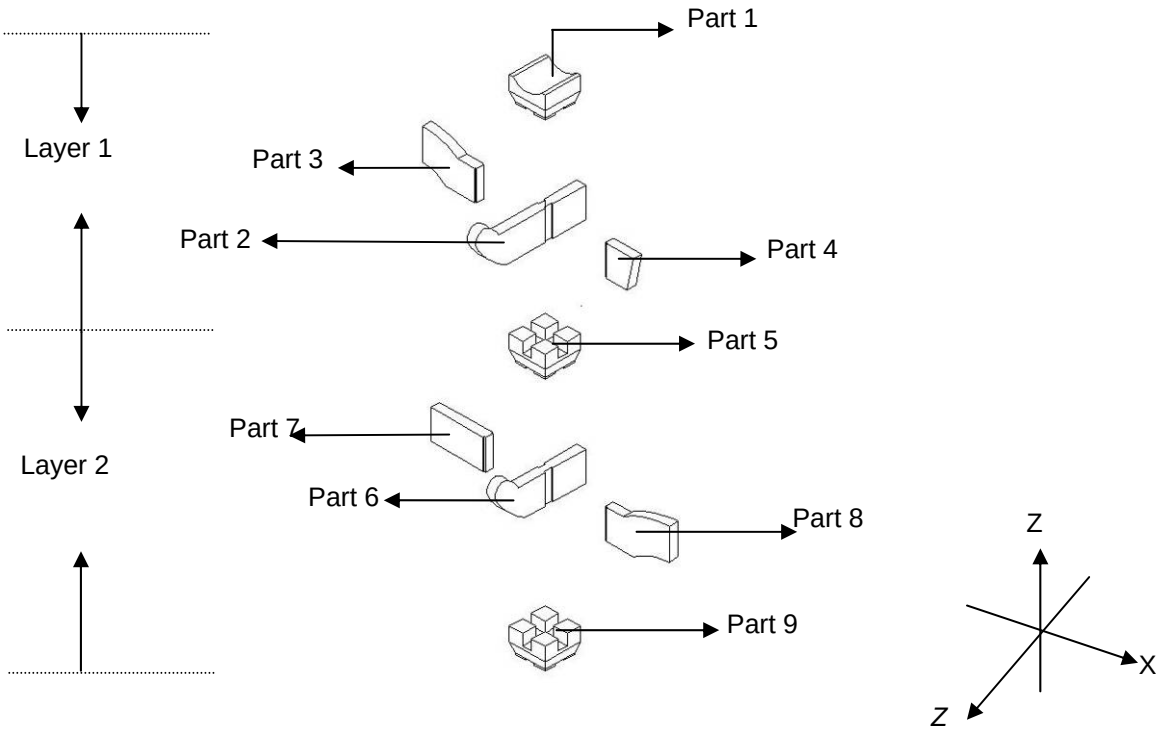

Figure 4.2.1 Two layers of a Dieh-Dou joint

As seen in the brief description in Chapter 2 a bracket set can have two or three layers according to its position along the height of the in-plane frame. Each layer consists of cross shaped cubic pieces, the Dou (parts 1, 5 and 9), continuous out-of-plane brackets (parts 2 and 6), that help to transfer the vertical loads from the purlins into the bracket set, and discontinuous in-plane beams (parts 3, 4, 7 and 8), which connect adjacent bracket sets and columns and form the in-plane (X-Z plane in Fig. 4.2.1) frame of the Dieh-Dou building.

In the experimental campaign, one full scale layer of Dieh-Dou set was reproduced (see Figure 4.2.2), and a series of test was performed to study the behaviour of such joint. One joint layer is comprised of Part 5, the Dou, Part 6, the out of plane continuous bracket, and Part 7 and 8, the in plane beams that connect the other bracket sets to the column. A second Dou, Part 9, is used to keep in plane and out of plane beams in position.

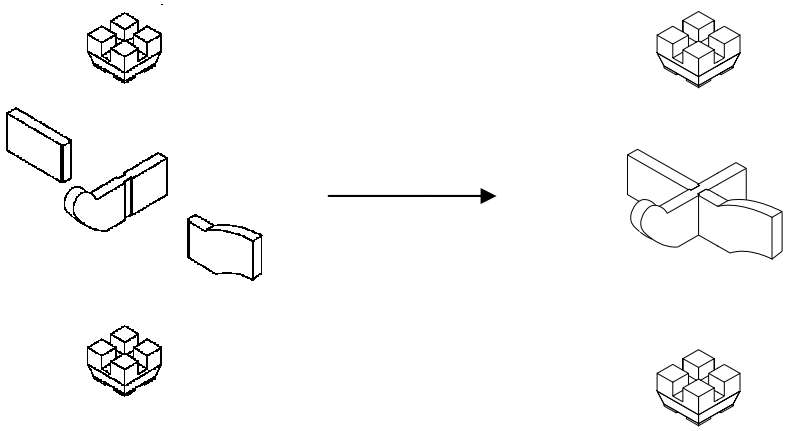

Figure 4.2.2 Construction of one layer of a Dieh-Dou joint

The in-plane beams, whose carving at the face end is often not properly done, so that they can sometimes be considered as just in contact with the out-of-plane elements (see Fig. 4.2.2), are the major concern in an accurate modelling of the structure using finite elements for the evaluation of its failure behaviour. From the survey of these structures after earthquake, it is clear that most of these in-plane elements suffered excessive rotations or were pulled out from their original positions, in some cases leading to the collapse of the frame.

To investigate the proportion of structures to determine there was standardization within Dieh-Dou buildings, Lee (2007) collected 24 “three main beams and five Dieh-Dou sets, 3-5 Type” (see Chapter 2) Dieh-Dou buildings from investigation drawing sources and found out that a high degree of similar proportioning existed.

Lee (2007) concluded that the construction of the two-sloped roof Dieh-Dou buildings always respects certain proportions in relations to the central space of the frame. Although details of joint dimensions were not included that the geometry of Dieh-Dou buildings elements is shown to be constrained around some average sizes with small variation. So the assumption of an average size for the test specimen was made following these findings, which would render results directly representative of the majority of real buildings without losing in accuracy.

Huang et al. (2003) recorded one Dieh-Dou dismantled frame during construction and pointed out that in this frame that the upper Dou (Part 5) are slightly smaller than lower ones (Part 9). For example the “a” dimension (see Fig. 4.2.3) for the upper ones is 230 to 240 mm while for the lower ones is 250 to 260 mm. Chao

(2004) recorded the dimension of San-Chun Dian temple Dous and found a value of 235 mm for “a”. From field survey and record drawings, a minimum value of 200 mm was found in all cases. Thus, as 200 to 250 mm is the range of dimensions of the Dou, an average value of 225 mm was chosen. In the Dieh-Dou building, the shape of Dou is normally square, but in some cases is octagonal; in the tests, the Dou was assumed as square for simplicity (see Fig. 4.2.4 and 4.2.5).

Because only one layer was considered, the height of upper Dou (Part 5 in Fig 4.2.3) was reduced and its upper surface was cut flat to accommodate the load jack, see Fig 4.2.4. Also, the bottom of Part 9 was flattened (Figure 4.2.5).

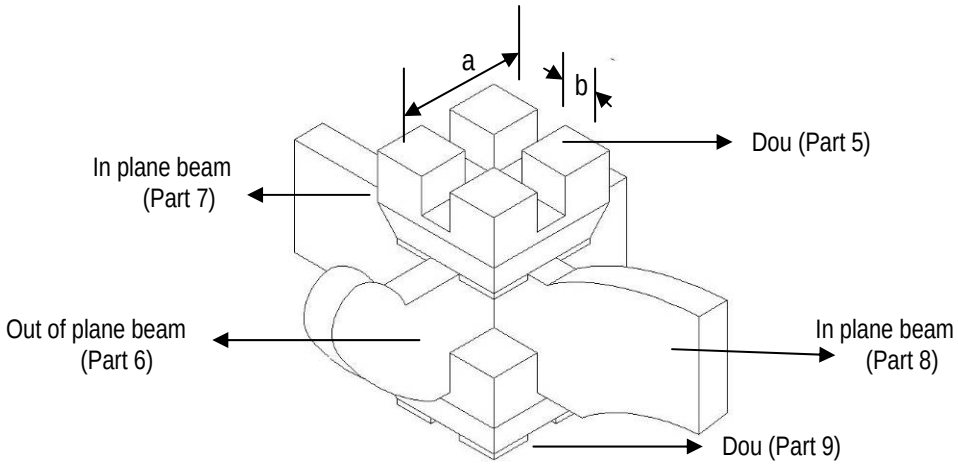

Figure 4.2.3 One layer of joint

In Dieh-Dou frames, the horizontal beam elements (main beams, binding beams and out of plane brackets) may differ in depth and width. However, the ends of these beam elements are always trimmed thin to fit in the notch of the Dou (Chapter 2); therefore, here only the dimension of the end part of beam (fitting in the joint) was considered. The average width of the notch of Dou is 60 mm, so this value was used for the test beams (Part 6, 7 and 8). The depth of beam was obtained from the average value of various survey drawings, being equal to 170 mm (see Fig.4.2.6 and 4.2.7). The dove-tail proportions were also taken from the available survey drawings.

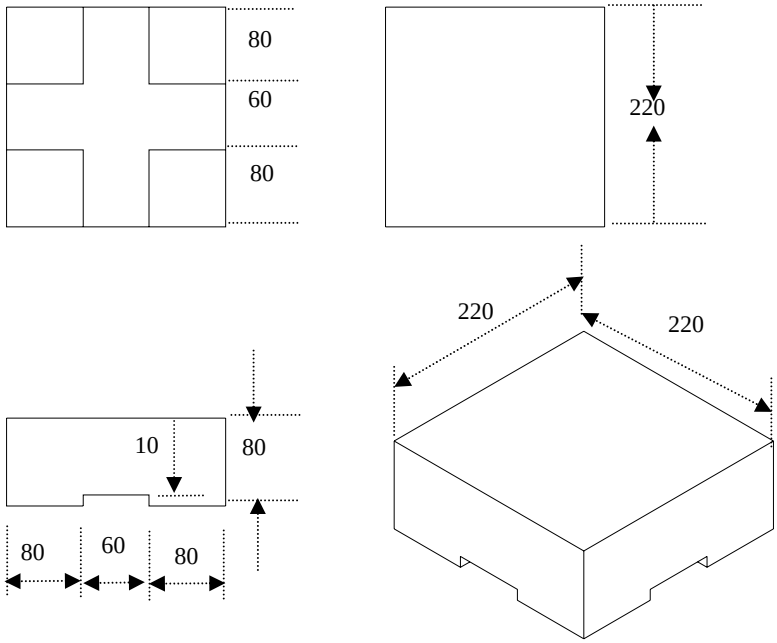

Figure 4.2.4 Test specimen dimensions of Part 5 (in mm)

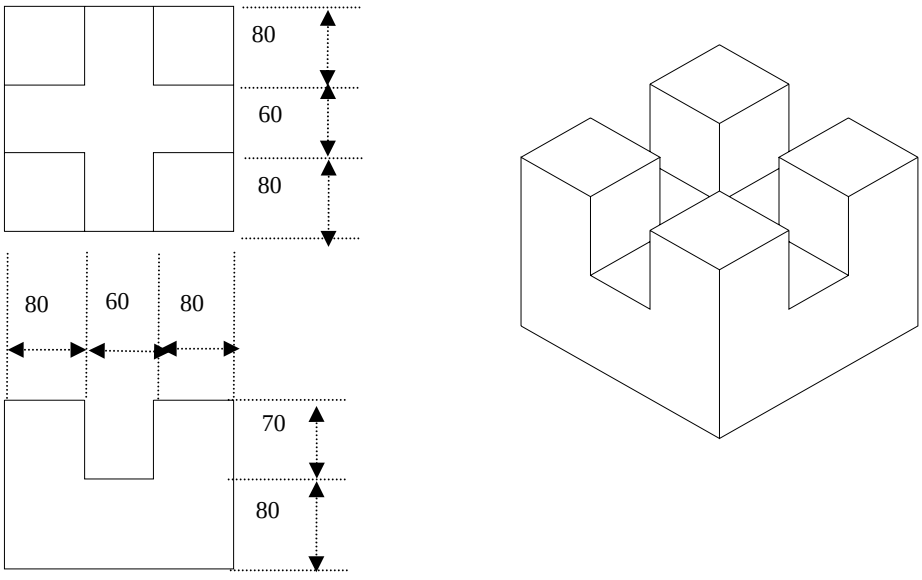

Figure 4.2.5 Test specimen dimensions of Part 9 (in mm)

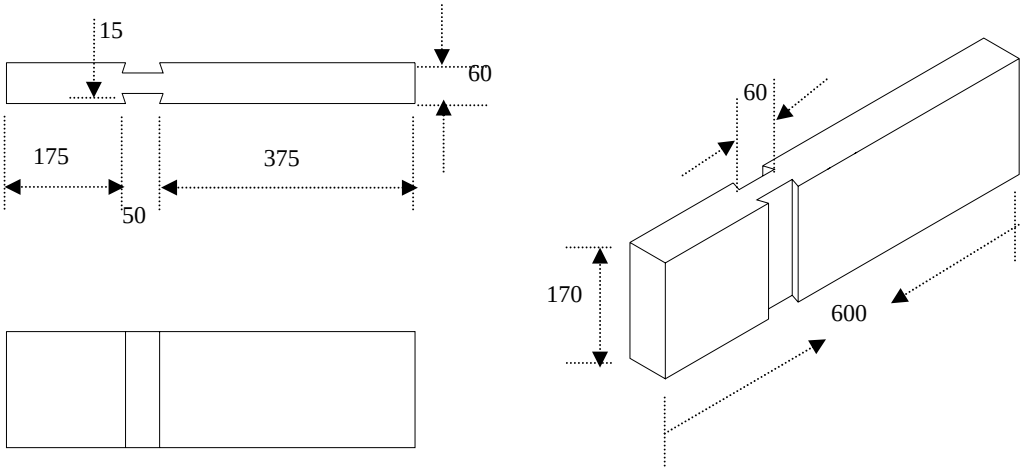

Figure 4.2.6 Test specimen dimensions of Part 6 (in mm)

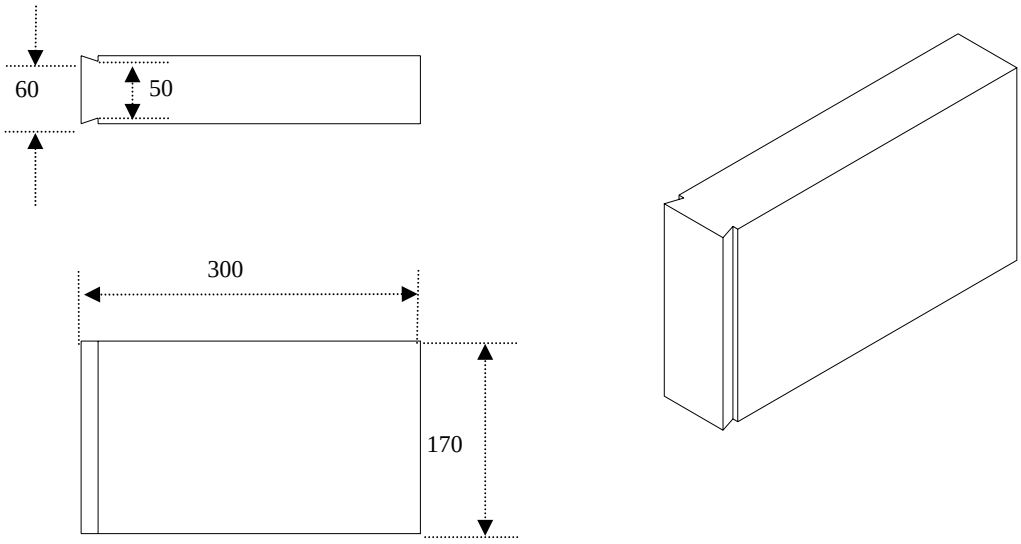

Figure 4.2.7 Test specimen dimensions of Part 7 and 8 (in mm)

4.2.2 Material tests

Tsai (1997) and Chang (2006) inspected wooden material of historic buildings on site and concluded that softwood was the most widely used and more than 80% was cedar.

Considering the timber pieces that will be used in the tests, the historic nature of the buildings and the high architectural and sculptural value associated with each component of the Dou-Gon and with their painting, to use joints directly extracted from existing frames was simply unattainable. Furthermore, there would have been high associated costs of transport to obtain cedar from Taiwan or other Asian areas.

The U.S. Wood Handbook (1999) defines the typical properties of many kinds of species. The Modulus of elasticity of dry Cedar (including different type of cedars) is in the range of 5500 to 7200 MPa, with an average of 6400 MPa. An aged pine wood was sourced from the components of a 200 year old roof, constituting the roof of a dismantled church in the UK southwest region. After laboratory testing, the Modulus of Elasticity of this pine wood was found to be 6500 MPa, and as such it was considered apt to represent Dieh-Dou frame joint in terms of material properties.

Before constructing the joint test specimens, small material specimens were prepared according to BS EN 408 and ASTM D198 standards to determine the other material properties. Figure.4.2.8 shows the static bending test (for MOE) and Figure 4.2.9 shows the results of compression test perpendicular to grain. The timber had a moisture content of 10% and average weight density of 400 kgf/m^3.

Figure.4.2.8 Static bending test (MOE)

Figure.4.2.9 Compression perpendicular to grain

Table 4.2.1 shows comparison of the material properties (parallel to grain) of test specimens and the average values from US Wood Hand Book. The results are very close apart from the compressive strength parallel to grain. In the literature, the compressive strength parallel to grain of Cedar can vary from 27 to 41 MPa for 12% MC wood and from 13.7 to 24 MPa for green wood, thus the 20 MPa of test

specimen is still reasonable although a bit lower than average. Tension strength perpendicular to grain was found equal to 1468 kPa in the test, while in the wood hand book is 1500 kPa. The Taiwanese code for timber design (2008) gives only the values of the permissible stresses which are two to three times lower that the test results; this is in line with the value of the safety factors implicitly included in the allowable stress provisions.

Table 4.2.1: Material properties (parallel to grain)

	Specific density (Kg/m^3)	MOE parallel to grain (MPa)	Compressive strength parallel to grain (MPa)	Static bending: fibre stress at proportional limit (MPa)
Test specimen	400	6500	20	46
Cedar (US. Wood Hand Book)	330	6400	32	47

The material characterisation shows that the choice of aged pine used to represent the Dieh-Dou joints is suitable to match the real values and is reasonably accurate for stiffness analysis. It will be shown in Chapters 6 and 7 that material ruptures are highly unlikely to occur in Die-Dou buildings as the stress levels are usually well below the strength limit.

4.3 Rotational tests

4.3.1 Test device and setting

A test programme is performed on a series of full-scale models where the aforementioned bracket set is reproduced and tested in a laboratory with the loading arrangement shown in Figure. 4.3.1.

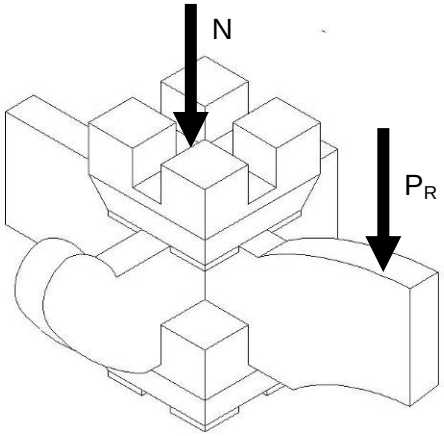

Figure 4.3.1 Loads applied for the rotational tests

The magnitude of the vertical load N is kept constant during each test while a vertical load (P_R) is increased incrementally up until failure, in order to evaluate the M-θ curve (and so the rotational stiffness K_R) for the beam under examination. Given the great similarity between the dimensions of the cross-sections of all these in-plane beam members in one Dieh-Dou frame, it is believed to be sufficient to test one typical specimen and apply the results to the other beams; as mentioned previously, from on-site survey and reference source is found that the ends of the beams are usually cut to 1 size to fit in the Dou-Gon set.

The vertical loads N represent the weight of the roof and of the elements above the joints. Fig. 4.3.2 shows the out of plane timber frame. The purlins that lay out-of-plane transfer the weight of the roof to the joint set. As seen from the figure, each layer has a different value of vertical load applied (N_1,N_2 and N_3). Considering the failure mode and construction features of Dou-Gon joint set, a different magnitude of vertical load (N) can affect the rotation capacity of the joint set.

Thus, it is decided to perform the test regime described above for two values of the vertical loads N. The weight of roof is calculated with reference to Chao (2004) from a building survey, while the self weight of timber is taken from the test (Table 4.2.1) as equal to 400 kg/m^3. A range of span lengths, purlins spacing and roof weights were observed in the survey of existing Dieh-Dou buildings as confirmed by Lee (2007) and used to determine an upper and lower bound value. The maximum load

is found being about 6.5kN and the minimum can be almost halved, so 3.25kN and 6.5kN are selected for the test program.

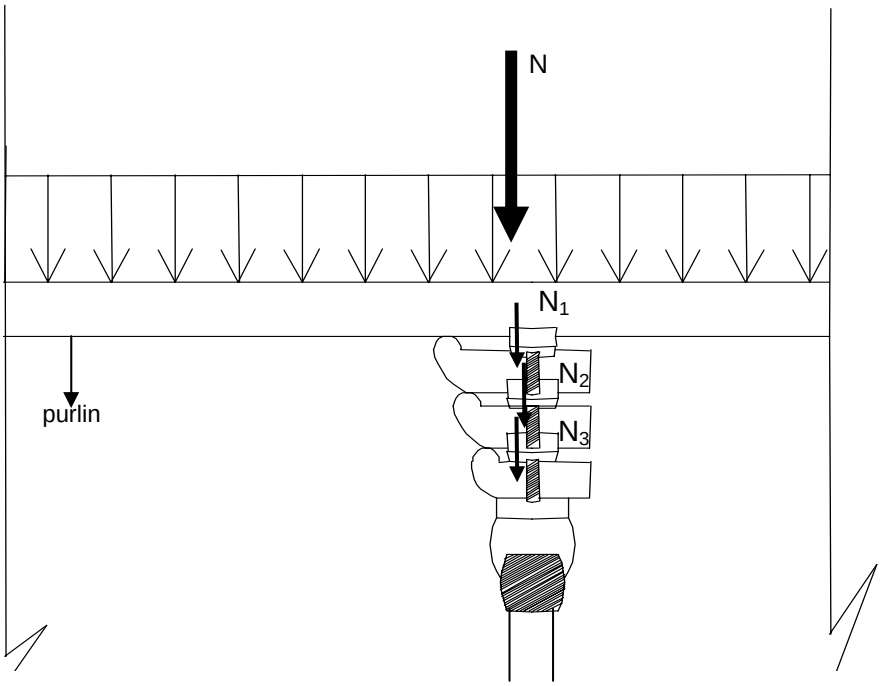

Figure 4.3.2 Loading of Dieh-Dou building (out-of-plane)

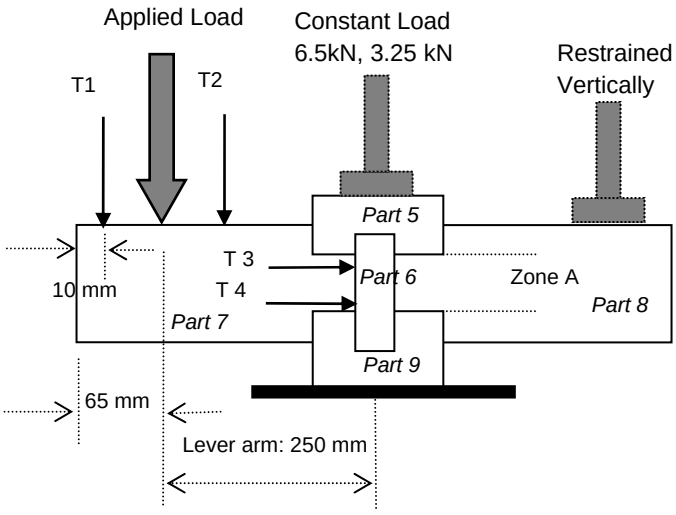

Figure 4.3.3 Test apparatus and applied jacks

Constant loads of 6.5kN (to represent as highly compressed set) and 3.25kN (representing a less compressed set) were applied to the upper Dou. Test RUL01 and RUL02 refer to the first load level, test RLL03 and RLL04 to the second. A restraining jack was positioned above Part 8 (see Fig. 4.3.3) to prevent the joint from rotating upwards during testing. In the real building, the other end of this beam (Part 8) is restrained by the other Dieh-Dou set. The pressure at this jack is monitored by a load cell.

A steel cylinder was inserted between the jack and the specimen to apply the point load and two transducers were fitted to Part 7 to record the displacements, so that the rotation of the beam under loading could be calculated. The apparatus is shown in Fig. 4.3.3. Transducers T1 and T2 were set to record the displacement of Part 7, while T3 and T4 allowed to measure the relative movement of Part 7 and Part 6 (see Fig 4.3.4).

4.3.2 Test results

Transducers T1 and T2 were used to measure the displacements of the timber beam under loading. The difference of vertical displacement between transducer 1 and 2, divided by their distance, provides a measure of the relative rotation of Part 7 to Part 6. The moment is calculated taking a lever arm from the centre of the load cell jack to the centre of the joint. The rotation and moment measurement are shown in Fig. 4.3.4. The moment-rotation relationship for tests 1 and 2 are shown in Figs. 4.3.5 and 4.3.6.

The rotational stiffness in the elastic range in tests RUL01 and RUL02, K_1, resulted 4.00E+4 and 4.09E+4 Nm/rad, respectively (see Fig. 4.3.5), with an average value of 4.045E4 Nm/rad. In tests RLL03 and RLL04 (see Fig. 4.3.6), where only 3.25 kN were applied on Part 5, stiffness K_2 are equal to 2.3E+4 and 2.5E+4 N*m/rad respectively, with an average value of 2.4E4 N*m/rad. In both set of tests the maximum moment associated with the linear behaviour was approximately 1000 Nm, while a nonlinear behaviour comprising an ascending and descending branch in the first case and a flat and descending branch in the second case were identified after this point.

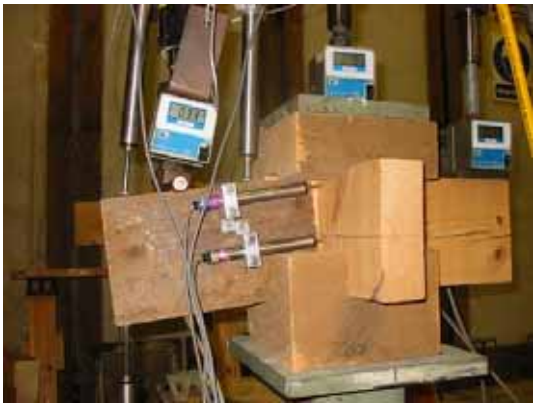

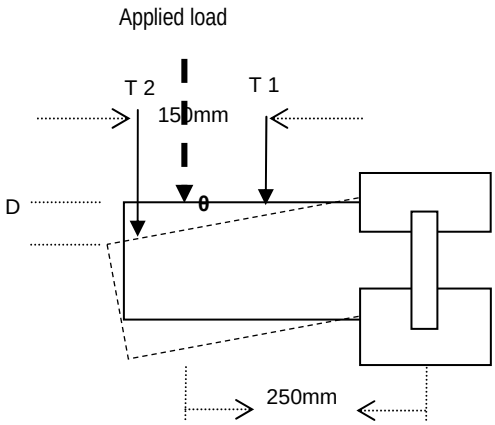

$$\theta = \tan^{-1}\frac{D_{T2} - D_{T1}}{150}$$

M (N*m) = (Applied Load) x 250 (mm)

Figure 4.3.4: Rotation and moment measurement

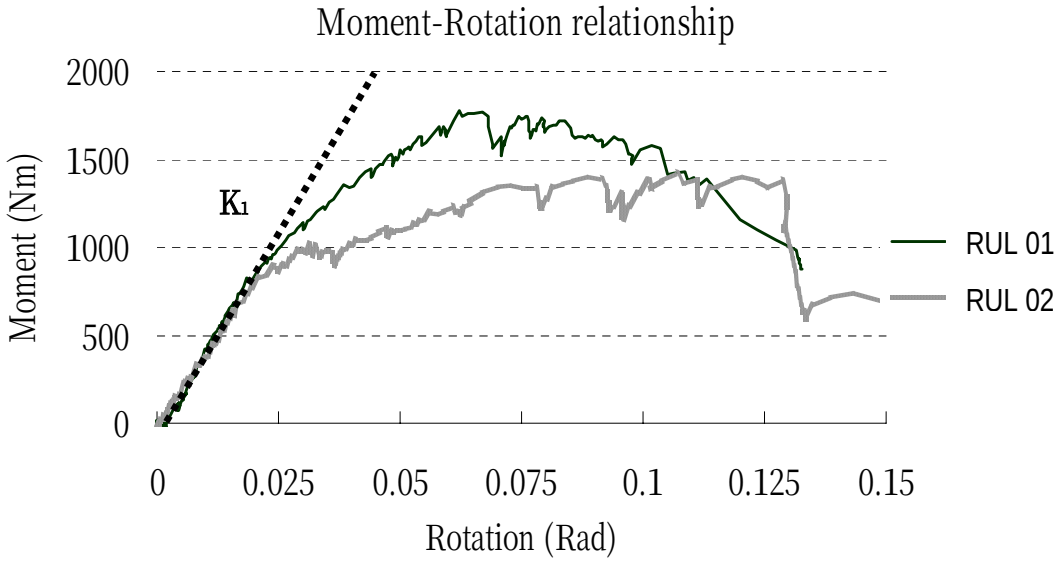

Figure 4.3.5 Moment-rotation relationship for tests RUL01 and RUL02

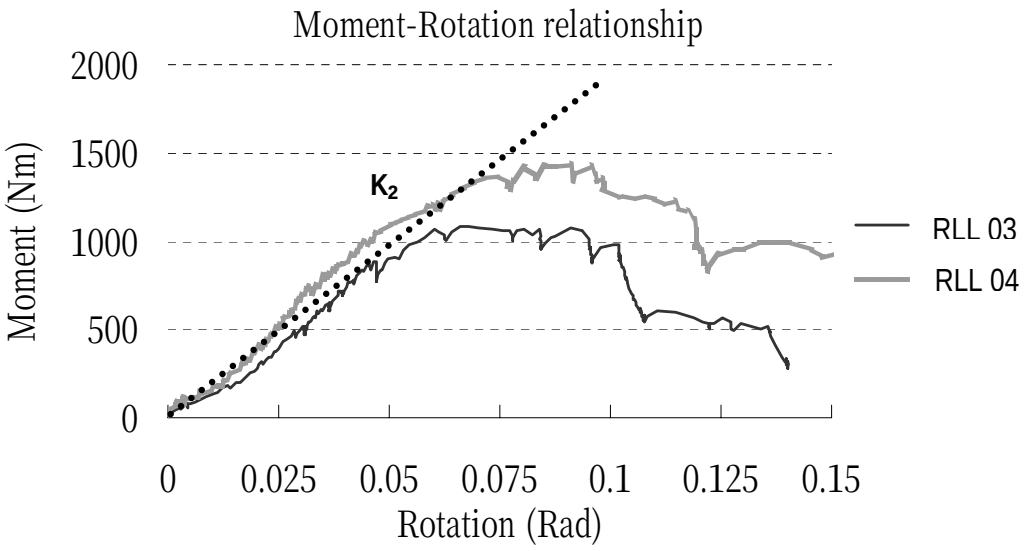

Figure 4.3.6 Moment-rotation relationship of test RLL03 and test RLL04

In tests RUL01 and RUL02 there is a sudden reduction of stiffness beyond the elastic limit. When a lower level of vertical load is applied (tests RLL03 and RLL04) the capacity at the end of the linear branch is similar to the previous tests but is reached for a higher deformation of the joint (0.05 radians versus 0.025) showing that in this case the stiffness in the linear stage is lower. A total maximum rotation of 0.125 radians was achieved at failure in all cases, with final failure due to the ripping off of the dove tail edges.

The values obtained from test results, although they cannot be considered to have a statistical significance for the various softwood species and timber conditions, can be used in the FE model for analysing the structural behaviour of Dieh-Dou buildings with acceptable approximation.

4.3.3 Mechanical failure

During loading two types of mechanical failures occurred. First, localized stresses occurred on the surface where the beam (Part 8) contacts with the upper Dou (Part 5). The top edge of beam was crushed due to the upper Dou providing restraint to the beam movement. Figure 4.3.7 shows the crushed fibres of top edge of beam

and Figure 4.3.8 shows a view from top, where the crushed part of the beam is shown and a vertical crack is highlighted.

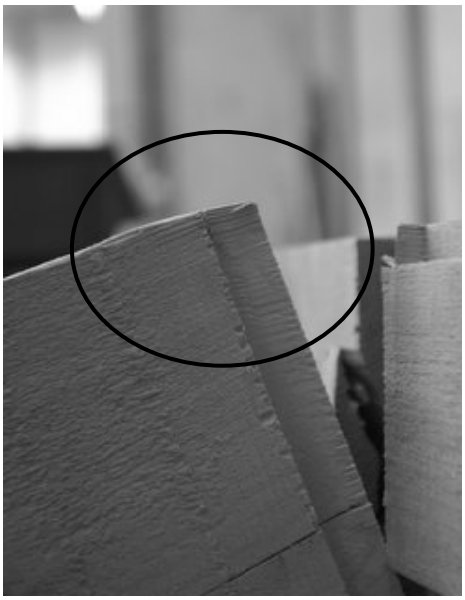

Figure 4.3.7 Crushing of top edge of beam

Figure 4.3.8 Crack highlighted by pen mark

Since the beam (Part 8) has deformed downward under jack loading, local deformation occurred in the lower part of the joint in contact with the lower Dou (Part 9), see Figure 4.3.9. However, as the in plane beam (Part 8) has a dove-tail connection with the continuous out of plane beam (Part 6, see Figure 4.2.6), a second type of failure occurred involving the ripping off of the dove-tail as the upper part of the beam tended to pull-out.

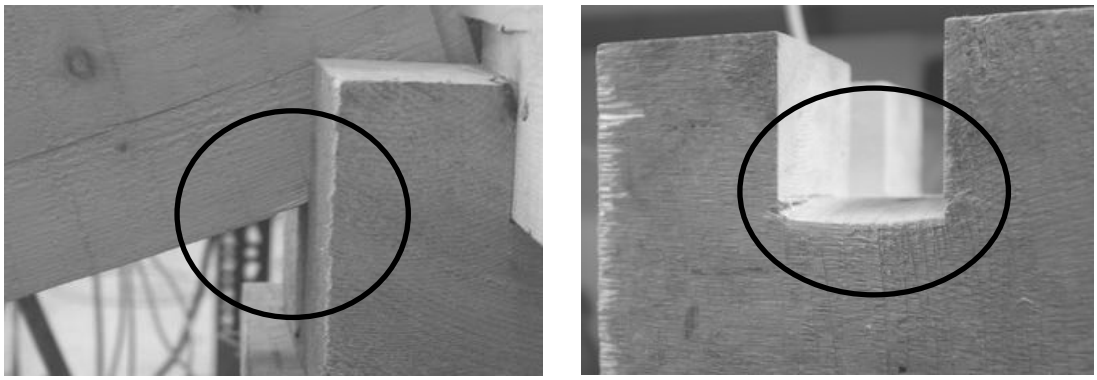

Figure 4.3.9 Local deformation of beam (Part 8) and lower Dou (Part 9)

The failure of dove-tail joint developed mostly on Part 6 (Fig.4.3.10). As the construction details of the joint set show, the upper and lower parts of the out of plane beam (Part 6) are restrained by the upper and lower Dou, whereas the middle part is not in contact with any timber element so this area becomes a zone weaker than the other parts in terms of pull-out resistance.

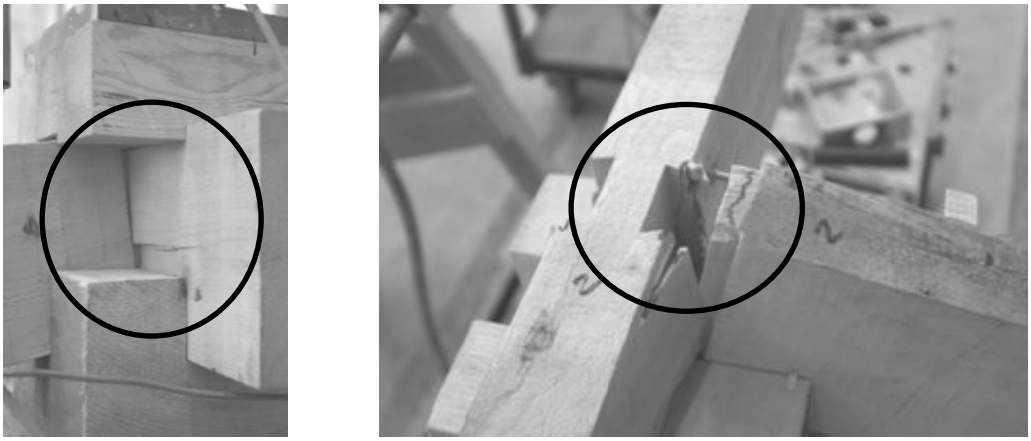

Figure 4.3.10 Failure of Dove tail joint

Figure 4.3.11 shows a horizontal section of a dove-tail between the in plane (Part 8) and out of plane beams (Part 9), where compression and tension stresses develop on the contact surfaces. In the physical test, see Figure 4.3.12, the tensile capacity of the fibres in the dove-tail of the out of plane beam (Part 6), where the stress is perpendicular to the grains, was exceeded and this initiated the failure mechanism. In the material tests discussed in the previous section it has been found that that tension strength perpendicular to grain is only 1.5MPa, confirming that the dove-tails subjected to tension are the weakest part of the joint.

In a related project, Lewis (2006) created two distinct 2-D FE models to simulate these two types of failures using shell elements of unit thickness in the vertical and horizontal plane respectively. The results of these two FE model highlighted the weak point of the joints and a check over the stresses when the failure load was applied confirmed that such elements were over the Tresca failure criterion. However, as the mechanisms of failure are not decoupled in reality but are combined, it is difficult to predict the failure load from a relatively simplified analysis that separates the effects.

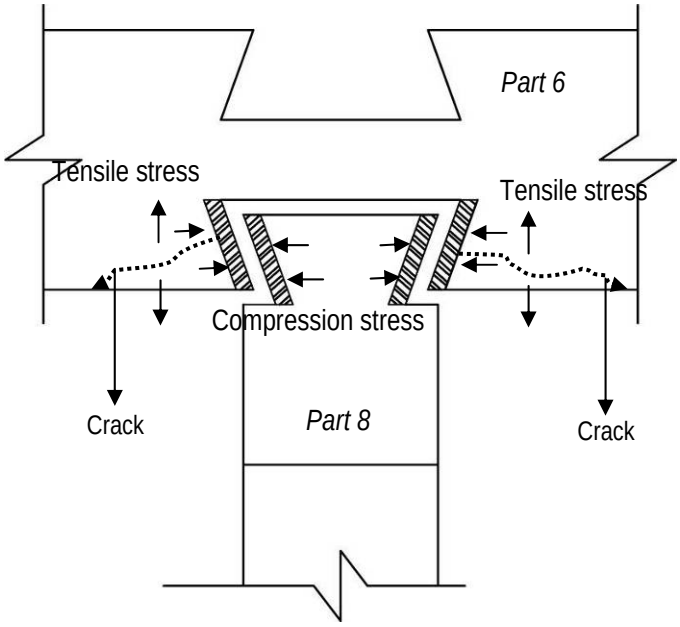

Figure 4.3.11: Stresses in the dove-tail joint

The mechanical failure observation confirmed that the rotational capacity of the joint depends on the level of load above upper Dou which governs the first type of failure, that occurs at the end of the linear branch, while the presence of the dove tail in the out plane and in plane beams governs the second part of failure and therefore the maximum joint ductility.

4.4 Translational tests

4.4.1 Test device and setting

The dimensions of the test specimens are the same as for the rotational tests. Two levels of vertical force, 6.5 and 3.25 kN were applied vertically as in previous tests, but this time the applied force was a pull-out horizontal force in the in-plane beam (Part 8). Figures 4.4.1 and 4.4.2 show the setting of pull out test.

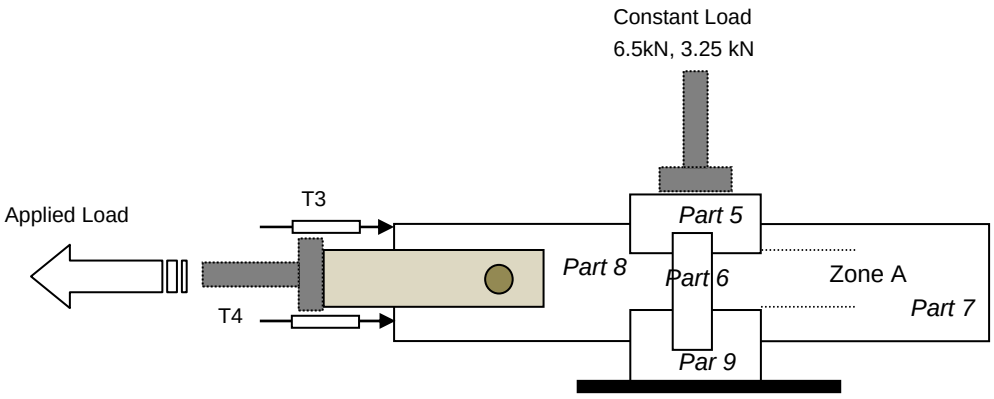

Figure 4.4.1 Test apparatus and applied jacks

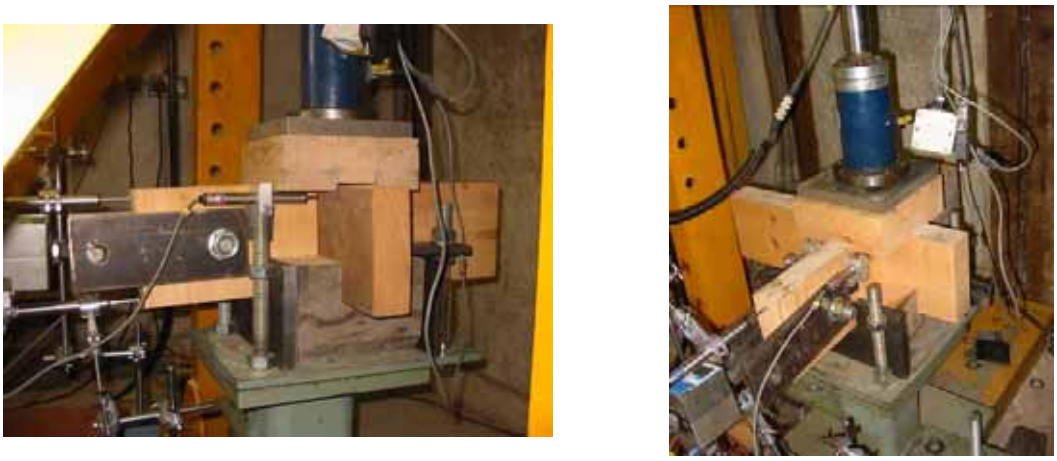

Figure 4.4.2 Photos of pull out set

The load to the in-plane beam was applied through a steel pin inserted in a hole drilled at beam mid-height, connected to the jack via two steel plates. Two additional transducers (T3 and T4 on Figure 4.4.1) were fitted on the end of the beam to measure the translation under loading, see Figure 4.4.2.

4.4.2 Test results

A 3.25kN vertical load was applied on tests PO01 and PO02, while tests PO03 and PO04 had a vertical load of 6.5kN, for the reasons discussed above. Transducers

T3 and T4 measured the displacement of beam (Part 8) under loading and these values against the pull out force were plotted on Figure 4.4.3, which includes the results of tests POS05 and POS06 which are discussed later.

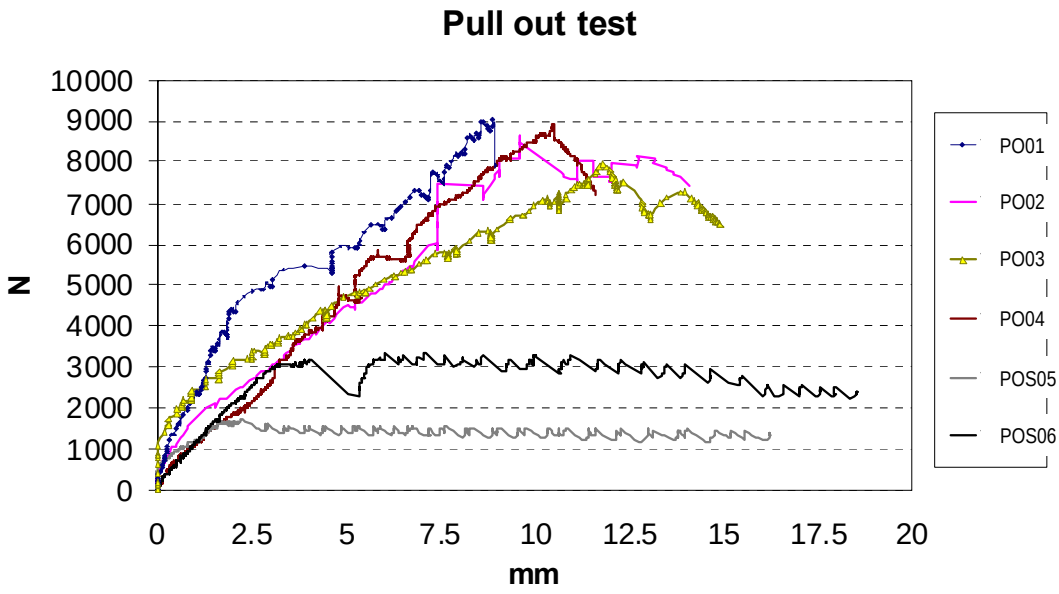

Figure 4.4.3 Results of pull out tests

The plots shows that the maximum pull out forces at failure were similar whether the vertical load was 6.5 or 3.25 kN, with a value varying between 8000 to 9000 N. The average initial axial stiffness of the joints was calculated as 1.8E3 N/mm in these four tests.

4.4.3 Mechanical failure

The failure modes of the four tests PO01 to PO04 were very similar. As can be seen from Figure 4.4.4 (left), the areas B of the out of plane beam (Part 6) were initially restrained by the upper and lower Dou, Part 5 and Part 9. When Part 8 starts pulling out, the unconfined area of Part 6 (A in Figure 4.4.1 and 4.4.4) started to crack and deflect. Once timber strength was overcome the areas A ruptured and Part 8 pulled out completely from the joint (see Figure 4.4.5).

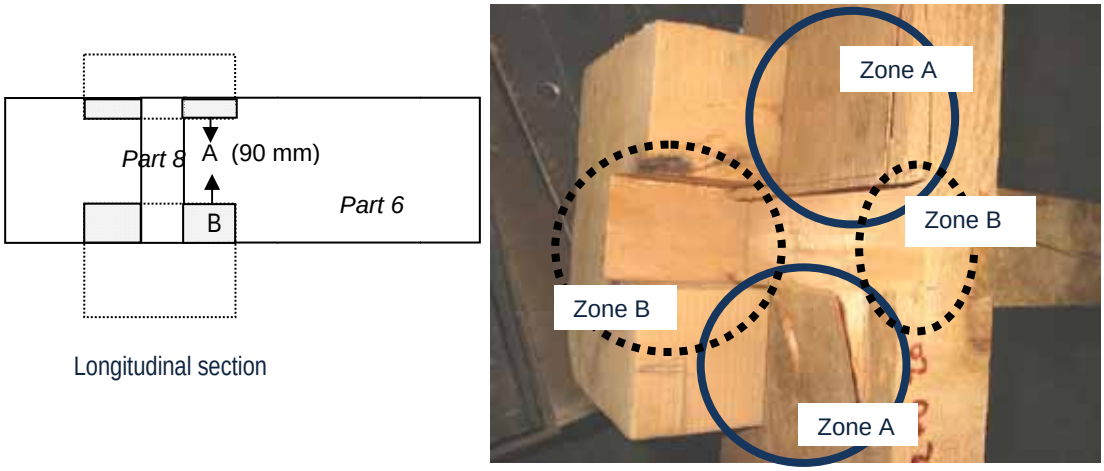

Figure 4.4.4 Pull out rupture of joint

From analysis of the ruptured pieces at failure it can be seen that the pull out failure is comprised of ruptures in both zones B and A: the dove tail tips of Part 8 sheared off at some points along the restraint offered by the Dou and the faces of the perpendicular out plane beam (part A) suffered tension failure (perpendicular to grain) and opened up allowing the in plane element (Part 8) to move out of position.

The ruptured area of Part 6 was observed from the tests. In some cases the area affected by the tensional separation was clearly visible (zone A at bottom of Figure 4.4.4), in others is more difficult to measure accurately (zone A at top of Figure 4.4.4), because it is not clear the exact extent of the area that really separated from the substrate. The extent of the dove tail parts which sheared off can be measured with better accuracy.

In the specimen shown, the area of one side of Zone A being ruptured is 80x50 = 4000 mm^2. In the material tests, the tension strength perpendicular to grain was found to be an average of 1480 kPa (with the typical value of Cedar being 1500 kPa), with a minimum of 1055 kPa. This means that to tear out the area of 4000 mm^2 a force of 4000 to 5500 N is approximately needed if only direct tension applies. As the ruptured area of the other side of Zone A in Part 6 was about 120x40 = 4800 mm^2, the force needed to pull out this zone is about 5000 to 7000 N. In Part 8, the total area of the dove-tail that sheared out (Zone B) is about 70x15 = 1050mm^2. The shear strength parallel to grain has not been measured, but according to the codes for a pine with the MOE, tensional and compression

strengths of specimen is about 5000 to 5500 kPa, which would imply a failure load of about 5500 N.


1


2

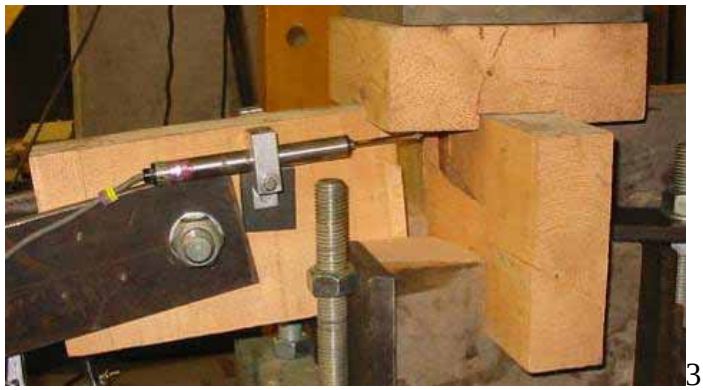
3

Figure 4.4.5 Sequence of beam pulling out and progressive failure of Part 6

If the total force needed to pull out the specimen is the sum of the forces needed to win the total resisting mechanisms, a force of about 14000-16000 N would be needed, which is higher than the 8000 N measured experimentally. However, this is strictly true if all ruptures would contribute contemporarily to the resistance, which is considered unrealistic. In particular, it is more likely that the dove tails of Part 8 (Zone B) would break first (being much more rigid) at a value of 5000 to 5500 N, after that the whole of the force needs to be resisted by the two faces (zone A) which would eventually rupture in tension allowing the beam to come out, and their total resistance in tension is 9000 to 12000 N, which is a figure quite close to what has been measured, especially considering that the tensile resistance of these faces, whose crack develop in a progressive “delamination” mode from the dove tail tip, may be lower than the experimental tensile strength measured on a specimen uniformly loaded in tension.

The assumption that Zone B breaks first cannot be confirmed as it is hard to observe the failure progression during tests as dove tail part and zone B are hidden by the timber specimen. Thus, it is difficult to assess how much is the effectiveness of the dove-tail angle in the resisting loads mechanism, i.e. to relate the load capacity to the depth of the dove tail. Compared with rotational tests, there is no local deformation occurring on the surfaces of in-plane beams in contact with the upper and lower Dou. The resistance to pull out force is provided by the dove-tail only, which explains why the pull out force is not affected by the vertical load as in the rotational tests.

As the reports of Dieh-Dou building failure show that, in fact, the dove-tail was rarely cut perfectly to fit in the joint set and in several cases the connection was flat straight without any tenon and mortise, a further series of pull out tests were performed to assess the translational resistance of a flat cut connection.

4.4.4 Straight cut joint failure tests

Tests POS05 (with vertical load 3.25kN) and POS06 (with vertical load 6.5kN), with the elements flat cut, were performed to understand how the connection behaves in the common case of a bad or non existing dove-tail connection. The setting of test is the same as previous pull out tests, but this time Parts 8 and 6 (Fig. 4.4.6) were cut straight. The result of test (pull out force versus displacement) is plotted on Figure 4.4.3.

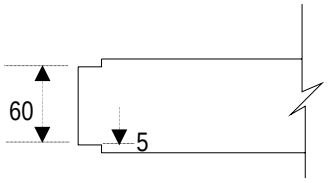

Figure 4.4.6 Joint of Part 8 in tests POS05 and POS06

The results show that in this case the friction is the critical mechanism of failure; when the vertical load is higher the resistance of the joint is higher (see Figure 4.4.3). In test POS06, with a vertical load of 6.5kN, the maximum pull out force was

3500N while in test POS05, with 3.25kN of vertical force, it was 1900N. The coefficient of static friction can be calculated dividing the horizontal pull out force by the vertical load applied, obtaining values of 0.53 and 0.58, with an average of 0.55, in line with codes predictions (which range from 0.5 to 0.6 for friction of timber to timber in dry specimens). After the maximum value was reached at the end of the elastic stage, the elements rapidly pulled out from the joint without material damage.

It can be concluded that in the real buildings, for all flat cut joints and for all cases where dove-tail joints are not made properly and their effect is conservatively disregarded, the maximum horizontal resistance depends on the vertical load applied and can be derived from a linear variation between 1900 and 3500 N according to the vertical load applied on the joint, having assumed that the friction coefficient is not affected by the applied load.

4.5 Cyclic load tests

In order to confirm the joint rotational behaviour under seismic loading, one cyclic test (RULC01) was performed and compared with the rotational static test. However, due to shortage of timber specimens, the geometry and construction of specimens was the same as for the monotonic rotational tests. The vertical load on the upper Dou was kept constant at 6.5kN. A steel device was designed to allow the in plane beam (Part 8) to move up and down following the cycles imposed by a computer controlled jack (see Fig. 4.5.1).

The cycle amplitude, in terms of vertical displacement imposed to the beam, was increased gradually; the jack forced the beam to move up and down 2.5mm for 10 times, then a series of cycles with 10 loads/unloads each followed with beam displacements of ±5, ±7.5, ±10, ±12.5, ±15 mm with an increase of 2.5 mm until failure. The joint failed at the cycle of vertical displacement equal to 25 mm. The result is shown in Figure 4.5.2.

Considering only elastic stage, disregarding the cycles at 25 mm (which degraded to irreversible behaviour and then to failure) the envelope of all cycles from 2.5 to 22.5 mm can be drawn in Figure 4.5.3 and the moment against rotation trend of this

cyclic test is shown in Figure 4.5.4. The rotational stiffness K in the positive side of the diagram (loads going downwards) equals 3.35E4 Nm/rad.

Figure 4.5.1 Cyclic test

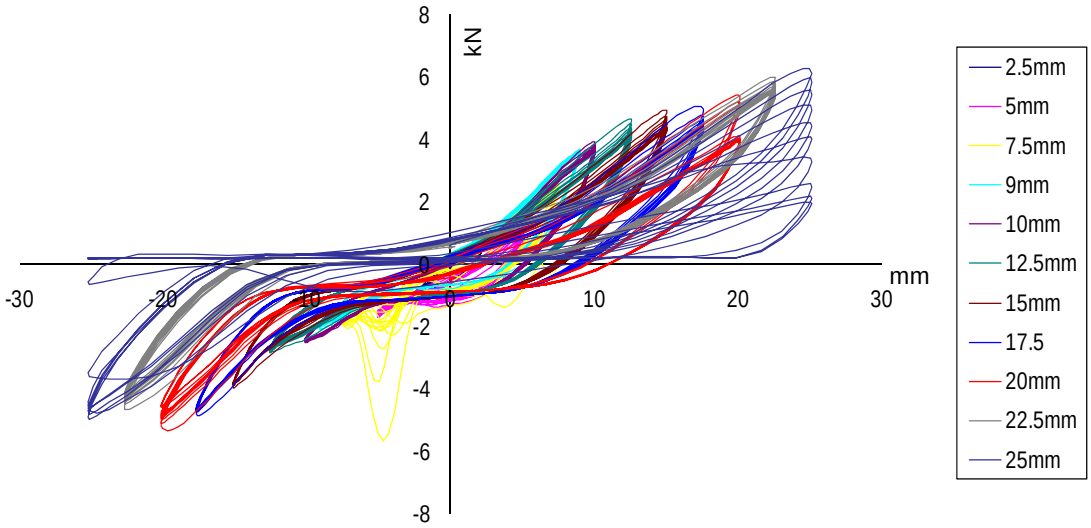

Figure 4.5.2 Load-displacement plot for the cyclic test

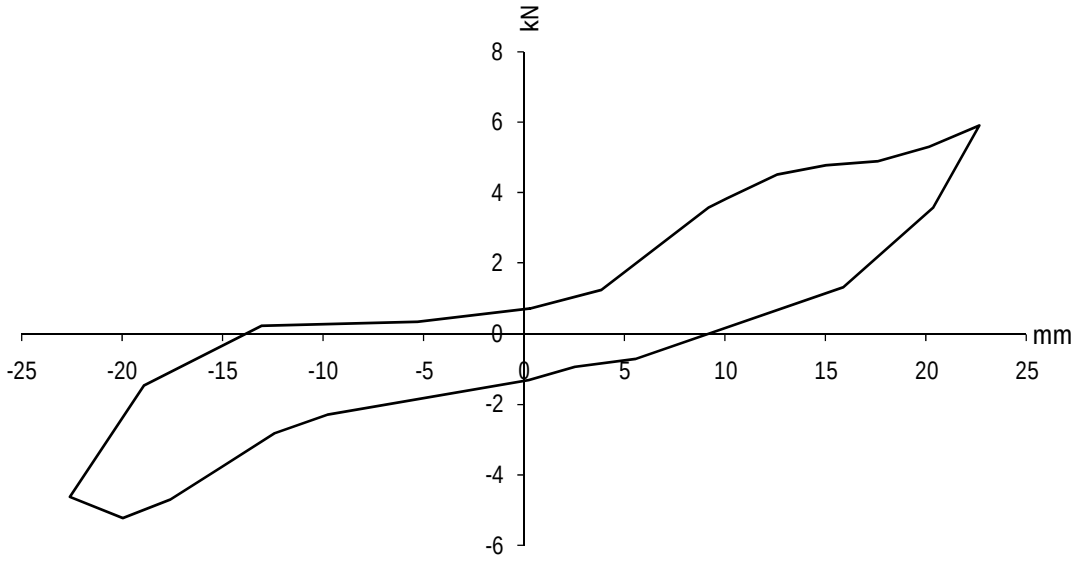

Figure 4.5.3 Envelope of load-displacement plot (cycles 2.5 to 22.5 mm)

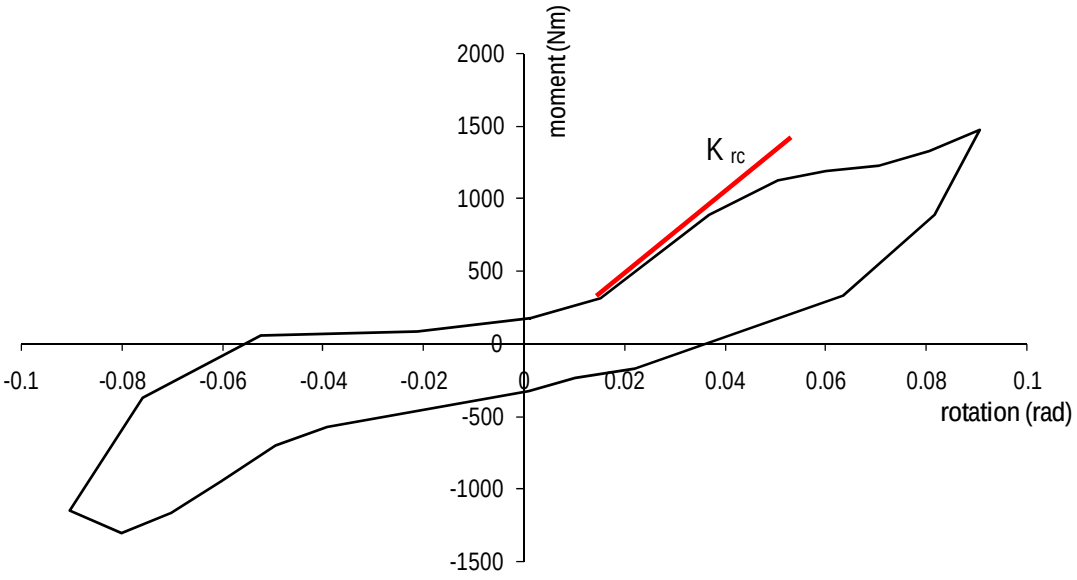

Figure 4.5.4 Envelope of moment-rotation plot (cycles 2.5 to 22.5 mm)

In the static tests the average rotational stiffness of RUL01 and RUL02 (with 6.5 kN vertical load) was 4.05E4 Nm/rad and the one of RUL03 and RUL04 (with 3.25 kN

vertical load) was 2.4E4 Nm/rad, while with the cyclic test RULC01 a value of 3.35E4 Nm/rad was obtained, which is somewhere in between the two. The moment capacity and the maximum rotation of static and cyclic tests are comparable, with the cyclic test values always slightly lower. This may be caused by parts of specimen starting to damage in the early cycles weakening the capacity of the joint.

Although this was a single test and firm conclusion can not be drawn, it appears that there is sufficient correlation to reasonably confirm the static test results can be used in the FE analysis. However, in order to assess Dieh-Dou buildings in a conservative manner, it will be prudent to adopt the lower bounds of the static test results in terms of stiffness and moment capacity.

4.6 Discussion and conclusions

The rotational and translational tests performed over one layer of joint set contributed to the estimate of the rotational and translational stiffness of these joints and allowed to understand their failure mechanisms. They are representative of the whole range of joints of the existing Dieh-Dou buildings, as both the dimensions and the material properties matched very well with average of actual values, giving confidence in the applicability of the results.

The rotational tests showed that stiffness changes according to the vertical load applied on the upper Dou. Values of 4.045E+4 Nm/rad and 2.4E+4 Nm/rad were calculated as joint stiffness for vertical applied loads of 6.5 and 3.25 kN respectively, that represent the upper and lower bound of the actual loads on the joint set. The mechanism of failure involves local crushing on the top edge of the in-plane beam and upper and lower Dou and rupture of the dove tail of the out of plane continuous beam. The first mode depends on the magnitude of the vertical load, while the second one is only governed by the effectiveness of the dove-tail connection, whose contribution cannot always be relied upon. Result of the cyclic loading confirmed the values of stiffness and the moment capacity obtained by the static test. Therefore, in a conservative approach, it is considered appropriate to disregard the post-elastic behaviour of the joint and assume it failed in rotation once the elastic stage limit is reached.

For the pull out tests, it was found that if the dovetail connections are properly made, the stiffness is 1.8E+3 N/mm and the maximum pull-out force around 8000 N in all cases. The failure of the joints with proper dove-tail involves the shearing off of the male dove tail part of the in plane beams and material tensile failure perpendicular to grain. No material failure is observed when the connection is flat cut, with the behaviour being purely frictional. Compared to rotational tests, the upper and lower Dou were not damaged in the pull out tests; this can explain why the translational stiffness is not affected by the vertical load. However, in the real situation where most dove-tails are not properly made and it is prudent to conservatively disregarded them, the maximum horizontal resistance depends on the vertical load applied and can be assumed to vary linearly between 1900 and 3500N according to the actual vertical load applied.

Overall the test results were satisfactory as they allowed identifying the failure modes of joint and obtaining the minimum and maximum strength capacity and stiffness values to be relied upon. Both values of rotational and translational stiffness can be used in the finite element modelling of the whole frame and the capacities used as failure criteria to evaluate the structural safety, which will be illustrated in the following chapters. In particular, how the difference of the value of stiffness of single joints will affect the overall structural behaviour will be analysed in the following Chapter 5.

Chapter 5
Finite element model and parametric study

5.1 Introduction

5.1.1 General

The lack of structural information and the complexity of construction make it difficulty to understand the real structural behaviour of Dieh-Dou buildings. According to Spyrakos (1994) "*The use of classic methods is probably the best way to analyse simple structures; nevertheless, their use is prohibitive when the physical system is complex. In such cases the best alternative is usually a solution obtained with the finite element method*." The structural system of a Dieh-Dou building, described in Chapter 2, cannot be analysed by hand if stiffness has to be considreed. Other research work has shown that numerical analyses with FE can be successfully employed to simulate Far East timber structures under earthquake loading (Fang, 2001).

Finite element analysis method is a numerical method that is widely used to solve problems covering almost the whole spectrum of engineering analysis. Rather than considering the structure as a continuum, finite element methods view the structure as an assembly of small finite sized parts, and the behaviour of such parts and the overall structure is obtained by formulating a system of algebraic equations that can be solved with a computer. The programming techniques behind finite element analysis can be complex and their understanding is essential if an engineer is developing a finite element code to solve a particular problem. However, the objective of this project is to assess Dieh-Dou building rapidly and efficiently, and an appropriate existing finite element code is therefore chosen to meet the goal; in this case, preliminary understanding of the fundamental concepts of finite element and knowledge of the capabilities and limitations of the computer program that will be used become a matter to consider.

ISCARSAH Principles and Guidelines (2003) indicate that two kinds of actions, (i) mechanical action and (ii) physical, chemical and biological actions, can act on historic buildings. The first action produces stresses and strain on the structure, while the second action usually affects materials and reduces their strength. Although it is important to account for both actions on historic structures assessment; it is the effect of mechanical actions due to earthquake that represent the big unknown for Dieh-Dou buildings. Thus, finite element models of Dieh-Dou frames are built assuming the materials are in normal condition with no decay. Once the structural evaluation has delivered its results, it will be possible to account for material characteristic's reductions that might have been highlighted for instance by non-destructive tests, to further refine the assessment work.

Hence, the strategy of the analysis is to simulate the structural response of Dieh-Dou buildings under static and dynamic actions by using finite elements, trying to reproduce in the model, as accurately as possible, all the characteristic features of these structures, especially the joints.

5.1.2 Choice of FE software

The commercial package ALGOR © (2008), available in the department of Architecture and Civil Engineering of University of Bath, introduced finite element analysis for personal computers in 1984. ALGOR © provides tools for different aspects of structural engineering and offers various modelling features, allowing analysing stresses and displacements due to static or dynamic loading applied constantly or varying with time; effects of large deflections under these loadings can be analyzed using a variety of nonlinear material models and a large library of finite elements.

The survey reports showed that Dieh-Dou frames were prone to be damaged in the timber joints, and the semi-rigid rotational and translational features of the joints play an important role on the structure; ALGOR © provides the opportunity of modelling these connections using combinations of springs and rigid elements under both static and dynamic loading. It is believed that the capabilities of the software can simulate Dieh-Dou frames appropriately, as described in detail in 5.2.

5.1.3 The choice of single frame analysis

Chapter 2 described the features of Dieh-Dou buildings, which are comprised of two parallel timber frames connected with purlins and enclosed by masonry walls. Literature reviewed in Chapter 3 shows there is lack of research on the behaviour of Dieh-Dou buildings, especially with regards to the structural conservation. It is essential giving primary emphasis to the preservation of the main timber frames, which contains several elements of artistic and architectural value, rather than the masonry walls.

Several architectural historians pointed out that the main feature of Dieh-Dou buildings is the two main timber frames that transfer the roof load to the ground, while the masonry walls are seen mainly as an enclosure. Fang et al (2001) disregarded the enclosing masonry wall in assessing a Chinese timber tower. The two Dieh-Dou frames and masonry walls are connected with purlins which are just sitting on the top of Dou-Gon joint sets and the masonry without a positive tensile connection (Chapter 2). This construction feature may allow the timber frames and masonry to vibrate independently, as discussed and analysed later in Chapter 6, where it will be shown that the structural resistance of the elements of the frames is not substantially affected by the 3D behaviour.

Hence, the lateral stability of a Dieh-Dou frame subjected to equivalent seismic action can be initially studied assuming a frame is an independent unit in the XZ plane and is analysed separately from the rest (see Fig. 5.1.1) with in-plane loading only.

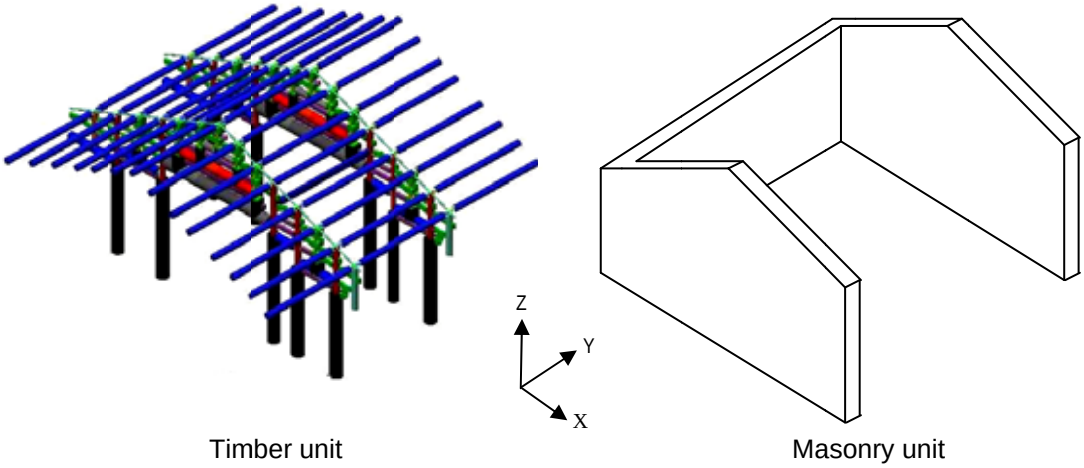

Figure 5.1.1 Timber and masonry constructions of Dieh-Dou building

5.2 Finite element model

5.2.1 Frame

Linear material model

A single Dieh-Dou frame is built on global X-Z coordinate in ALGOR, see Figure 5.2.1. The FE model is built assigning firstly a node to each support of the frame in the global coordinates, and then additional nodes are created that correspond to the centre of the connected members. More nodes are added where concentrated forces and moments are applied and also within members of variable cross-section. Once the coordinates of the nodes have been defined, beam elements are used to link nodes (Fig.5.2.1).

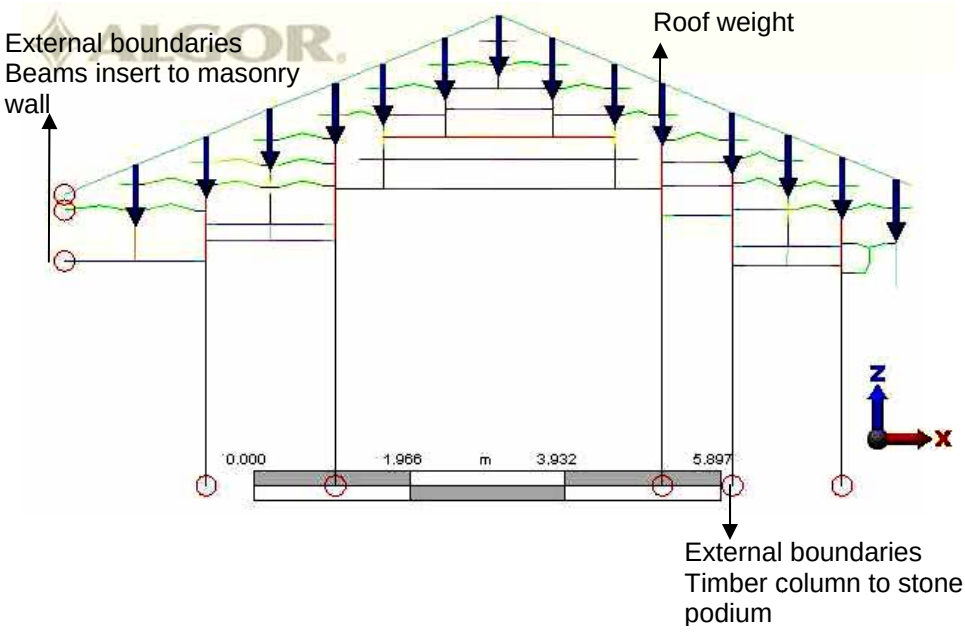

Figure 5.2.1 ALGOR model of Dieh-Dou frame

External Boundaries

(i)Column end

The boundary conditions are used in ALGOR to define the supporting point of the structure by fixing the appropriate degrees of freedom in the global coordinate system. In the Dieh-Dou frame FE model, built by beam elements, the 'Nodal

Boundary Condition' is the option for simulating the supports of frame. There are two external supports, the nodes of columns sitting on the stone podiums and those of the beams inserted into the lateral masonry walls, see Figure 5.2.1.

Figure 5.2.2 is the close up of a tenon of a timber column that would insert into the stone podium. Compared to the size of the column, the tenon is very small revealing the weakness of the joint.

Figure 5.2.2 Tenon of column

Figure 5.2.3 Rotation of column

Huang & Sheu (2001) studied the failure modes of Dieh-Dou buildings through observation after the 1999 Chi-Chi earthquake and showed that the wooden columns could easily sway (see Fig. 5.2.3, showing a frame whit no purlins on top) as they only have such a tiny joint with the stone podiums. Therefore, the joint is likely to behave almost as a spherical hinge without any rotational constraint and it is hence modelled releasing the rotational degrees of freedom (d.o.f.) of the node to ground of the columns. On the other end post-earthquake survey also shows that the tenon of the columns does not shear off, and hence it is effective in providing translational constraint between the column and the stone podium, and hence the translation d.o.f. are set to fix. In the Dieh-Dou buildings, the floor is paved by stone or brick and the stone podiums are fixed upon them. The survey shows that the podiums normally remained in position after earthquake, thus the stone podiums in FE model of Dieh-Dou frame were ignored and treated as part of the rigid support.

(ii)Joint of frame and masonry wall

The wooden elements of the frame are supported over the enclosing masonry wall without a specific connection, see Chapter 2. It is therefore assumed that the masonry wall will allow the timber beam to rotate and translate horizontally, see Figure 5.2.4. In the 2D model a “Nodal Boundary Condition Object” was hence added on the node at the end of beam with the Tx and Ry d.o.f. released and the others restrained.

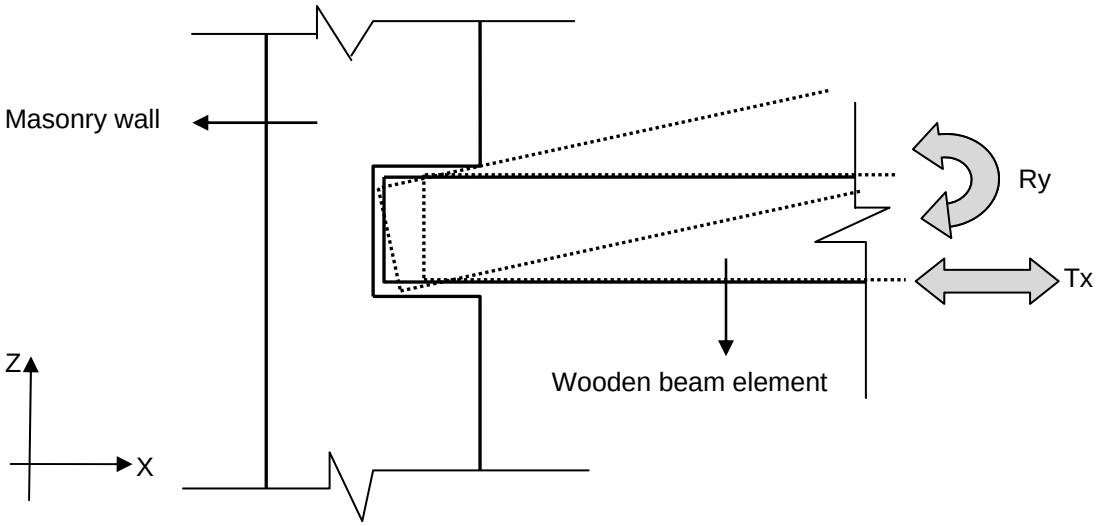

Figure 5.2.4 Beam and masonry wall connection

Vertical Load

The roof of Dieh-Dou buildings is formed by purlins, roof tiles, and roof ridge (Chapter 2), which added together form the weight of roof. The purlins are assumed having the same characteristic of other wooden element discussed in the test section of Chapter 4, with a mass of 400 kg/m^3. Chao (2004) observed the San-Chuan-Dian, a Dieh-Dou building in Tainan, during dismantling and recorded all its geometrical details. Above purlins, wooden rafters are laid perpendicularly with a 18 cm spacing between each other. Thin bricks are placed upon these wooden rafters and the roof tiles are jointed with mortar (see Figure 5.2.5).

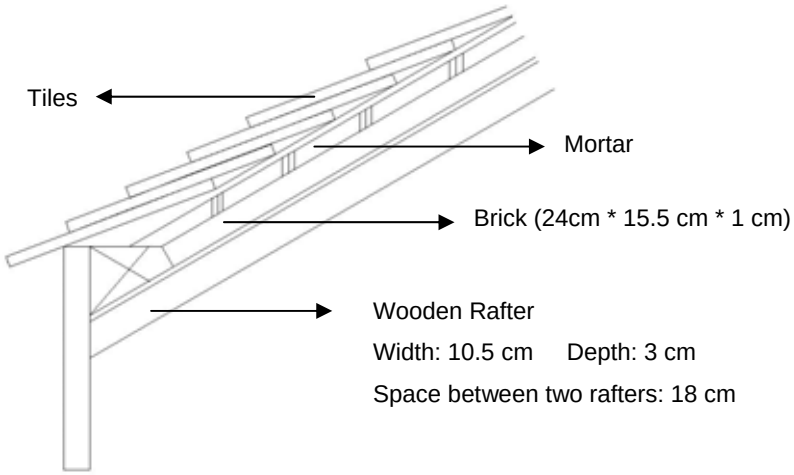

Figure 5.2.5 Typical section of roof

The surface of roof consists of two types of tiles, plate shape tiles and tube shape tiles, see Figure 5.2.6. The plate shape tiles are laid over the bricks on a mortar bed, and overlap for two thirds of the length. Tube shape tiles then cover the space between two rows of plate shape tiles. The tiles are set in mortar. According to Chao (2004), the specific weight of these bricks and tiles is about 1900 kg/m^3, while the wooden rafters are 390 kg/m^3. Chao (2004) calculated the weight of roof cladding (including wooden rafters, bricks, mortars, tube and plate shape tiles) of San-Chuan-Dian on site, and concluded that the average weight was 80 kg/m^2.

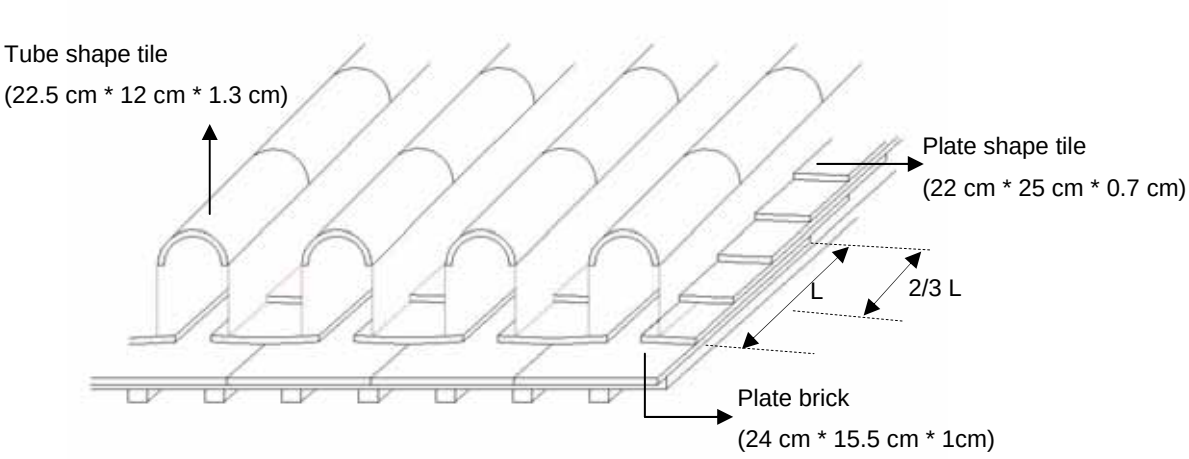

Figure 5.2.6: Roof cladding

Figure 5.2.7 shows an out of plane section of Dieh-Dou building, where “D” and “F” represent the distance of Dieh-Dou frames to the walls and “E” defines the spacing of the two frames (Fig. 5.1.1). Although frame and masonry wall might have different vertical stiffness, it was decided, in favour of safety, to redistribute equally the weight of roof cladding above “D” and “F” between masonry wall and Dieh-Dou frame, while the roof weight in “E” is shared between the two frames.

One significant feature of Dieh-Dou buildings’ roof is the ridge, which complete the building with its unique Asian style shape and beautiful decorations, see Chapter 2. According to Chao (2004), the average weight of the whole of the roof ridge of San-Chuan-Dian is about 430 kg/m, and only acts on the apex purlin.

The total vertical load is finally applied as a point load to each purlin connection location, see Fig 5.2.1.

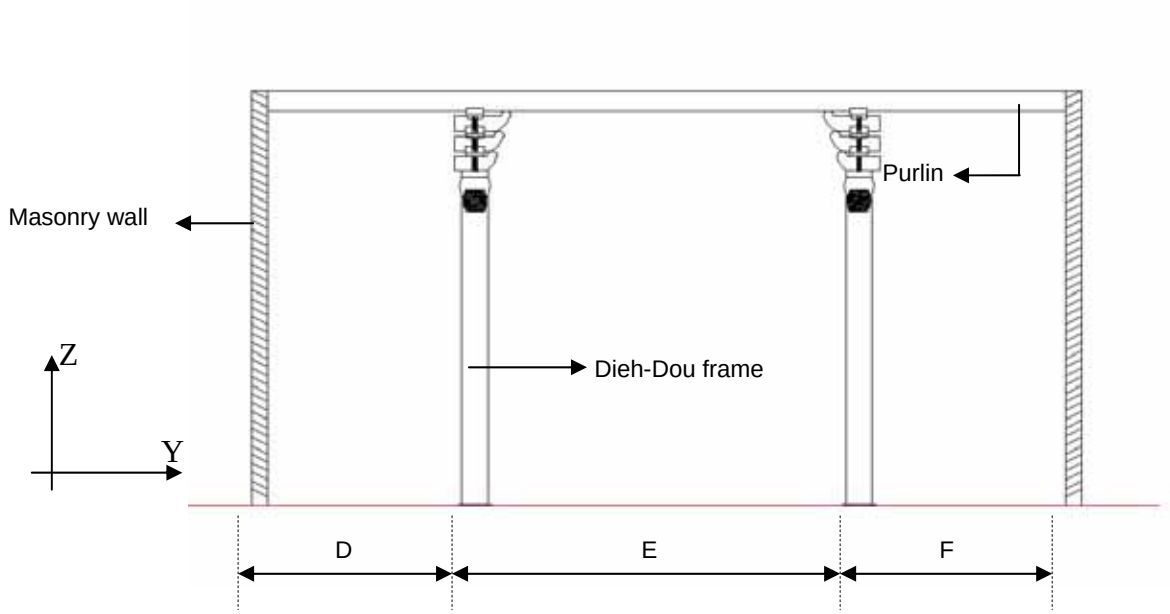

Figure 5.2.7 Building out of plane section

5.2.2 Beam Elements

Although there may be advantages in the use of area or volume elements, which can provide more information compared to line elements (beam or truss element), the Dieh-Dou frames, as described in Chapters 2 and 3, are prone to fail by global failures of the linear elements and their connections rather than localized material

damage, making the choice of using beam elements a rational one. Also, the goal of finite elements analysis in this work is to examine the overall behaviour and vulnerability under earthquake of the frame and provide a quick and easy method to identify the weak parts of structure, not an in-depth of the failure mechanism of one particular detail. Consequently, considering that most elements in the frame have either a predominantly flexural or axial behaviour, and that for most of them one dimension is almost one order of magnitude bigger than the other 2, beam elements are believed able to supply all information required to be compared with appropriate failure criteria leading to the safety evaluation of the structure.

The cross sectional area, torsional resistance, flexural moment of inertia, section modulus and shear area are defined for each element and applied in the model, together with the material properties in accordance with Chapter 4.

5.2.3 Joint simulation

In the modelling of beams, the FE elements are usually defined on the neutral axis. In Dieh-Dou buildings, most members are thick, so there is the need to consider appropriate offsets from neutral axis to model them properly. Fig. 5.2.8 shows the idealized joint of beam connecting with column. There are different ways to model the offset, like inserting a very stiff element, using a rigid element or multipoint constraints (MPC) equation (Liu & Quek, 2003).

A rigid element is available in many commercial software packages, including ALGOR ©. The feature of the rigid element in ALGOR is the same as employing a MPC equation.

The concept of the MPC equation is basically the assumption that nodes A and node B are connected by a rigid body and they are enforced to follow rigid body movement. In ALGOR, a rigid element functions as a rigid body and the DOFs of its two nodes can be modified. Hence, the translation along X and rotation about Y of the rigid body can be eliminated and replaced by two spring elements to account for the translational and rotational stiffness of the joint, whose values can then be inserted accordingly.

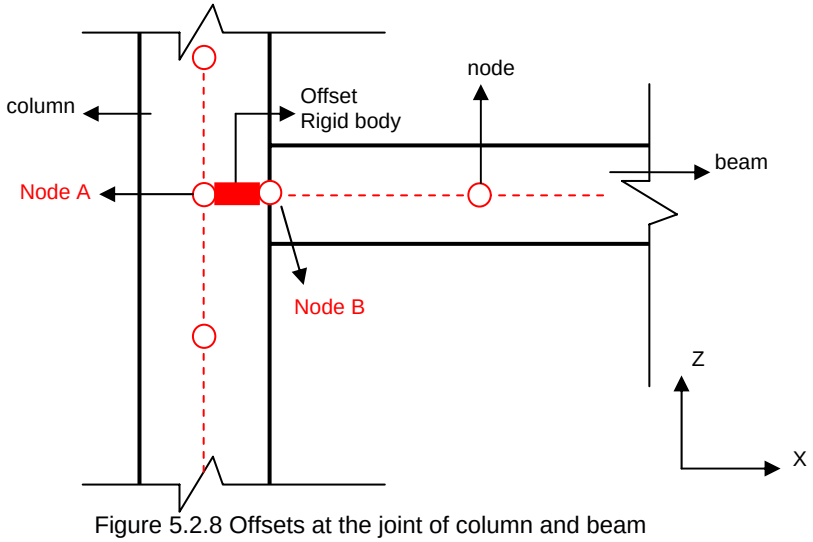

Figure 5.2.8 Offsets at the joint of column and beam

In ALGOR, a spring element is defined between two nodes and can be assigned a rotational or translational stiffness. There are two types of spring element: a spring whose stiffness is assigned in all directions and a DOF spring where the stiffness can be allocated in a specified direction in both nodes of the element. Although a spring element cannot transmit the remaining forces or moment to the next element connected, the coupling with the rigid element supplies the remaining DOFs.

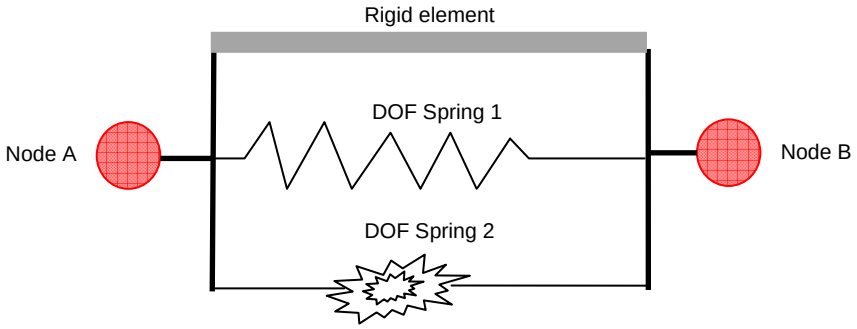

Figure 5.2.9 Joint simulation

Figure 5.2.9 depicts the Dou-Gon joint set and beam to column joints in the finite element modelling, with the rigid element and the translational and rotational stiffness elements between node A and B shown. In the rigid element, Tx and Ry are left unlocked while the other degrees of freedom are assigned the rigid stiffness value, while DOF Spring Elements 1 and 2 are assigned the appropriate

translational or rotational stiffness respectively, with units of N/m or Nm/rad as calculated in Chapter 4.

One of the advantages of using FE modelling is that it allows easy examination of all different factors which can affect the structural behaviour. From the in-situ post earthquake survey it was found that the failure modes of Dieh-Dou frames tended to involve the joints rather than material rupture in the elements; it is therefore assumed that the rotational and translational stiffness of the joints play an important role in the structural behaviour. Hence, based on the finite element model discussed above, a parametric study involving translational and rotational stiffness was performed and the results are presented in the remainder of the chapter.

5.3 Parametric study on joint stiffness

5.3.1 Modelling of the Guan-Shi family temple

The main hall of Guan-Shi family was chosen as an example to investigate the effect of joint stiffness. Main hall of Guan-Shi temple is a typical “three main beam and five Dou-Gon joint set“ type of Dieh-Dou frame. The height of the frames is 593 cm, which falls in the range of the highest built (Lee, 2007). This building is located near the epicentre of the Chi-Chi earthquake and the earthquake record station nearby (TCU076) recorded a peak ground acceleration of more than 250gal, equal to 0.25g (Hsu, 2002).

The Guan-Shi family Temple is located in Nan-Tou county, where the Chang family community established in 1894 and began to consider the construction of a family temple. Although there is no documentary evidence, the temple is believed to have been built just after 1894. In the Japanese occupation period, from 1897 to 1899, the Guan-Shi Temple compound was used as a military office. The temple was then damaged by a typhoon, after which it was rebuilt by the Chang Family in 1911. The Guan-Shi family temple compound consists of a Main hall, Front hall, Terrace and Yards (Hsu, 2002).

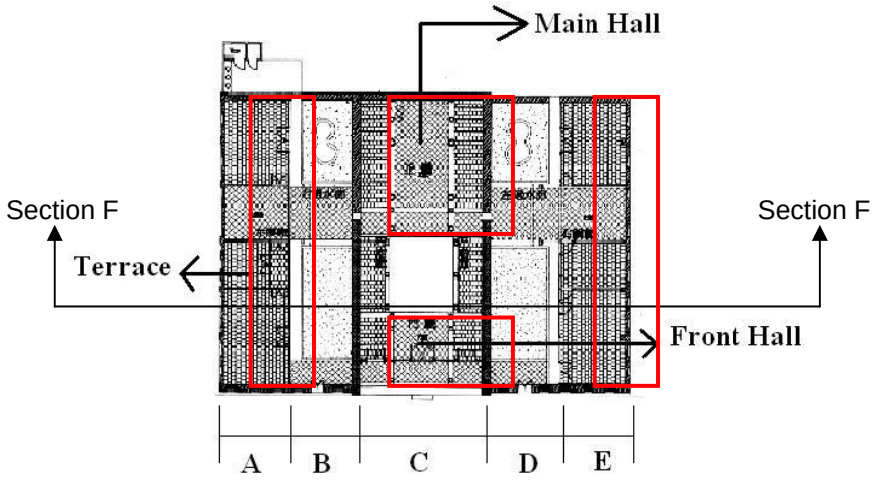

Figure 5.3.1 Plan of Guan-Shi Temple (Hsu, 2002, adapted)

Figure 5.3.1 shows the plan of Guan-Shi family temple. Section C is the main part of temple, and includes the Front hall, Main hall and a Yard between these two halls. Sections B and D are two Yards, while sections A and E are two Terraces. The Main hall and Front hall are Dieh-Dou timber structures while the right Terrace consists of masonry with a trussed roof and the left Terrace is built using the Chuan-Dou structural system. Both are used for storage space and rooms (see Fig 5.3.2).

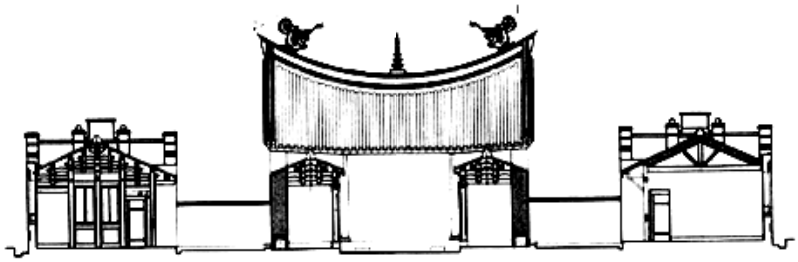

Figure 5.3.2 Section F of Guan-Shi Temple (Hsu, 2002)

The main buildings of the temple, the Main hall, is used for ceremonial purposes. Fig. 5.3.3 shows a drawing of the whole main frame and a photo of the main space of the frame post earthquake.

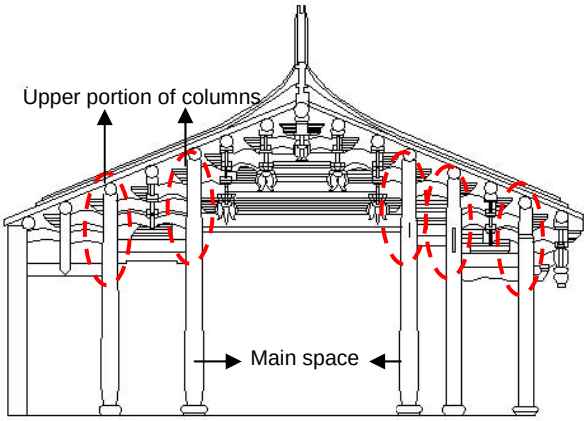

Figure 5.3.3 Main hall of Guan-Shi Temple

In the finite element model, built as described above the cross sections of the various elements were inserted accordingly to the real building taking appropriate consideration of all elements with reduced sections due to the mortise or scarfing to accommodate the intersecting members, like in the columns in Fig 5.3.4.

Figure 5.3.5 shows the model with the extruded elements. The vertical loads from the self weight and the roof weight over the purlins were calculated from the geometry of the Main hall of Guan-Shi temple and applied as described previously. Su (2003) indicated that the seriously damaged and collapsed buildings were mostly found in the zones where the recorded North to South and East to West peak ground accelerations were more than 300 gal (980 gal equals 1.0 g, so 300 gal is about 0.3g). In this preliminary analysis, lateral forces equivalent to an acceleration of 0.33g are considered, in accordance with the provisions of Taiwanese code (see Chapter 6).

Figure 5.3.4 Holes in the upper portion of columns

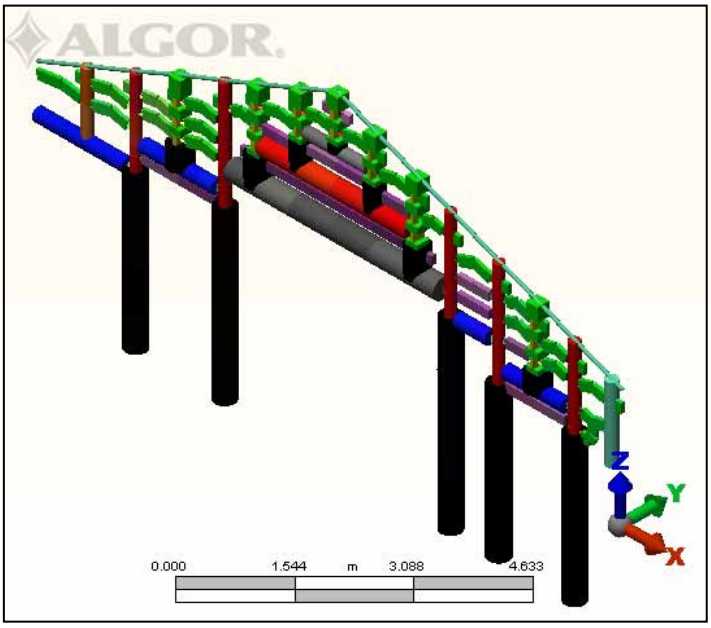

Figure 5.3.5 Extrusion of FE model

5.3.2 Variation of rotational and translational stiffness

Due to the limited number of laboratory test that could be realistically carried out during the project duration, the sensitivity of the model and the frame to variation in value of translational and rotational stiffness of the joints was studied by a parametric analysis.

Two parametric factors, rotational and translational stiffness are analysed by four groups of models. The first group is used to study the influence of rotational stiffness, while second to fourth group study the effects of the translational stiffness.

In the first group of models, the translational stiffness of all joints was kept constant at a value of 1.8E+6 N/m (the minimum value obtained by pull out tests), while the rotational stiffness of the Dou joints was varied between 4.0E0 to 4.0E9 Nm/rad (in the Dou joints in Chapter 4, the average result of joint rotational test was 4.045E4 Nm/rad). This allowed identifying the range of rotational stiffness for which the most substantial change in lateral displacement was obtained. These series of models were classified as Group 1.

The second part of the parametric study entailed keeping the rotational stiffness constant in the Dou joints (at the extreme and median value of the range identified above) and varying the translational stiffness between 1E4 and 1E8 N/m; in other words, the finite element models with rotational stiffness 1E4, 1E5 and 1E6 Nm/rad where coupled with translational stiffness 1E4 to 1E8 N/m, and categorised as Group 2, Group 3 and Group 4 respectively. Table 5.3.1 illustrates the details for each of the groups of analysis.

Table 5.3.1 Rotation and translational stiffness of FE model

	Rotational stiffness (Nm/rad)	Translational stiffness (N/m)
Group 1	4E+0 < Kr < 4E+9	1.8E+6
Group 2	4E+4	1.8E+4 < Kt < 1.8E+8
Group 3	4E+5	1.8E+4< Kt < 1.8E+8
Group 4	4E+6	1.8E+4 < Kt < 1.8E+8

The results of the parametric study and their implications are examined in the following.

5.3.4 Results and discussions

One of the characteristic features of Dieh-Dou buildings is that the roof is heavy compared to the whole structure but is only supported by four or five columns. Fang et al (2001) indicated that in buildings with such characteristics this heavy mass may lead, under seismic load, to excessive lateral movements. Huang & Sheu (2001) identified, as a cause of collapse of Dieh-Dou buildings, the excessive swaying of the roof causing the columns to rotate excessively. Also, the survey and discussion on failure modes presented in Chapter 3 show that Dieh-Dou buildings were often damaged because elements slipped out of their original position leading to collapse, while very few were the cases of structural failure due to material rupture. Thus, structural sway plays an important role on such buildings.

Although there is lack of testing and literatures that clearly specify a drift limitation for Dieh-Dou frames, the Taiwanese "*Code for the Design and Construction of Timber Buildings*" (2008) and "*Design of Buildings for Earthquake Resistance*" (2005) specify that, for buildings in general, the storey drift under seismic loads should not exceed 0.005. Furthermore, Miyamoto et al (2004) used a limiting drift criterion of 0.008 to evaluate the deformation of Japanese historic timber buildings. These values are taken as a reference to compare the results of the numerical parametric study against.

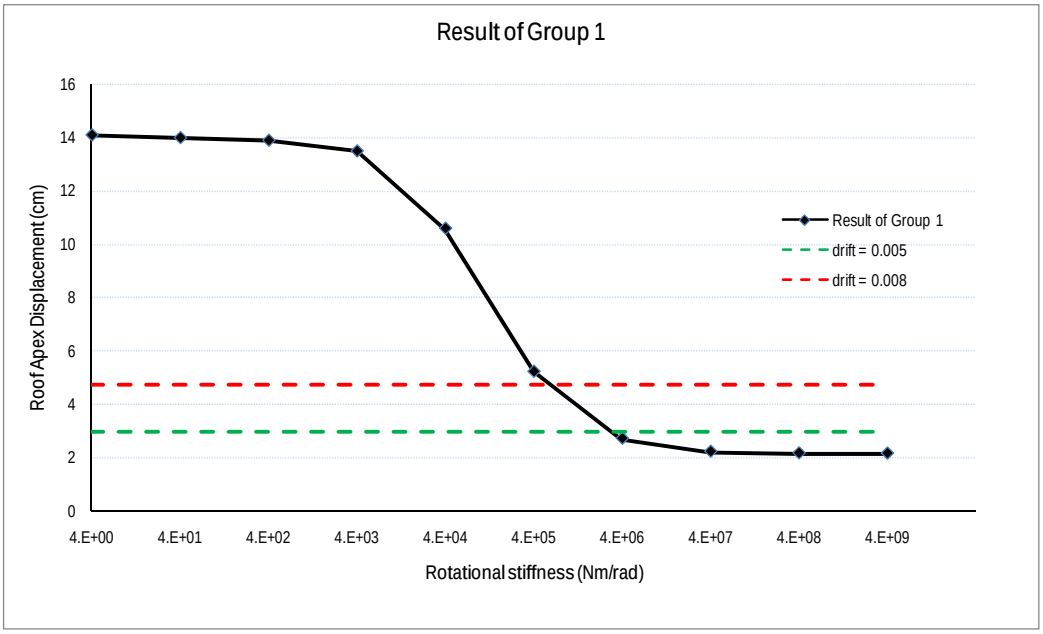

Figure 5.3.6 Result of Group 1

Results are shown in Figure 5.3.6 for Group 1 and in Figure 5.3.7 for Groups 2 to 4. The result of Group 1 clearly shows that for constant translational stiffness, when the rotational stiffness is below 4E3 Nm/rad the structure tends to behave as if the joints are hinges, while for stiffness values above 4E7 Nm/rad as if they are fixed, showing that these two extreme comprise the range of values for which the behaviour of these joints can be classified as semi-rigid.

So when translational stiffness is constant the behaviour can be classified as:

for	Rotational stiffness < 4E3 Nm/rad →	Hinge
for	Rotational stiffness > 4E7 Nm/rad →	Fixed
for	4E3 Nm/rad <Rotational stiffness < 4E7 Nm/rad →	Semi-rigid

The rotational tests of Dou-Gon joints performed in Chapter 4 and Chang's formula (Chang 2006) for mortise and tenon beam to column joints lie in the range of 2E+4 to 3.8E+5 Nm/rad, showing they are in the range of semi-rigid.

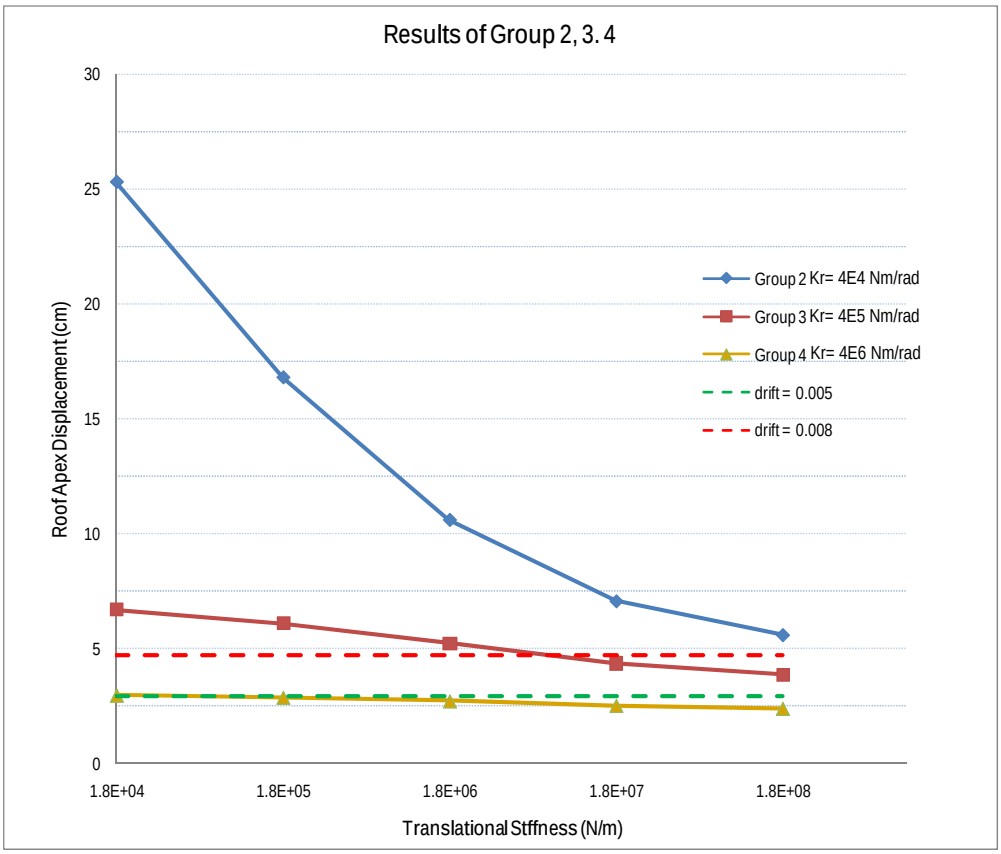

Figure 5.3.7 Results of Group 2, 3 and 4

Comparing the results of Group 2 to 4 in Figure 5.3.7, it is clear that the effects of variation in rotational stiffness are amplified when the translational stiffness is lower.

For example, when the translational stiffness is 1.8E+8 N/m, the roof apex displacements of group 2 (rotational stiffness 4E+4 Nm/rad), group 3 (rotational stiffness 4E+5 Nm/rad) and group 4 (rotational stiffness 4E+6 Nm/rad) are 5.59, 3.84, and 2.4 cm, respectively, with the value of the first one being 2.33 times the third. However, when the translational stiffness decreases to 1.8E+4 N/m, the ratio of the first to the third is 8.52 times.

When the rotational stiffness is near to rigid, see Fig 5.3.6 and Fig. 5.3.7, the influence of translational stiffness reduces. In Group 4, where the rotational stiffness was kept constant at 4E+06 Nm/rad, the roof apex displacement of the model with translational stiffness 1.8E+04 N/m is 2.97 cm, while for the model with 1.8E+06 N/m it just diminishes to 2.4 cm.

When comparing the results of the various Groups with the drift limitations, it appears that to satisfy the limit of the Taiwanese earthquake code the joints of Dieh-Dou frames should be practically rigid. However, this limitation have been derived for concrete and steel modern framed buildings which are generally stiffer than Dieh-Dou frames, that are built by small pieces of timber which are susceptible to substantial relative displacement. Moreover, rigid joints can result in higher stresses in the elements and cause local material rupture, a phenomenon not observed in the post earthquake survey of Dieh-Dou frames. Thus, the drift limit of 0.005 proposed by Taiwanese codes appears excessively conservative to judge the damage limitation of Dieh-Dou frames.

The drift criteria used by Miyamoto for Asian-style timber structures (Miyamoto et al 2004) seems more reasonable than the Taiwanese code limit, as it account for the superior degree of deformability honed by these structures. When compared with the values of stiffness obtained in the test results of Chapter 4, this drift criterion corresponds to the deformation of the upper range of semi-rigid connection behaviour (see Fig. 5.3.6). However for a frame with translational stiffness of 1.8E+06 N/m and rotational stiffness comprised between 4E+4 to 4E+5 Nm/rad in all joints, the result show that the roof apex drift for the applied load of 0.33g is over the damaging criterion of 0.008 (Fig. 5.3.7), indicating the structure may have seriously damaged.

The results of this parametric study showed the importance of modelling the stiffness of this joints properly, as variation in both rotational and translational stiffness can lead to major difference in global structural deformability. Either assuming these joints are rigid or pinned and ignoring the finite translational stiffness, which is usually done, is proved to be incorrect and may lead to misleading results.

Having determined the characteristics of the FE models for Dieh-Dou buildings to account for their peculiar joint arrangement and their qualitative behaviour under horizontal loads, a quantitative study to identify the criticality of the various elements of the structure will be performed in the following Chapter 6 using static, dynamic and nonlinear analysis methods. The effect of 3D analysis versus 2D will also be discussed in the following chapter.

Chapter 6
Assessment Methodology and Procedure

6.1 Introduction

6.1.1 General

Historic building conservation involves several aspects of professional knowledge, combining both science and culture. Although both issues are indispensable for heritage, in a seismic zone like Taiwan the natural disasters threaten the safety of heritages and may destroy them through potent earthquakes.

The International Scientific Committee on the Analysis and Restoration of Structures of Architectural Heritage (ISCARSAH) was founded by ICOMOS (International Council of Monument and Site) in 1996. This committee (ISCARSAH) has authored the ICOMOS Charter - Principles for the Analysis, Conservation and Structural Restoration of Architectural Heritage (ISCARSAH Principles) in 2003 and also provided guidelines (Recommendations for the analysis, conservation and structural restoration of architectural heritage, 2003) for conservation and restoration purpose. These documents provide a general overview of the works involved in conservation, such as information and investigation of heritage history, analysis of structural behaviour, diagnosis and evaluation procedures.

The historic buildings are different from building to building, country to country, as they can vary in structural systems, materials, environment, so it is difficult to specify a standard that include details of assessment for a specific structure. However, following the principle provided in these documents, an evaluation method suitable for Dieh-Dou frames can be established.

The guideline for ISCARSAH Principles (2003) reveals that the evaluation of heritage safety should be based on both qualitative analysis (review of original documentation, observation) and quantitative analysis (experimental, mathematical), hence a purely quantitative method used for new construction may not necessarily

be accurate nor reliable for historic buildings. Therefore, both qualitative and quantitative analyses are used in the Dieh-Dou building assessment.

The qualitative analysis applied to Dieh-Dou buildings has been discussed in Chapter 3 in the form of study of a past earthquake event (the 1999 Chi-Chi earthquake) through field surveys and literature review, that revealed the damage pattern of the building and the overall structural behaviour under seismic action. In order to have more evidence on the Dieh-Dou frames behaviour and form the basis of comparison for a quantitative analysis, two reference buildings located between 5 to 10 km alongside the Chelungpu fault are considered.

In the quantitative analytical approach, mathematic models are used and theoretical damage can be calculated. Structural analysis is an indispensable tool to understand the flow of the stresses and identify critical areas; if combined with the qualitative approach, the results can be accurate and give reliable methods to predict Dieh-Dou buildings behaviour under earthquake. A review of the provisions of Eurocode 8 and Taiwanese code for the structural analysis under earthquake loading is given in the following.

6.1.2 Taiwanese codes and Eurocode

Dieh-Dou frames are timber structures; however, there are no design or assessment codes and standards directly related to their peculiar structural form. The "*Code for the Design and Construction of Timber Buildings*" (2008) was first issued in 2003 in Taiwan and then revised in 2008. Although information regarding timber as material is generally provided, nothing is included that bears directly to the Dieh-Dou buildings structural system, and the earthquake resistance of timber structures is not discussed in this document.

The "*Design of Buildings for Earthquake Resistance*" (2005), first issued in 1974, defines how to design new buildings under earthquake loads. Two seismic analysis methods are suggested in this document, namely static analysis and dynamic analysis (Table 6.1.1). Here, the lateral force method is used for the static analysis, while dynamic analysis includes response spectrum analysis method and time history analysis. Section 8 of this Code is for the evaluation and strengthening of existing buildings; however, the text of this section is very general and no type-

specific method of assessment is defined. Also, this code is mainly aimed to steel and concrete structures.

In order to establish the most appropriate assessment method for Dieh-Dou building, the Eurocode, the common standard now used in European countries, is considered as a suitable reference. The Eurocodes comprise 10 parts and include the standard EN 1998 Eurocode 8 - "*Design of structures for earthquake resistance*" (2004), aimed at the protection of civil engineering structures in seismic regions. In this code, four method of analysis are proposed for the earthquake design of new buildings, see Table 6.1.1. For the purpose of providing information of how to deal with existing structures, Eurocode 8 contains Part 3, named "*Assessment and retrofitting of buildings*". Five analysis methods are suggested in Eurocode 8, Part 3, (Table 6.1.1)

Table 6.1.1 Earthquake analysis methods of Taiwanese code and Eurocode-8

	Suitable for use	Methods of Analysis
Taiwan - *Design of Buildings for Earthquake Resistance*	New buildings	Lateral force method Response spectrum analysis Time history analysis.
Eurocode 8-1 *General rules, seismic action and rules for buildings*	New buildings	Lateral force method Modal response spectrum Non-linear static (pushover) Non-linear time history dynamic
Eurocode 8-3 *Assessment and retrofitting of buildings*	Existing buildings	Lateral force analysis Modal response spectrum Non-linear static (pushover) Non-linear time history dynamic *q*-factor approach

The common aim of the different methods is ensuring the structures are safe under seismic actions, with different degree of complexity and applicability. The suitability of the above methods for the analysis of Dieh-Dou buildings is discussed in the next section.

6.1.3 Analysis methods for Dieh-Dou buildings

The Taiwanese code" *Design of Buildings for Earthquake Resistance"* (2005) states that buildings with height less than 50 meters or less than 15 storeys, and with plan and elevation of regular geometry can be appropriately analysed using static analysis rather than dynamic analysis. For tall buildings that consist of two parts of very different stiffness, whose geometry is regular and have rigid horizontal diaphragms, the two parts of the building can be calculated by static analysis separately. In all other cases the dynamic analysis should be applied. According to these rules the Dieh-Dou buildings, which are regular in plan and elevation and they are basically made of one storey (the roof), can be analysed using the static lateral force method.

In the Eurocode 8-3 for assessment, choice of the analysis method depends on the knowledge level of the target building. The knowledge level is determined depending on available information on geometry, construction detail, and material of the building. Hence, three levels are defined and corresponding allowable analysis methods are indicated as in Table 6.1.2

Table 6.1.2 Knowledge levels and analysis methods of Eurocode 8-3 (2005)

Knowledge levels		Methods of Analysis
KL1	*Limited knowledge*	Lateral force analysis Modal response spectrum analysis
KL2	*Normal knowledge*	Lateral force analysis Modal response spectrum analysis Non-linear static (pushover) analysis Non-linear time history dynamic analysis *q*-factor approach
KL3	*Full knowledge*	Lateral force analysis Modal response spectrum analysis Non-linear static (pushover) analysis Non-linear time history dynamic analysis *q*-factor approach

As the knowledge level detail is assessed in terms of geometry, detailing and material, the knowledge of Dieh-Dou buildings in this respect can be summarised as follows:

i) geometry: The Dieh-Dou buildings are considered historic buildings in Taiwan, and in many cases were built more than one hundred years ago. Differently to recently built existing buildings, there are no original drawings as they were constructed before the introductions of codes and standard, using the working knowledge of carpenters transmitted in the workshop from generation to generation (Lee, 2003). The geometry of Dieh-Dou buildings is available therefore from survey only, and might differ from case to case and within the same building from structure to structure.

ii) details: In Eurocode 8-3, the construction details which qualify the seismic behaviour of the structure include detailing of reinforcement in reinforced concrete, connection between steel members, presence of floor diaphragms to lateral resisting structure, the bond and mortar jointing of masonry and the nature of any reinforcing elements in masonry. The description above concentrates on masonry, concrete and steel and details of timber structures are not included. As discussed in the previous Chapters, the details of Dieh-Dou buildings are hard to obtain, especially the joints, without dismantling them. The details of Dieh-Dou buildings were recorded from few cases while under construction or reconstruction. The stiffness of Dou-Gon joint was obtained from laboratory tests in the present research project.

iii) *material*: As mentioned in previous Chapters, the Dieh-Dou frames are made of softwood timber, but no particular type of timber has been consistently used. Even in the same building, various species of softwood can be identified, and of different age. The mechanical properties adopted are therefore from surveys and from average characteristics of the Asian softwood species.

The discussions above reveal that there is a general lack of original construction drawing and records of Dieh-Dou buildings leading to no direct information of construction details and mechanical properties. The present research is contributing

to an improvement in such knowledge, especially in terms of details. In any case, following the scheme of Eurocode 8-3 the Dieh-Dou buildings would be classed in between KL1, *Limited* knowledge, and KL2, *Normal knowledge*, implying the lateral force analysis and modal response spectrum analysis are certainly suitable for Dieh-Dou building assessment but there might be shortage of information for other analysis methods, especially the *q*-factor approach which strongly relies on the ductility of certain elements to reduce the seismic forces applied in the analysis.

Apart from selecting the analysis method according to the level of knowledge of the existing building, there are also limitations on each analysis method. According to Eurocode 8-1 for new design, the first judgement on analysis type is the structural regularity. Dieh-Dou buildings meet the criteria for both plan and elevation regularity, meaning they are allowed using simplified planar model and lateral force analysis. Lateral force analysis is allowed if buildings meet the condition:

$$T_1 \leq \begin{cases} 4 * Tc \\ 2.0\,s \end{cases} \qquad (6.1.1)$$

Here, T_1 is the fundamental period, which as a first approximation can be calculated with

$$T_1 = C_t * H^{3/4} \qquad (6.1.2)$$

As Dieh-Dou buildings are neither moment resistant space steel frames nor resistant space concrete frames, C_t is equal to 0.05, while H is the height of the building. Lee (2007) concluded his survey of 33 Dieh-Dou buildings stating that the height of frame with three main beams and five Dieh-Dou sets, which are the most commonly used, is comprised in the range between 5.5 to 6.5 meter. Thus, according to Formula (6.1.1) and (6.1.2), the fundamental period of Dieh-Dou building can range from 0.179 s to 0.2 s, and this would comply with the requirements in (6.1.1). Tc is the upper limit of period of the constant spectral acceleration of the two recommended elastic spectra. Because Taiwan is located in highly seismic zone, response spectrum Type 1 is taken as recommend in the document for earthquake magnitudes of more than 5.5. Within Type 1, the values of Tc ranges, depending on soil types, between 0.4 s and 0.8 s. The soil type corresponding to Tc equal 0.4 is rock or other rock-like geological formation, including 5 meter of weaker superficial

material. Assuming an average conservative value of 0.5 means that the fundamental period T_1 should not exceed 2 seconds, which is over the upper bound of Dieh-Dou building as calculated above, making the lateral force analysis applicable.

According to Eurocode 8-1 the modal response spectrum analysis is applicable to all types of buildings. Alternatively, non-linear analysis methods, such as non-linear static (pushover) analysis and non-linear time history dynamic analysis may also be used, but only if properly substantiated with respect to the seismic input.

As discussed above, Dieh-Dou buildings meet the conditions of Taiwanese code and Eurocode for the lateral force and modal response spectrum analysis. Lateral force analysis, in particular, is a simplified method and gives the advantages of being easy to understand for all people involved in the field in the need of performing quick assessment of seismic capacity of Dieh-Dou buildings.

However, the lateral force and modal response spectrum approaches are both linear analyses and may not necessarily be conservative enough for historic buildings. Some parts of the structures may start to fail or be disconnected for lower values of force or displacement and dramatically reduce the overall capacity of the building or change its stiffness, as observed in the post earthquake survey. Thus, a non-linear static pushover analysis can supplement the linear analyses efficiently; as it is believed that it can allow identifying the progressive failure of the elements under seismic load and give a more precise indication of the damage pattern.

In time history analysis, the post-elastic behaviour of the elements of the structural model should be adequately accounted for to cater for the energy dissipation in the cycles of loading and unloading (Eurocode 8-1, 2004). This analysis method requires precise input data of the acceleration history related to specified earthquake event in the building location and a very high knowledge level is required to perform this analysis properly and obtain reliable and meaningful results. The lack of full knowledge of Dieh-Dou frames would substantially affect the confidence in the results of time history dynamic analysis, as apart from the single cyclic test performed in this project with a dove-tail type connection data on the dynamic behaviour of the joints is unavailable.

However, a non-linear time history dynamic analysis would be the closest estimate of the actual response of the building to a specific earthquake. A simplified single degree of freedom (SDOF) model is employed to perform a time history analysis using the input data based on results of the modal analysis and pushover analysis.

Hence, the four methods below are considered for the analysis of Dieh-Dou buildings:

- *Lateral force analysis*
- *Modal response spectrum analysis*
- *Non-linear static (pushover) analysis*
- *SDOF time history analysis*

The first three methods are analysed with FE and results are discussed in Chapter 6, while the SDOF time history analysis results will be described in Chapter 7.

The guidelines for ISCARSAH Principles (2003) indicate that modern codes are to be treated with caution when dealing with historic structures, as requirement to improve the strength may lead to the loss of historical uniqueness. Hence a flexible approach needs to be adopted for historic buildings. With this in mind, the three analyses described above and the failure criteria are discussed in the following paragraph.

6.2 Methods of Analysis

6.2.1 Linear lateral force analysis

For lateral force analysis in the Taiwanese Code the total lateral force is first calculated by the following formula:

$$V = \frac{I}{1.4\alpha_y}\left(\frac{S_{aD}}{F_u}\right) * W \qquad (6.2.1)$$

where

I : building importance factor

a_y : behaviour factor

F_u: structure coefficient

S_{aD}: coefficient of spectrum

In Formula (6.2.1), the building importance factor *I* is related to the type of occupational function of the building; buildings involving the critical maintenance of human lives after earthquakes have higher values of importance factor implying the buildings should sustain larger lateral forces. Dieh-Dou buildings can be considered as third category, which is grouped under public buildings, and the importance factor is 1.25.

The value of the behaviour factor depends on the material and structural system of the building and ranges from 1 to 1.5. As Dieh-Dou buildings are not specifically included in the document, in favour of safety this value is taken equal to 1. The value of structure coefficient F_u equals 1.4 for timber.

The coefficient of spectrum $S_{aD,}$ is function of the fundamental period, ground soil type and location of the building. Although this code provides a formula to estimate the fundamental period of the building similar to (6.1.2), the actual fundamental period of the Dieh-Dou frame analysed will be calculated to define the value of S_{aD}.

Formula (6.2.2) is provided in Eurocode 8-1 (2005) to calculate the value of horizontal force for lateral force analysis. The shear force F_b is determined, which will then be distributed on each of the building storeys in a triangular shape as per the typical first mode of vibration. The base force F_b is expressed as:

$$F_b = S_e(T_1)*m*\lambda \qquad (6.2.2)$$

Where

- $S_e(T_1)$ is the ordinate of the elastic spectrum at period T_1
- m is the total mass of the building above the foundation
- λ is a correction factor

The elastic response spectrum at period T_1, $S_e(T_1)$, depends on the fundamental period, soil condition and location. The soil and location factors are only included in the various European Countries National Annex of this document, while the correction factor equals 1 for single storey buildings.

In the following analysis, the lateral force will be calculated with Formula 6.2.1 provided by the Taiwanese code, as the appropriate parameters for the soil type and site location of the buildings can be taken from the zonation map included in the code.

Once forces, stresses and displacements are obtained for all members from the FE analysis, then failure criteria is applied similarly to the previous methods to assess failure of joints and members. The result will then be compared with real failure after the 1999 Chi-Chi earthquake and response spectrum and pushover analysis.

6.2.2 Modal response spectrum analysis

Vibrations due to seismic loads and wind can create significant stresses in structures; seismic action is often the main cause of damage or collapse of historic buildings (Croci, 2000). There are several ways to deal with structural dynamic; however, natural frequencies and mode shapes are often required for dynamic analysis. Hence, the first stage of a dynamic analysis is to perform a modal analysis to understand which natural frequencies and modal shapes are most affecting to the structure. Theoretically, a continuous construction has an infinite number of modes; however, usually only one or a few modes considerably affect the structural behaviour the most, in relation to the percentage of mass participating in that vibration shape. Given the many structural elements and connections forming the Dieh-Dou buildings, a modal analysis and spectral superposition is considered necessary to evaluate the error made in the assumption of lateral force analysis. In brief, a response spectrum is a plot of maximum response, i.e., maximum acceleration, velocity, or displacement to a specified dynamic input acting on all possible SDOF system of increasing periods (Spyrakos, 1994).

The modal response of the Dieh-Dou frames are analysed by the finite element software ALGOR ©, where the mass of the fully-loaded roof is lumped at the junction with each purlins. The first ten modes of the structures are examined to evaluate their frequency, modal effective mass, participation factor and modal shape. Following the natural frequency analysis, a modal response spectrum analysis is performed where accelerations are applied to the model, and the displacement results acquire a physical value.

Seismic codes suggest the use of elastic and design response spectra. Fig. 6.2.1 shows an example of graph of elastic response spectra provided by Eurocode 8-1 (2004). The lines differ in terms of soil types (A to E in the figure) and building damping ratio. A 5% damping ratio is usually used in the graphs. Spyrakos (1994) indicates that the damping ratio for timber structures can range from 5% to 12%. Thus, a response spectrum with 5% damping ratio can be conservatively employed for Dieh-Dou frames in the analysis.

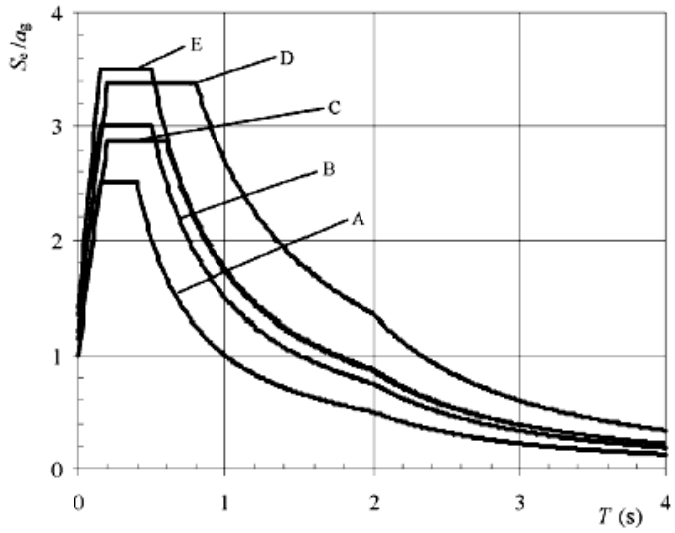

Figure 6.2.1 Design response spectrum (Eurocode 8-1, 2004)

However, the purpose of applying a response spectrum on Dieh-Dou building is not for a design goal, but to validate the numerical modelling by comparing with the post-earthquake failures observed. A real earthquake spectrum is then best employed, instead of a design one. The response spectra used for Dieh-Dou frames

are obtained from accelerometer recordings during the 1999 Chi-Chi earthquake at locations close to the analysed buildings.

The response spectrum analysis is based on the results from the modal analysis, which is performed by the software beforehand. After the analysis, there are two common ways in which the software can calculate the response in terms of combination of all results, i.e. the square root of the sum of squares (SRSS) and the complete quadratic combination (CQC). According to Spyrakos, (1994), the most commonly used combination method is the SRSS. The SRSS usually provides good maximum response estimates when the structure has well separate modes, but not when the structure has several closely spaced natural frequencies. Therefore, when the cluster factor $(f_i-f_{i-1})/f_{i-1}$ is greater than 0.1, SRSS is acceptable. The Dieh-Dou frames will be shown to have a predominant first mode of vibration with insignificant participation factor of the subsequent modes; a SRSS is therefore employed in the analysis to combine the minor frequencies.

6.2.3 Nonlinear static step by step pushover analysis

According to Elnashai (2001), the use of inelastic static pushover analysis in earthquake engineering can be traced from the early seventies, where load-displacement curves of single degree of freedom system used to represent multi-degree of freedom structures were evaluated by finite element methods or hand calculations to obtain the initial and post-yield stiffness, the yield strength and the ultimate strength. Since then, inelastic static pushover analysis has been developed and modified accordingly to adapt to the seismic assessment.

Grierson et al (2006) indicated that although nonlinear dynamic analysis can catch structural behaviour accurately, but it requires significant calculation effort; pushover analysis can be seen as a viable and attractive alternative to dynamic analysis. As the feature of pushover analysis is applying increasing lateral load until the control point of a structure sways to a predefined target lateral displacement, this analysis method allows to trace the sequence of stress increase, localised yielding or other forms of failure, and final collapse mechanism. Goel and Chopra (2005) analysed results of six buildings under 20 different ground motions and confirmed that a modal pushover analysis procedure provides good estimates of member forces when compared with nonlinear response time history analysis.

Cardone (2007) tested a pair of 1 to 3.3 scale RC frames, with and without infill masonry walls on the shaking tables then compared the results with numerical models analysed by pushover analysis. This work proved pushover analysis was able to predict the seismic response of the building with adequate accuracy. Inel et al. (2008) employed pushover analysis to re-evaluate building damage during earthquake in Turkey, and showed that structural characteristics and local failures can be identified properly.

D'Ayala (2005) applied pushover analysis to historic masonry buildings in Turkey, comparing analytical approach and in-situ post earthquake damage, showing that this method can accurately predict vulnerability and collapse mechanisms for historic buildings. In addition, Lourenco (2005) reveals that nonlinear methods can point out damage of historic building and significant information also can be obtained from numerical models to minimise strengthening on heritage structures.

The brief review conducted above shows that a nonlinear static pushover analysis has the advantage of identifying failure patterns and inelastic deformation of structure. It has also proved accurate when compared with experimental tests and in-situ observation. However, the structural features of Dieh-Dou buildings are very different than the reinforced concrete, steel and masonry structures that were involved in the great majority of previous reviewed work. Hence, the feasibility and modifications of a nonlinear static pushover analysis applied on Dieh-Dou frames is thoroughly investigated in the following.

In the definition of Eurocode 8-1 (2004), pushover analysis is "*a non-linear analysis carried out under conditions of constant gravity loads and monotonically increasing horizontal loads; it may be applied to verified structural performance of newly designed and existing buildings"*. Therefore, this method is based on the premise that the response of the structure is mainly controlled by a single vibration mode; generally, the fundamental vibration mode is chosen as the dominant response mode and higher modes are ignored (Grierson et al 2006). Modal pushover analysis (Chopra & Goel, 2002) and advance inelastic static pushover analysis (Elnashai, 2001) were performed to account for higher modes for taller buildings. Because the simple conventional pushover analysis requires a single fundamental response and the shape of the mode is invariant through the loading history, it is clear that classic pushover analysis should best be used for the prediction of the seismic

displacement response of low-rise to mid-rise buildings (Grierson et al 2006; Cardone 2007).

Dieh-Dou buildings are considered as low-rise building. In addition, the roof of a Dieh-Dou timber frame can be seen as a large mass supported by four, five or six columns (see Fig. 6.2.2). There are no internal infill walls in between these columns, hence it can be reasonably thought as having a top mass with a column with the whole structure having a single degree of freedom (see Figure 6.2.2 right); this responds to the requirements of a classic pushover analysis, where effects of higher modes are neglected.

Various lateral force patterns have been proposed for pushover analysis, such as uniform, triangular or multi-mode distribution (Eurocode 8-1 2004, Chopra & Goel 2002, Cardone 2007). Clearly for Dieh-Dou buildings, governed by the fundamental mode, a single uniform lateral force pattern regardless of elevation is appropriate. The great majority of the lateral force comes from the roof load transferred from the purlins to the frames. It is therefore appropriate for these forces to be applied laterally at each purlin connection as in the lateral force analysis discussed previously. The lateral load is applied in increments of 0.033g.

There are normally two possibilities of target limitations for the pushover analysis, either displacement or load. The analysis is carried out until the displacement of a specified node, in general the roof apex, reaches the target limit or until a maximum specified load is reached. Although the displacement-control procedure is likely to be more suitable for existing buildings (Grierson et al 2006), however, it is difficult to decide an ultimate displacement for Dieh-Dou buildings as there is lack of fundamental research suggesting the ductility of these frames.

Therefore, in the present analysis, the value of lateral force obtained from the Taiwanese code used for the lateral force analysis is considered as a target. The idealization of a capacity curve in a pushover analysis, illustrating an elastic-perfectly plastic behaviour, is shown in Figure 6.2.3.

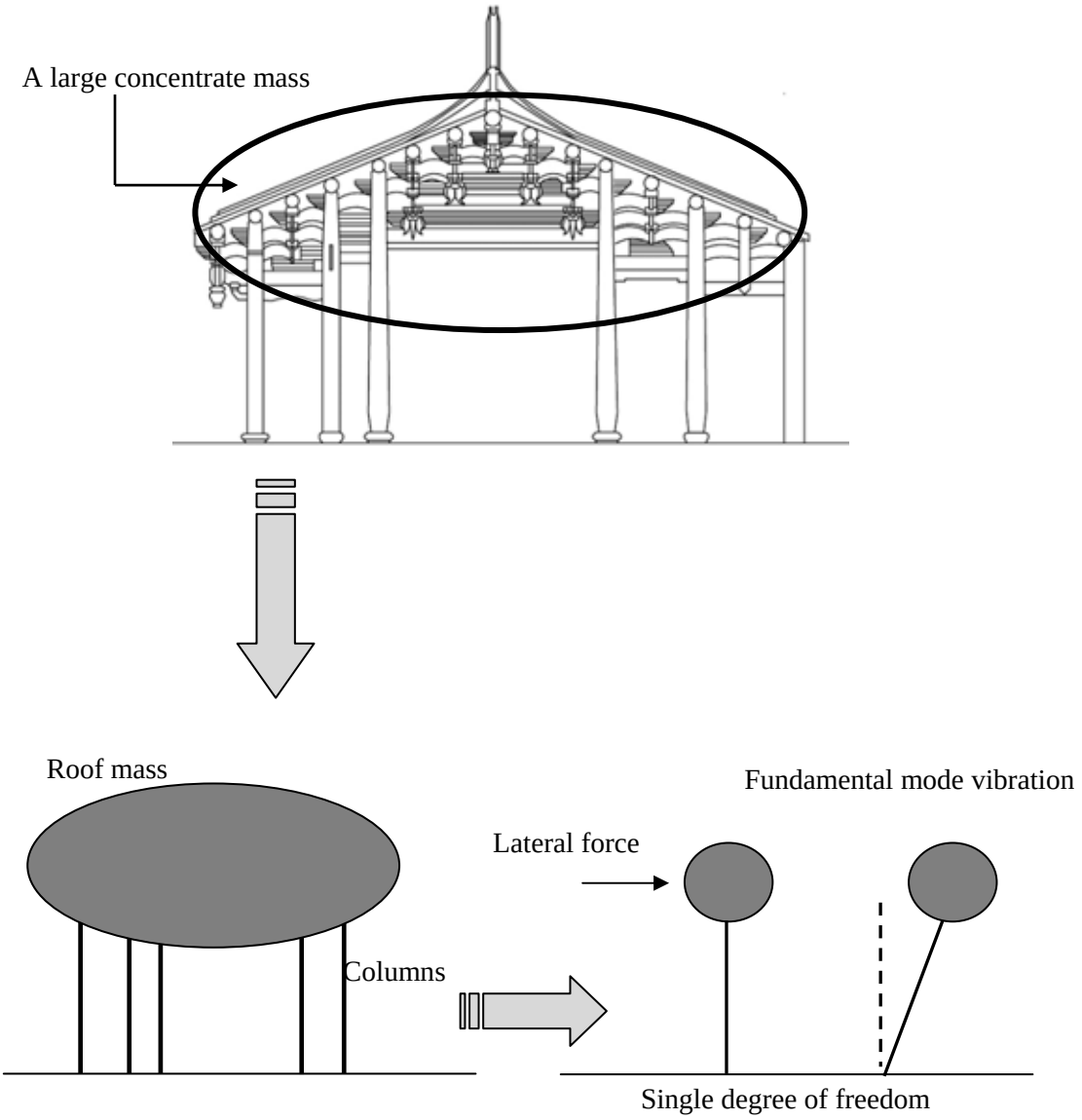

Figure 6.2.2 Schematization of a Die-Dou frame

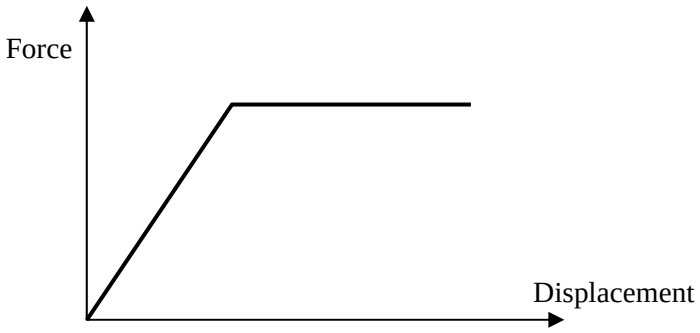

Figure 6.2.3 Idealized lateral force versus displacement chart in pushover analysis

6.2.4 SDOF time history analysis

According to Spyrakos (1994), although structures have an infinite number of degrees of freedom, when the behaviour can be identified as predominantly affected by a single parameter, the study of a single degree of freedom (SDOF) system may be very useful. Clough and Penzien (1993) indicate that a system subjected to dynamic loading, in its simplest form, is represented by a mass, the elastic properties (stiffness) and an energy-loss mechanism (damping). In the simplest SDOF model, each of these properties is assumed to be a single physical element. Fig. 6.2.4 shows a SDOF system that can represent a Dieh-Dou frame.

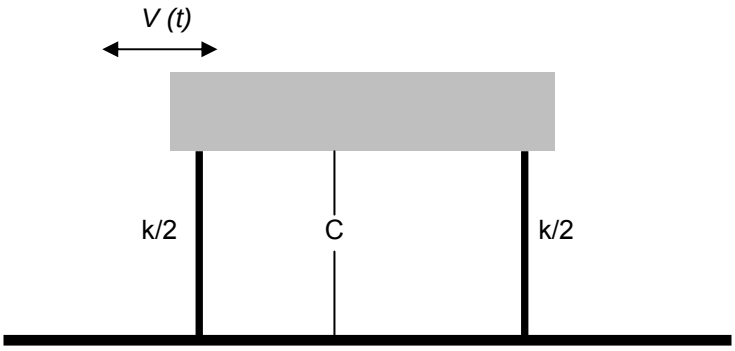

Figure 6.2.4 SDOF of Dieh-Dou frame

The rigid horizontal girder simulates the roof of the structure, while the two columns supporting the roof mass are assumed weightless. The magnitude of the girder displacement caused by the ground motion depends on the stiffness of the columns. The overall stiffness K, the roof mass and natural frequency are related through the expression $f\ 2\pi = (k/m)^{0.5}$. The frequency of the structure is obtained from modal analysis. In accordance with common practice for timber structures, the structural damping is set as 5%.

This SDOF analysis was performed using a program, in the open source Processing environment, written by Dr. C.J.K. Williams for educational purposes in the department of Architecture and Civil Engineering of University of Bath. Fig. 6.2.5 shows a frame of the program's graphic output. The height of the building is defined according to the geometry of the target structure, and the frequency value is obtained from modal analysis with FE.

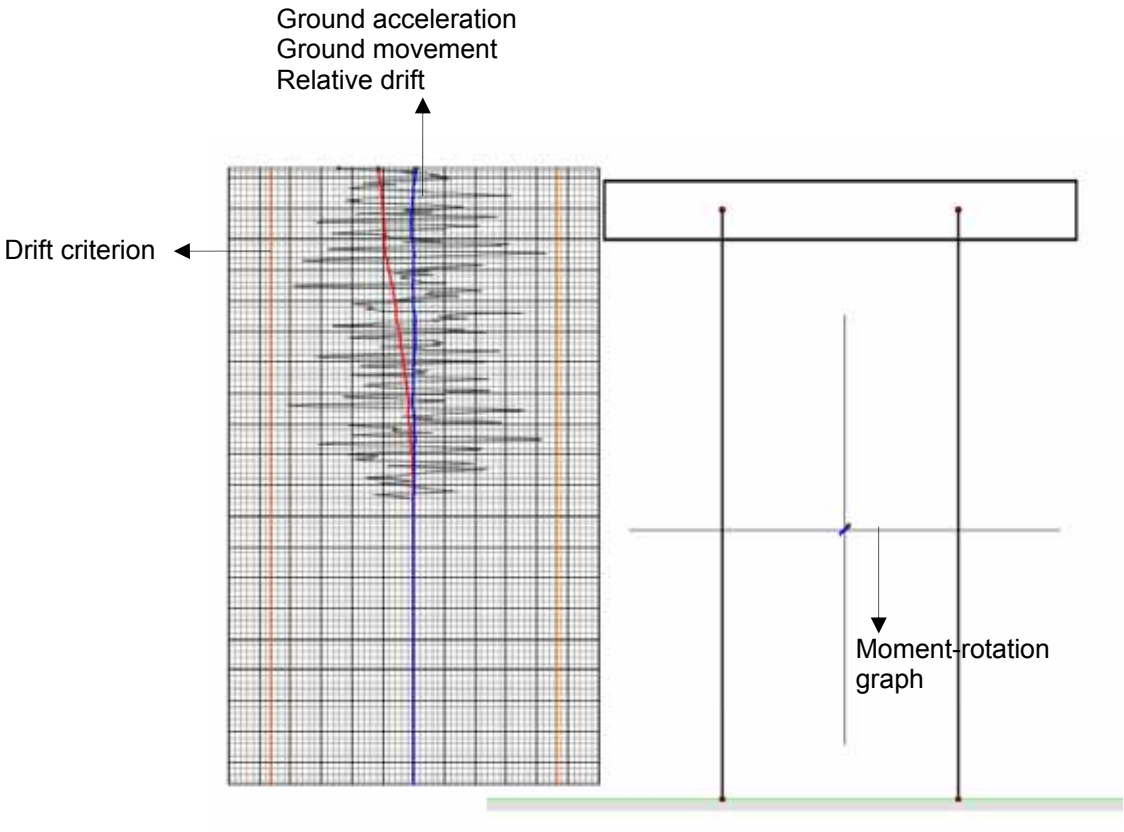

Figure 6.2.5 An instantaneous of the SDOF time history analysis animation

In the calculation, the moment-rotation characteristics of the idealised columns are defined as elasto-plastic and the limit rotation that describes the yield criterion is inserted, corresponding to the drift limit of the Dieh-Dou frame. The algorithm used for the integration of the equations of motions is the Euler-Cromer algorithm, codified as follows:

$$\ddot{\theta} = -2\omega\beta\dot{\theta} - \frac{\ddot{\alpha}_0}{h}\cos\theta_0 + \frac{g}{h}\sin\theta_0 - \omega^2\theta_0 \qquad (6.2.3)$$

Where $\ddot{\theta}$ is the rotational acceleration at the current step, β is the damping factor, $\dot{\theta}$ the velocity at the current step, $\ddot{\alpha}_0$ is the ground movement and its time derivative, θ_0 is the rotational displacement at the previous step, g is the gravity constant , h is the reference height of the structure, ω is the circular frequency of the structure, and

$$\Delta\dot{\theta} = \ddot{\theta}\Delta t\ ,\ \Delta\theta = \dot{\theta}\Delta t \tag{6.2.4}$$

$$\Delta\dot{\alpha} = \ddot{\alpha}\Delta t\ ,\ \Delta\alpha = \dot{\alpha}\Delta t \tag{6.2.5}$$

Where θ is the rotation of the columns from the vertical and α is the ground displacement as obtained from integration of the accelerogrammes. To avoid ground movement drifting due to numerical errors a quantity $\alpha\Delta t/1000$ is subtracted from α each time step

At each integration step the current value of the rotational displacement is checked against the yielding and failure limit.

6.3 Diagnosis

6.3.1 Global observation

The qualitative data from post earthquake surveys shows the Dieh-Dou frames were easy to lean, with the eave parts deformed more than other zone of the structure (see Chapter 3). Thus, the results obtained from lateral force analysis, response spectrum analysis, and step by step pushover analyses are observed and compared with the qualitative data aforementioned.

Storey drift limitation is used in various codes to check the lateral deflection of the buildings. In the Taiwanese Seismic Code (2005) the newly designed buildings are examined by checking the permissible stresses and the maximum drift, which is limited to 0.005 as a limiting damage criterion. In Eurocode 8-1 (2004), however, three drift limitations are made, according to different structural configurations, and a factor is included which is to be defined fro each Country in the National Annex. In the American standard for assessment FEMA 356 (2000), for woods stud walls, three values of lateral drift are considered, equal to 0.01, 0.02 and 0.03 for the structural performance levels limiting threatening immediate occupancy, life safety and collapse prevention, respectively.

Miyamoto et. al (2004) used a drift damage limitation of 0.008 to evaluate Japanese traditional timber structures. Although the Japanese structural system is not exactly the same as the Dieh-Dou frames, the similarity of material and Asian-style construction is evident and this value is adopted as a further reference.

The storey drifts can represent a damage limitation for structures under seismic action especially in relation to serviceability conditions. However, it is difficult to judge the level of damage of the building once this limit is surpassed. A ductile structure leads to higher tolerable drifts, and timber joints, for example, are more flexible than concrete ones, making them theoretically superior in dissipating energy, so the same magnitude of drift on timber structures may not cause such harm on the structure as in a concrete ones will. The Dieh-Dou buildings are built by several pieces of timbers and there is no metal connection between them, and this can allow deformation at the joints preventing the formation of very high stress concentrations Therefore, global drifts limitations are important to define mostly in relative comparative terms and for understanding the potential severity of the damage, but cannot give an absolute definition of whether the building or its element are collapsed. Local failure observations are therefore important to define.

6.3.2 Local observation

The basic concept for designing a new building in seismic region is to ensure the building remains safe in the specific return period of earthquake, which in general depends on the usage and importance of the building. However, design codes contain often quite generous safety factors that render the structural margin over collapse very high.

As the structural behaviour and analysis methodology for Dieh-Dou buildings have not been codified to date in Taiwan, this project proposes some numerical methods to assist in this task. It is then necessary to validate the method by comparing the results of the structural modelling and analysis to the status of the building after an earthquake against which the structure should be verified and assessed for.

In an assessment exercise, the interest is on the actual level of stress of the elements rather than the permissible stress, therefore the ultimate stress capacities

are considered as the limiting material failure criterion and compared with the FE results for all structural members of the Dieh-Dou frame under the assumed loading.

Apart from the material failure, the surveys of Dieh-Dou buildings showed that the joints are easily pulled out from their original position. This type of failure, in which the material is not damaged but the elements are dislocated, is considered as the second failure criterion to be checked against the FE analysis results and named as joint failure. The two types of failure, material failure and joint failure, are quantified below.

6.3.2.1 Material failure

For the material failure, combined bending and tension, combined bending and compression and shear stress are examined. All the material capacities for bending and axial stress are taken from the results of the material tests (presented in Chapter 4) and from the Wood Handbook (1999), where no material tests were available. Once the applied stress is greater than the failure capacity the member is considered failed for material damage.

The members subject to axial tension and bending are checked with the formula (6.3.1)

$$\frac{\sigma_{m,a,//}}{\sigma_{m.scm,//}} + \frac{\sigma_{t,a,//}}{\sigma_{t,scm,//}} \leq 1 \qquad (6.3.1)$$

Where, $\sigma_{m,a,//}$ is the resulting bending stress from the FE analysis, $\sigma_{m.scm,//}$ is the material strength capacity in bending and $\sigma_{t,a,//}$ and $\sigma_{t,scm,//}$ represent the resulting tension stress and the material strength capacity in tension, respectively.

For the elements subject to axial compression and bending, the interaction formula of British Standard (BS 5268-2; 2002), shown as equation (6.3.2), is used as failure criterion:

$$\frac{\sigma_{m,a,//}}{\sigma_{m.adm,//}\left(1-\frac{1.5\sigma_{c,a,//}}{\sigma_e}\times K_{12}\right)} + \frac{\sigma_{c,a,//}}{\sigma_{c,adm,//}} \leq 1 \qquad (6.3.2)$$

However, as formula (6.3.2) is for allowable stress design, it is converted in the form (6.3.3):

$$\frac{\sigma_{m,a,//}}{\sigma_{m.scm,//}\left(1 - \frac{1.5\sigma_{c,a,//}}{\sigma_e} \times K_{12}\right)} + \frac{\sigma_{c,a,//}}{\sigma_{c,scm,//}} \leq 1 \qquad (6.3.3)$$

where $\sigma_{m,a,//}$ and $\sigma_{m.scm,//}$ represent the applied bending stress and the bending strength defined above, $\sigma_{c,a,//}$ indicates applied compressive stress obtained from ALGOR © and σ_e is the Euler critical stress $\pi^2 E/(L_e/i)^2$ to account for buckling. In the latter, E is the modulus of elasticity (equal to 6400 MPa) taken from the material tests, L_e is the effective length of the compression member that depends on the element restraint and i is the element minimum radius of gyration. The elements of a Dieh-Dou frame are all linked with other members and although the joints are not perfectly rigid, they are effectively restrained in position and direction and therefore the coefficient 0.7 for the ratio of effective to actual length is taken from BS 5268; Le/i represents the slenderness ratio of the compression members. The factor K_{12} in formula 5.5 and 5.6 is a modification factor related to the slenderness ratio, E and $\sigma_{c,//}$ and is taken from Table 22 of BS 5268. In formula (6.3.3) $\sigma_{c,scm//}$ represents the compression strength parallel to grain.

Finally, for the material failures in pure bending and in shear, the bending and shear stresses are simply compared with the bending rupture and shear strength.

6.3.2.2 Joint failure

The joint failure criteria can be grouped into pull out failure, rotational failure of joints (for horizontal members) and column failure.

In Chapter 4, the series of pull out tests performed in laboratory with full scale samples of one layer of Dou-Gon joint were described; the results indicated that the

maximum pull out forces at failure were similar and did not depend on the magnitude of vertical load applied (with a value varying between 8000 N and 9000 N) if the dove-tail connection was perfect, but reduced to 3000 N and 1500 N when applied loads were 6500 N and 3250 N respectively in the case of poor fit of the dove-tail joint (then relying on the timber to timber friction, as expected).

In Dieh-Dou buildings, the dove-tail joints are supposed to be carved properly; however, survey showed that in several cases the classic straight cut tenon and mortise arrangement was used. As dove-tail and tenon and mortise are hidden inside the whole joint set, it is virtually impossible to observe these connections without dismantling them. In addition, the survey post-earthquake showed that the pull out failure is a common feature and an extensive cause of damage for Dieh-Dou frames. Thus, in a conservative approach, the lower bound capacity of 1500 N is set as the pull out criterion. In other words, this means assuming the end of the members close to being straight cut, as shown in Fig. 6.3.1 and minimising the weight of roof over the joint.

Differently from pull out tests, the rotational tests showed that the results, in terms of stiffness, always depend on the magnitude of the vertical load. However, although the rotational stiffnesses were different, the maximum moment resisted by the joint was found to be always around 1000 Nm (see Chapter 4), after which the residual capacity is highly dependant of the configuration of the end of the member and cannot be consistently relied upon. Therefore, if the bending moment in the model is found to exceed this value, then the joint will be considered as failed in rotation.

The foot of the column has a very shallow timber pin into a stone base; the failure criteria here is that lateral force on the end of column exceed the shear capacity of the shallow pin plus the friction between timber and stone, see Fig. 6.3.2.

The coefficient of static friction for timber pieces to stone were calculated from laboratory tests, obtaining values of 0.53 and 0.58, with an average of 0.55, in line with codes indications (which range from 0.5 to 0.6 for friction of timber to timber in dry specimens). The frictional limit is then calculated by multiplying by 0.5 the vertical load, conservatively.

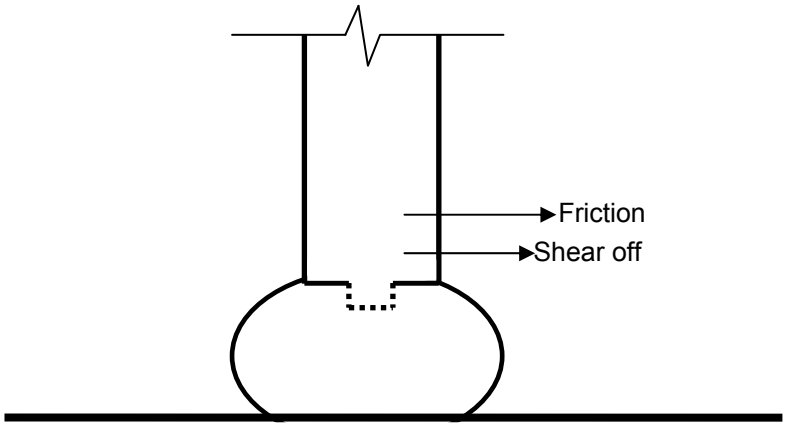

Figure 6.3.2 Resistance forces on the end of column

The width of the shallow pins is about 60 mm, with a surface area of about 3600 mm^2. The capacity of shear perpendicular to grain is 2.5 to 3 times of shear capacity parallel to grain (Kelly, 1990). The shear strength parallel to grain is 5 MPa, see Chapter 4, implying the capacity perpendicular to grain is 12.5 to 15 MPa. To shear off the dowel pin in the end of column require at least 45000 Newton. Once the numerical model result foot end force is more than criteria above, then the columns are assumed to be sliding from their original position and so no more horizontal force could be transmitted to the ground by releasing beam end in mathematical model. Due to the particular connection with the ground described above and following observation form survey, it is further assumed that the columns are able to rotate and do not transmit moment.

6.4 Application 1

Main hall of Guan-Shi family temple

6.4.1 Introduction of Guan-Shi family temple

The main hall of Guan-Shi temple was used for the parameter study of the stiffness in Chapter 5, where information regarding this temple is included. The finite element model was built in the software ALGOR © environment using beam elements and semi-rigid connections in the manner previously described.

In the parametric study on Chapter 5, all joints were assigned one value of stiffness which was then varied with the purpose of observing the relationship between the magnitude of stiffness and structural displacement. In the current analysis, the stiffness of each joint is assigned according to its location in the building and hence to the change of stiffness with weight described in Chapter 4. The rotational stiffness of Dou-Gon joints located in the upper layer is 2.4E4 N*m/rad; while the one for the joints in the lower layer is 4.05E4 Nm/rad. The results of the parametric study in Chapter 5 show that both values fall in the range of semi-rigid behaviour, slightly closer to hinge behaviour. The applied translational stiffness of all joints is equal to 1.8E6 N/m, in accordance with the lower bound of the test results of Chapter 4

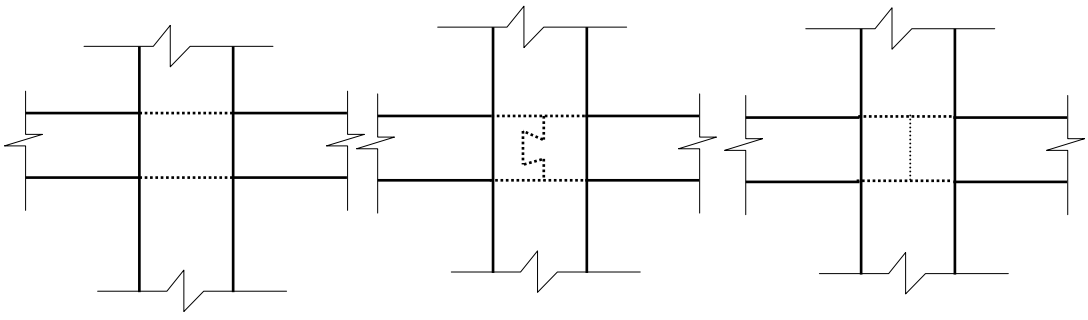

Figure 6.4.1 Three types of beam-to-column joints in Chuan-Dou frames

The stiffness of the classic beam-to-column joints are taken from the formula proposed by Chang (2006) for the Taiwanese Chuan-Dou timber buildings. The joints of the Chuan-Dou frame, which is the other type of Taiwanese historic buildings described in Chapter 2, as classified into three types, continuous connection, dove-tail connection and flat cut connection, see Figure 6.4.1, with the rotational stiffness values calculated by formulas (6.4.1), (6.4.2) and (6.4.3), respectively.

$$K_{I,C} = 691.12 \times \frac{C_W{}^3 \cdot B_w \cdot E_\perp}{B_d} + 446.83 \qquad (6.4.1)$$

$$K_{I,DT} = 6.223 \times B_w \cdot E_\perp + 446.83 \qquad (6.4.2)$$

$$K_{I,FC} = 104.48 \times \frac{C_W{}^3 \cdot B_w \cdot E_\perp}{B_d} + 72.026 \qquad (6.4.3)$$

where

C_w: column width (m)

B_w: beam width (m)

B_d: beam depth (m)

$E_\perp$: modulus of elasticity of timber perpendicular to grain (kg/cm^2)

K is kgm/rad

From the site survey, three types of beam-to-column joints were identified, namely continuous, flat cut and scarf connection (see Figure 6.4.2). The continuous connections are usually between the corridor beams and the eave beams; in other words, the corridor beam and eave beam are one single piece of timber. The curved beams and decorative beams are cut flat in the end and directly placed on the excavated holes of columns. The main beams and the inner end of the corridor beams are shaped as scarf joint and then inserted into columns.

Compared to the Chuan Dou connections of Fig.6.4.1, the continuous and flat cut beam to column joint are very similar and the stiffness values were calculated with formula (6.4.1) and (6.4.2), respectively. The scarf connection of Dieh-Dou frame is assumed to behave between a dove-tail and flat cut, as the joint is not as tied as dove tail but can resist more moment than a flat cut joint. However, there is lack of data to be certain of the rotational stiffness of this type; therefore, given the limited number of scarf joints present in the frame, the rotational stiffness of this scarf connections are assumed as flat cut joint, which is a lower bound and makes the analysis conservative. Fig 6.4.3 shows the locations of beam to columns and Dou-Gon joints. Finally, the translational stiffness of all joints is 1.8E6N/m.

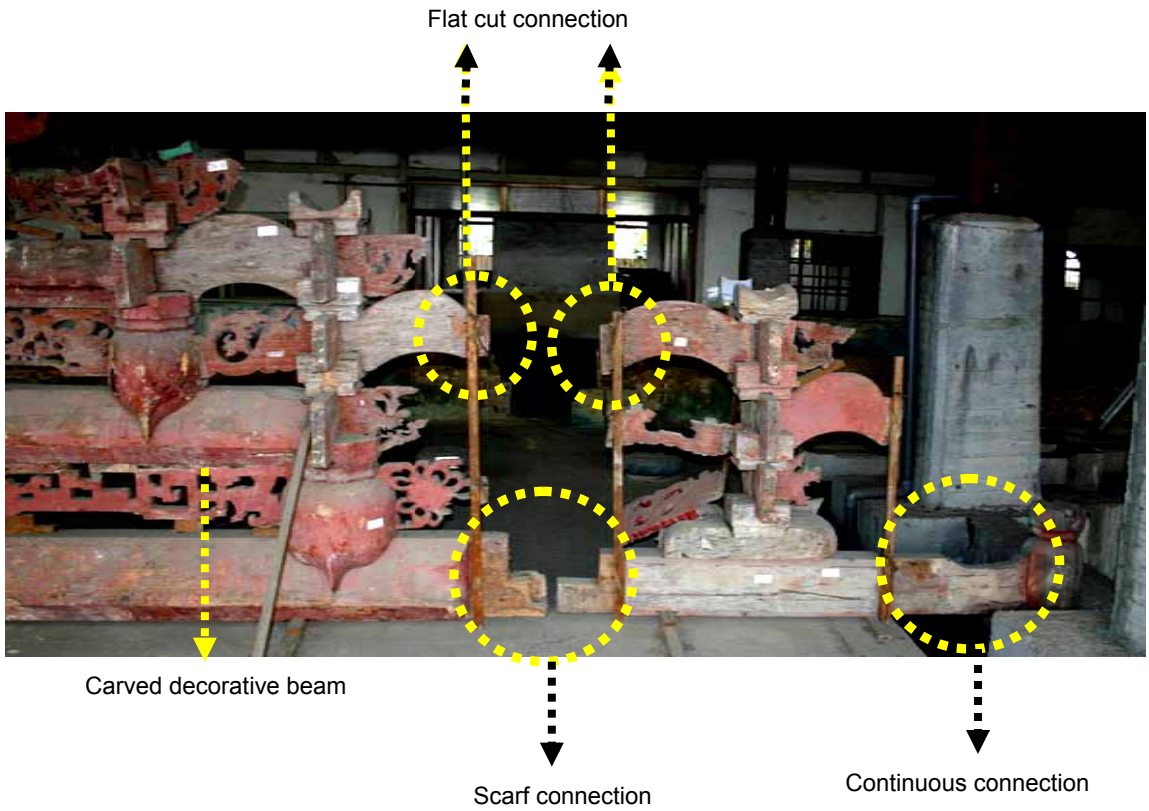

Figure 6.4.2 The three different types of beam to column joints in Dieh-Dou frame

The survey record of Guan-Shi family temple (Hsu, 2002) reports that the main hall building collapsed. The left frame was covered by the debris of the roof, and it was difficult to assess and record its condition. In the right frame, the columns were still connected by corridor beams and some binding beams (Fig. 6.4.4). From the report, it is shown that corridor beams and binding beams in zone A1 were missing and all binding beams located in A2 and C2 pulled out from their position during earthquake. In addition, the binding beams of C1 were damaged. However, in the central zone B, the three main beams and 5 Dou-Gon joints sets and binding beams remained connected and virtually undamaged post-earthquake.

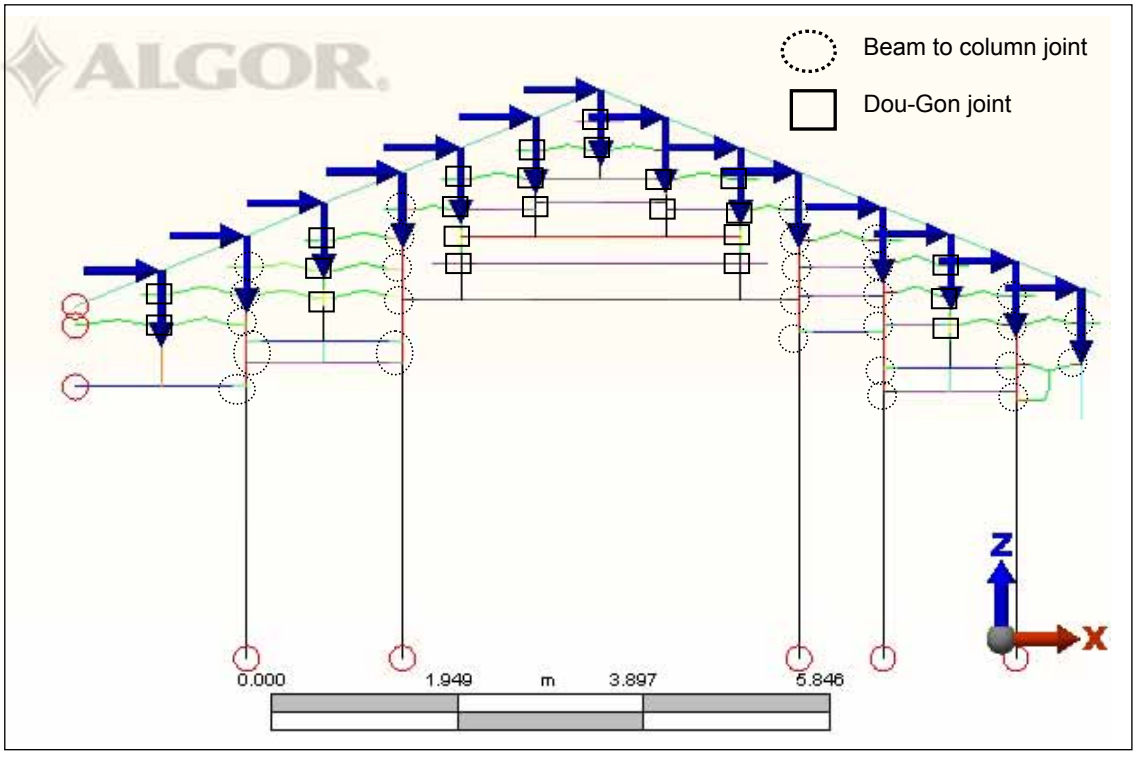

Figure 6.4.3 FE model

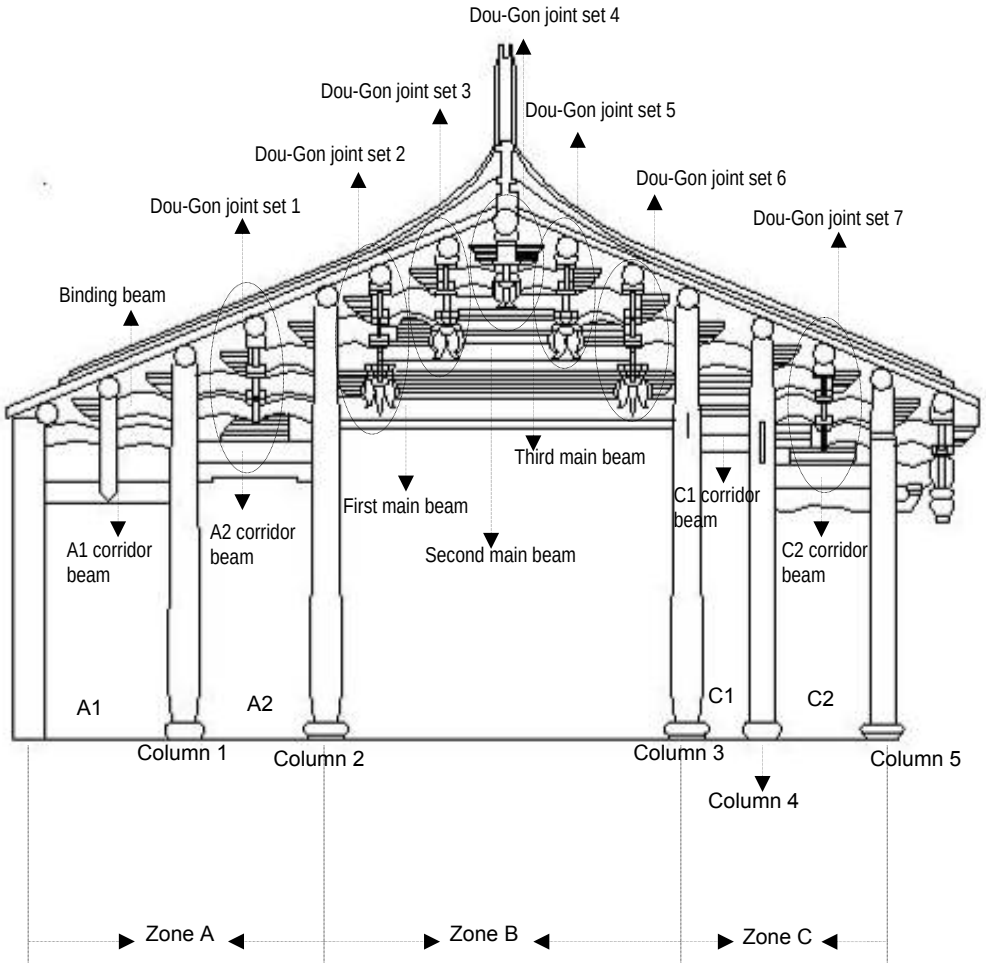

Figure 6.4.4 Dieh-Dou frame of Guan-Shi hall

6.4.2 Result of modal analysis

Natural frequency modal analysis (GS-NF) is performed first. The finite element model described in Chapter 5 was used with the values of stiffness at the joints discussed in section 6.4.1; the appropriate value of mass corresponding to roof weight is lumped over the purlin connection position while the mass of the frame is distributed through the elements geometry. A total of 10 modes are calculated. Circular frequency, frequency and period of each mode are listed in Table 6.4.1. Modal effective mass and participation factor in X and Z direction are included in the same table.

Table 6.4.1 Results of natural frequency modal analysis of Guan-Shi main hall

Mode number	Circular frequency (rad/sec)	Frequency (Hertz)	Period (sec)	Modal effective mass in X direction (%)	Modal effective mass in Z direction (%)
1	5.5136E+00	8.7752E-01	1.1396E+00	97.40	0.00
2	5.6724E+01	9.0279E+00	1.1077E-01	0.01	11.97
3	7.6905E+01	1.2240E+01	8.1700E-02	0.02	33.84
4	8.3953E+01	1.3362E+01	7.4842E-02	0.20	0.00
5	9.3129E+01	1.4822E+01	6.7467E-02	0.04	0.55
6	1.1678E+02	1.8586E+01	5.3805E-02	0.37	0.07
7	1.3382E+02	2.1298E+01	4.6953E-02	0.06	0.70
8	1.5138E+02	2.4093E+01	4.1505E-02	0.25	0.09
9	1.6466E+02	2.6207E+01	3.8158E-02	0.01	0.63
10	1.7962E+02	2.8588E+01	3.480E-02	0.02	5.41

The results indicate that the natural period of the first mode is 1.139 second and its natural frequency is 0.87752 Hertz. It is seen that the first mode has the great majority of mass participation factor in the X-direction, over 97%, confirming the assumption that Dieh-Dou frames behave as a one DOF oscillator with a large mass placed over columns. In the Z direction, the second and third mode contribute with the 12% and 34% of the total vertical mass, with the rest allocated to much higher vibration modes. The substantial difference in frequency between the second and third mode from the first also indicate that horizontal and vertical vibration are substantially decoupled. The calculated values, of course, do not take into account the non-elastic nature of the joints, the effect of friction, and the effect of a possible lack of fit. For these reasons, they need to be considered as indicative of the behaviour rather than the exact value of the real structure.

At the beginning of this chapter, Eurocode 8-1 (2004) was taken as reference document for determining the most appropriate analysis method of Dieh-Dou buildings. This document provided a method to estimate the natural period of the structure in order to confirm if the structure can be analysed with simple lateral force analysis. The formula identified that the natural period should not exceed 2 seconds, a criteria easily met by the first mode period of 1.1396 seconds. However, estimating the first fundamental period by the formula 6.1.2 provided by Eurocode 8-

1 shows a very different result, erroneously suggesting that the structure is much stiffer than what it is (0.2 versus 1.14 seconds). It is, therefore, essential to perform a modal analysis of a historic building with peculiar structural characteristics rather than simply rely on simplified code formulas derived for modern construction.

There is a dearth of in-situ measurements of Dieh-Dou buildings natural frequency that could be used to validate the obtained results. Shiao et al (2003) built a 3D model of a Dieh-Dou building using finite element software STAAD Pro and found that first mode in the plane of the frames was 1.34 seconds, a value higher but reasonably close to what has been found in the present analysis, which confirms the great deformability of these structures.

Figure 6.4.5 illustrates the first 10 mode shapes, where is clear how the deformation of first mode is that of the whole building swaying laterally. Modes 3, 4 and 5 capture the deformed shape of the eave, which clearly vibrates independently of the rest of the structure. This matches the damage to the eaves reported in Chapter 2.

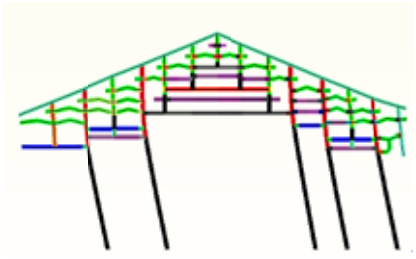

Mode 1

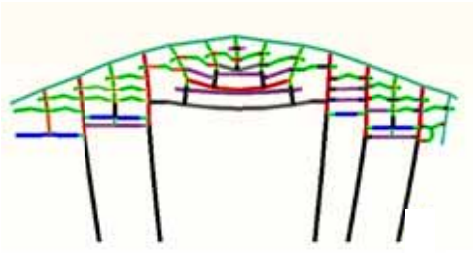

Mode 2

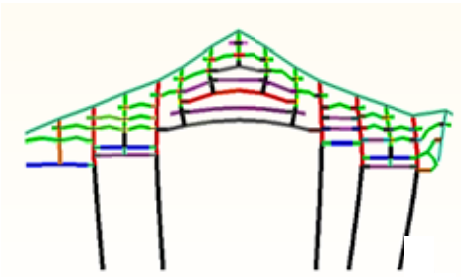

Mode 3

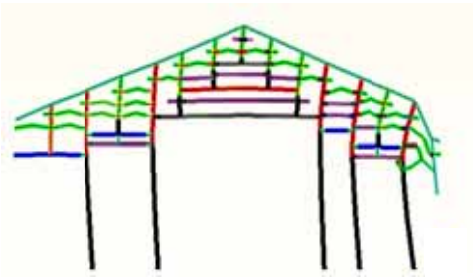

Mode 4

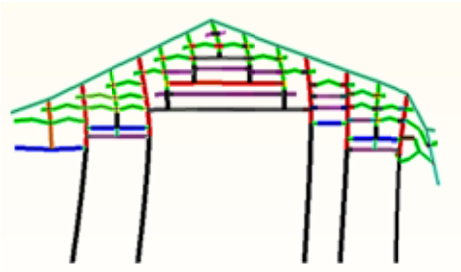

Mode 5

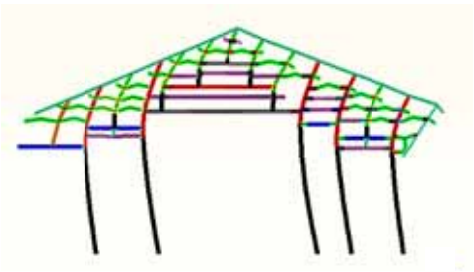

Mode 6

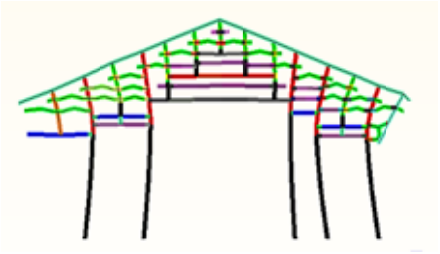

Mode 7

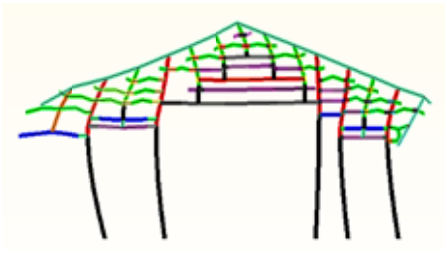

Mode 8

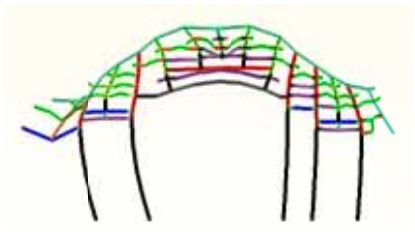

Mode 9

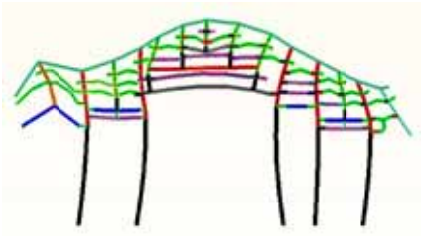

Mode 10

Figure 6.4.5 First 10 modes of GS-NF

6.4.3 Results of lateral force analysis

The total lateral force was calculated according to the formula (6.2.1) of the Taiwanese code, where the spectrum coefficient S_{aD} is a function of: the fundamental period, T_1= 1.14 s, the location of the building, Nan-Tou county, and the soil condition. All the three different soil conditions in the code were considered, as the exact soil profile under the building was unknown. The results imply a total lateral force of 0.225, 0.288 and 0.328 of the vertical weight for the three ground conditions, respectively, that correspond to the ground types B, C and D of the Eurocode (very dense sand or stiff clay, medium-dense sand or clay and loose cohesionless soil). If the lateral force is calculated disregarding the factors in formula (6.2.1) it is equivalent to the ordinate of an elastic rather than design spectrum, and the values are 0.252, 0.322 and 0.367. Also, it will be shown in paragraph 6.4.4 that the ordinate of the real response spectrum for the Chi-Chi earthquake in the location of the building was approximately 0.3-0.35g. Therefore, it was decided to apply a lateral force equal to 0.33 of the vertical weight.

The Taiwanese code provides a method to distribute loads into different floors. As the Dieh-Dou frame is basically one floor only (the roof), the total load was spread and applied at the roof level at each point of connection of the purlins with the frame Fig. 6.4.6.

Two analyses were performed, named GS-LF1 and GS-LF2, the former with lateral loads applied in the +X global direction and the latter in the –X direction, see Fig 6.4.6, to account for the lack of symmetry of the frame.

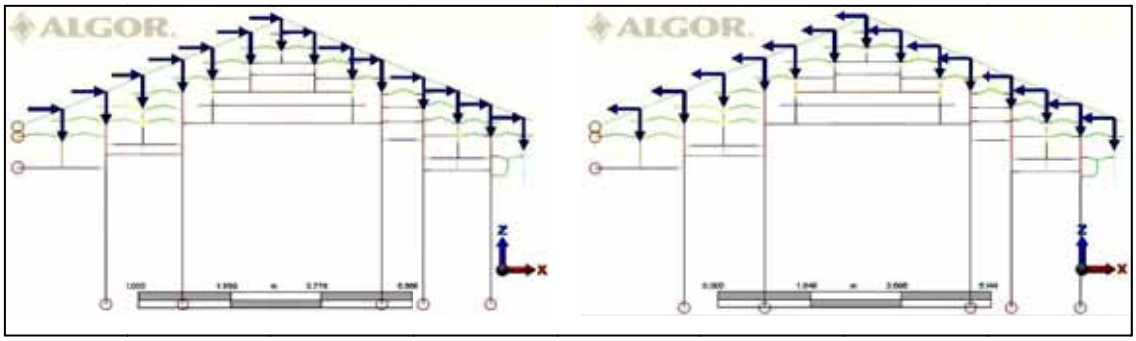

GS-LF1 model GS-LF2 model

Figure 6.4.6 FE model of lateral force analysis of Guan-Shi main hall

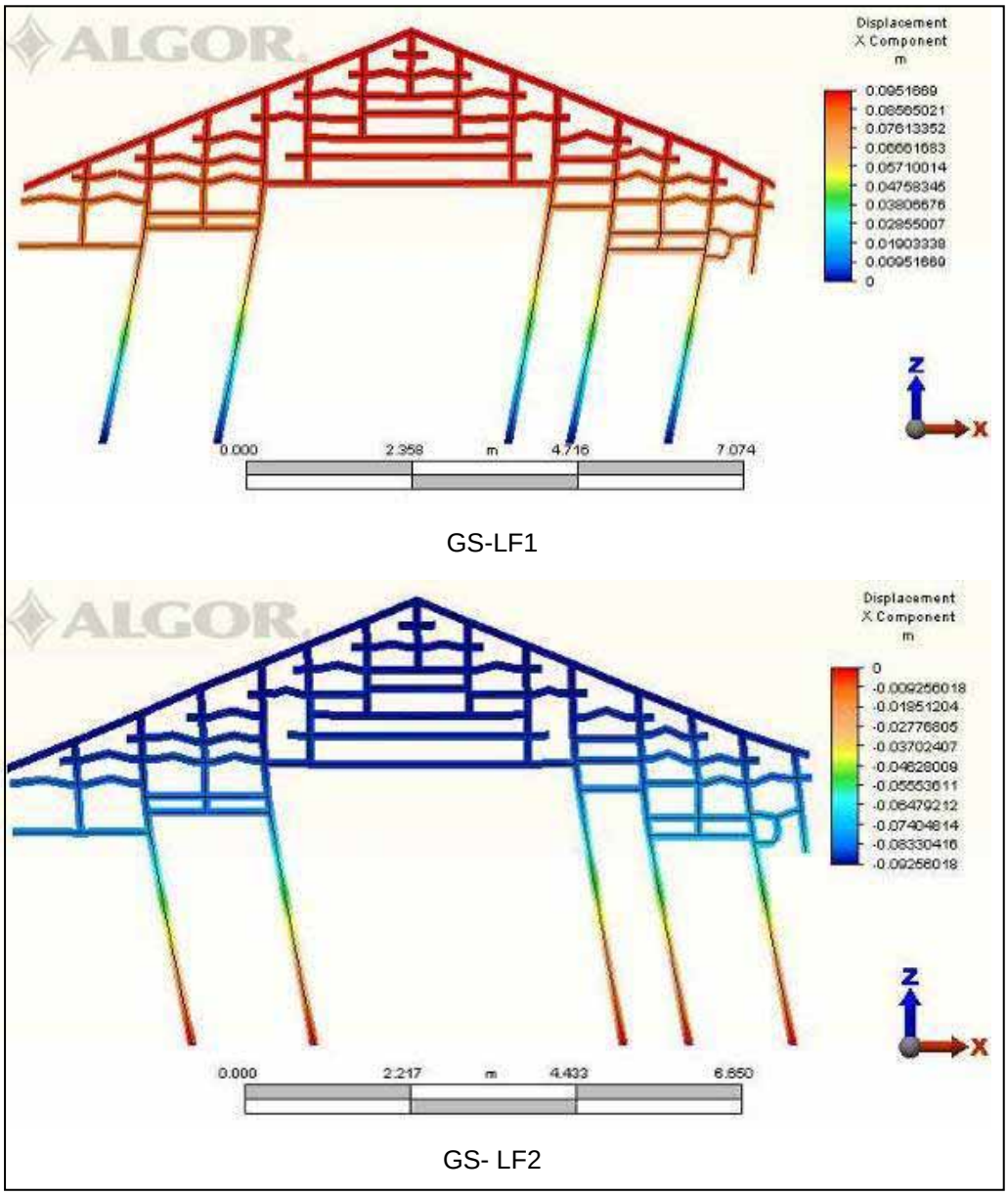

Figure 6.4.7 Deformed shape of GS-LF1 and GS- LF2 with a 5 scale factor on horizontal displacement

The deformed shapes of GS-LF1 and GS-LF2 are plotted in 6.4.7.

To evaluate the global behaviour, the roof apex displacement is considered. In model GS-LF1 the horizontal displacement at the apex is 94 mm, while the result of GS-LF2 is 92 mm, indicating that the global response is almost symmetric, despite the asymmetric layout. The total height of frame is 5930 mm, meaning that the drift of GS-LF1 is 0.0159 and the drift of GS-LF2 is 0.0155.

To evaluate the local behaviour of the frame elements, stresses, forces and moments are taken from the results of the finite element analysis and compared with failure criteria discussed in section 6.2. Structural members and joints of GS-LF1 and GS-LF2 are checked. In both cases, no material failures have been found. However, joints pull out and rotational failure occurred in both cases. Figure 6.4.8 and Fig. 6.4.9 shows the failure pattern of GS-LF1, and GS-LF2, respectively.

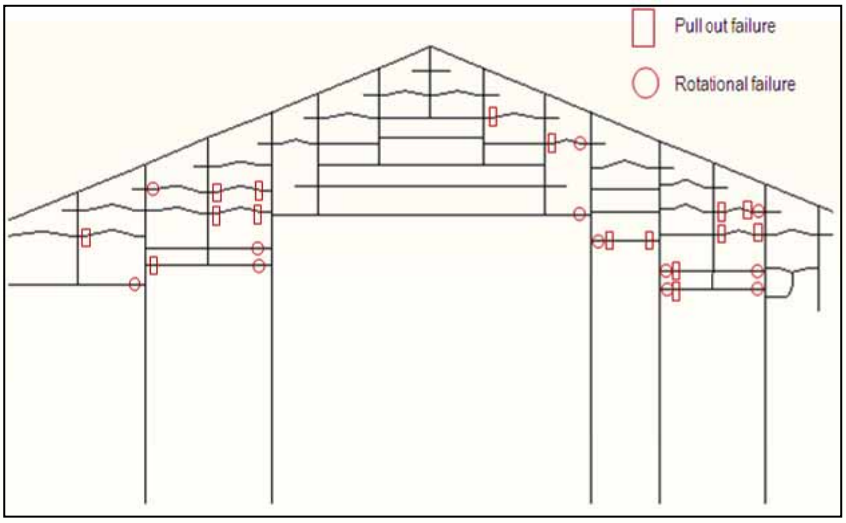

Figure 6.4.8 Joints failures of GS-LF1

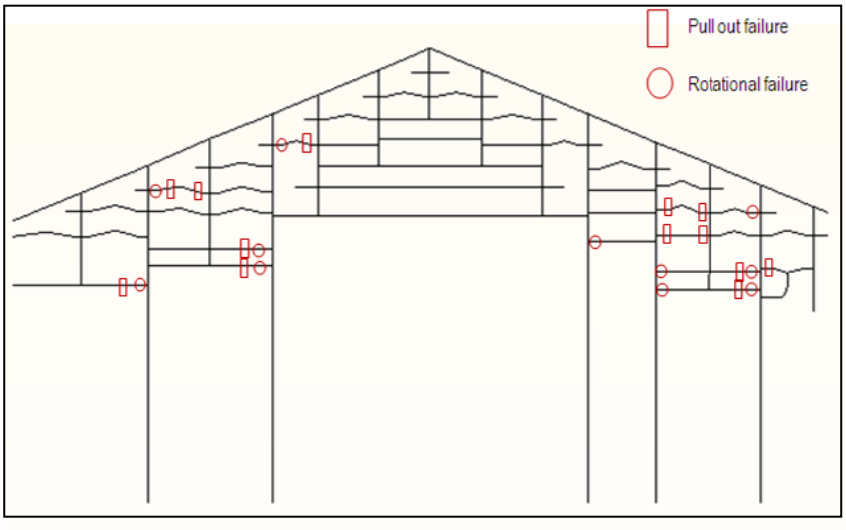

Figure 6.4.9 Joints failures of GS-LF2

From both patterns it appears that failures are less likely to happen in the main space of the frame than the outer parts. Such results match well, in both cases the

observation on the Guan-Shi main hall frame in the post-earthquake survey, which, as already mentioned, record that the central part of frame remained practically intact.

Table 6.4.2 lists the results of GS-LF1 and GS-LF2 in terms of displacement and failure. Besides the already noted greater roof apex displacement of GS-LF1, the total number of joint failure is also greater. The first main beam recorded a rotational failure in GS-LF1 (Fig 6.4.8) while no damage is found in GS-LF2 (Fig 6.4.9), implying that this beam is the critical element of the main space (central part, B) and the slight asymmetry of the structure might affect it differently in the two directions of swaying.

Results of post-earthquake surveys and damage modes of other Dieh-Dou frames discussed in Chapter 3 reveal that the eave is a vulnerable zone of the frame. From the deformed shapes and number of failed elements, this weakness of the eave can be confirmed by the analytical modelling as all the connection elements in the bay behind the eave are pulled out.

Table 6.4.2 Results of lateral force of Guan-Shi main hall

	Lateral force direction	Roof Apex displacement	Number of material failure	Number of pull out failure	Number of rotational failure
GS-LF1	+X	94 mm	None	16	12
GS-LF2	-X	92 mm	None	13	11

6.4.4 Results of response spectrum analysis

In the reports of the Institute of Architects (1999) after Chi-Chi earthquake, it was pointed out that there are more than 400 earthquake record stations spread in Taiwan (of total area 35801 km^2); among them, 24 stations, located near the rupture fault, recorded more than 250gal (0.25g) peak ground acceleration during this event. Guan-Shi family temple is located in Nan-Tou County, where the rupture fault passed. Hsu (2002) indicated that Guan-Shi family temple was close to record

station TCU 076, which is 1 of the 24 stations listed. The exact location of Guan-Shi family temple and record station TCU 076, that are 1.2 km distant between each other, is shown in Table 6.4.3. The Guan-Shi temple was about 18 km from the epicentre of the earthquake.

Table 6.4.3 Location of Guan-Shi family temple and record station TCU 076

	Longitude	Latitude
Guan-Shi family temple	120.6884 East	23.9128 North
TCU 076	120.4054 East	23.5447 North

The reports of the Institute of Architects (1999) contain the accelerometer readings from these 24 stations, which were transferred to a response spectrum having assumed a 5% damping in the three directions (North-South, North-East and Up-Down). Fig. 6.4.10 shows the response spectrum for the East-West direction at station TCU 076, corresponding to the +X direction of the frame.

In order to insert the spectrum into ALGOR ©, the plot is redrawn and approximated as shown in Fig. 6.4.11.

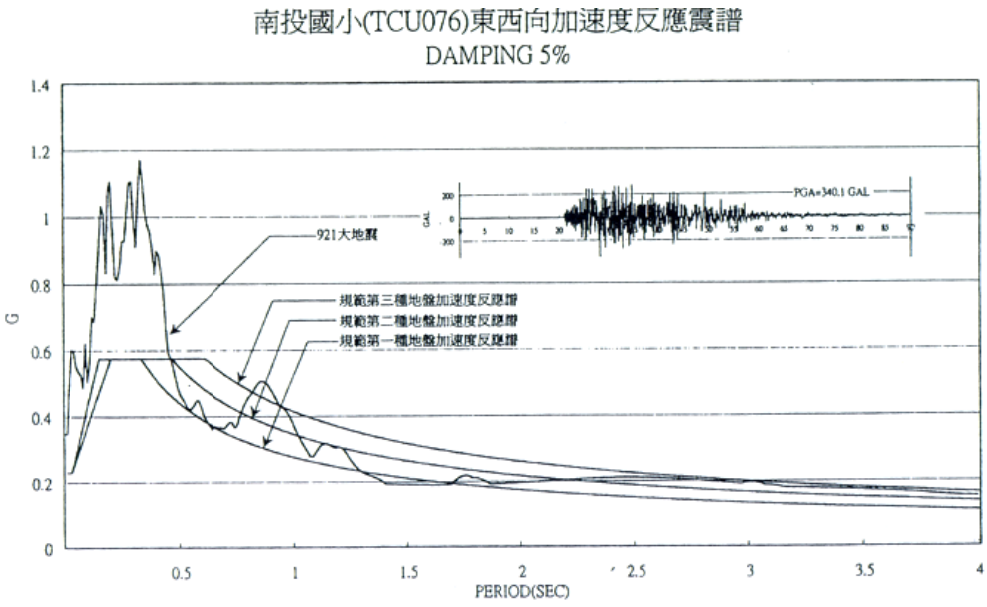

Figure 6.4.10 TCU 076 response spectrum from reports of the Institute of Architects (1999)

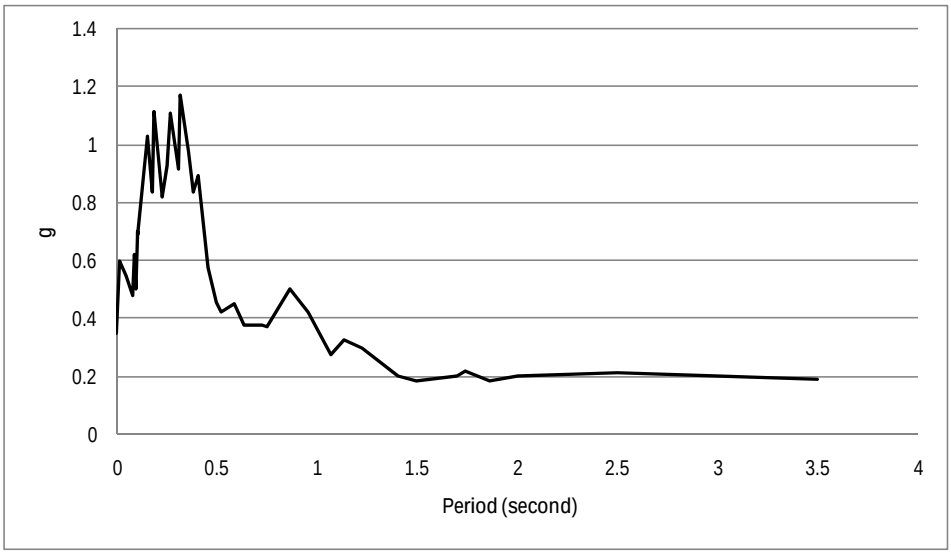

Figure 6.4.11 Response spectrum of East-West of TCU 076

As all the structure's modes are considered in the response spectrum, the natural frequency modal analysis previously performed is used. It has to be noted that the acceleration corresponding to the natural period of the structure (1.14 seconds) is of the order of 0.3-0.35g, in good agreement with the value assumed in the lateral force analysis. Figure 6.4.12 shows the deformed shape of the response spectrum analysis (GS-RS).

The roof apex displacement in the response spectrum of Guan-Shi main hall (GS-RS) is 107.5 mm with a drift of 0.018. As far as failure criteria are concerned, results again show that no material failure occurred, while joint failures are depicted in Fig. 6.4.13.

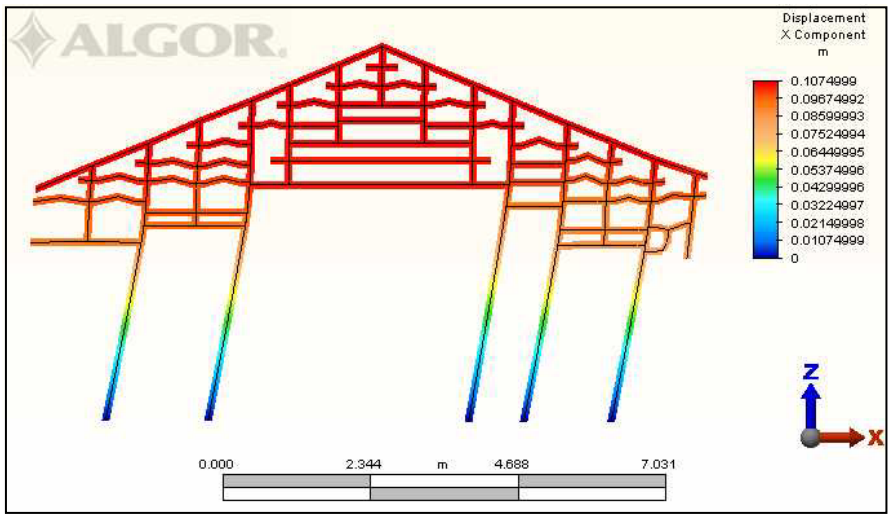

Figure 6.4.12 Result of response spectrum analysis (GS-RS)

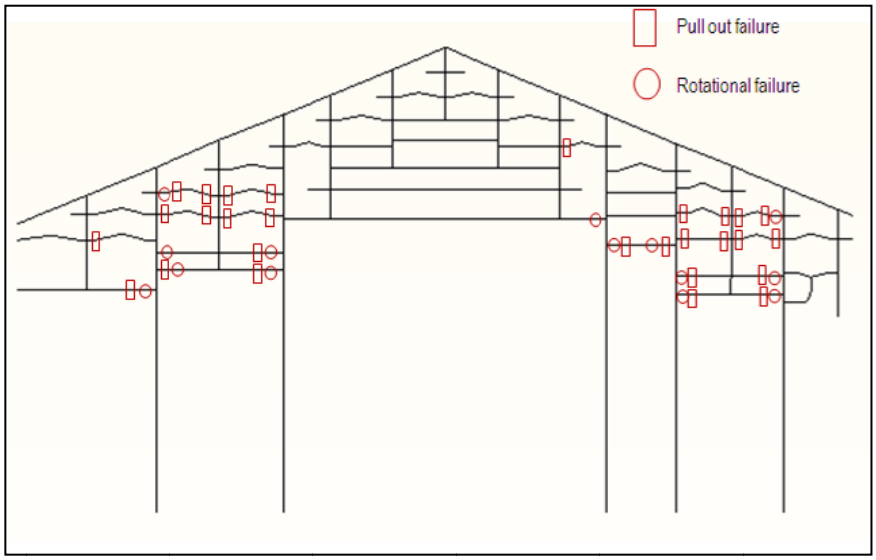

Figure 6.4.13 Joints failures from response spectrum (GS-RS)

A total of 27 joints pulled out in this analysis and there were 14 rotational failures, a higher number of damaged joints than in lateral force analysis, Table 6.4.2. The central part of the frame (zone B) suffered much less failure than the outer parts (zone A and C), similarly to the lateral force analysis. Zones A-2 and C-2, at the connection with Column 1- 2 and 4- 5 respectively (see Figure 6.4.4), present the highest proportion of damage. It appears that a FE analysis with proper rotational and translational stiffness and appropriate criteria can identify the zones of Dieh-Dou frames likely to be damaged and generally critical under earthquake.

It should be noted that in the two lateral bays, the total number of failure in the GS-RS model is equal to the summation of the GS-LF1 and GS-LF2 models. This is due to the superposition of effect procedure chosen, the SRSS method, which sums up all effect as positive. It can be considered that this is realistic as cycle reversals would occur during an earthquake, so that the overall damage is the results of successive right and left sway.

6.4.4 Results of nonlinear static pushover analysis

In the introduction to the nonlinear static step by step pushover analysis of section 6.2.2, it was discussed how the classic pushover analysis is based on the first mode of vibration of the structure. The modal analysis of Guan-Shi main hall frame shows

that the in-plane fundamental mode has the great majority of the proportion of participating mass, equal to 97.40% in X direction, see Table 6.4.1. The finite element model is the same as the lateral force and response spectrum analysis. As the lateral force analysis showed the behaviour of the structure to be similar but slightly critical in the +X direction, the pushover analysis is performed along +X. A target lateral force, which is the same value used previously, of 0.33 of vertical weight is set as the final step of pushover analysis.

The pushover analysis is run as a succession of elastic runs opportunely modified depending on the output of the previous run, with the aid of a Visual Basic routine interfaced with the ALGOR © output environment opportunely written to help with the lengthy process of analysing each element at each step and identifying the critical elements to be deactivated in the next step. This choice has been made as the software did not feature the possibility of running a pushover analysis automatically accounting for the deactivation of the spring elements used to model the joints.

For each incremental run, there are two possible results:

- One or more failures occur
- No failure is found, neither material failure nor joint failure

In the first case, the corresponding element or joint is deactivated or released in the numerical model and a subsequent run is performed under the same lateral load as the previous and the checking procedure repeated. In the second case, a new load increment is applied and the procedure is repeated

In the step-by-step analysis of the Guan-Shi main hall frame, a total of 27 steps were performed until the lateral force target, 0.33g, was reached. Details of failures at each step are illustrated in Appendix A. Figure 6.4.14 shows the relationship between structure displacement and lateral equivalent acceleration.

The result of step by step analysis shows that elements start to fail, when the lateral load is still relatively low. At step 06, where the lateral equivalent load acceleration is 0.009g, the roof apex lateral displacement surpasses the drift of 0.005. Up to step 08 (Fig. 6.4.15), where lateral equivalent load is 0.132g, there are only pull out

failures, and this phenomenon highlights the importance of translational stiffness and pull out capacity in these timber buildings built by small pieces stacked and without metal nails. Traditionally, the pull out capacity and translational stiffness are disregarded during analysis, but this study shows that for such buildings this feature needs to be considered for an accurate modelling as these elements tend to be dislocated and this can reduce the global stiffness of the structure.

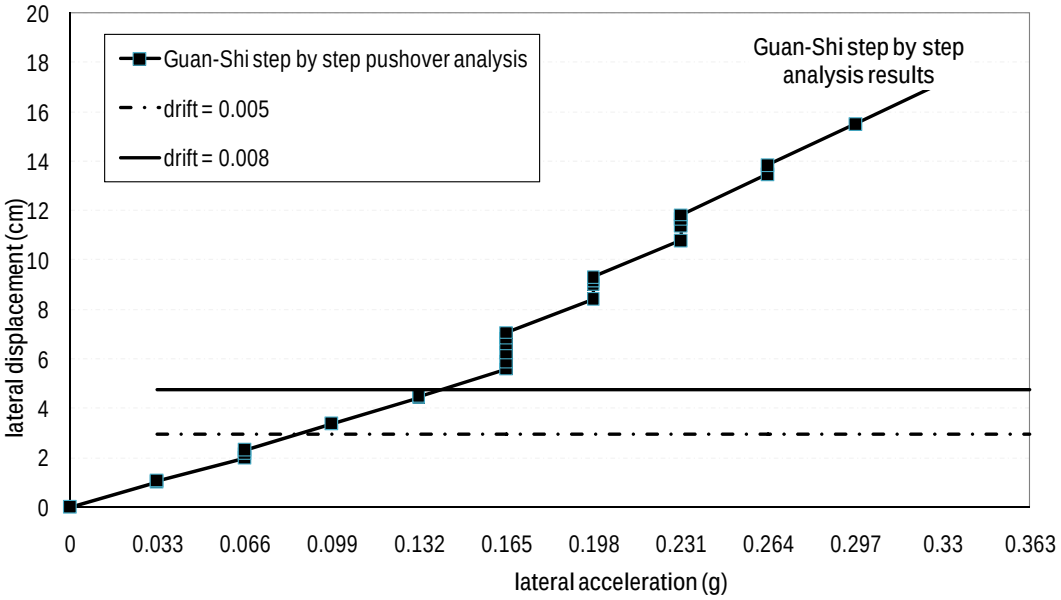

Figure 6.4.14 Structure displacement and lateral equivalent acceleration (Guan-Shi)

In the 9th step, where the lateral equivalent acceleration reached 0.016g, that is half of the total value applied, joint rotational failures started to occur. At this step, the roof apex met the drift of 0.008. At step 12, while lateral equivalent acceleration remained 0.016g, and at load equal to 0.165, several failures occurred implying this is a critical stage for Guan-Shi main hall frame.

At step 18, the roof apex displacement is close to the maximum reached in the lateral force analysis (GS-LF 1 and GS-LF 2); however, the lateral force at this step is only 60% of the lateral analysis. At step 19 the structural drift is close to the result found with the response spectrum analysis. At step 27, where step by step analysis ended and the lateral equivalent acceleration is 0.33g, a roof apex displacement of 176 mm is reached, nearly double than in the lateral force analysis. Failures up to these stage and details are shown in Fig. 6.4.15 and Table 6.4.4.

Table 6.4.4 Details of steps surpassing the elastic target drifts (Guan-Shi main hall)

	Lateral force (Equivalent g)	Roof Apex displacement	Drift	Material failures	Number of pull out failures	Number of rotational failures
Step 06	0.009g	3.38cm	0.0057	None	5	None
Step 08	0.132g	4.50cm	0.0075	None	6	None
Step 09	0.165 g	5.58 cm	0.0094	None	8	2
Step 12	0.165 g	6.62 cm	0.0111	None	10	7
Step 18	0.198 g	9.31 cm	0.0157	None	11	14
Step 19	0.231 g	10.80 cm	0.0182	None	11	18
Step 27	0.330 g	17.56 cm	0.0296	None	15	26

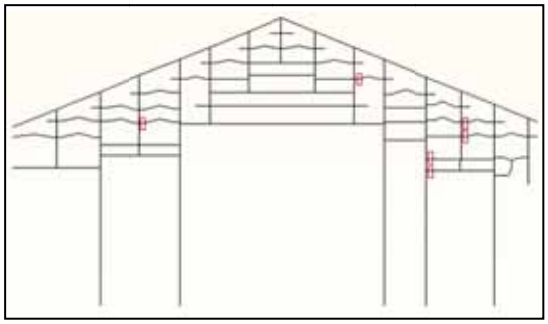

Failures up to step 08

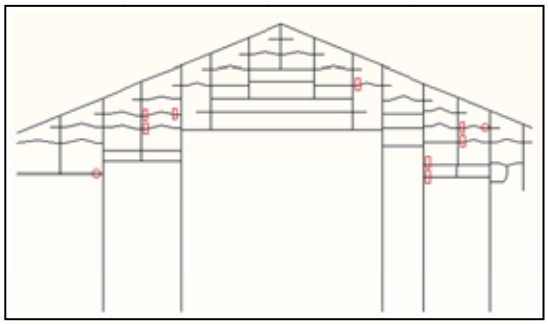

Failures up to step 09

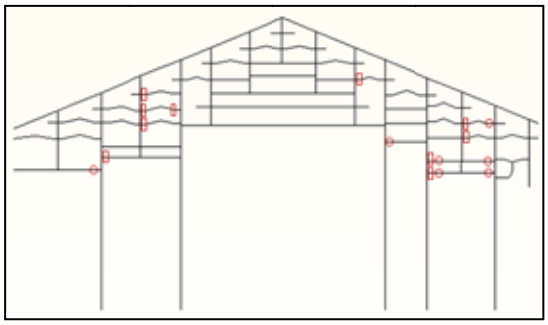

Failures up to step 12

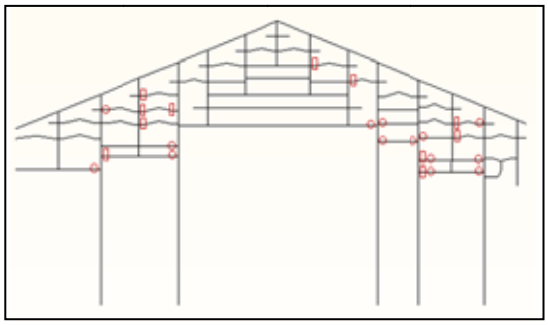

Failures up to step 18

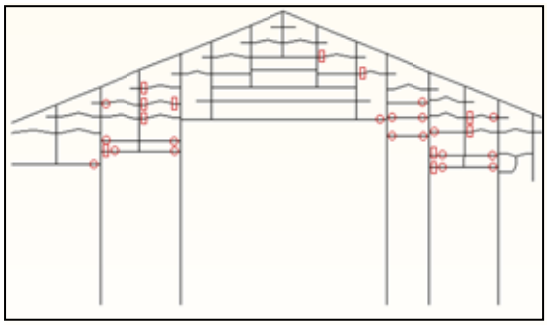

Failures up to step 19

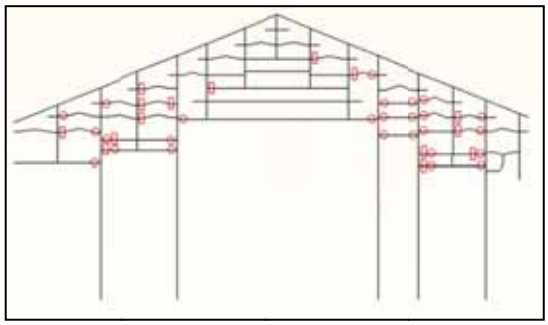

Failures up to step 27

Figure 6.4.15 Failure up to steps 08, 09, 12, 18, 19 and 27 (Guan-Shi temple frame)

The frame initially suffered pull out failures, then rotational failures, mostly located outside the zone of the main span. This compares well with the failure survey of Guan-Shi family temple main hall frame post earthquake, where the elements of corridor parts were pulled out while the elements of the main span were still in position and kept contributing to the lateral transfer of load.

In the step by step analysis the lateral load increased when no failures occurred, but there were many steps under the same load with increased failed number of joints. To better visualize the energy dissipated by the structure during failure, Fig. 6.4.14 was modified to account for the non-linear elastic behaviour in which all increasing lines, representing the steps where no failures occurred, are joined together, as are the horizontal lines, representing the steps where failure occurred, see Fig. 6.4.16.

From Fig.6.4.16 it is clear that two different slopes can be identified on the oblique line, with the slope changing at 0.165g, implying that the frame is stiffer until the equivalent acceleration is 0.165g. The initial structural stiffness is drawn as a dotted line. Thus, the failures at the level of 0.165g, step 09 to step 14, greatly affect the structural stiffness, see Appendix A. The two elastic drift criteria are also drawn in Fig. 6.4.16, showings that the greater of the two clearly identifies the end of the elastic stage of the analysis.

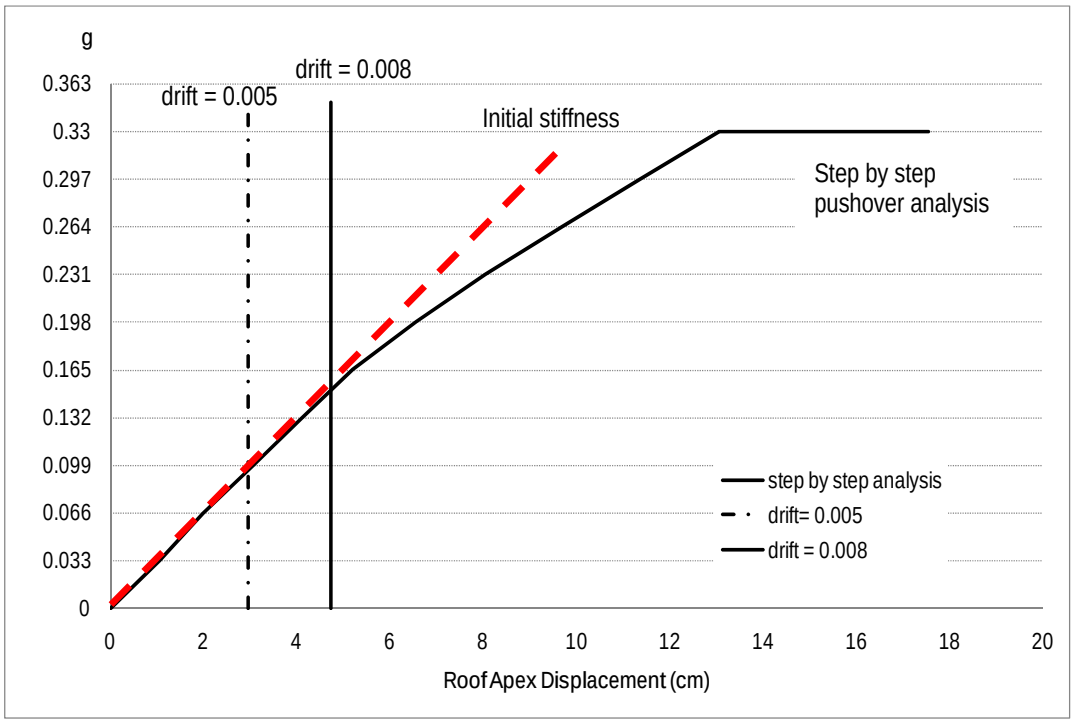

Figure 6.4.16 Results of step by step analysis (Guan-Shi temple frame)

6.4.5 Comparison of failures between the three analyses

The survey made by Hsu (2002) after the 1999 Chi-Chi earthquake indicated that the central part of the right frame of the Guan-Shi temple (Zone B) remained mostly intact, while most horizontal elements in the right and left zones of the frame (Zones A and C) were separated from columns. The left zone of the frame had the majority of the elements disconnected from the columns.

The results of all three analyses show that the central part of frame, Zone B, remains intact, which matches with the actual observation. In the Zone C-1 of the real frame the lower horizontal beam was disconnected from the central zone, with the upper one still connected. The lateral force analysis GS-LF1 (Fig. 6.4.8), the response spectrum analysis GS-RS (Fig. 6.4.13), and step 15 (Appendix A) of the pushover catch this failure, while lateral force analysis GS-LF2 (Fig. 6.4.9) does not, confirming that forces directed along +X are more critical.

When comparing lateral force analysis GS-LF1 (Fig. 6.4.8) and response spectrum analysis (Fig. 6.4.13), is seen that the majority of elements of areas A-2 and C-2 failed in the response spectrum analysis and lost connection with columns, while a smaller number of failed elements were found with the lateral force analysis GS-LF1. When compared with the actual failure pattern, it can be concluded that in this case the response spectrum analysis was more accurate. In the pushover analysis, to match with the result of response spectrum analysis and real failure in terms of failed elements we have to reach step 19, with a lateral equivalent acceleration of 0.231 g and roof apex displacement of 10.8 cm. It is also seen that roof apex displacement between response spectrum analysis and step 19 of step by step analysis are very close, 10.75 cm versus 10.8 cm. Furthermore, step 19 is the first step when the structure enters the second slope in the capacity curve, see Fig. 6.4.16, where the stiffness of the frame starts to decrease. These clearly show that the failure of the connection in pull out is drift sensitive rather than capacity sensitive as one might be inclined to initially think.

The structural stiffness under these three analysis methods is plotted in Fig. 6.4.17. It is shown that

$$K\text{-}LF > K\text{-}PO1 > K\text{-}RS > K\text{-}PO2 \qquad (6.4.1)$$

where K-PO1 is the step by step analysis up to 0.165g (step 18, 0.165g) and K-PO2 is after step 19 (0.198 g). The equivalent lateral acceleration in the response spectrum is estimated as 0.325g, because the first period of vibration, with 97.4 % mass participation in X direction, is 1.139 sec (Table 6.4.1) and the correspondent value in the response spectrum of the record station of the 1999 Chi-Chi earthquake is 0.325g (Fig. 6.4.11).

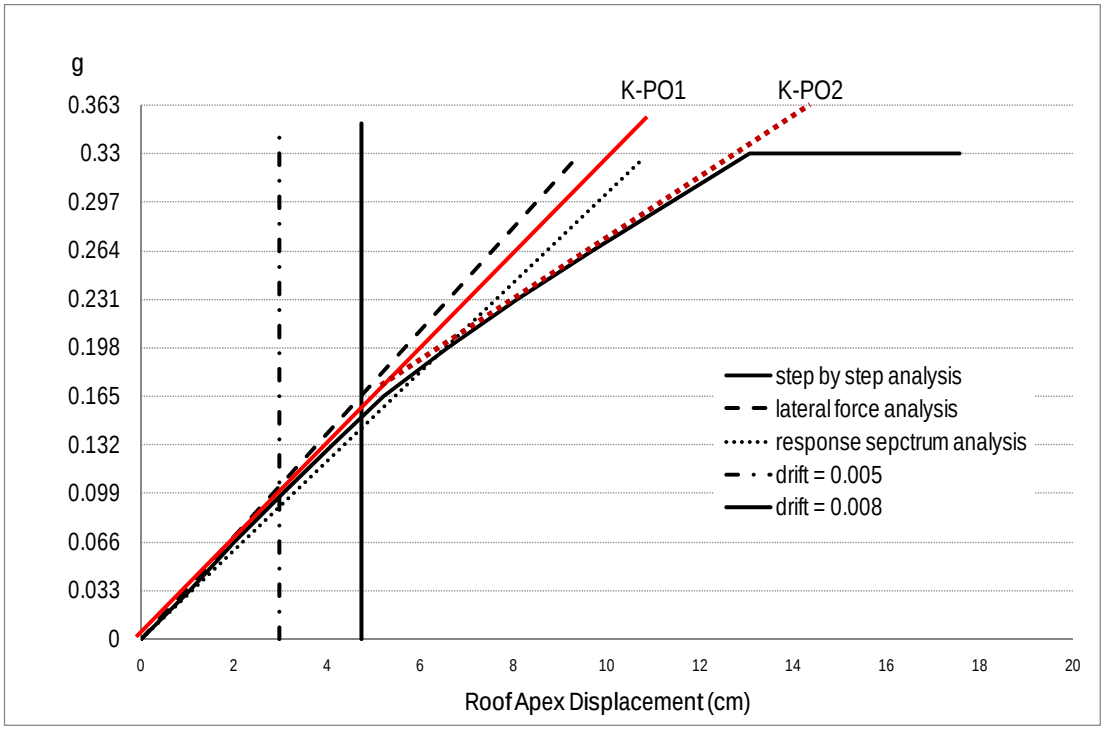

Figure 6.4.17 Structural stiffness according to the three analyses

In conclusion, it is shown the finite element model proposed in this project can be used to analyse a Dieh-Dou frame realistically. The response spectrum analysis, with spectrum taken from the real earthquake event, compared reasonably with the actual frame as the failure pattern matches the reality well, identifying the fact that rather than for material failures the elements of this buildings fail at the connection in terms of pull out or excessive rotation. From modal analysis, it is shown the Dieh-Dou frame fundamental period is much higher than the peak of response spectrum of the Chi- Chi earthquake (Fig. 6.4.11), which makes the timber frame suffer lower inertia load than, for example, a masonry structure would in such strong seismic event, as the first period of 1 storey masonry walls can be between 0 and 0.5 seconds. This can explain why the masonry walls encasing the frames and

providing lateral support, generally fail sooner and separate from the timber structure.

Lateral force analysis is shown to be sufficiently close to response spectrum analysis in terms of displacement and failure mode, although the pushover analysis is the one most capable to identify the criticality and the importance of the elements, also allowing to assess the loss of stiffness of the structure as the loads increase, and is, therefore, needed to get the most accurate picture, as it will be shown later in the discussion in section 6.6.

For getting quick results, lateral force analysis can be applied; however, its lack of ability to catch the progressive failure pattern may render it slightly unconservative, and it is suggested that to assess structures under strong seismic events like the 1999 Chi-Chi earthquake with lateral force analysis, opportunely conservative safety factors are adopted.

In order to confirm the applicability of the analysis methods described above for the Guan-Shi family temple and draw more general conclusions, a second Dieh-Dou building is analysed in the following section.

6.5 Application 2
Main hall of Dou-Shan family temple

6.5.1 Introduction of Dou-Shan family temple

The Dou-Shan Hsiao family temple is located on Changhua County, in the central part of Taiwan. According to the Dou-Shan Temple Commission (2008), it was first built between 1796 and 1820, and later major construction works were undertaken in 1880 by the Hsiao family. The temple compound consists of six independent buildings: main hall, front hall, and four additional buildings used nowadays as galleries and offices. Yards and gardens surround the buildings. The Main hall and front hall were built by timber frames enclosed with masonry walls and the frames

are in Dieh-Dou style, while the other four additional side buildings are of modern construction.

Two Dieh-Dou frames forming the main hall are laid parallel with the same layout, which is shown in Fig. 6.5.1. Each frame can be subdivided as central main space (zone B in Fig. 6.5.1), and two sets of lateral bays (zone A and C). The central main space is symmetric with three main beams and five Dou-Gon joints set, typical as main hall and similar to the Guan-Shi temple analysed previously.

The extreme bay in zone A is linked to the masonry wall, while zone C is the entrance area of the main hall buildings and fronted by the eaves. The outer right column of zone C shown in Fig 6.5.1 is made of stone for two thirds of its height and timber for the remaining third. This mixture of two materials supporting the eaves is occasionally seen in Dieh-Dou buildings, and differs from the previous example.

Hsu (2003) surveyed the Dou-Shan temple after the 1999 Chi-Chi earthquake. His reported that, although the temple is located in an area where peak ground accelerations of 250 to 400 gal (0.25 to 0.4g) were recorded, the main and front hall of the temple were still standing, however a few elements were missing or damaged. The enclosed masonry walls were severely cracked but did not collapse. Furthermore, pull –out of joints was observed in several locations.

Fig 6.5.2 and Fig, 6.5.3 highlight the elements that were reported missing or damaged by Hsu's post earthquake survey (2003) and government report (http://web.cca.gov.tw/imfor/921/14.htm), in the left and right frame, respectively. The majority of the damaged elements are located in the bay corresponding to zone C.

The failure pattern can be used as comparison with the results of the FE analysis, where one frame of the main hall is built in ALGOR © with the corresponding rotational and translational stiffness. Similarly to the Guan-Shi temple, lateral force, response spectrum and pushover analysis are performed and described in the following section.

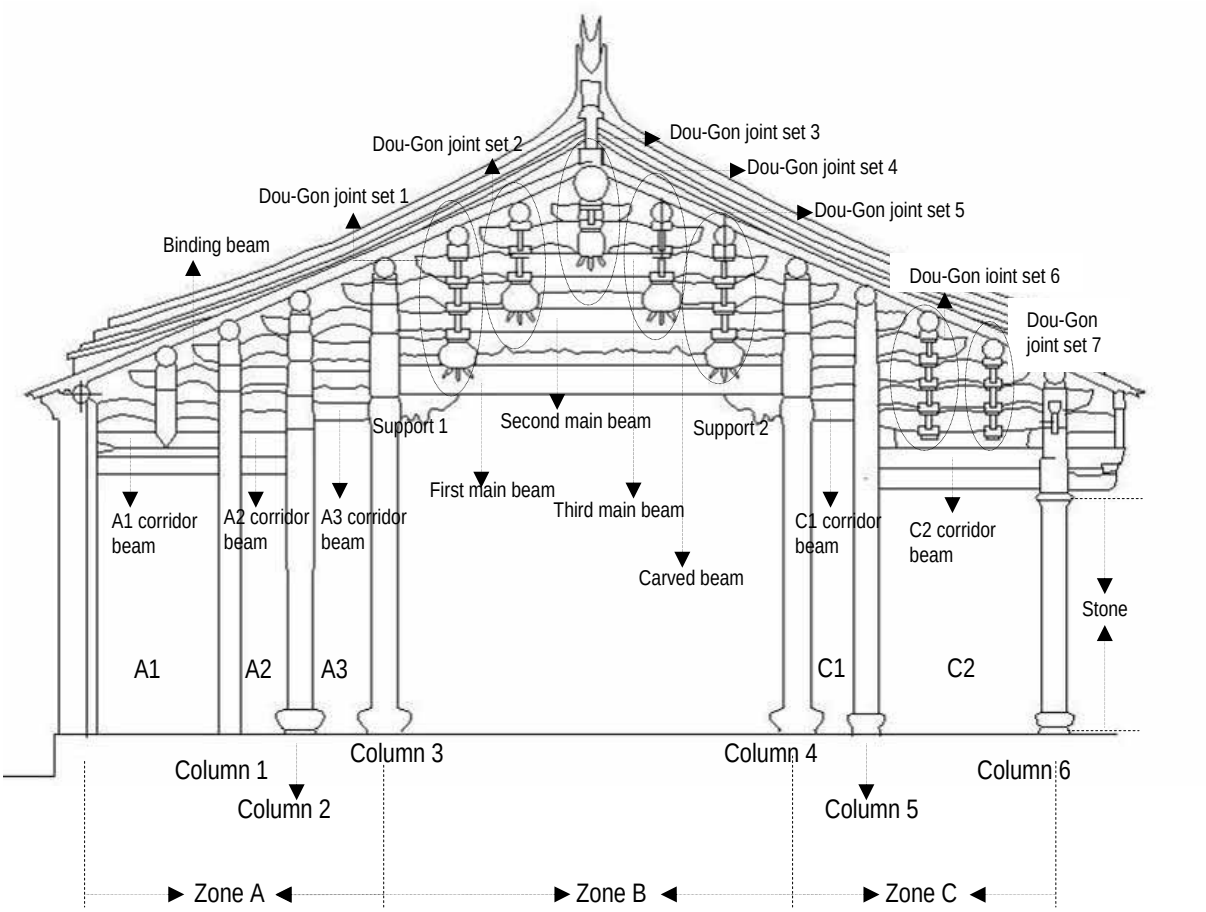

Figure 6.5.1 Dieh-Dou frame of Dou-Shan main hall

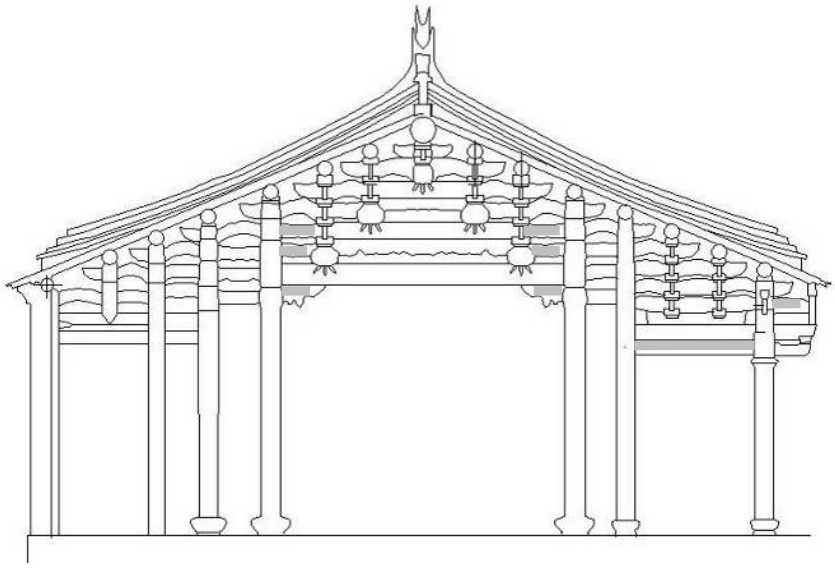

Figure 6.5.2 Damaged elements of Dou-Shan main hall timber left frame

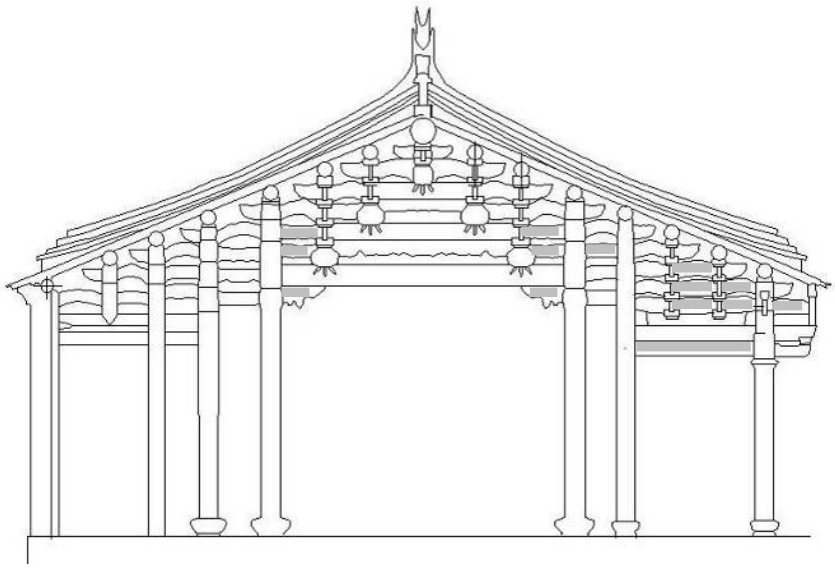

Figure 6.5.3 Damaged elements of Dou-Shan main hall right timber frame

6.5.2 Modal analysis

The Finite element model DS-NF was created to calculate the free oscillation elastic frequencies of the frame as already seen in the previous examples. Circular frequency, period of each mode, and modal effective mass in X and Z direction are summarised in Table 6.5.1. In addition, the first 10 modes are shown in Fig. 6.5.4.

Table 6.5.1 Results of nature frequency modal analysis of Dou-Shan main hall frame

Mode number	Circular frequency (rad/sec)	Frequency (Hertz)	Period (sec)	Modal effective mass in X direction	Modal effective mass in Z direction
1	6.7439E+00	1.0733E+00	9.3168E-01	97.28%	0.00%
2	5.9186E+01	9.4197E+00	1.0616E-01	0.05%	8.11%
3	7.7998E+01	1.2414E+01	8.0556E-02	0.11%	32.34%
4	8.6600E+01	1.3783E+01	7.2555E-02	0.31%	3.22%
5	9.3031E+01	1.4806E+01	6.7539E-02	0.08%	1.84%
6	1.4908E+02	2.3726E+01	4.2147E-02	0.01%	2.27%
7	1.5264E+02	2.4293E+01	4.1164E-02	0.46%	0.87%
8	1.6558E+02	2.6354E+01	3.7945E-02	0.04%	0.30%
9	1.7079E+02	2.7182E+01	3.6789E-02	0.01%	0.06%
10	1.9336E+02	3.0771E+01	3.2498E-02	0.01%	0.48%

The results point out that the natural period of the first mode is 0.93168 s and natural frequency is 1.0733 Hertz. The first mode has the great majority of mass participation in the X direction, over 97%. The mode 3 shape, where there is a contribute of 32.34% of excited vertical mass, indicates that Zone C-2 (see Fig. 6.5.1) deformed more than other zone. Failures resulting in this area are due to vertical excitation. Due to the modest stiffness of the connections, many of the modes are local ones.

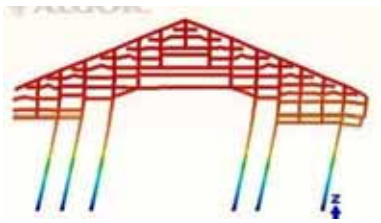

Mode 1

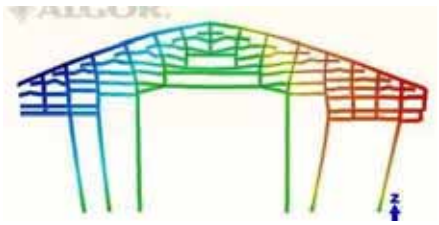

Mode 2

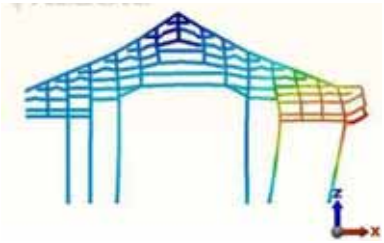

Mode 3

Mode 4

Mode 5

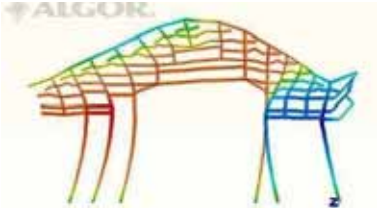

Mode 6

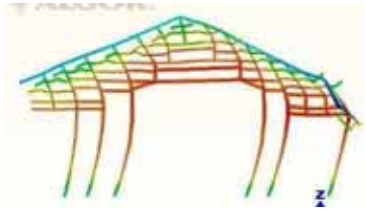

Mode 7

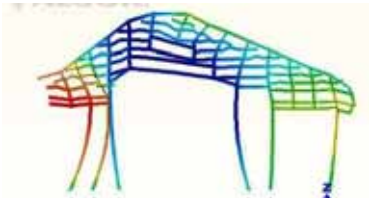

Mode 8

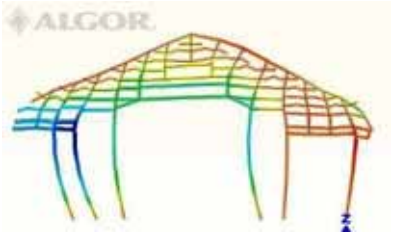

Mode 9

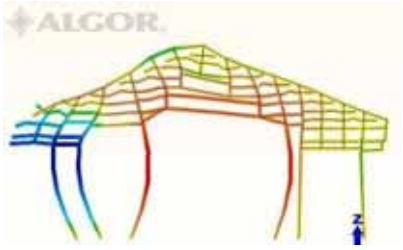

Mode 10

Figure 6.5.4 First 10modes of Dou-Shan main hall frame

6.5.3 Results of lateral force analysis

Two analyses were performed with lateral force, namely DS-LF 1 and DS-LF 2. In DS-LF 1, lateral forces were applied in the +X direction (Fig. 6.5.5), while in DS-LF 2 forces were applied in the –X direction (Fig. 6.5.6). The timber properties are as described in the previous chapter; while the mass density of the stone in the beam elements simulating the eave column was set as 2700 kg/m^2, and the MoE as 5E+10 N/m^2.

Fig. 6.5.7 and Fig. 6.5.8 illustrate the deformed shape of the FE model under equivalent acceleration 0.33g, amplified by a factor of 5. A summary of the results of these two analyses is listed in Table 6.5.2.

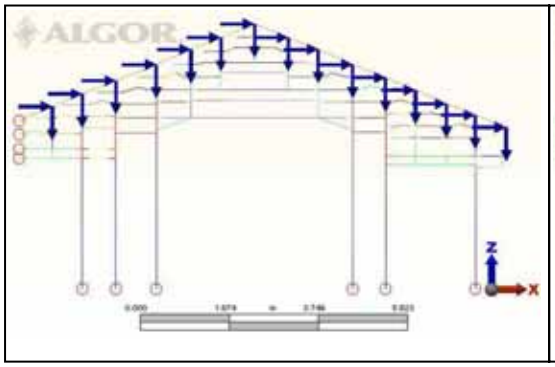

Figure 6.5.5 DS-LF 1 model

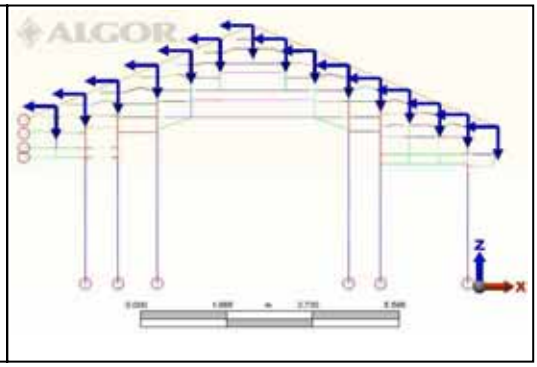

Figure 6.5.6 DS-LF 2 model

Table 6.5.2 Results of lateral force of Dou-Shan main hall

	Lateral force direction	Column 6 simulation	Roof Apex displacement	Number of material failure	Number of pull out failure	Number of rotational failure
DS-LF1	+X	1	65.07mm	None	10	8
DS-LF2	-X	1	64.69mm	None	14	8

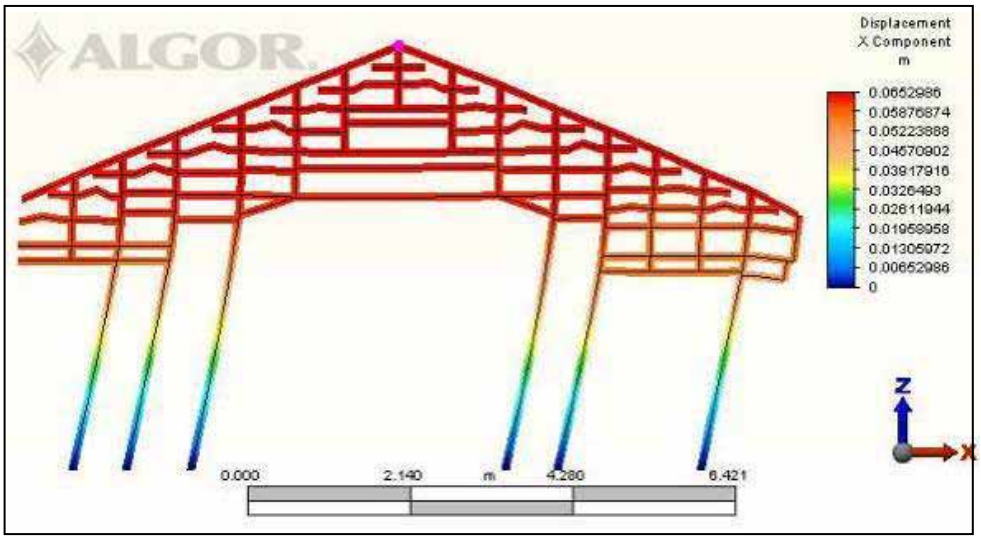

Figure 6.5.7 Deformed shape of DS-LF 1

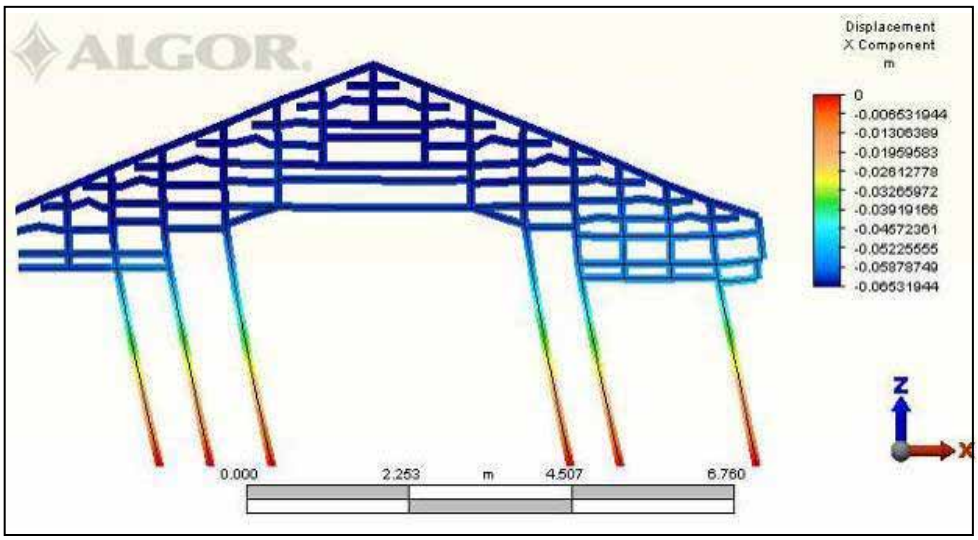

Figure 6.5.8 Deformed shape of DS-LF 2

The height of Dou-Shan main hall is 559 cm, so the drifts of 0.005 and 0.008, are equal to 2.795cm and 4.472 cm, respectively. Roof apex displacements in these two analyses are over these drift values, suggesting that some damage occurs in the frame, although they are substantially smaller than in the Guan-Shi temple. According to the report, the building remained standing post earthquake with some elements' failure, and this global behaviour matches with the finding of the computer simulation.

The results of these two models are very similar, in terms of roof apex lateral displacements and numbers of joints failures. The patterns of failure in both

analyses (Fig. 6.5.9 and Fig. 6.5.10) show that Zone C is more vulnerable than Zone A and the central part Zone B. The two bracket supports under the first main beam (Fig. 6.5.1) are damaged in both analyses. The binding beams connecting columns 3 and 4 with the first series of Dou-Gon joints are failed in DS-LF 2 and DS-LF 1 respectively.

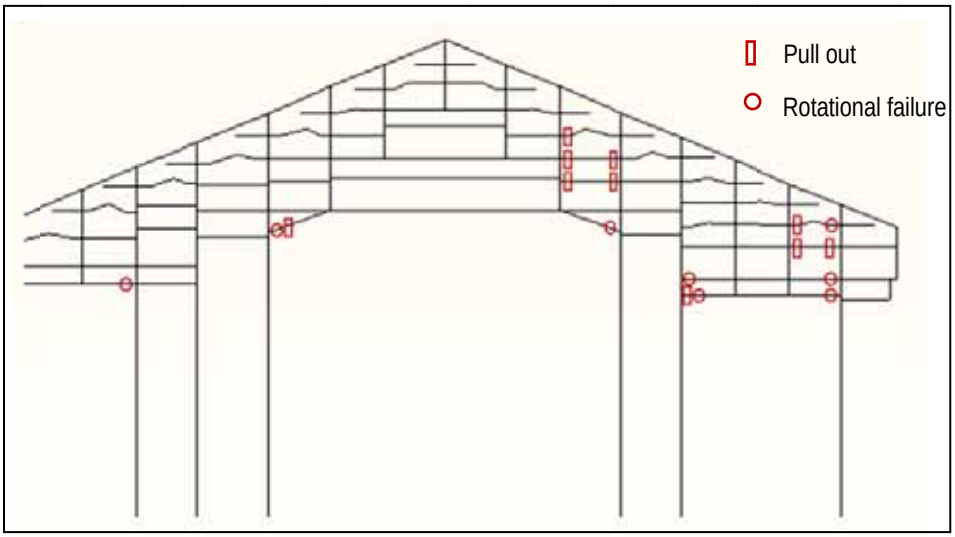

Figure 6.5.9 Joint failure of DS-LF 1

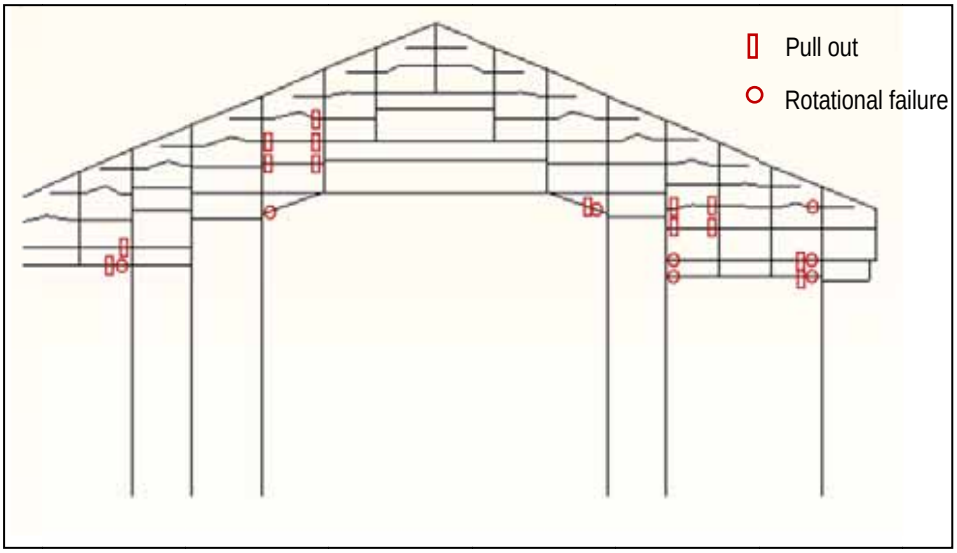

Figure 6.5.10 Joint failure of DS-LF 2

6.5.4 Results of response spectrum analysis

Hsu (2003) indicated that Dou-Shan family temple is located 9 km from seismic station TCU 122 (see Table 6.5.3) and 24 km form the epicentre of the earthquake.

Record station TCU 122 is one of the 24 stations located near the rupture fault and recorded over 250gal peak ground acceleration during the 1999 Chi-Chi earthquake (Institute of Architects, 1999). The data of TCU 122 is translated into a response spectrum with 5% damping in three directions (North-South, East-West, Up-Down) in the report of the Institute of Architects (1999). Response spectrum of East-West of TCU 122, associated to the +X direction of the frame, was taken as redrawn in Fig 6.5.11. The natural frequency analysis of DS-NF was used to perform response spectrum analysis DS-RS.

Table 6.5.3 Location of Dou-Shan family temple and record station TCU 122

	Longitude	Latitude
Dou-Shan family temple	120.608278 East	23.892413 North
TCU 122	120.3657 East	23.48760 North

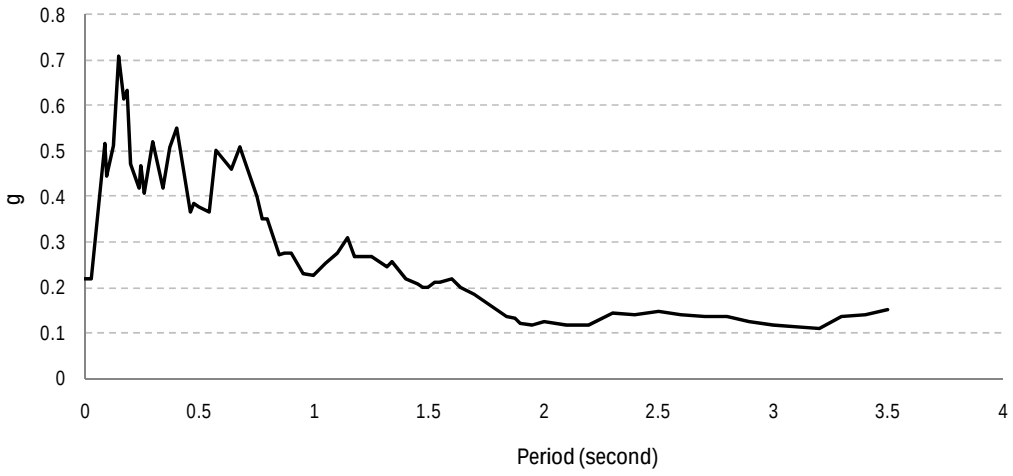

Figure 6.5.11 Response spectrum of East-West of TCU 122

The result of response spectrum on Dou-Shan main hall indicates the roof apex displacements is 55 mm. This value is greater than both drift damage limitations but lower than that recorded in the lateral force analysis, where an equivalent acceleration of 0.33g was applied. Here, according to results of natural frequency analysis (Table 6.5.2) and response spectrum (Fig. 6.5.11), the equivalent

acceleration at period 0.93168 seconds is about 0.26g, which is lower than former one, explaining the difference.

There is no material failure in the response spectrum but 10 joint pull out and 6 rotational failures were found, see Fig. 6.5.12. The total numbers of joint failures are also lower than DS-LF 1 and DS-LF 2, but the difference is not large.

In the central zone B, response spectrum model (DS-RS) also correctly predicts the failure of the inclined supporting brackets. Zone C2 shows more joint failures than other zones, confirming the lateral force analysis and matching post earthquake observation.

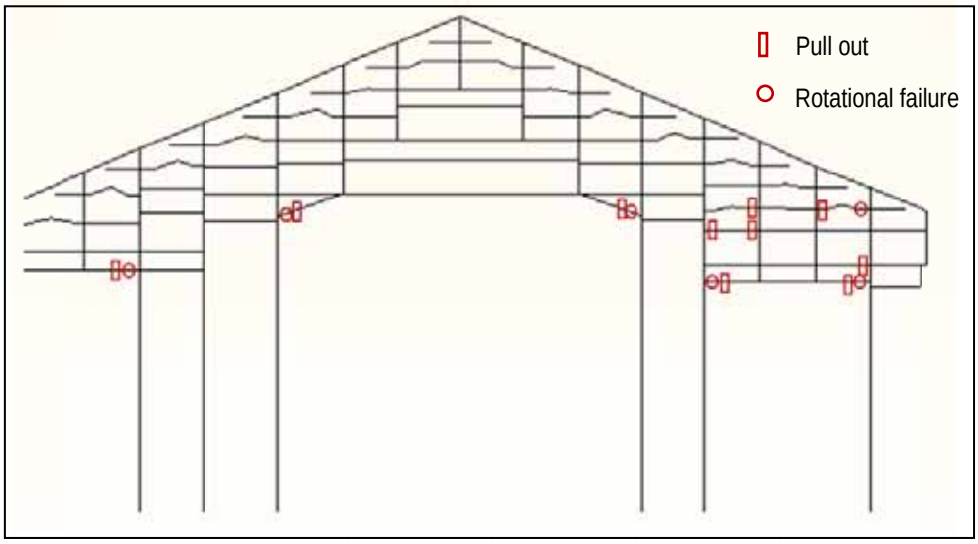

Figure 6.5.12 Joint failure of response spectrum of Dou-Shan main hall

6.5.5 Results of nonlinear static pushover analysis

In analogy with the Guan-Shi temple simulation, forces are applied along +X direction with a target value of 0.33g. A total of 24 steps were performed until the equivalent acceleration of 0.33g was reached. Details of each step are listed in Appendix B. Fig. 6.5.13 plots the relationship of structure displacement and lateral equivalent acceleration. It is shown that lateral equivalent accelerations equal to 0.099g and 0.198g resulted critical for Dou-Shan main hall frame. At steps 08 and 13 the roof apex displacement overcame the limits of 0.005 and 0.008 respectively, see Table 6.5.4.

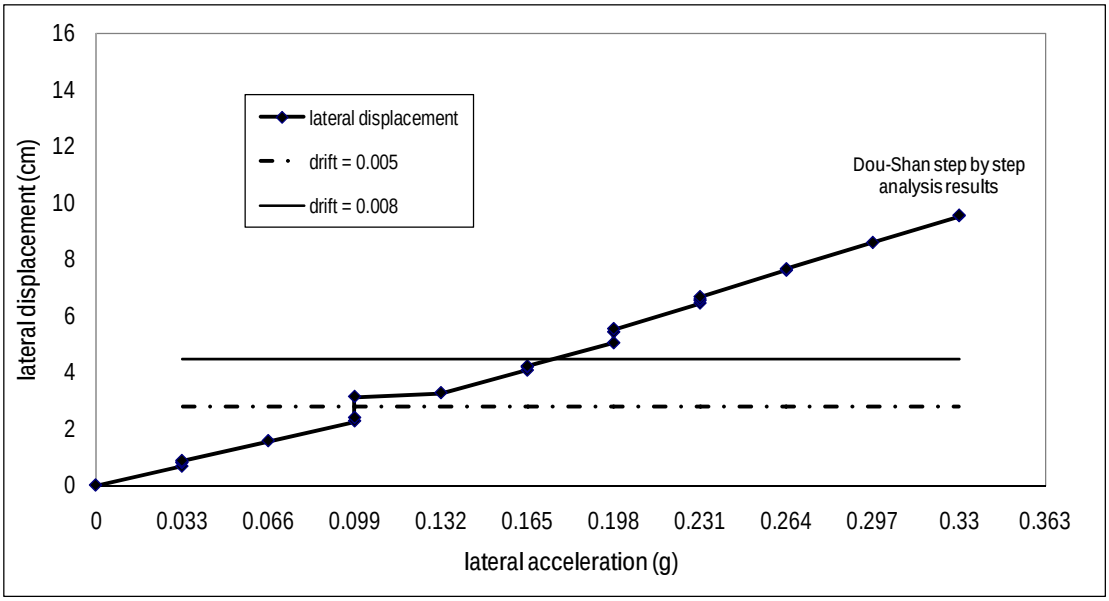

Figure 6.5.13 Structure displacement and lateral equivalent acceleration

Table 6.5.4 Details of steps over the elastic drifts (Dou-Shan main hall)

	Lateral force (Equivalent g)	Roof Apex displacement	Drift	Material failure	Number of pull out failure	Number of rotational failure
Step 08	0.099 g	31.37 mm	0.0056	None	11	2
Step 13	0.198 g	50.40 mm	0.0090	None	13	6
Step 16	0.231 g	64.44 mm	0.0110	None	13	8
Step 23	0.330 g	95.35 mm	0.0170	None	13	12
Step 24	0.330 g	95.60 mm	0.0171	None	13	12

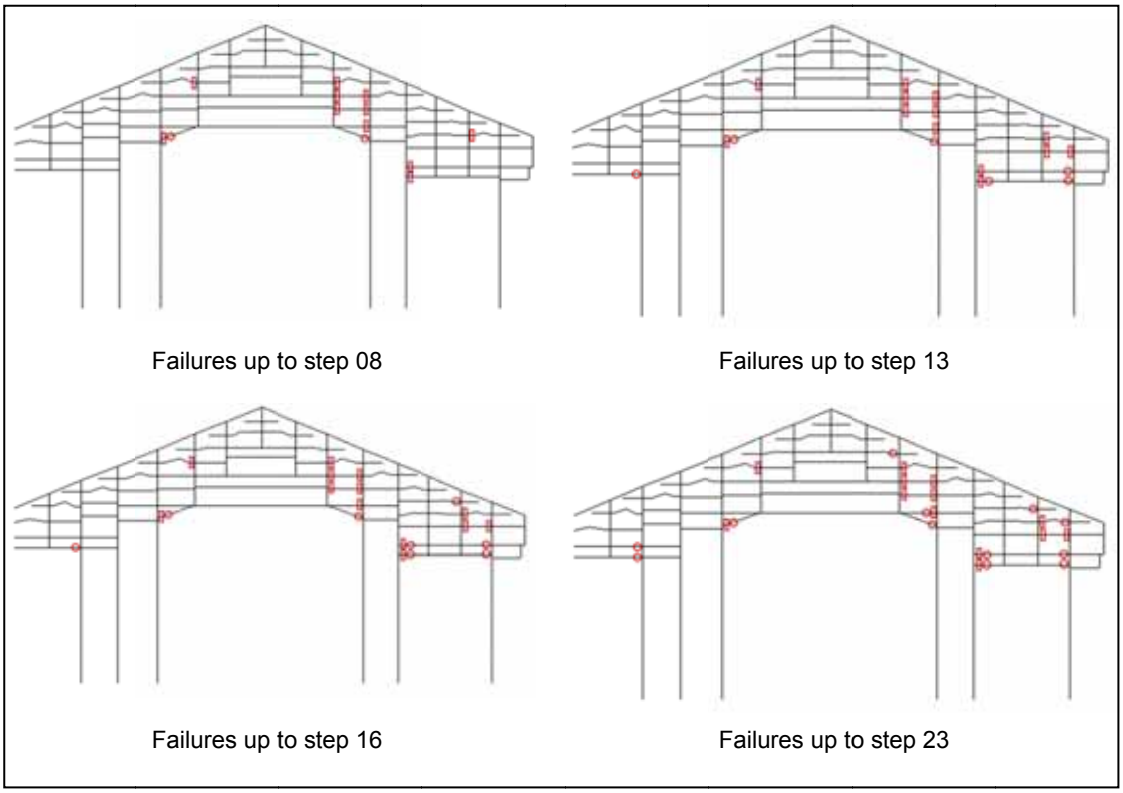

Figure 6.5.14 Failures up to step 08, 13, 16 and 23

At step 08 (Fig. 6.5.14), which is the last step where lateral equivalent acceleration was 0.099g, 6 out of 9 failures are the same as observed in the real right frame (Fig. 6.5.2). At steps 13 and 16, equivalent to 0.198g and 0.231g, respectively, the resulting failures are already similar to those in the post-earthquake observation, where support elements (1 and 2) located between the first main beam and columns 3 and 4 are damaged in the FE model and in reality. This step by step analysis also catches failures of the C2 corridor beam, the binding element on C2 zone and binding element linking the Dou-Gon joint set 5 with column 4. At step 23, the last one, for a total displacement of 96 mm, more failures appear, such as the A1 corridor beam and one binding beam between joint sets 4 and 5.

Fig. 6.5.15 shows the elasto-plastic behaviour of the frame compared with the drift damage criteria. The structure starts to lose its initial stiffness when accelerations exceed 0.165g, implying that elements failing up to step 12 are the critical for the structure. The first drift damage criterion is within the elastic range of the frame's structural behaviour.

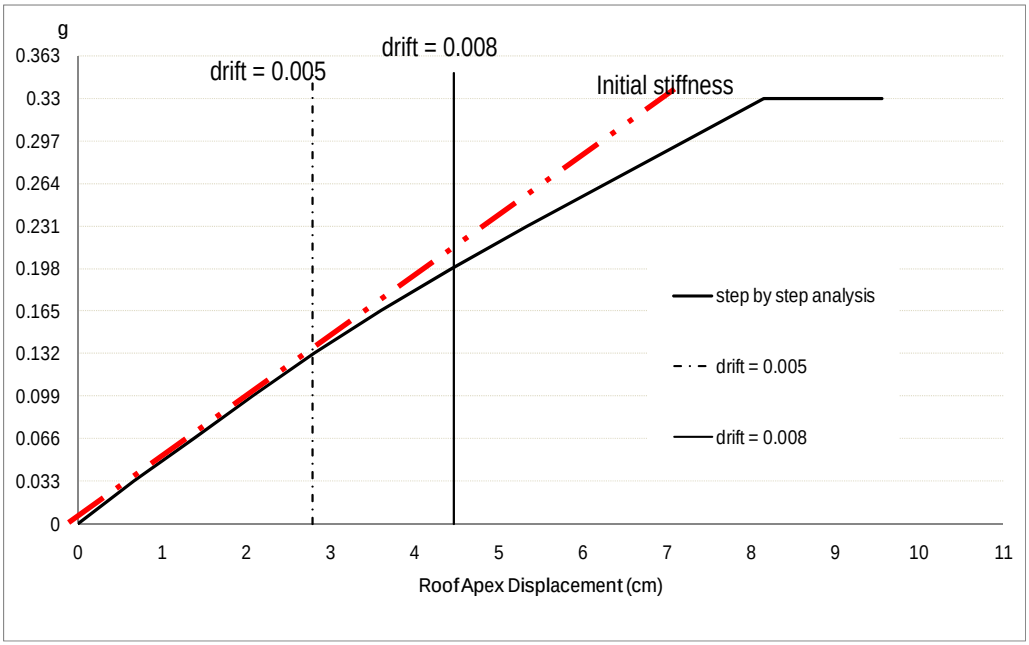

Figure 6.5.15 Results of step by step analysis (Dou-Shan temple frame)

6.5.6 Comparison of failure between the three analyses

The report on the post earthquake conditions of Dou-Shan temple showed that the right frame suffered more damaged than the left (Fig.6.5.2), and as such it was chosen as reference to for the analysis, in favour of safety. First of all, Zone A remained intact, while in central zone (B) the bracket supports 1 and 2 failed together with some binding beams. The right bays, zone C, is the most vulnerable part of the frame. As described, all three analyses catch the global behaviour and failure pattern of the frame.

In the lateral force analysis, both DS-LF 1 and DS-LF 2 match well with the right frame post earthquake. However, it is the sum of these two models that identifies the majority of the elements actually failed, in agreement, as already explained in the previous section with the alternate sways due to reversal of acceleration and displacement direction during a seismic event. .

In the response spectrum analysis both sides are considered and summed together as the results are calculated by SRSS. However, DS-RS has less failures than DS-LF 1 and DS-LF 2. The reason, discussed above, is that the equivalent acceleration corresponding to the first mode of the frame is 0.26g rather than 0.33g, and the higher modes have very modest contribution, so that the total excitations remains

smaller than the equivalent static one. The failure mode of zone C obtained by response spectrum however matches well post-earthquake observed failures.

In this case, the failures in the step by step pushover analysis are very similar to the lateral force analysis and response spectrum. At the same target load of 0.33g, lateral force analysis results in 65 mm roof apex, displacement while the value is 95.6 mm in the pushover analysis. But DS-LF 1 and step 24 result in very similar failure patterns and both match well with the observation in Fig. 6.5.2.

Fig. 6.5.16 shows the structure stiffness and capacity in the three analysis compared with the drift criteria. It is shown that structure stiffness due to lateral force (K-LF) is higher than those due to response spectrum (K-RS) and initial stiffness of step by step pushover analysis (K-PO1); however, the values of K-LF, K-RS and K-PO1 are quite close.

At the level of the equivalent acceleration of 0.26g that was sustained by the structure in the 1999 Chi-Chi earthquake according to the first mode of vibration, the roof displacement in lateral force analysis is slightly over the drift of 0.008, which matches with the survey post earthquake that revealed damage only in a few elements.

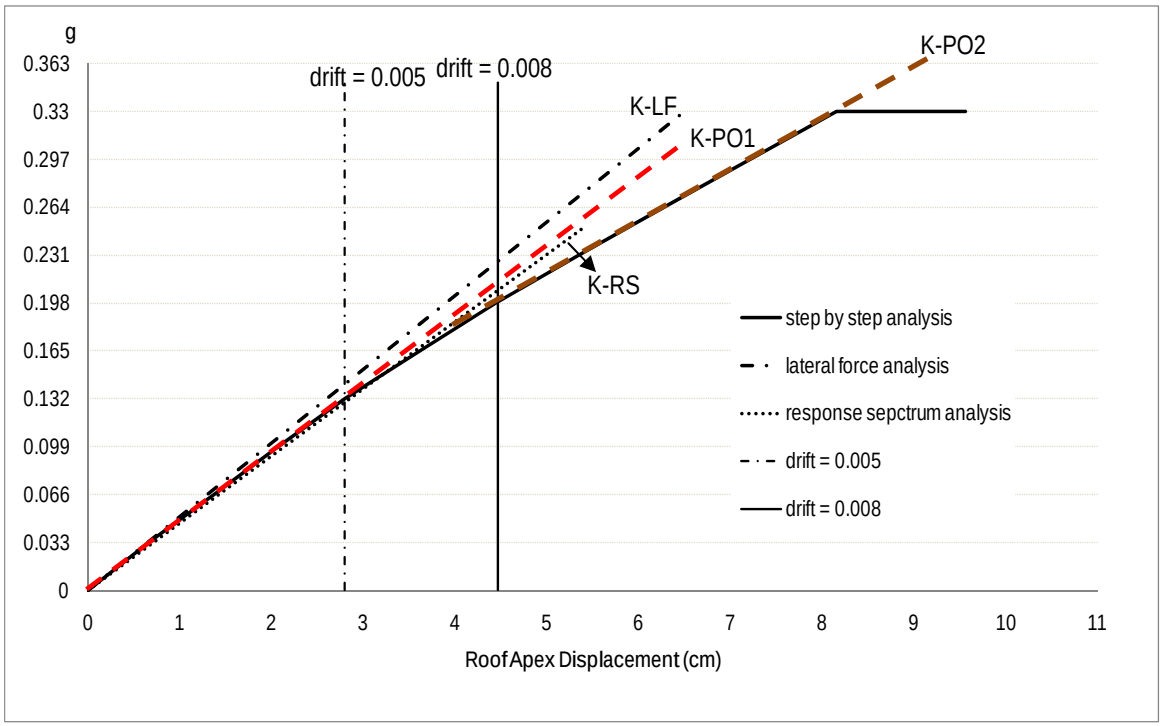

Figure 6.5.16 Structure stiffness according to the three analysis (Dou-Shan)

6.6 Discussion of analytical modelling

6.6.1 Comparison between the two reference buildings and the three analyses

In both buildings it has been found that the first period of vibration is in the region of 1.0 seconds and it has the great majority of participating mass, over 97% (Table 6.4.1 and Table 6.5.1); this confirms the assumption that Dieh-Dou frames can be simulated by a single DOF oscillator.

Eurocode 8-1 (2004) was taken as reference document for determining the most appropriate analysis method of Dieh-Dou buildings. The formula identified that the natural period should not exceed 2 seconds, a criteria easily met by the first mode period of both frames, which are 1.1396 and 0.932 seconds. However, estimating first fundamental period by the formula (6.1.2) provided by Eurocode 8-1 shows a rather different result (0.2 seconds), indicating the frames are stiffer than reality. It is, therefore, essential to perform a natural frequency analysis for this building type rather than simply rely on simplified formula from codes derived for modern construction.

All three analyses can catch the actual failure trend reasonably well, identifying the lateral zones (A and C) as the critical for both buildings, further demonstrating how in general in Dieh-Dou frames these zones are the first to be damaged, as discussed in Chapter 3. However, as Dieh-Dou frames vary greatly from one another, not having being built following standards, the differences between buildings may ultimately affect the capacity. Figure 6.6.1 shows the curve obtained from the step by step pushover analysis for both buildings, outlining that the Dou-Shan frame is stiffer than the Guan-Shi frame.

Fig. 6.6.1 indicates that at lateral equivalent load 0.165g both frames start to lose stiffness. Defining the displacement at this 0.165g as the elastic limit displacement Δ_y and the final step drift as ultimate displacement Δ_u, the ductility of Guan-Shi main hall frame (μ_c) is 3.3, while for Dou-Shan is 2.6. There is clearly lack of literature and data on the ductility of Dieh-Dou frames to further confirm this result; however, D'Ayala (2005) indicates the ductility of facades of masonry structures is in the region of 3.0, so these values seem of a reasonable order of magnitude. To the author's knowledge, no other experimental or numerical study has been currently

performed to quantify ductility in this type of traditional Asian style frames. In fact, the classic concept of ductility cannot be directly applied to this category of buildings, as it is strictly related to post-yielding behaviour of the material, which does not really applies here.

As the three analyses on both buildings show a good qualitative comparison with reality, we can conclude that simulating Dieh-Dou frames by finite element model considering the proper joint rotational and translational stiffness is a correct approach. The drift damage limiting criteria of 0.008 represents a reference value to evaluate the potential level of damage in the building, but it needs to be supplemented by a failure pattern to assess the structure properly. The analysis has demonstrated how for these buildings the joint failures are critical, in terms of both pull out or excessive rotation, rather than the material failure of the timber itself.

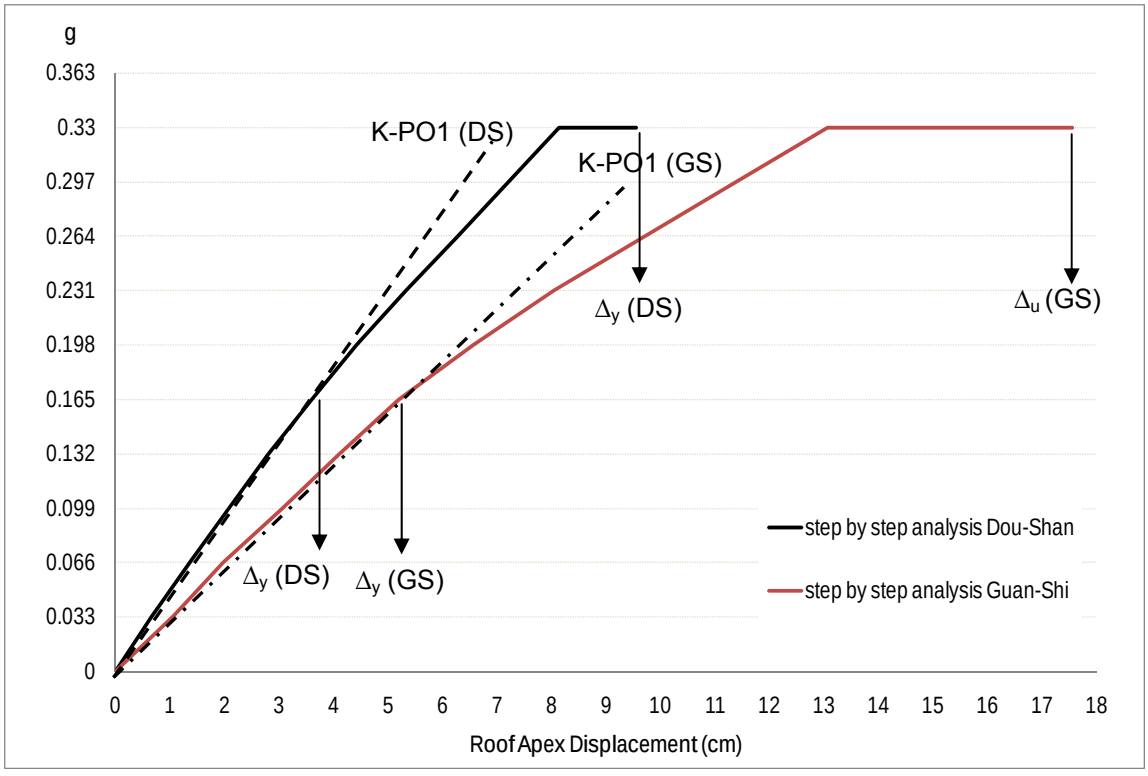

Figure 6.6.1 Structural capacity of two frames

When comparing the three analysis methods with the post earthquake surveys is shown that all of them can map and predict the vulnerable parts of the structure, but with different degrees of refinement. An advantage of the response spectrum analysis undertaken is that it is based on the natural frequency response of the

building under the actual accelerometer reading and can therefore reassure about the actual forces experience by the structure. Lateral force analysis is easy and quick to perform and still shows good agreement with the other two analyses, especially up to the end of the linear stage (see Fig. 6.4.18 and Fig. 6.5.16). The nonlinear pushover analysis is the most accurate, as it can identify the variability in structural stiffness and the sequence of failures in the frame.

Table 6.6.1 shows the ratio between the correctly predicted to actually failed elements, as identified from the survey reports, for the three different analysis methods. The elements reported missing in Guan-Shi right frame are shown in grey in Fig. 6.6.2 (with the ones correctly predicted by pushover analysis in red), while the ones for the Dou-Shan temple were shown in Fig. 6.5.2. In all cases the predictions are good, especially taking into account the fact that the surveys were not undertaken immediately after the earthquake and some of the elements reportedly missing may have been removed afterwards and not necessarily been damaged during earthquake.

Table 6.6.1 Percentage of correctly predicted failed elements

	Lateral force analysis (+X/-X)	Step by step pushover analysis	Response spectrum analysis
Guan-Shi	60%	75%	65%
Dou-Shan (right)	70%	65%	50%
Dou-Shan (left)	85%	65%	65%

From Table 6.6.1 it can be seen that in the case of the Guan-Shi temple, that actually withstood a high earthquake load and was heavily damaged, the step-by step analysis is the most accurate, allowing to identify three quarters of the actually failed elements. One reason why the lateral force analysis is slightly unconservative in this case may be because this building has experienced, at its first period of vibration, a force slightly in excess of the actual lateral load applied, but also because the excitation clearly took the structure well into the non linear behaviour. In the case of the Dou-Shan temple, which suffered relatively minor damages, the lateral force analysis proved to be the most accurate to catch the reportedly failed elements. This can be explained by the fact that this building is more pronouncedly

asymmetric and the pushover analysis should be performed in both directions to be able to catch all critical elements. In this case the building suffered a lower earthquake load at its natural period than 0.33g, which explains why the lateral force load of 0.33g results in more elements failed.

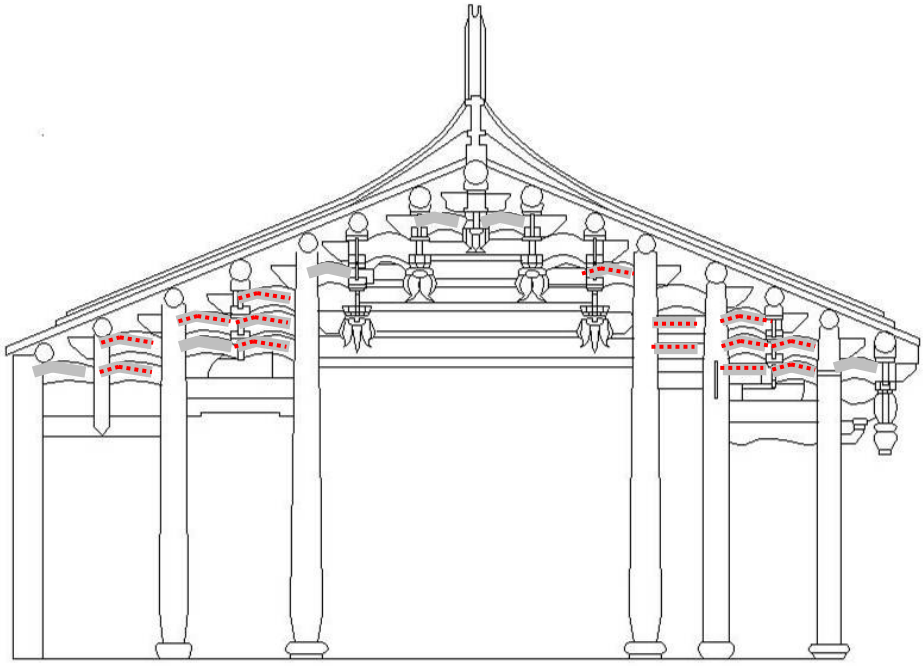

Figure 6.6.2 Failure of Guan-Shi main hall (right frame) and step by step prediction

In conclusion, the study shows that it is possible to accurately evaluate the critical elements in a Dieh-Dou frame using such a FE modelling and failure criteria, and that the proposed pushover analysis is the most accurate method of identifying the failure pattern, when the analysis is perfomed in both directions for non-symmetric frames. However, a simpler lateral force analysis can identify the local failure pattern with almost equal accuracy and, when appropriate safety factors are employed, be conveniently used to assess these structures.

6.6.2 Effects of vertical seismic excitation and 3-D behaviour

Vertical seismic excitation

In the previous analysis it was assumed that the vertical seismic component can be neglected and only horizontal force were considered acting together with the gravity

loads. However, Eurocode 8-1 (2004) indicates that in high seismic zone, the vertical component of the seismic action need to be taken into account in cases when there are beams supporting columns, a condition that is met in the Dieh-Dou buildings as Dou-Gon joint sets are sitting on main beams or corridor beams.

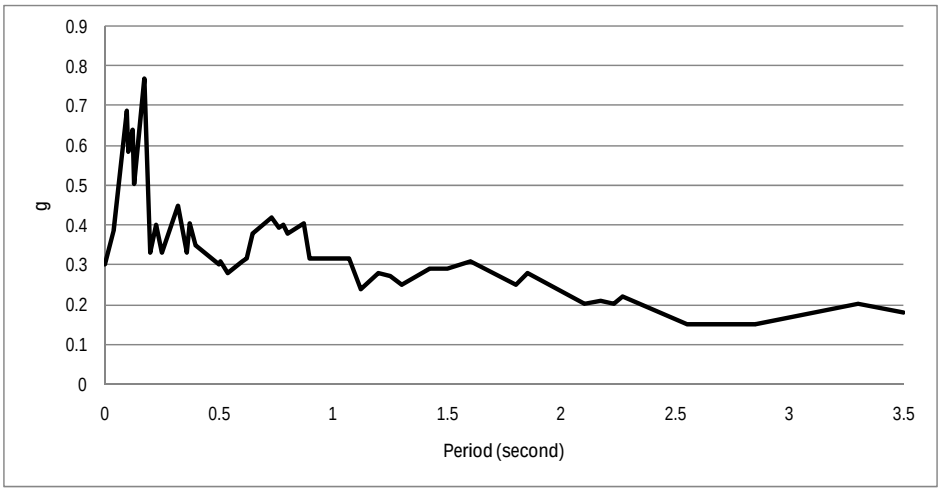

Figure 6.6.3 Response spectrum of Up-Down of TCU 076

Thus, the Guan-Shi main hall frame, which showed the higher total effective mass participation factor in the z direction, of the two case studies, was taken as reference building to run a vertical response spectrum analysis. The FE model (GS-RSV) has the same layout and mechanical characteristics as GS-RS, and the vertical spectrum recorded during the 1999 Chi-Chi earthquake has been used, see Fig. 6.6.3.

Three cases are considered according to the following combination of effects:

(i) E_{Edz}

(ii) E_{Edx} "+" 0.3 E_{Edz}

(iii) 0.3E_{Edx} "+" E_{Edz}

where

"+" implies "to be combined with"

E_{EdZ} represents the action effect due to response spectrum in Z direction, results of GS-RSV

E_{Edx} represents the action effect due to response spectrum in X direction, results of GS-RS
the value of 0.3 is recommended by Eurocode 8-1 (2004)

In terms of displacements, GS-RSV resulted in 0.259 mm of roof apex displacement in X direction and 1.05 mm in the vertical Z direction. From the examination of combination (i) neither material nor joint failure occurred.

The failure results of combinations (ii) and (iii) are shown in Fig. 6.6.4 and Fig. 6.6.5, respectively.

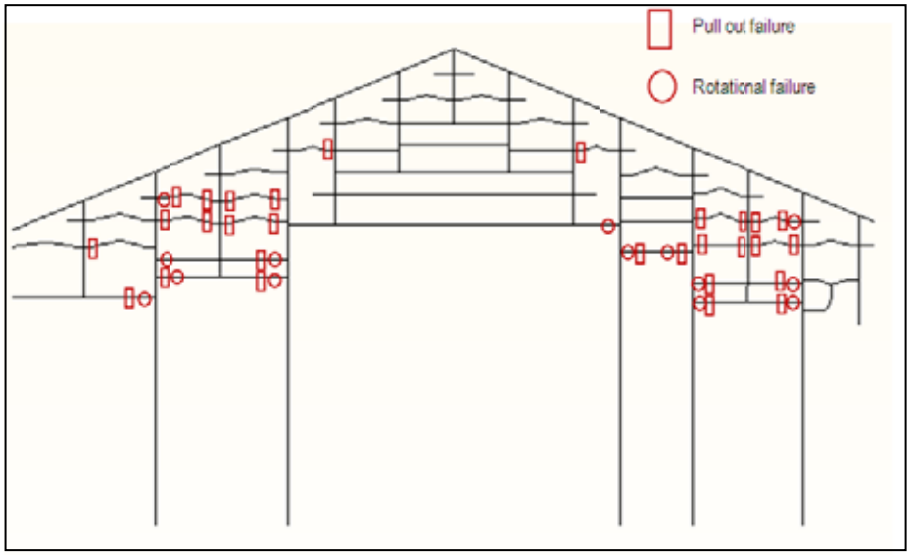

Figure 6.6.4 Result of check (ii)

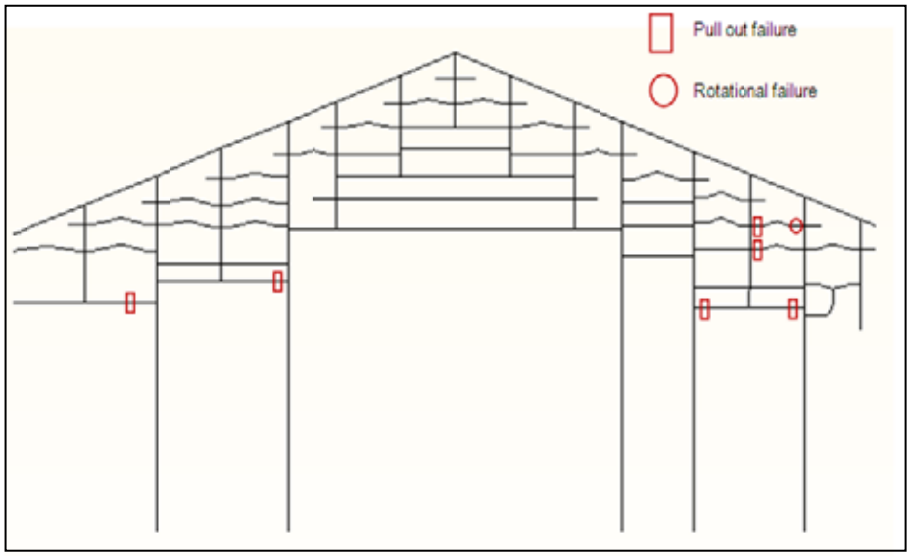

Figure 6.6.5 Result of check(iii)

They both show that the effects of the vertical excitation component on the frames are negligible, as check (ii) results in only one additional failure out of forty-two encountered with the horizontal force only, while check (iii) results in too fewer failure to be realistically comparable with the in situ survey. These checks prove correct the hypothesis that vertical load can be neglected.

3-D behaviour

In the analyses carried out so far, the behaviour of a single frame has been taken into account. In order to examine the effects of 3D behaviour, a response spectrum analysis is performed where both frames and the purlins are modelled.

The first two models, GS-3D 01 and GS-3D 02 (Figure 6.6.6) take into account the effect of masonry walls in terms of restraint offered by the connection with masonry at the end of the purlins.

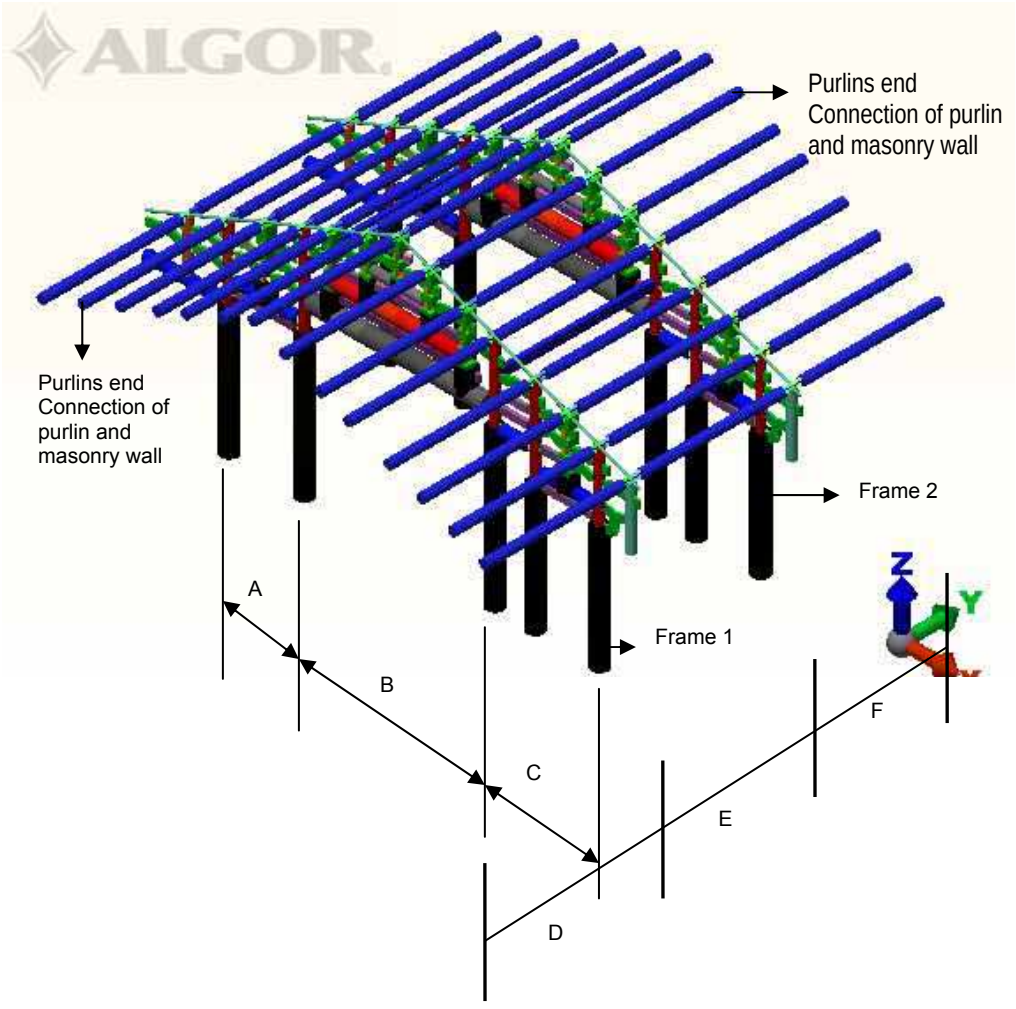

Figure 6.6.6 GS-3D 01 and GS-3D 02 model

Purlins of Dieh-Dou buildings are simply supported onto the masonry walls without a specific tension resisting connection. Also, Taiwan is in a high humidity climate zone and the end of timber purlins sitting on the top of masonry are often found rotted (Fig. 6.6.7). Therefore, the purlins would rely at best only on friction with the wall to resist the pull out force due to an earthquake component along Y. Hence, the two models simulate the two possible extremes of the restraint condition, i.e. free movement (GS-3D 01) or restrained movement (GS-3D 02) in Y direction. Also, no restraint to rotation was assumed for the purlins at both connection with the masonry and the top of the frames.

The first 20 modes of vibration were considered. Table 6.6.2 lists frequency, period and modal mass participation for the first five modes of both models, and Fig.6.6.8 shows the first two modes of GS-3D 01 and GS-3D 02.

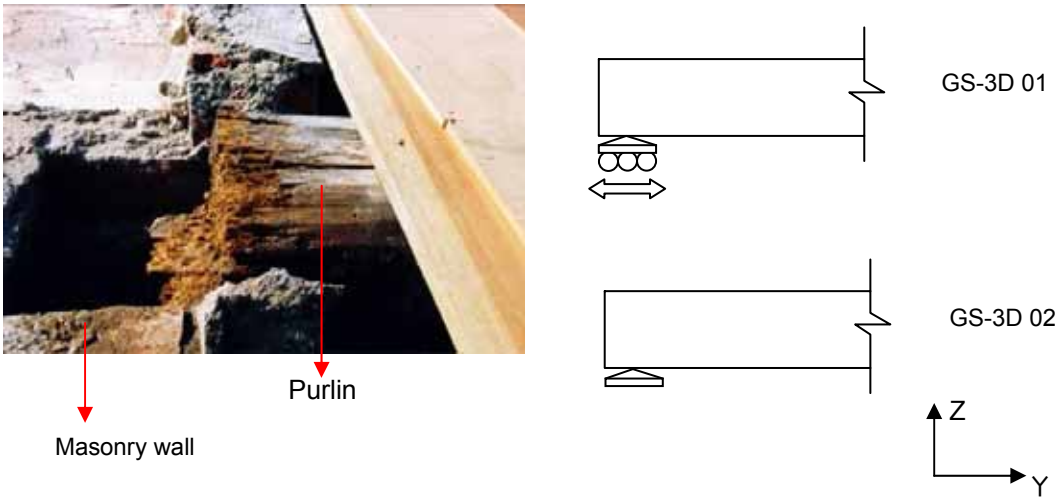

Figure 6.6.7 Purlin connection with masonry wall

The results show that assuming no Y direction restraint to the purlins from the masonry (GS-3D 01), the first mode of vibration of the building is in Y direction, while the second mode is in X direction, with the great majority of the total mass in each direction excited in these first two modes. The periods of the first and second mode are 1.31 and 1.18 s, respectively. It is noted that the period of vibration and the participating mass in the X-direction are practically the same that in the single frame analysis. However, considering the connection with masonry wall fully effective (GS-3D 02), the first mode is in X direction, where again the period of vibration and participating mass is the same of the in-plane single frame models.

Table 6.6.2 Modal analysis results for GS-3D 01 and GS-3D 02

	Mode number	Frequency (Hertz)	Period (sec)	Modal effective mass in X direction	Modal effective mass in Y direction	Modal effective mass in Z direction
GS-3D 01	1	7.5999E-01	1.3158E+00	0	95.02	0
	2	8.4377E-01	1.1852E+00	96.15	0	0
	3	9.9527E-01	1.0047E+00	0	0.6	0
	4	1.2198E+00	8.1979E-01	0	0.15	0
	5	2.0282E+00	4.9304E-01	0	1.75	0
GS-3D 02	1	8.4377E-01	1.1852E+00	96.15	0	0
	2	1.0825E+00	9.2378E-01	0	0	0
	3	6.9799E+00	1.4327E-01	0	37.23	0
	4	8.0932E+00	1.2356E-01	0	0	15.03
	5	8.5771E+00	1.1659E-01	0	0.71	0

In order to observe the effect of the out-of-plane forces on the failure pattern of the building, a response spectrum analysis is undertaken applying the actual recorded spectrum on GS-3D 01 and GS-3D 02 in both X and Y direction, while Z direction is disregarded as it has been proved it does not contribute in an appreciable way.

The results indicate that roof apex displacements of frames 1 and 2 in the X direction are very similar in both models, equal to 113.3 and 113.0 mm respectively, while the displacement in Y direction is 120.7 mm for the GS-3D 01 model and 5.6 mm for the GS-3D 02 model.

The frames are then checked for the joint failure and material failure criteria, considering the biaxial bending and shear in the interaction formula of the material failure criteria. Although there is an increase in the timber stresses especially in the columns (as expected), still no material failure are found, with the most stressed elements being at around 55% of the characteristics strength. The pattern of joint failures is exactly the same that in the single frame, with only two additional joint failure in GS-3D 01 (Fig. 6.6.9) if compared with the single frame response spectrum analysis.

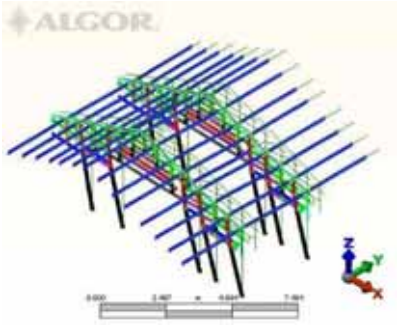

GS-3D 01 mode 1

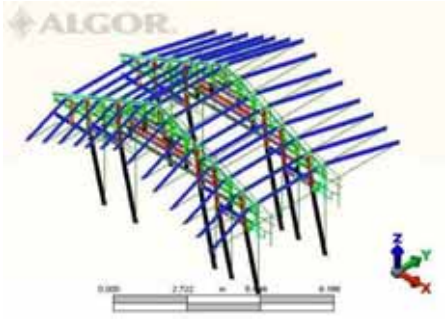

GS-3D 01 mode 2

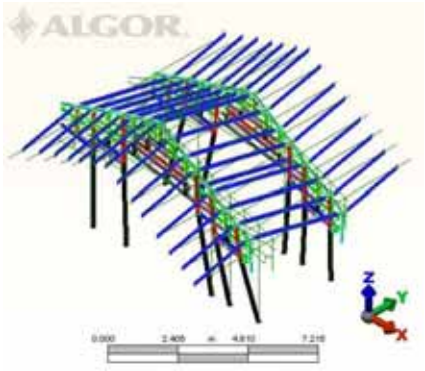

GS-3D 01 mode 3

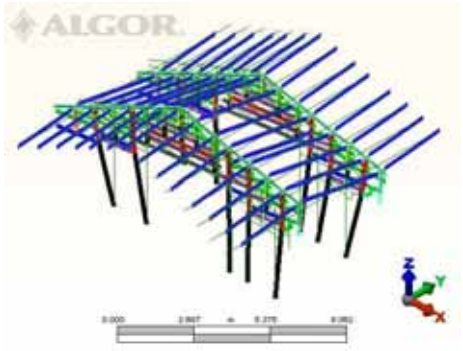

GS-3D 01 mode 4

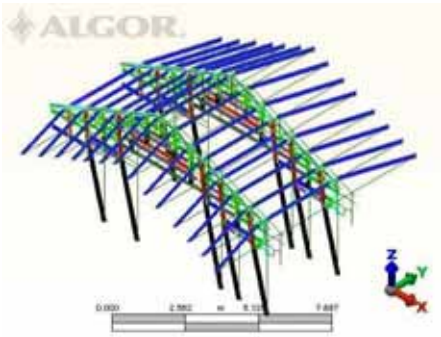

GS-3D 02 mode 1

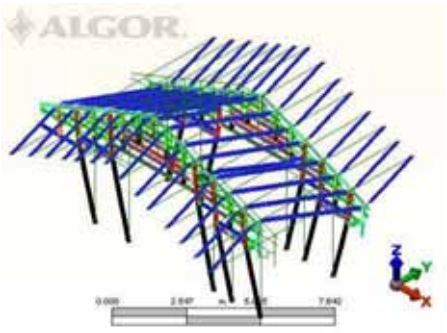

GS-3D 02 mode 2

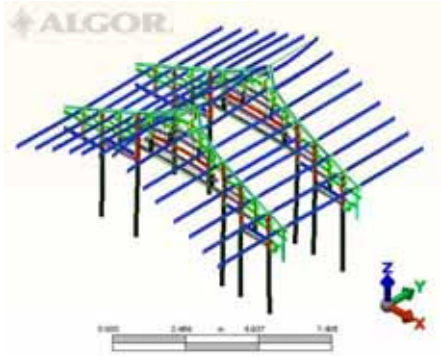

GS-3D 02 mode 3

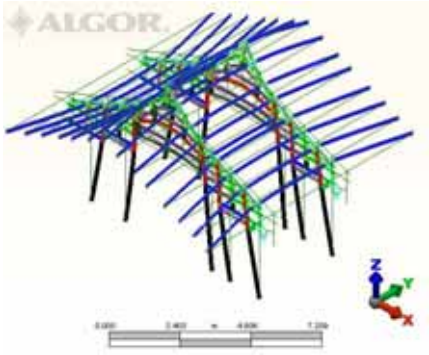

GS-3D 02 mode 4

Figure 6.6.8 First 4 modes of GS-3D 02 and GS-3D 03

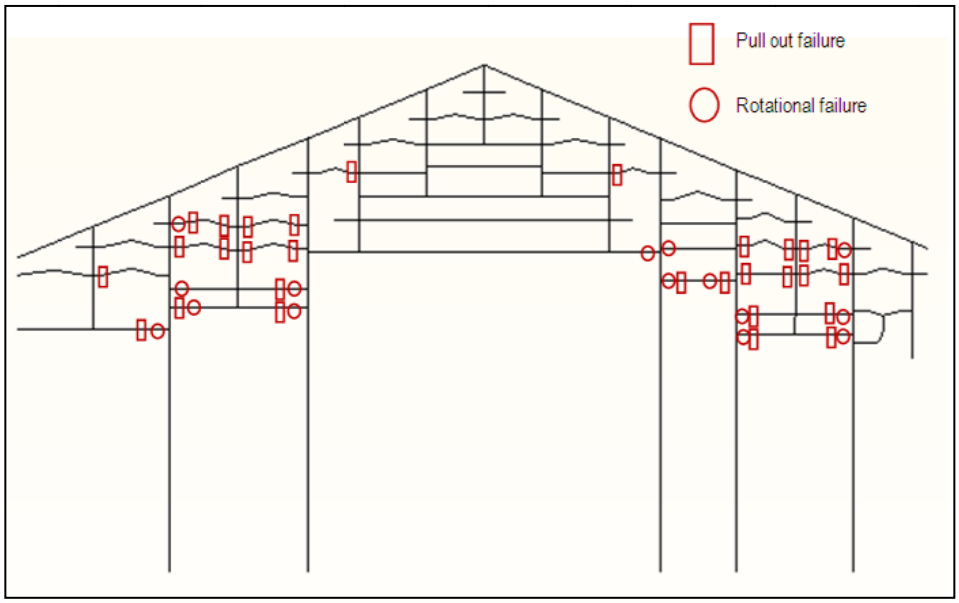

Figure 6.6.9 Failure of GS-3D01 model

In reality there is a certain frictional restraint to pull out the purlins from the masonry. Considering the static frictional coefficient between purlins and masonry equal to 0.55 and assuming this resistance is lost when the force on the purlin in the Y direction surpasses 0.55 times the vertical load, from model GS-3D 02 it is found that all the connections of the purlins in both zones D and F (see Fig 6.6.6) have a force 1.5 to 2 times in excess of this limit, meaning these purlins can pull out during a seismic event and are likely to fall to the ground resulting in the roof collapse, as in fact happened in the actual building. The same situation can occur if the masonry walls collapse during the earthquake, which has also been shown to be relatively common form the survey in Chapter 3.

At this stage, the two Dieh-Dou frames are linked together by the purlins in the central zone E of Fig 6.6.6 only. Therefore, a third model (GS-3D 03, see Fig. 6.6.10) has been set where the purlins in the outer zone are removed.

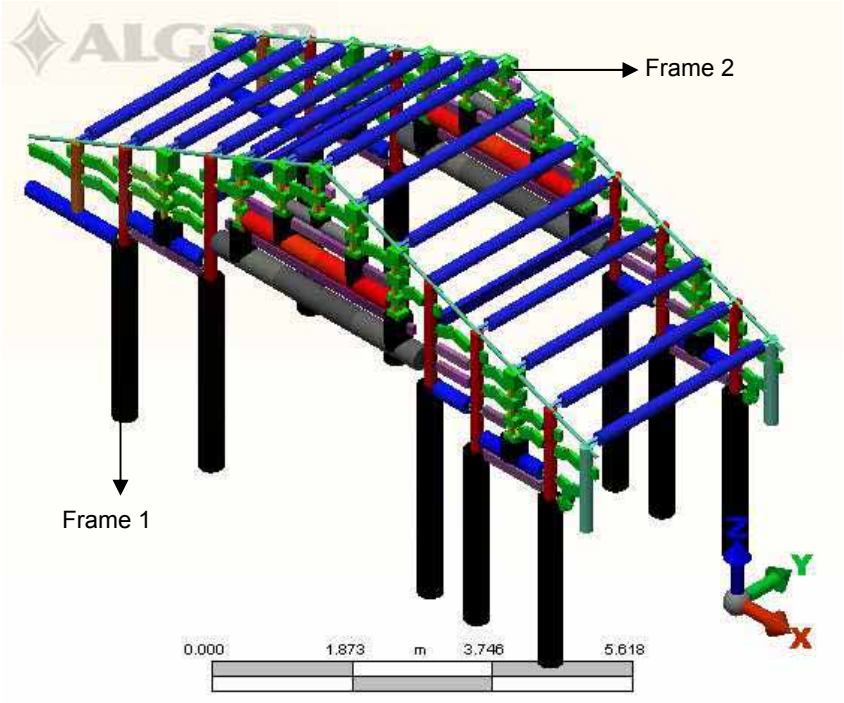

Figure 6.6.10 GS-3D 03 model

Table 6.5.3 shows the results of the modal analysis, while the shapes of the first two modes are plotted in Fig. 6.6.11 and the joint failure pattern in Fig. 6.6.12 obtained with the response spectrum analysis. All results, including the joint failures, are practically coincident with those of model GS-3D 01, confirming that there are no major differences between 2D and 3D modelling in terms of behaviour of the single frames.

Table 6.6.3 Modal analysis results of GS-3D 03

Mode number	Frequency (Hertz)	Period (sec)	Modal effective mass in X direction	Modal effective mass in Y direction	Modal effective mass in Z direction
1	7.8033E-01	1.2815E+00	0	96.59	0
2	8.5502E-01	1.1696E+00	97.50	0.02	0
3	1.0559E+00	9.4525E-01	0	1.09	0
4	2.7161E+00	3.6818E-01	0	0	0
5	3.2183E+00	3.1072E-01	0	0.93	0

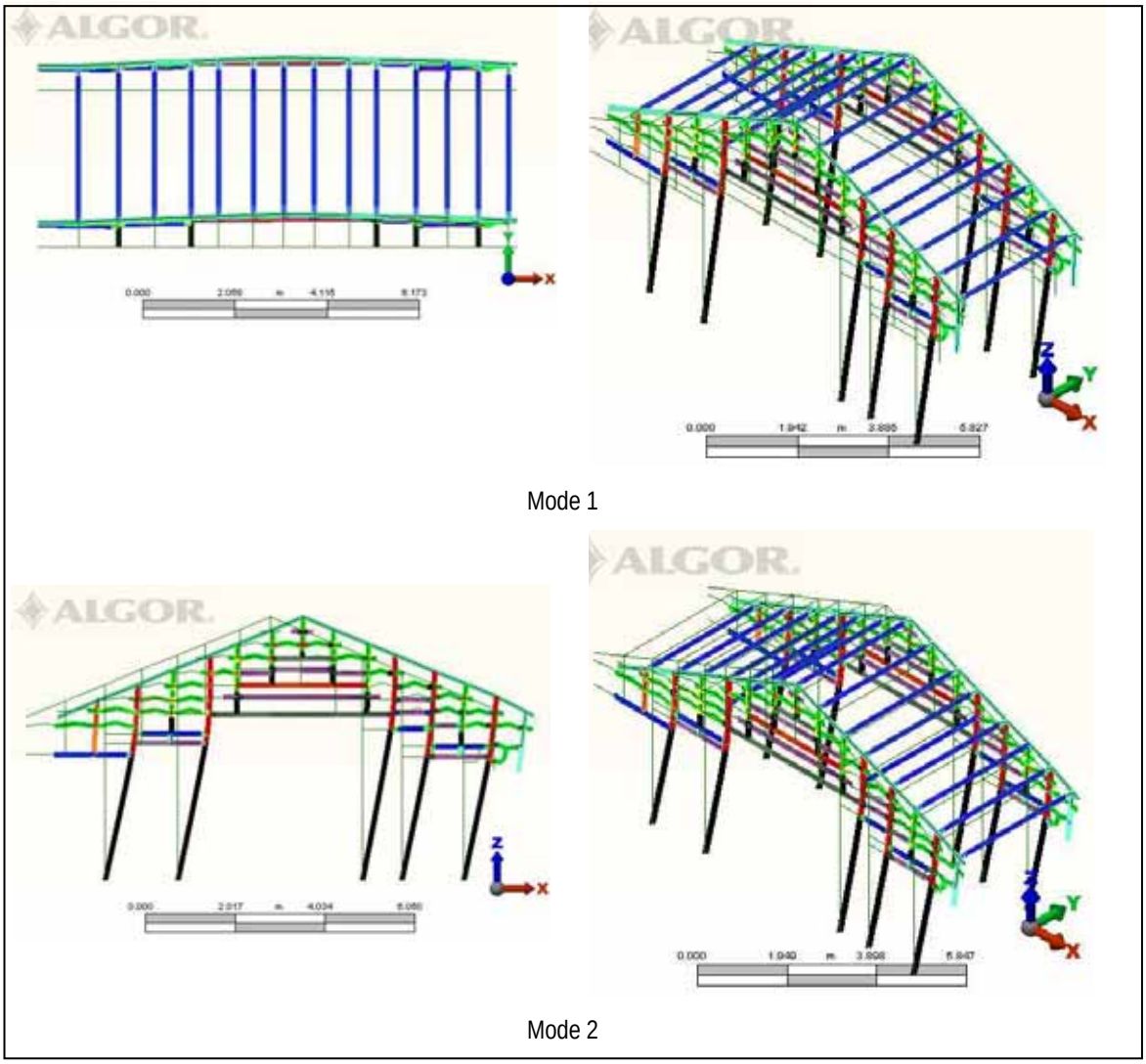

Figure 6.6.11 First two modes of GS-3D 03 model

However, in order to avoid collapse of the purlins in between the frames when the frames vibrate in opposite directions (although the present 3D model shows these modes to have an insignificant mass participation in Y direction) it is important that their connection with the top of the frame is as firm as possible. Otherwise, the collapse of the whole building could be initiated by the purlins (and the roof) falling in between the frames, leaving the frames prone to out of plane instability.

In conclusion, the 3D analysis has shown that, provided that the out of plane stability is guaranteed by ensuring a stable connection between the top of the purlins and the frames, it is appropriate to assess the frames with a single in plane model only, as their criticality in terms of lateral movement, joint failures and material failures is not affected by the out of plane forces. It has been shown that even if the outer

masonry walls collapse the system made by the two frames and the purlins in between can resist the earthquake forces (out of plane, but not in plane).

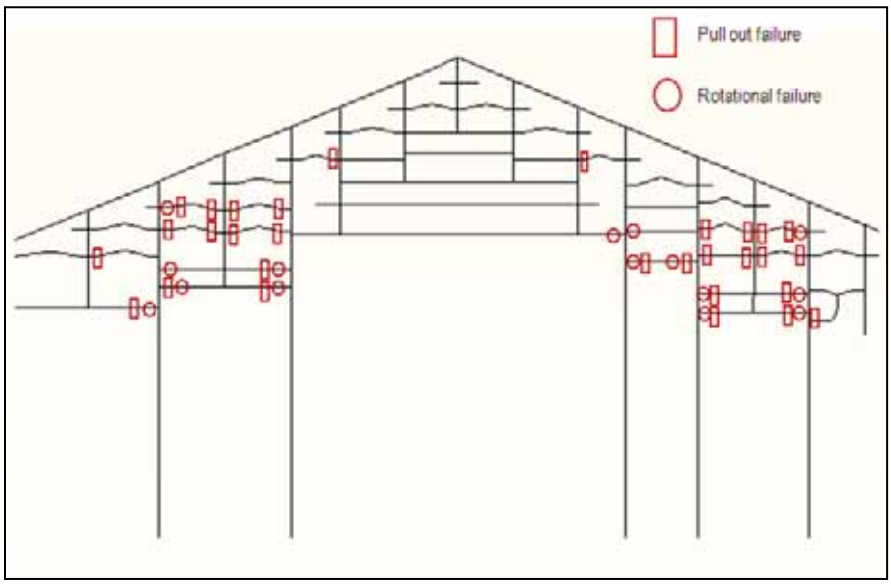

Figure 6.6.12 Failures in GS-3D 03 model

6.6.3 Conclusions

A Dieh-Dou building is comprised of two timber frames, three masonry walls and roof. The structural behaviour under seismic load has been properly modelled with finite element analysis.

The results show that:

- if the purlin connections with masonry walls are able to resist the horizontal loads in the-out-of plane direction, or
- when the masonry falls or the purlins pull out from the wall, if the central set of purlins are properly connected at the top the frames, then

the vulnerability of the structure, in terms of displacement and local failure is equivalent to that evaluated with a single frame 2D analysis, which therefore can be used to carry out the preliminary assessment of these frames to estimate their seismic vulnerability.

In highly seismic zone, vertical action is also a potential hazard for structures. Taking vertical load into account combined with the horizontal component, it has been shown that the effects are practically coincident to those of horizontal action

only, so it is possible to ignore the vertical component of the earthquake for Dieh-Dou buildings in the first instance.

It is seen that all three analyses performed (lateral force, step by step pushover analysis and response spectrum) can accurately predict the vulnerability of the frames, when compared with post earthquake reports. In all cases, joint failures are critical than material failures, which is the peculiar feature of these buildings. The degree to which one analysis outperforms the others depends on the intensity of the lateral action and associated expected drift. For both frames it is seen that the 0.008 drift criterion provides a good estimate of the elastic limit. Hence if the expected spectral demand in terms of acceleration or base shear is substantially greater than the capacity associated with the 0.008 demand drift, a nonlinear analysis is preferable to correctly estimate failure and overall sway.

In the analysis is found, as confirmed by the actual observation, that the critical elements of Die-Dou frames more prone to failure are situated in the outer zones of the frame, while the central zone with the main beams remains relatively undamaged. Therefore, are these outer zones that would merit further attention to improve the performance of the frames under earthquake.

Among the analyses, the step by step pushover analysis is the most accurate, as it can allow identifying the succession of failure and give a good picture of the reduction in stiffness experienced by the frame due to the progressive damage. However, it may be necessary to perform the analysis in both directions, if the structure is asymmetric. Moreover, this nonlinear assessment method can also provide knowledge on the structural “ductility”, help to define the elastic range of the structure and identify the critical elements that reduce the building stiffness excessively.

The capacity curves show that up to the linear elastic stage the three analyses are in good agreement, in terms of predicted structural stiffness. The lateral force analysis is shown to be sufficiently accurate to be used to assess the vulnerability of these buildings and it may be very helpful as a quick tool for a first screening of these structures. If appropriate safety factors are applied, lateral force analysis can be sufficiently conservative.

Chapter 7
Seismic improvement of Dieh-Dou frames

7.1 Introduction

The Dieh-Dou timber frames not only have a structural function, but also represent art and culture of Taiwan. The post-earthquake surveys and numerical analysis show that they are easily damaged under earthquake. In order to prevent failures, it may be necessary to enhance their capacity. However, as discussed by D'Ayala and Wang (2006a,b) with reference to the 'no originality to be changed' approach defined for Asian timber heritage in the *Principles for Conservation of Heritage in China* (2004) document, interventions should be considered only when proven necessary by safety considerations or the preservation of the structural integrity.

In the previous Chapter 6, a finite element modelling with proper rotational and translational stiffness and an assessment methodology employing lateral force, response spectrum and step by step pushover analysis with appropriate failure criteria has been shown, by way of comparison with post earthquake survey, to be an adequate tool to predict and indentify the vulnerability of Dieh-Dou frames.

In particular, the results have shown that, whether the masonry walls are able or not to restrain the purlins horizontally, the vulnerability of the Die-Dou frame in terms of in plane deformation and the related local failure of its historically valuable elements, is equivalent to that evaluated with a single frame 2D analysis. Therefore, the structural performance of the single frames can be improved by strengthening the frame and evaluating the effectiveness of the procedure with a 2D analysis.

The improvement of the overall out of plane stability of the whole structure, which may benefit from strengthening of the masonry walls (with associated improvement of the degree of restraint between the purlins connection with the masonry) and the connection between the purlins and the frames themselves, may merit further attention and should be object of future work.

The assessment of the main hall of Guan-Shi and Dou-Shan temples, combined with the survey results, showed that the central parts (zone B) of the frames are intact but the outer parts (zone A and C) are prone to failure. From a heritage point of view the central part (zone B) of the frame is the most important, as there are important paintings on the surface of timber members, while the outer zones are of less significance in this respect. Hence, elements of the zones A2 and C2 of Guan-Shi main hall and C2 of Dou-Shan main hall (Fig. 7.1.1), which contained the great majority of the failed elements, are selected for strengthening.

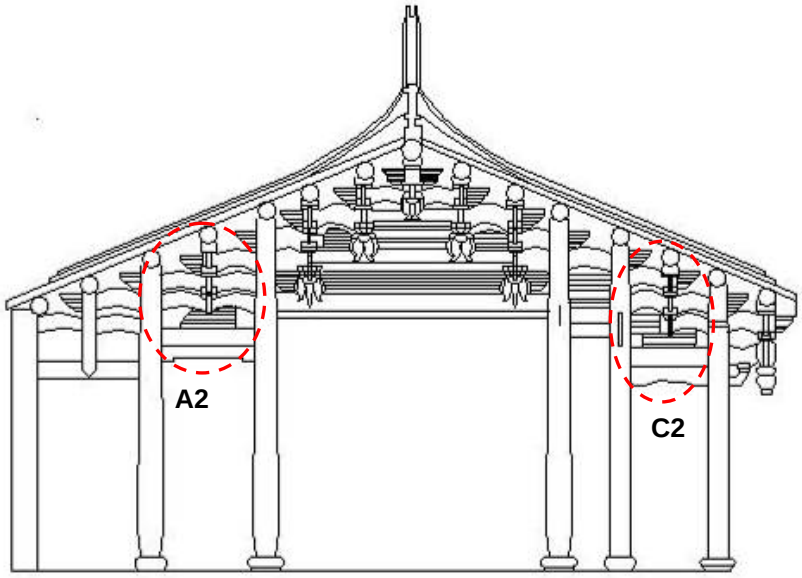

Guan-Shi

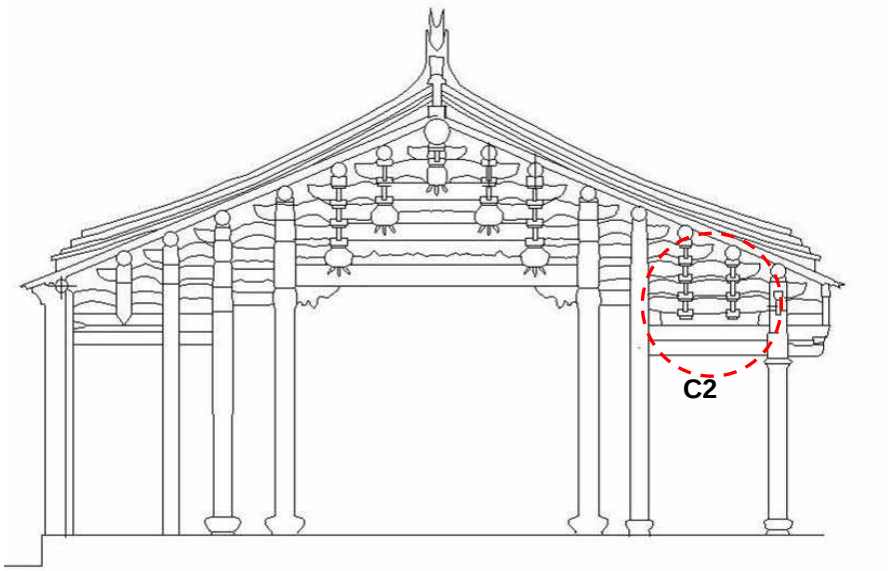

Dou-Shan

Figure 7.1.1 Elements selected for strengthening

7.2 Methods of strengthening and failure criteria

Yeomans (2003) states that there are four possibilities for strengthening and repairing historic timber structure, which are:

(1) Timber is replaced with timber
(2) Timber is supplemented by other material
(3) Steel or other material is used to replace the timber
(4) Supplementary structures that act either independently of the original, simply provide it with support, or which act in consort with the original structure

Considering that timber members of Dieh-Dou frames are a heritage in themselves, the strengthening effort should also be concerned with issues of reversibility. Hence, replacement of timber elements by either timber pieces or other material should be avoided. In order to maximise the retention of historic material and still strengthen the structure so that it is able to safely support earthquake loads, the second option is considered the most appropriate, i.e. supplement the timber with other material.

Yeomans (2003) pointed out that the most commonly used fasteners in timber structure strengthening work are bolts and screws. Chen (2008) proposed three strengthening methods on Chuan-Dou joints considering the “reversibility” and “originality” principles. These three methods, designed to increase the mortised beam to column joints’ rotational stiffness and ultimate moment, use steel plates and screws, steel plates and bolts and carbon fibre (CFRP) strips, respectively. Figure 7.2.1 shows details of the three methods adopted by Chen (2008).

Chen (2008) applied these strengthening methods to beam to column Chuan-Dou joints (Chang 2006). Rotational tests were performed in laboratory, where the efficiency of rotational stiffness and ultimate moment capacity were compared with the unstrengthened joints. The results show that these methods can substantially increase the rotational stiffness and moment capacity of Chuan-Dou joints. The tests of Chen (2008) focused on rotational features, while survey and numerical analysis results indicate that translational behaviour is critical to Dieh-Dou buildings under earthquake. Thus, both rotational and translational stiffness and associated capacity need to be considered.

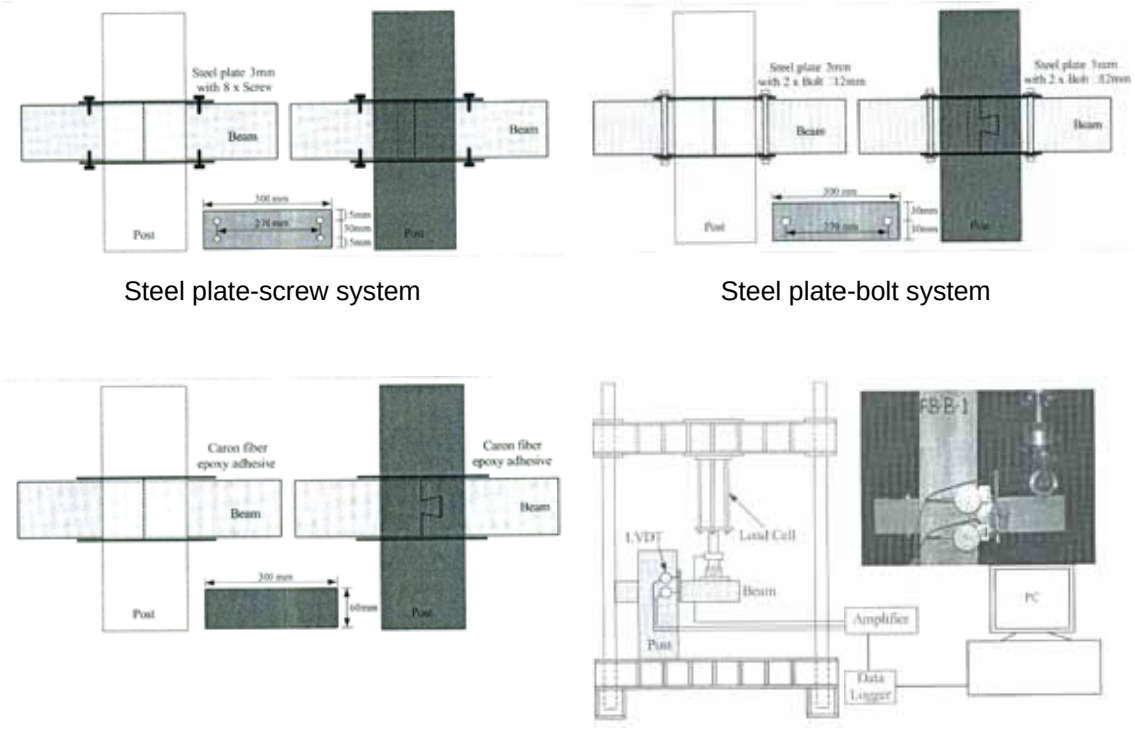

Steel plate-screw system

Steel plate-bolt system

CFRP strip system

Test device

Figure 7.2.1 Beam to column strengthening tests (Chen 2008)

In terms of rotational stiffness and joint moment capacity, the steel plate-screw method is shown to be the less efficient. Also, as the screws do not guarantee a part to part connection, it is believed it can have lower efficiency in preventing pull out, too. The carbon fibre strip and steel plate-bolt methods are the most efficient. However, CFRP needs to be glued on the surface of the elements and there is no problem with that in Chuan-Dou buildings, as there is no painting on the surface of timber elements of the residential houses. However, for Dieh-Dou building, this permanently glued strip would affect negatively the artistic value of the timber element and also be irreversible. Hence, taking structural strengthening efficiency and cultural preservation into account, the steel plate-bolt method is considered the most appropriate, as it mixes efficiency with a degree of reversibility.

Chen (2008) indicated that for dove-tail joint, strengthening with the steel plate-bolt system with 3 mm thick plates and 12 mm diameter bolts, as shown in Figure 7.2.1, could increase the rotational stiffness from 1.74E+4 Nm/rad to 3.70E+4 Nm/rad, while the ultimate moment was increased from 1156 Nm to 2120 Nm, when

compared to the unstrengthened case. The increase in rotational stiffness and moment capacity due to the strengthening was 2.13 and 1.83 times, respectively.

In order to evaluate the effect of a potential strengthening of the aforementioned outer zones of the frames, the rotational and translational stiffness are updated in all elements of zones A2 and C2 of Guan-Shi main hall and C2 of Dou-Shan main hall models. As both the values of the joint stiffness and ultimate moment capacity found by Chen in the unstrengthened case are in good agreement with the values found in the Dieh-Dou joints loaded with 3.25 kN vertical load (see Chapter 4), it is assumed that the increase in stiffness and moment capacity due to the strengthening would be of the same magnitude, although this would need to be verified by further testing on strengthened Dieh-Dou joints.

In terms of translational stiffness, it is easily checked that this strengthening arrangement will render the joint axially rigid. The pull out capacity is limited by the shear capacity of a 12 mm bolt and the associated bearing capacity of the 3 mm plate and the timber. With standard commercially available steel and bolt grades and the softwood considered, a minimum allowable axial capacity of 12 kN is easily guaranteed limited by the bearing of the steel plates, which can be set as failure criterion for the strengthened joints, so as to designate the plate as sacrificial with respect to the historic timber element.

Modal analysis, lateral force analysis and response spectrum are performed and results checked with the updated failure criteria in the following section.

7.3 Analysis results

Modal analyses were first performed to observe the natural periods of these two frames after strengthening. Table 7.3.1 lists natural periods, frequencies and mass participations of the first 6 modes, while Fig 7.3.1 and Fig 7.3.2 show the first 6 modal shapes of Guan-Shi temple (GS-NF S) and Dou-Shan temple (DS-NF S), respectively after strengthening.

Table 7.3.1 Results of modal analyses of two frames with strengthening

	Mode number	Frequency (Hertz)	Period (sec)	Modal effective mass in X direction (%)	Modal effective mass in Z direction (%)
Guan-Shi (GS-NF S)	1	1.1392E+00	8.7778E-01	97.6	0
	2	9.3110E+00	1.0740E-01	0.01	13.66
	3	1.2355E+01	8.0938E-02	0.02	32.1
	4	1.3803E+01	7.2446E-02	0.11	0.02
	5	1.5030E+01	6.6536E-02	0.05	0.76
	6	2.1590E+01	4.6317E-02	0.11	0.29
Dou-Shan (DS-NF S)	1	1.1951E+00	8.3673E-01	97.51	0
	2	9.6882E+00	1.0322E-01	0.05	10.28
	3	1.2669E+01	7.8934E-02	0.04	31.92
	4	1.4248E+01	7.0187E-02	0.07	2.53
	5	1.7516E+01	5.7089E-02	0.06	1.28
	6	2.4416E+01	4.0957E-02	0	1.99

The results indicate that strengthening of zones A2, C2 of Guan-Shi main hall and C2 of Dou-Shan main hall renders both frames more rigid, as expected, and the first natural periods reduce from 1.14 to 0.88 seconds for Guan-Shi main hall and from 0.93 second to 0.84 seconds for Dou-Shan main hall. Still the first modes of both buildings have the great majority of mass effective in X direction, similarly to the unstrengthened situation.

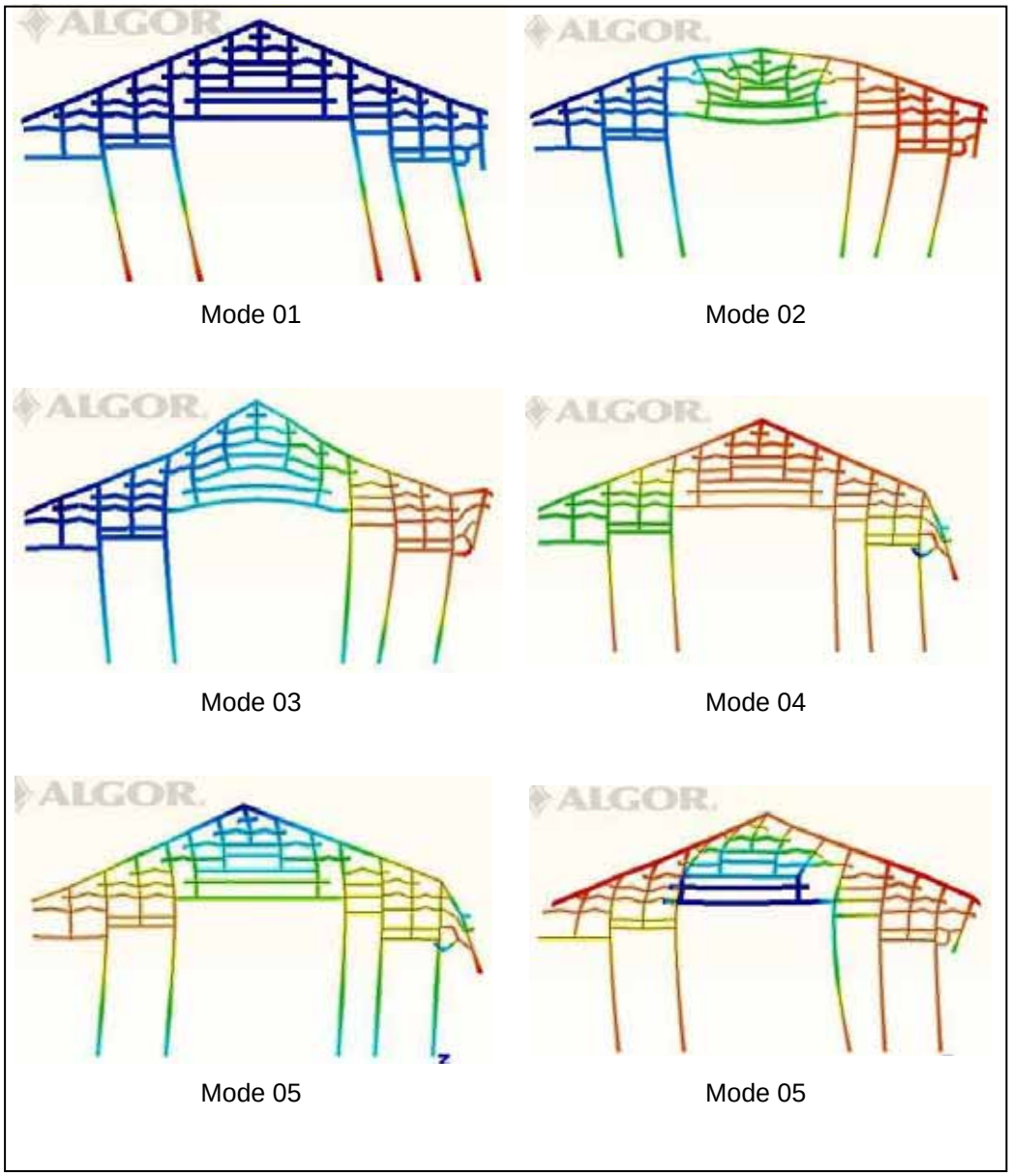

Figure 7.3.1 First 6 modes of Guan-Shi frame with strengthening

In the lateral force analysis for Guan-Shi main hall, whether the force equivalent to 0.33g is applied in the +X direction (GS-LF S01) or in the –X direction (GS-LF S02), the roof apex displacement decreased in both cases when compared to the unstrengthened situation (see Table 7.3.2). Compared to the results before strengthening, the roof apex displacement and number of local joint failure reduced,

showing that this strengthening strategy can improve the structural capacity to resist horizontal forces.

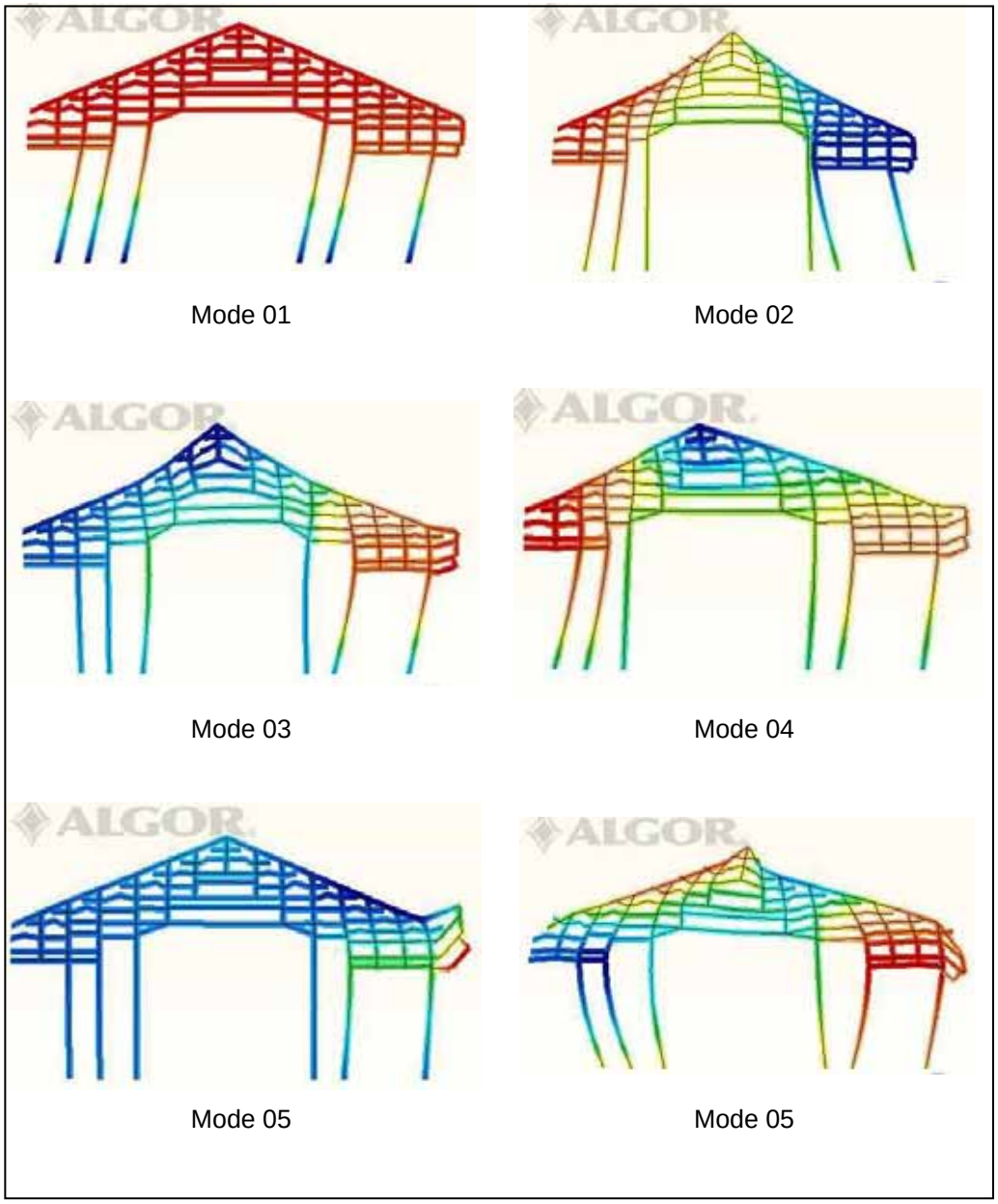

Figure 7.3.2 First 6 modes of Dou-Shan frame with strengthening

For Dou-Shan temple, although again in both models, with force applied in the +X direction (DS-LF S01) and –X direction (DS-LF S02) the roof apex displacements decreased, the differences were lower, passing from 65.1 mm to 51.8 mm for DS-LF S01 and from 64.7 mm to 52.2 mm for DS-LF S02, respectively, as this structure

was already more rigid than the previous. The number of joint failures also decreased by strengthening the elements of C2 area, but they are still in similar number to the frames without strengthening (see Table 7.3.2). The joint failures of Guan-Shi main hall and Dou-Shan main hall before and after strengthening are shown in Fig. 7.3.3 and 7.3.4.

Table 7.3.2 Results of lateral force of Guan-Shi and Dou-Shan main hall with strengthening

Strengthened (Unstrengthened)	Lateral force direction	Roof Apex displacement	Number of material failures	Number of pull out failures	Number of rotational failures
GS-LF S01 *(GS-LF 01)*	+X	55.4mm *(94.3mm)*	None	3 *(16)*	2 *(12)*
GS-LF S02 *(GS-LF 02)*	-X	54.6mm *(92.2mm)*	None	3 *(13)*	2 *(11)*
DS-LF S01 *(DS-LF 01)*	+X	51.8mm *(65.1mm)*	None	7 *(10)*	5 *(8)*
DS-LF S02 *(DS-LF 02)*	-X	52.2mm *(64.7mm)*	None	10 *(14)*	5 *(8)*

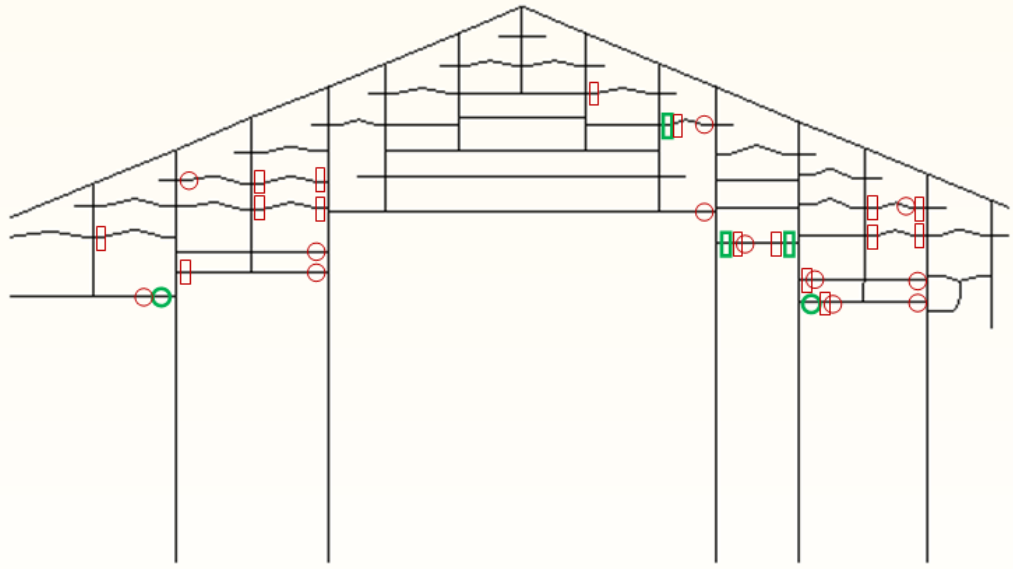

GS-LF S01 & GS-LF 01

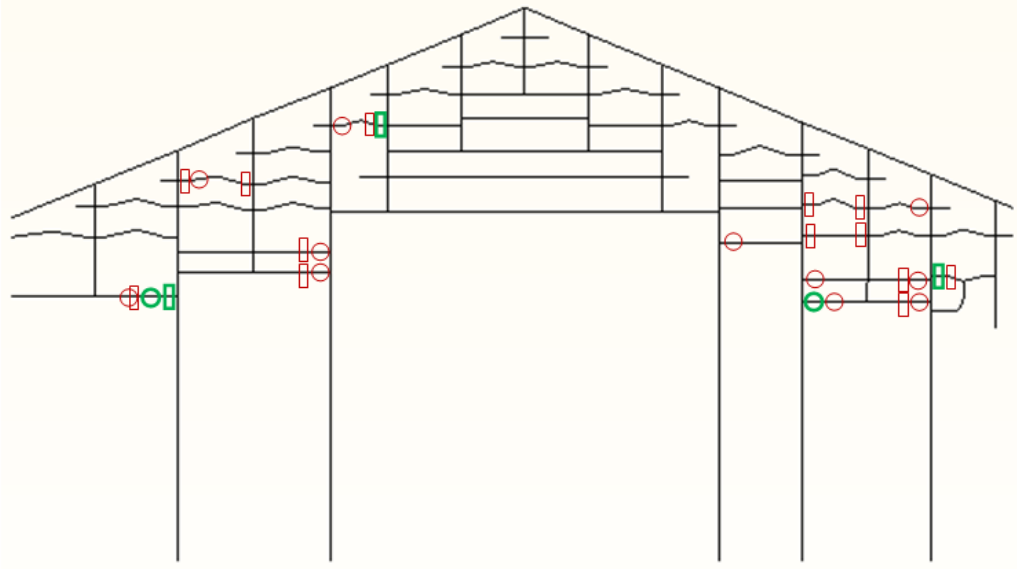

GS-LF S02 and GS-LF 02

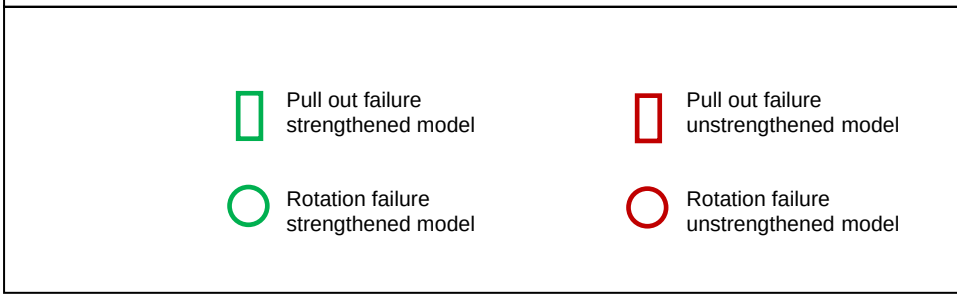

Figure 7.3.3 Joint failures of Guan-Shi frame before and after strengthening (lateral force analysis)

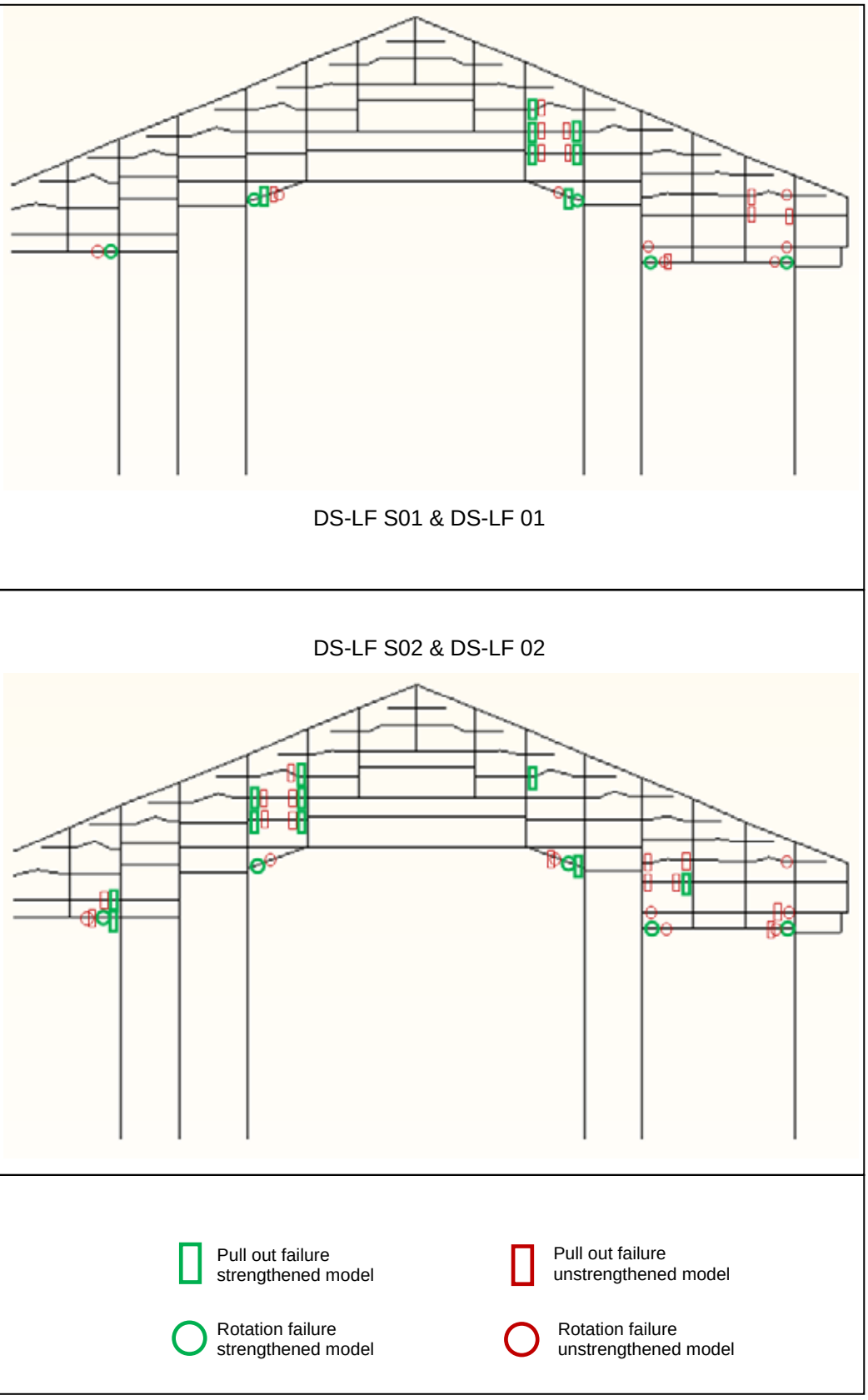

Figure 7.3.4 Joint failures of Dou-Shan frame before and after strengthening (lateral force analysis)

When the response spectrum analysis is performed for the strengthened frame, the roof apex displacement of the Guan-Shi main hall (model GS-RS S) is 96.2 mm, so the reduction from the unstrengthened situation (where the displacement was 107.5 mm) is much less than that found with the lateral force analysis, where a roof apex displacement of 55.4 mm was obtained (see Table 7.3.2).

Also, although the joints failures were reduced in number, a shear failure occurred this time, see Table 7.3.3. Figure 7.3.5 show the variation of shear forces in Guan-Shi temple after strengthening according to the response spectrum analysis (GS-RS S), while Fig. 7.3.6 indicates the location of material failure and joint failures of Guan-Shi and Dou-Shan temple.

Table 7.3.3 Results of response spectrum of Guan-Shi and Dou-Shan main hall with strengthening

Strengthened (Unstrengthened)	Roof Apex displacement	Number of material failures	Number of pull out failures	Number of rotational failures
GS-RS S *(GS-RS)*	96.2mm *(107.5mm)*	1 (None)	7 *(28)*	7 *(14)*
DS-RS S *(DS-RS)*	54.7mm *(52.1m)*	None	3 *(10)*	5 *(6)*

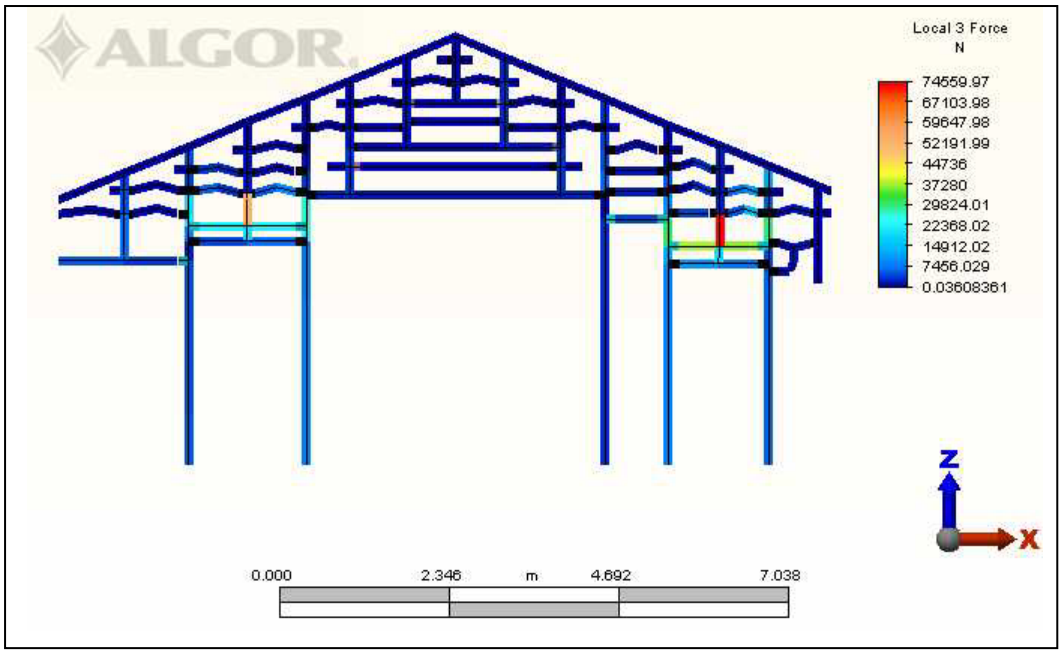

Figure 7.3.5 Shear force result of response spectrum (Guan-Shi)

This difference of behaviour between the lateral force and response spectrum occurs because, when the first period reduces, the equivalent lateral load increases and the structure now experiences a load higher than 0.33g. Therefore, in the case of Guan-Shi building, the response spectrum is more realistic or, in other terms, the applied lateral force should be increased to match the value found from the spectrum to become equivalent.

In Dou-Shan temple (DS-RS S), the roof apex displacement is quite similar between unstrengthened and strengthened situation (54.7 mm versus 52.1 mm respectively, see Table 7.3.3), but joint failures are still reduced after strengthening. Differently from the previous building, in the Dou-Shan temple the equivalent load from the real earthquake spectra is still below 0.33g even after the (slight) reduction of period due to the strengthening, so in overall terms, for this building the lateral force analysis is conservative.

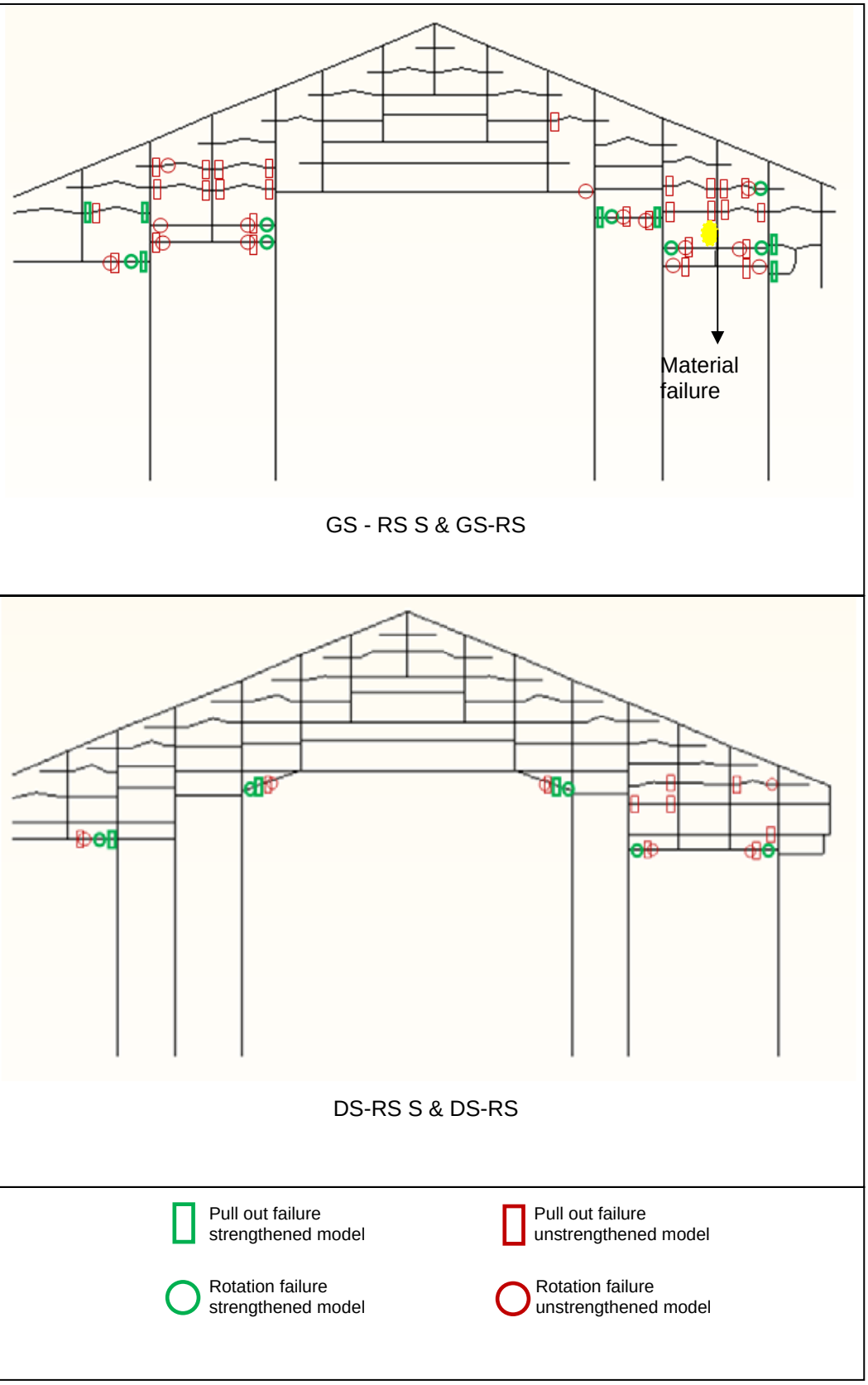

Figure. 7.3.6 Failures before and after strengthening
(response spectrum analysis)

7.4 Optimisation of strengthening

The results of these analyses outline that enhancing rotational and translational stiffness by strengthening the outer zones of the frame may not always be a convenient solution for Dieh-Dou timber frames under seismic loading, as the first period may be excessively reduced and potential material failures invocated. Hence, the extent and applicability of a strengthening scheme would need to be carefully assessed on a case by case basis, depending for example on the amount of identified vulnerable elements of the frame.

An extensive strengthening makes the whole structure stiffer, meaning the natural period of the building decreases leading the structure to potentially take more load, according to both real earthquake spectra and envelop design spectra (see FEMA 356, 2000). For example, before strengthening, the first period of Guan-Shi main hall was 1.14 second, which under the 1999 Chi-Chi earthquake spectra would have led to an acceleration of about 0.325g, while after strengthening all elements of the outer zones the load raised to about 0.5g. This corresponds to the fact that although the structural capacity of the critical elements increased, the higher load resulted in total displacements not dissimilar to the model without strengthening, which means that stresses on the other unstrengthened elements increase, potentially leading to material failures.

On the other hand, in the two case studies presented it has been shown that increasing ultimate moment and pull out capacity can significantly reduce joint failures. Therefore, strengthening of the Dieh-Dou frames is possible and can be very effective, but proper consideration needs to be given to the change of stiffness caused to the structure and special care needs to be taken in ensuring that the vulnerability of the elements is not worsened in any case by the strengthening scheme, especially that material failures are not created in the structure. The approach should be that the benefits of the strengthening have to be accurately weighed against the drawback in the most critical cases to understand the frame behaviour properly.

Two partial strengthening strategies were proposed for Guan-Shi temple, in addition to the one previously discussed, referred to as the ‘full strengthening’. The first

partial strengthening approach, represented by Model GS-RS PS01, involves strengthening all elements of A2 and C2 zones, see Fig. 7.4.1, apart from the two straight corridor beams, differently from the previous case. Finally, in model GS-RS PS02, only the ends of the binding beams that link with the Dou-Gon joint sets central to the zones were strengthened (see Fig. 7.4.1 right).

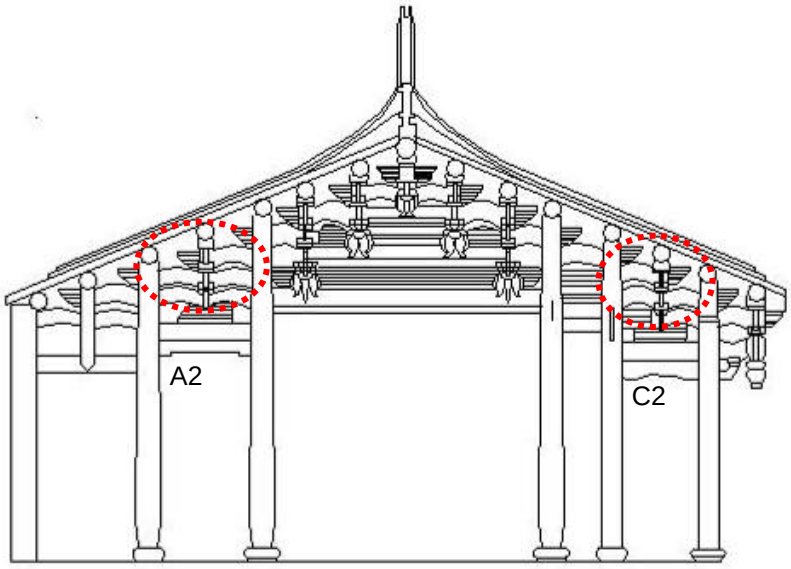

GS-RS PS01

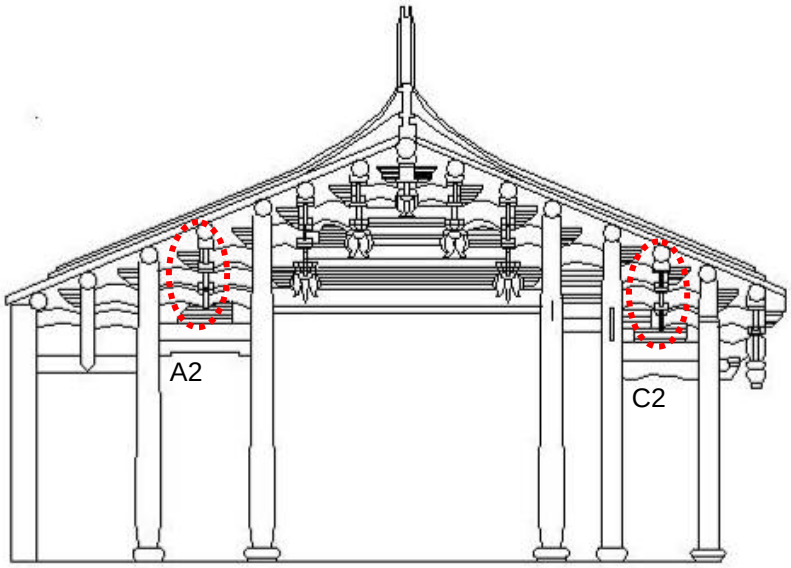

GS-RS PS02

Figure 7.4.1 Elements selected for partial strengthening of Guan-Shi temple

Table 7.4.1 Results of modal analyses of GS-RS PS01 and GS-RS PS02

	Mode number	Frequency (Hertz)	Period (sec)	Modal effective mass in X direction (%)	Modal effective mass in Z direction (%)
GS-RS PS01	1	1.0117E+00	9.8841E-01	97.64	0
	2	1.0160E+01	9.8430E-02	0.01	2.36
	3	1.4538E+01	6.8784E-02	0.13	0.73
	4	1.6002E+01	6.2494E-02	0	37.66
	5	2.2041E+01	4.5369E-02	0.07	0.33
	6	2.5035E+01	3.9945E-02	0	0.17
GS-RS PS02	1	9.0374E-01	1.1065E+00	97.44	0
	2	9.6837E+00	1.1009E-01	0.01	12.29
	3	1.2260E+01	8.1566E-02	0.02	33.51
	4	1.3417E+01	7.4535E-02	0.18	0
	5	1.4849E+01	6.7344E-02	0.04	0.58
	6	1.9149E+01	5.2220E-02	0.33	0.09

The analysis shows (see Table 7.4.1) that the first periods of these two frames are in between the unstrengthened (GS-RS) and fully strengthened (GS-RS S) being equal to 0.99 and 1.1 second for GS-RS PS01 and GS-RS PS02, respectively. When the response spectra of the 1999 Ch-Chi earthquake were applied, the results show that a partial strengthening can eliminate material failure and slightly reduce the roof apex displacement compared to the full strengthening (GS-RS S), while the total amount of joint of failures are somewhere in between GS-RS and GS-RS S. Fig. 7.4.2 shows the joint failures of GS-RS PS01 and GS-RS PS02.

Table 7.4.2.Results of response spectrum of Guan-Shi under different strengthening strategies

Strengthened (*Unstrengthened*)	Roof Apex displacement	Number of material failures	Number of pull out failures	Number of rotational failures
GS-RS PS 01	95.0mm	None	8	9
GS-RS PS 02	94.6mm	None	13	10
GS-RS S	96.2mm	1	7	7
GS-RS	*107.5mm*	*None*	*28*	*14*

Table 7.4.2 indicates that a partial strengthening of zones A2 and C2 is efficient for Guan-Shi main hall frame, as no material failures are caused by the intervention and the number of joint failures is significantly reduced compared with the unstrengthened situation. However, as the stiffness and consequently the forces on the structures are increased, the overall displacements can not be greatly reduced. It is also shown that although the strengthening was mainly designed to increase moment capacity, it is specifically effective in reducing pull out failure more than rotational failures. Moreover the difference between the two partial strengthening strategies highlight the improved behaviour obtained by strengthening both ends of the tie beams, rather than only the connection within the Dou-Gon, indicating the effect of continuity across the Gon of the beams connecting the corridor columns. However, the stiffening of this area in PS1 leads to concentration of stresses at the interface with the eaves element, producing failures here, in a zone already recognised as vulnerable.

This implies that strengthening may not always be necessary for all Dieh-Dou buildings; for example, in the case of the second building studied (Dou-Shan main hall), it is not easy to demonstrate how the reduced vulnerability of a few element would justify the damage to the originality of the structure. However, in the case of Guan-Shi main hall, which was subject to a large number of failures and to substantial global sway, leading to collapse, such a strengthening scheme may be necessary and should be tailored appropriately, maybe reducing the number of unnecessary strengthened elements in the outer zone to mitigate the stiffness increase and avoid material failures or failure in neighbouring unstrengthened connections.

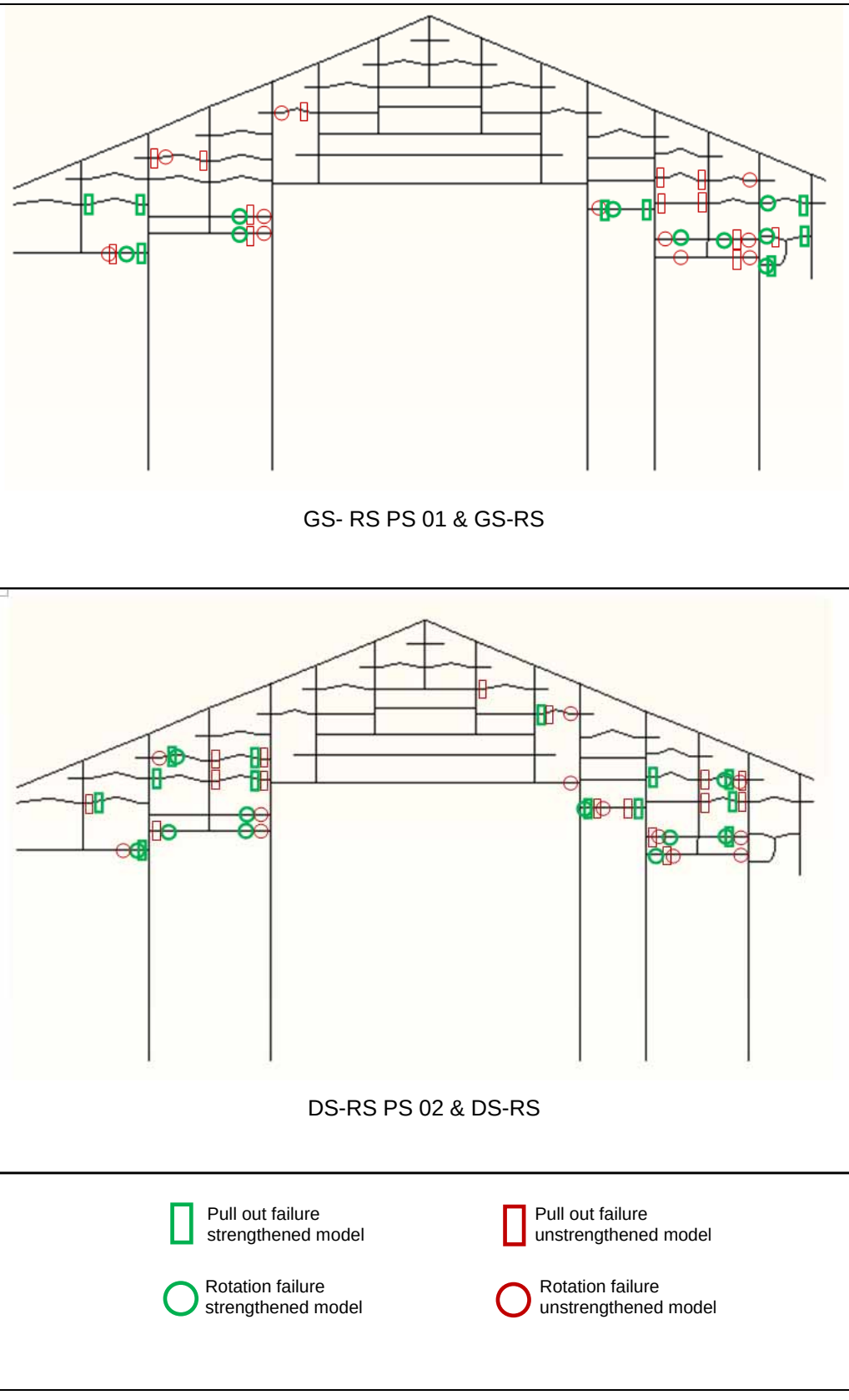

Figure 7.4.2 Failures of DS-RS PS 01 and DS-RS PS 02
(response spectrum analysis)

These analyses results highlight the sensitivity of these buildings to changes in stiffness. Taking the location of Guan-Shi family temple into account, the design spectra from the Taiwanese seismic code (Design of Buildings for Earthquake Resistance, 2005) can be drawn, see Fig. 7.4.3. The exact soil type for this site is unknown; however, considering all three types of soil considered (Type 1 for very dense sand or stiff clay, Type 2 for medium-dense sand or clay and Type 3 for loose cohesionless soil), it is seen that the fundamental period of the Dieh-Dou frames in both the unstrengthened and strengthened situations lie in the range of 0.8 to 1.2 seconds, which is in the descending branch of the response spectra.

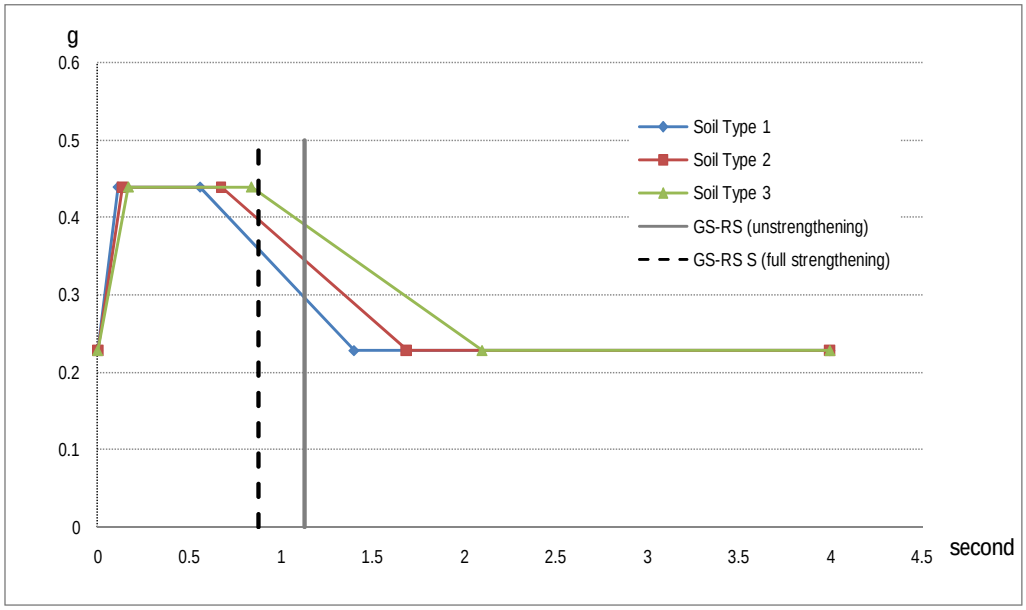

Figure 7.4.3 Elastic spectra for Guan-Shi temple following Taiwanese Code

Clearly, the vulnerability is dependant on the level of the assumed force due to the earthquake, which in the cases described above was taken from the current Taiwanese code with the 475 years return period and compared with the real Chi-Chi earthquake spectrum, showing it was slightly unconservative for the first building (Guan-Shi) and slightly conservative for the second (Dou-Shan). An aptly increased importance factor or an earthquake with a higher return period may be assumed where considered necessary, which would lead to a conservative prediction even in cases of such strong earthquakes as the 1999 Chi-Chi.

7.5 Proposed methodology and conclusions

The results of the analyses on Guan-Shi and Dou-Shan frames show that it is very important to perform a proper assessment before embarking in a strengthening scheme that may not be needed.

In the pushover analysis performed in Chapter 6 it was shown that the drift limit of 0.008, used by Miyamoto et al (2004) for Asian timber buildings, clearly identifies the limit of the linear stage for both buildings, so it is reasonable to use this criteria as the division between damage Level 1 and damage Level 2, which in Chapter 3 were defined as no damage and incipit of element pulling out, respectively. Although a drift of 0.005 is a limit for Taiwanese code, this value seems unduly conservative for Dieh-Dou buildings, as they are fairly deformable structures.

Under elastic analyses (lateral force and response spectrum), the roof apex displacement of Dou-Shan frame, that suffered only limited damage, resulted lower than 70 mm (corresponding to a drift of 0.0125) in both strengthened and unstrengthened situation. The limited benefit of a strengthening that would only dangerously increase the stiffness is not justified, as this building showed sufficient capacity to withstand the earthquake with limited damage. Hence, a second drift limit of 0.013 is proposed: it is assumed that if, as a result of a simple elastic analysis a drift lower than this limit is obtained, then the structure does not need to be strengthened. Although there may be some joint damage, the construction of Dieh-Dou frames allows carpenters to replace these few damaged elements, minimizing the disruption to originality.

Figures 7.5.1 and 7.5.2 show the load-displacement plots for both Guan-Shi and Dou-Shan temple frames with the various drift and proposed damage levels, where the 0.02 and 0.03 drift limits are those defined by the American standard for assessment FEMA 356 (2000) for wood stud walls corresponding to life safety and collapse prevention, respectively. Although the timber buildings defined in FEMA 356 (2000) are quite different to Dieh-Dou frames, it can be seen that these damage levels correspond well with the result of nonlinear analysis.

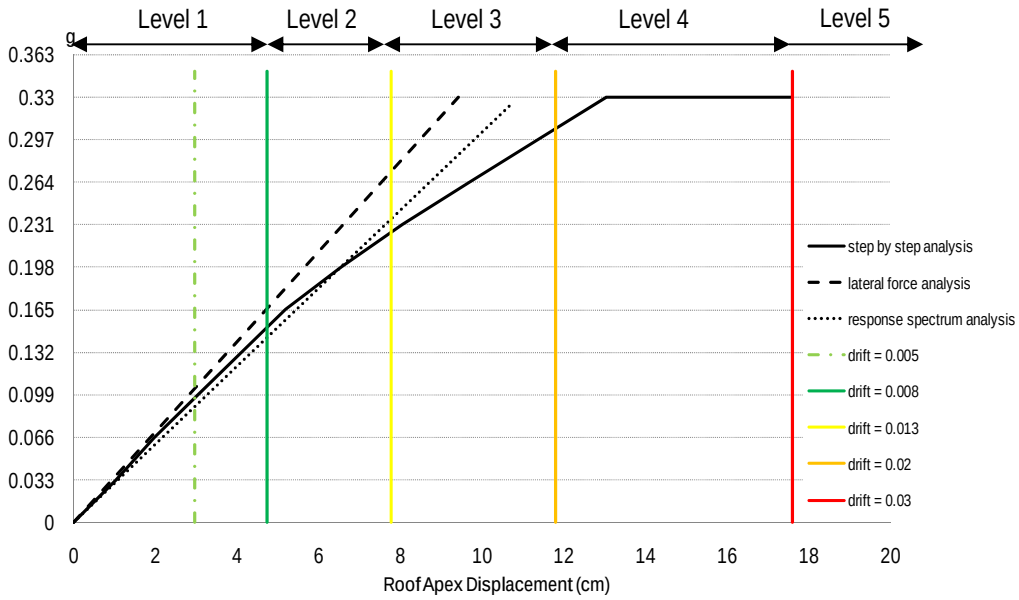

Figure 7.5.1 Guan-Shi frame analyses results and proposed limit drift

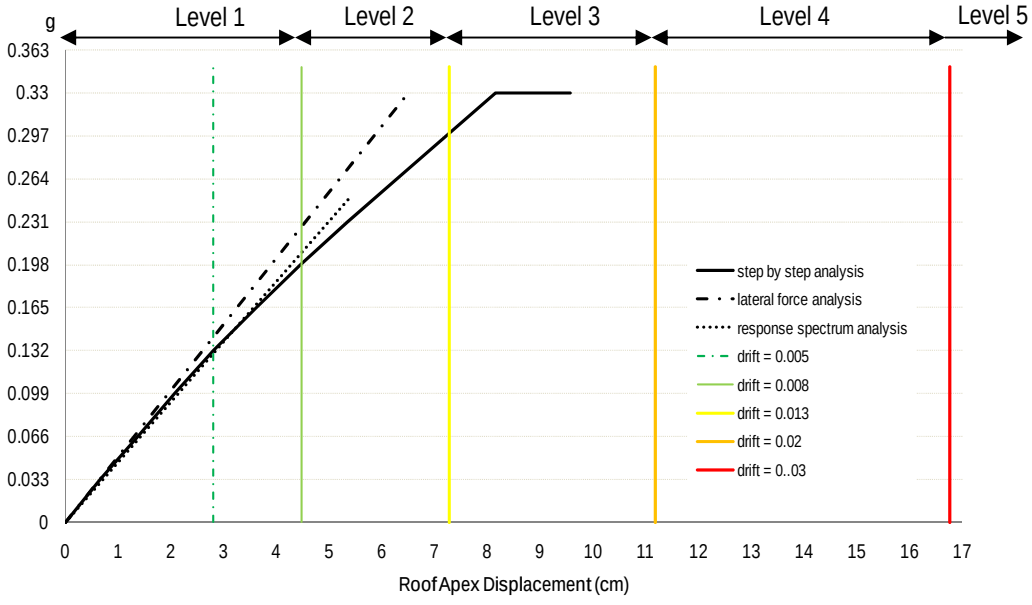

Figure 7.5.2 Dou-Shan analyses results and proposed limit drift

The nonlinear analysis represents the demand of strength and lateral drift necessary in the structure to withstand a given lateral acceleration. For Guan-Shi temple in order to withstand 0.33 g we have a demand of lateral drift of 0.03, which takes it to the brink of collapse, while for Dou-Shan the demand is in between 0.013 and 0.02, still well below the life safety risk. Comparing with the damage levels established in Chapter 3, 0.02 can be seen as the mark between damage levels 3 and 4, meaning that once drift exceeds this value the structure is likely to have suffered extensive damage. The drift 0.03 is set as collapse criteria separating levels 4 and 5.

However, checking the displacements alone is not sufficient, as the stability of the Dieh-Dou buildings becomes critical because of the joints' failures, while their historical values and uniqueness also is mainly embedded in the Dou-Gon joints. This implies that a frame, although originally stiff for its framing arrangement, has a too high proportion of failed joints or, on the other side, that a frame is more deformable but experiences less failures. Table 7.5.1 lists the percentage of failed joints in a frame for all analyses undertaken before and after strengthening, clearly showing that when the number of joints failed does not exceed 20-25% of the total in a frame, the structure may still be safe.

From the above considerations, it is proposed that the approach summarised in the flow chart of Figure 7.5.3 is followed for the assessment and strengthening of Die-Dou frames, where both checks on drift and percentage of failed elements should be accounted for in the assessment and strengthening outcome.

For a building like Dou-Shan, on the basis of drift demand form the elastic analysis there is no need to conduct non linear analysis and no need to strengthen, while in the case of Guan-Shi the elastic drift demand is above 0.013 and the joint failure is more than 20%, hence non linear analysis is needed. The nonlinear analysis results in a damage level 4 to 5 so there is need of strengthening. After strengthening, the elastic drift is between 0.013 and 0.02 but the joint failure can be reduced below 20%, so no further action is necessary. Clearly, it has to be checked that no material failure are introduced by strengthening the structure.

Table 7.5.1 Percentage of failed joints

		Before strengthening		After strengthening	
Guan-Shi	Lateral force	GS-LF01	32.9%	GS-LF S01	6.8%
		GS-LF02	24.7%	GS-LF S02	5.5%
		GS-LF01 + GS-LF02	43.8%	GS-LF S01 + GS-LF S02	9.5%
	Response spectrum	GS-RS	41.1%	GS-RS S	16.4%
				GS-RS PS01	19.2%
				GS-RS PS02	24.7%
	Step by step pushover	GS-PO	49.3%	---	---
Dou-Shan	Lateral force	DS-LF01	16.7%	DS-LF S01	10.4%
		DS-LF02	18.8%	DS-LF S02	13.5%
		DS-LF01 + DS-LF02	27%	DS-LF S01 + DS-LF S02	17.7%
	Response spectrum	DS-RS	11.5%	DS-RS S	5.2%
	Step by step pushover	DS-PO	21.9%	---	---

In conclusion, the uniqueness of Dieh-Dou construction, with timber pieces stacked together without any metal connections, makes the whole structure flexible; although this feature leads the structure to be prone to large deformations, on the other hand it helps the structure to dissipate the energy and this greatly helps to avoid material failures. As the timber elements of Dieh-Dou frames have precious painting on the surfaces, material failure is to be avoided as much as possible. The material failure will make the original pieces loose authenticity and replacement with new timber element is against good principles of conservation. Thus, the owners of these buildings and Taiwan Authorities should be aware that before strengthening these buildings, an appropriate assessment has to be undertaken, and the methodology applied in this research project is shown to be a valuable tool to achieve that goal.

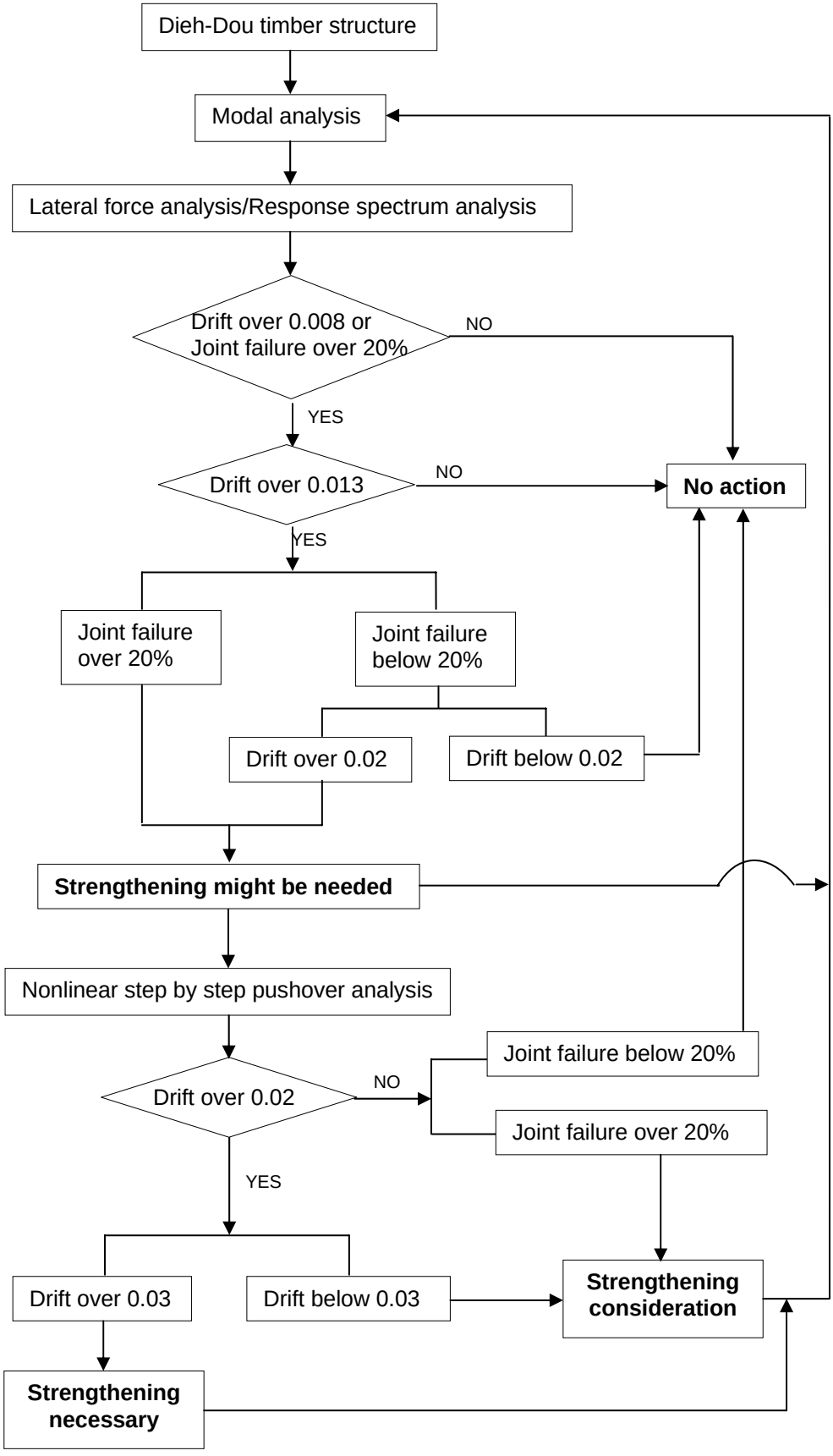

Figure 7.5.3 Proposed assessment and strengthening strategy

7.6 SDOF time history analysis

The numerical analysis and post-earthquake survey report show that the Dieh-Dou structure behaves approximately as a single degree of freedom (SDOF) in which the roof moves as a rigid body and the lateral displacement of the roof is the major movement. Thus, the Guan-Shi temple was selected for this SDOF time history analysis. From the modal analysis, the frequency of Guan-Shi temple is 0.877 Hertz, while the height is set as 4.46m corresponding to the gravity centre of the roof, see Fig.7.6.1.

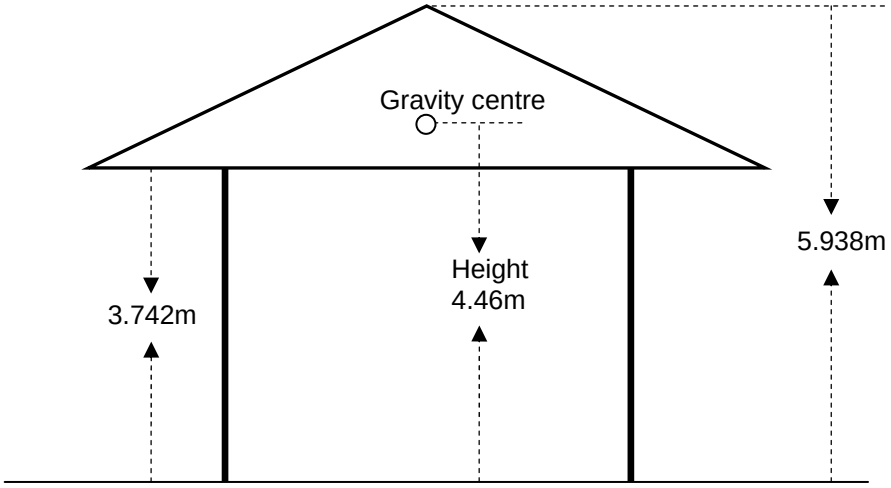

Figure 7.6.1 Height of Guan-Shi frame

From the Chi-Chi earthquake record of station TCU076, provided by the Central Weather Bureau of Taiwan, 70 seconds of the seismic excitation was applied as ground input in the time history analysis program described in the previous Chapter. The yield drift in the SDOF time history analysis was selected as equal to 0.03, to compare with the drift limit found in the previous analyses.

The result graph in Figure 7.6.2 shows that maximum roof apex drift in this SDOF time history was below 0.02, falling in the range of damage level 3, considered to produce structural damage but not collapse. However, Guan-Shi frame was seriously damaged during the Chi-Chi earthquake and partially collapsed. This difference may be caused by the fact that, for its unique construction feature and proneness to element pull-out rather than material yield failure, a SDOF can be an excessively simplification of the problem.

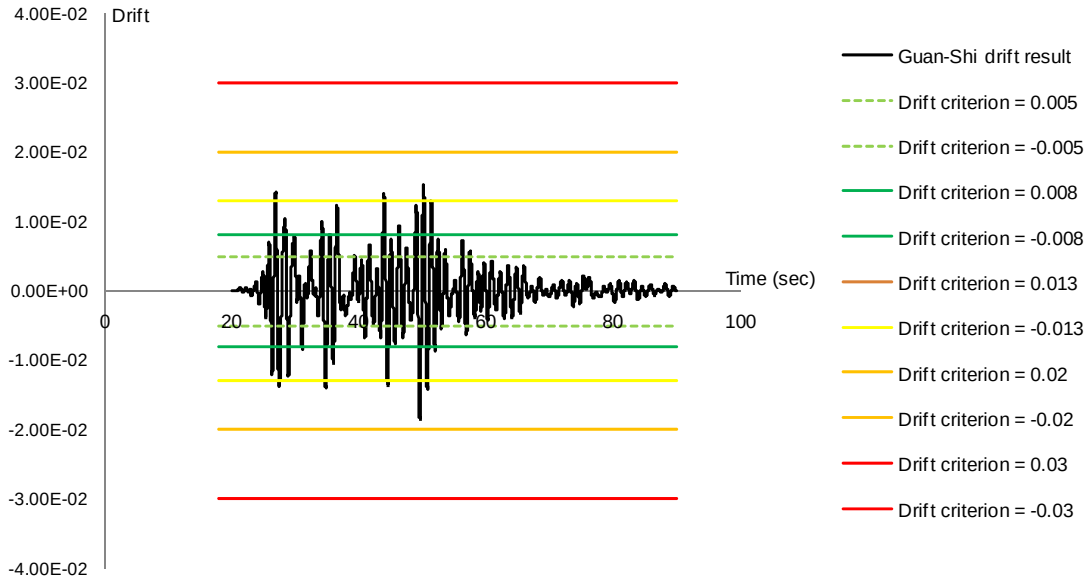

Figure 7.6.2 Result of SDOF time history analysis

The SDOF time history analysis can be a simple and quick method to assess structures under real earthquake and predict shakedown through defined criteria. It can be shown that a slight reduction in stiffness, possibly due to the repeated load, will cause the drift to exceed the 0.03 limit and the result to be in line with that of the previous analyses. It is also worth noting that short peaks of acceleration may not cause significant drift so that a static pushover could be over-safe.

Chapter 8
Conclusions and recommendations

8.1 Conclusions

This research has comprised a thorough investigation on the parameters influencing the seismic vulnerability of the Dieh-Dou timber frames in Taiwan through post-earthquake survey, experimental testing and numerical analysis, indicating the way for a rational procedure to assess and repair such structures.

The major task in the conservation of the historical Dieh-Dou timber buildings in Taiwan is to understand their structural behaviour. Taiwan is located in a highly seismic zone and these unique heritage buildings, constructed without following any code or standard, are prone to collapse under earthquake.

By collecting reports and by a field survey of Die-Dou buildings affected by the 1999 Chi-Chi earthquake, it was found that the most common features affecting the failure and the structural behaviour of the Dieh-Dou are:

- The connection of the columns with ground can be considered pinned
- The horizontal elements of the frame are easily pulled out from the joints or dislocated but rarely suffer material rupture
- The movement of the frames can be substantial before collapse

It is commonly recognized in the literature that timber joints are semi-rigid. However, the focus of previous researches was on the rotational stiffness, while in Die-Dou frames the translational characteristics are at least as important. Hence, an experimental campaign of laboratory testing on full-scale specimens of the traditional Dou-Gon joints was undertaken that permitted to obtain rotational stiffness, translational stiffness, moment capacity and pull out capacity of the joint elements.

A parametric study using finite element modelling revealed the sensitivity of the structural behaviour to the changes in rotational and translational stiffness, highlighting the importance of a proper modelling of the joint stiffness for Die-Dou frames.

The result of the laboratory testing was implemented in the FE numerical model and three seismic analyses (lateral force, step by step pushover and response spectrum) were performed on two reference buildings located in proximity of the epicentre of the Chi-Chi earthquake, for which an earthquake record was available. The results, when compared with the post earthquake survey, showed that the proposed FE modelling can successfully be employed to assess the vulnerability of the frames, as the critical zones could be accurately identified.

Lateral force analysis is the easiest and showed reasonable agreement with the other methods, because the great majority of the mass is excited by the first lateral mode of vibration in the plane of the frames. However, the natural frequency of these building cannot be accurately calculated with the simplified formulas of the codes, so a modal analysis is always necessary. The Dieh-Dou frames are found to have a relatively high first period of vibration; this is beneficial as it ensures they are not subjected to the high peaks of the spectral accelerations. The nonlinear step by step pushover analysis is the most accurate of the three methods as it can identify the variability in structural stiffness, the sequence of element failures and the ductility of the frame.

It was found that the effects of the vertical component of the earthquake excitation are negligible and can be disregarded. A 3D analysis of the whole building confirmed that a 2D analysis of a single frame is sufficient to assess its vulnerability even if the external masonry walls are collapsed, on condition that a proper connection is guaranteed between the purlins and the top of the frames.

The analysis results concluded that joint failures, especially those involving elements pull out, are critical rather than material failures. The elements more prone to failure are situated in the outer zones of the Dieh-Dou frame, while the central zone with the main beams remains relatively undamaged.

Strengthening the joints of the critical outer zones of the frames is the logical choice to reduce the number of failures and is an effective way to repair these structures. However, the strengthening increases the global stiffness and reduces the fundamental period of vibration, leading to an increase of force on the structure that can cause unwanted material failures and unnecessary reduction of safety factors elsewhere in the frame. Therefore, the extent of the strengthening should be carefully optimised following the assessment, also taking into account the value of preservation of the precious elements forming the Die-Dou buildings.

8.2 Recommendations and future work

From the findings of this research, it is recommended that the assessment of Die-Dou frames is undertaken using FE models that include both the rotational and translational stiffness found from this study.

A procedure to guide in the strategy of assessment and strengthening has been proposed, where both checks on limit drift and percentage of failed elements are accounted for in combination. Lateral force and response spectrum analyses can be initially performed in accordance with the provisions of the Taiwanese code, where the first period of vibration is calculated from a modal analysis. If the structure is found to be critical, before strengthening a step by step pushover analysis with a target force equal to the lateral force is the most appropriate approach. For both the lateral force and pushover analysis, it may be required to consider both directions as dissymmetry of the frame can result in different critical elements.

Future work may include verifying the proposed methodology against other Die-Dou buildings whose post-earthquake survey report are available, to adjust and confirm the validity of the proposed drift and damage level limitations. Further study is needed on the effectiveness and applicability of the strengthening procedures to the elements of Die-Dou buildings identified as critical.

A simple single degree of freedom model can be created that can take into proper account the general behaviour of Dieh-Dou frames with relation to its peculiar joint

failures. A time history could then be performed which would also consider the progressive loss of stiffness with the progressing of the failure.

Also, it has been shown that is important, to guarantee these buildings from out of plane instability, to assess the connections between the purlins and the saddles at the top of the frames, which in the traditional construction rely on friction only. Therefore, further work considering eventual options for strengthening these connections and involving a strengthening of the masonry walls and their connections with the purlins, together with the finding of the present research, would ensure these precious heritage structures can survive earthquakes.

References

9-21 Cultural Heritage Rescue Team, *http://www.arch.ncku.edu.tw/921/*

ALGOR v23, 2008, Algor, Inc., Pittsburgh, PA, USA

ASTM D198, 1984, *Standard Test Methods of Static Tests of Lumber in Structural Sizes,* American Society for Testing and Materials

BS EN 408, 2003, *Timber structures – structural timber and glued laminated timber – Determination of some physical and mechanical properties,* British Standard Institution, London

BS 5268-2, 2002, *Structural use of timber – Part 2: Code of practice for permissible stress design, materials and workman ship,* British Standard Institution

Cardone, D., 2007, Nonlinear static methods vs. experimental shaking table test results, *Journal of Earthquake Engineering*, v 11, n 6, November, pp 847-875

Chao, C.-C., 2004, "*Structural behaviour of traditional Die-Do Wooden Frame – Illustrated by the San-Chuan-Dian of listed heritage Tain-Nan, Tainan*," Master dissertation of national Cheng-Kung University, Taiwan (In Traditional Chinese)

Chang, W.-S., 2006, *On rotational performance of traditional Chuan-Dou timber joints in Taiwan*, PhD dissertation of National Cheng Kung University, Taiwan

Chang, J.-S.; **Lin, T.-C.** & **Yeh, C.-H.**; 2002, *Investigation of Damage Factors and Improvement for Ancient Monument and Historic Building Damaged in the 1999 Chi-Chi and Cha-Yi Earthquake*, National Centre for research on Earthquake Engineering, Taiwan (In Traditional Chinese)

Chang, Y.-H, 2004, *A study on Dismantling and Rehabilitation Procedures of Diehdou Wooden Structure in Traditional Remains of Taiwan – in the Case of Hsing-Chi Temple of Tainan*, Master dissertation of National Cheng Kung University, Taiwan (In traditional Chinese)

Chen, C.-J., 2008, The study on Improved Mechanical Properties of Reinforced Traditional Chuan-Dou Timber Joints in Taiwan, *Journal of Cultural Property conservation,* v 1 (3), pp 5-14

Chen, M.-H., 2004, *The study of In-Situ Investigation on Damages of Traditional Dieh-Dou Timber Frames in Taiwan*. Master dissertation, National Cheng Kung University (In Traditional Chinese)

Chen, T.-S., 2007, *The Study on the Planning for the Traditional Dei-dou Timber Frames in Temples Built During the Japanese Period in Taiwan by Using 3D Scanning Laser Ranger*, Master dissertation, National Cheng Kung University, Taiwan (In Traditional Chinese)

Chopra, A.K. & **Goel, R.K.**; 2002, A modal pushover analysis procedure for estimating seismic demands for buildings, *Earthquake Engineering and Structural Dynamics*, v 31, n 3, March, 2002, p 561-582

Clough, R. W.; Penzien, J, 1993, *Dynamic of structures*, McGraw-Hill, Inc,

Croci, G.; 2000, "*The Conservation and Structural Restoration of Architectural Heritage*", Computational Mechanics Publication

Cultural Heritage Preservation Law, 1982, Taiwan (In Traditional Chinese)

D'Ayala, Dina F., 2005, Force and displacement based vulnerability assessment for traditional buildings, *Bulletin of earthquake Engineering*, 2005, v 3, pp 235-265

D'Ayala, D. & **Forsyth, M.**, 2007," *What is conservation engineering?*" In *Structure and Construction in Historic Building*, edited by Michael Forsyth, Blackwell Publishing

D'Ayala, D. & **Wang, H.**, 2006 (a), Structural preservation of Chinese architectural heritage *Journal of Architectural Conservation*, No.1, Vol.12, March, pp 53-70

D'Ayala, D. & **Wang, H.**, 2006 (b), Conservation practice of Chinese Timber structure – "No originality to be changed" or "Conserve as found", *Journal of Architectural Conservation*, No.2, Vol.12, July, pp 7-26

Dong, Weimin; **Morrow, Guy**; **Tanaka, Akio**; **Kagawa, Hideo**; **Chou, Lun-Chang**; **Tsai, Yi-Ben**; **Hsu, Wenko**; **Johnson, Laurie**; **Anne, Craig Van**; **Segawa, Shukyo**;

Yeh, Chin-Hsun; **Wen, Kuo-Liang** & **Chiang, Wei-Ling**, "*Event Report for the 1999 Chi-Chi Earthquake"*, Risk Management Solutions Inc., Menlo Park, California, USA

Dou-Shan Temple Commission, 2008, "*Dou-Shan Temple*", published by Dou-Shan Temple Commission, Taiwan (in Traditional Chinese)

Elnashai, A.S., 2001, Advanced inelastic static (pushover) analysis for earthquake applications, *Structure Engineering and Mechanics*, Vol. 12, No. 1, pp 52-69

EMS 98, 1998, **"**European Macroseismic Scale 1998", *European Seismological Commission, Subcommission on Engineering Seismology*, Working Group Macroseismic Scales, G. Grünthal Ed. Luxembourg.

Eurocode 8, 2004, BS EN 1998-1:2004, *Design of structures for earthquake resistance – Part 1: General rules, seismic actions and rules for buildings*, British Standard Institution, London

Eurocode 8, 2005, BS EN 1998-3:2004, *Design of structures for earthquake resistance – Part 3: Assessment and retrofitting of buildings*, British Standard Institution, London

Fang, D. P., **Iwasaki, S.**, **Yu, M. H.**, **Shen, Q. P.**, **Miyamoto, Y.** & **Hikosaka, H**., 2001, Ancient Chinese timber architecture. I: Experimental study, *Journal of Structural Engineering*, November, pp 1348-1357

Fang, D. P., **Iwasaki, S.**, **Yu, M. H.**, **Shen, Q. P.**, **Miyamoto, Y.** & **Hikosaka, H**., 2001, Ancient Chinese timber architecture. II: Dynamic characteristics, *Journal of Structural Engineering,* November, pp 1358-1364.

FEMA 356, 2000, *Prestandard and Commentary for the seismic rehabilitation of buildings*, American Society of Civil Engineers, Federal Emergency Management Agency, November ,USA

Fijishima, G. (survey and writing), **Chan, H.-L.** (translating and editing), 1999, *Taiwanese architecture,* Taiuan Publishing Co. (In Traditional Chinese)

Fu C.-C., 2005, Symbolic, architecture and artistic decorations in structural elements in traditional architecture in Taiwan, In *Proceeding of Structural Studies, Repair and Maintenance Architecture IX*, Vol. 83, pp. 35-42.

Goel, R. K. & **Chopra, A. K.**, 2005, Extension of Modal Pushover Analysis to Computer Member Force, *Earthquake Spectra*, Vol. 21, No. 1, pp 125-139

Grierson, D. E., **Gong, Y.** & **Xu, L. E. I.**, 2006, Optimal performance-based seismic design using modal pushover analysis, *Journal of Earthquake Engineering*, v 10, n 1, January, 2006, p 73-96

Guo, Q., 1999, "*The structure of Chinese timber architecture"*, Minerva Press, UK

Hanazato, T., **Fujita, K.**, **Sakamoto, I.**, **Inayama, M.** & **Ohkura, Y.**, 2004, Analysis of earthquake resistance of five-storied timber pagoda, *Proceeding of 13th World Conference on Earthquake Engineering*, Paper No. 1223, August, Vancouver, Canada

HAZUS-MH MR3, 2003, Multi-Hazard Loss Estimation Methodology, *Earthquake model*, Technical Manual, Department of Homeland Security Emergency Preparedness and Response Directorate, Federal Emergency Management Agency (FEMA), USA

Hsu, U.-C., 2002, *Investigation project of historic building – Guan-Shi Chang family temple in Nan-Tou*, Nan-Tou County, Taiwan, (In Traditional Chinese)

Hsu, U.-C., 2003, *Investigation project of historic building – Dou-Shan temple*, Chang-Hua County, Taiwan, (In Traditional Chinese)

Huang, P., **Chang, J.-S.** & **Shu, T.-C.**, 2003, *Investigation of joint and structural feature of Dieh-Dou timber frame*, Architecture and Building Research Institute, Taiwan (In Traditional Chinese)

Huang, P. & **Sheu, M. S.**, 2001, *A study on seismic failure and maintenance of historic buildings. I: Bamboo and timber construction,* Council for Cultural Affair, Taipei (In Traditional Chinese)

Inel, M., **Ozmen, H. B.** & **Bilgin, H.**; 2008, Re-evaluation of building damage during recent earthquakes in Turkey, *Engineering Structures*, v 30, n 2, February, pp 412-427

Institute of Architects, 1999, *Survey of the Chi-Chi earthquake and building assessment and repair report,* Taiwan Institute of Architects (In Traditional Chinese)

Ipekoglu, Basak, 2006, An architectural evaluation method for conservation of traditional dwellings, *Building and Environment*, March, v 41, n 3, pp 386-394

ISCARSAH Principles, 2003, *Principles for the Analysis, Conservation and Structural Restoration of Architectural* Heritage, ICOMOS, available at the website www.international.icomos.org/charters.htm (accessed March 2009)

Jaishi, B., **Ren, W.-X.**, **Zong, Z.-H.** & **Maskey, P. N.**, 2003, Dynamic and seismic performance of old multi-tiered temples in Nepa, *Engineering Structures*, v 25, n 14, December, pp 1827-1839

Jokilehto, J., 1999, "*A History of Architectural Conservation"*, Elsevier, London

Kelly, A., 1990, "Concise Encyclopedia of Composite Materials", MIT press, Massachusetts, USA

King, W.S., **Yen, J. Y.** & **Yen, Y.N.**, 1996, Joint characteristics of traditional Chinese wooden frames, *Engineering Structures*, Vol. 18, No. 8, pp. 635-644

Lee, C.-L., 1988, *Investigation of Ian-Shan Temple*, Council for Cultural Affairs, Taipei County Government & Lee Chian-Lang Research Studio (In Traditional Chinese)

Lee, C.-W., 2007, "*The Study of Component Types of Four-Gold-Columns Extent of Die-dou Timber Frame*" Master dissertation, National Cheng Kung University, Taiwan (In traditional Chinese)

Lee, C.-L., 2003, *Pictorial matter of ancient Taiwanese architecture*, Uan-Low publication company, Taiwan (In Traditional Chinese)

Lewis. G W., 2006, *Dieh-Dou joints in Taiwanese timber frames,* BEng (hons) dissertation, Department of Architecture and Civil engineering, University of Bath, UK

Lin, H.-C., 1995*, Handbook of traditional building*, Artist publication company, Taiwan, (In Traditional Chinese)

Liu, G.-R. & **Quek, S. S.**, 2003, *Finite Element Method: A Practical Course*, Butterworth-Heinemann, UK

Lourenco, P. B. ,2005, Assessment, diagnosis and strengthening of Outeiro Church, Portugal, *Construction and Building Materials*, v 19, n 8, October, 2005, pp 634-645

Miyamoto S., **Miyazawa K.**, **Irie Y.**, **Wu J.**, **Nomata Y. O.** & **Goto**, 2004, A study on seismic performance and seismic diagnosis, seismic retrofit of Japanese temple, *Proceeding of 13th World Conference on Earthquake Engineering*, Paper No. 853, August, Vancouver, Canada

Morris, E. T., **Black, R. G.** & **Tobriner, S. T.**, 1995, Report on the Application of Finite Element Analysis to Historic Structures: Westminster Hall, London, *The Journal of the Society of Architecture Historians*, Vol. 54, No. 3, September, pp 336-347

Nara Document on Authenticity, 1994, ICOMOS, available on the website http://www.international.icomos.org/naradoc_eng.htm (accessed March 2009)

Parisi, M. A. & **Piazza, M.**, 2002*,* Seismic behaviour and retrofitting of joints in traditional timber roof structures, *Soil Dynamics and Earthquake Engineering*, v 22, n 9-12, October/December, pp 1183-1191

Principle for the Conservation of Heritage Sites in China, 2004, ICOMOS China, Agnew, D and Demas, M. (Eds.), Getty Conservation Institute, Los Angeles.

Principle for the Preservation of Historic Timber Structure, 1999, ICOMOS, http://www.international.icomos.org/charters/wood_e.htm (accessed March 2009)

Shiao, J.-P., **Lee, C.-Y.**, **Hung, C.-Y.**, **Lee, T.-M.**, **Cheng, T.-W.**, **Lee, P.-H.** & **Wu, C.-M.**, 2003, *Historic timber frame structure investigation-–– Illustrated by Dieh-Dou frames,* Architecture and building research, Ministry of Interior, Taiwan (In traditional Chinese)

Shu, T.-C., 2000, *The Study of the Joint Systems in the Wooden Structure of Taiwan Listed Historic Buildings,* Master dissertation, National Cheng Kung University, Taiwan (In Traditional Chinese*)*

Song, C.-S, 2004, *The Research on the split of wooden beams using Epoxy resin repair*, Master dissertation, National Cheng Kung University, Taiwan (In Traditional Chinese*)*

Spyrakos, C. C., 1994, *Finite element modelling in engineering practice*, Algor, Inc. Publish Division Pittsburgh, PA, USA

Su, I.-W., 2003, "*A Study of the Earthquake Damage and Retrofit of Taiwan's Traditional Temple*", Master dissertation, National Cheng Kung University, Taiwan

Survey of 9-21 Chi-Chi earthquake buildings damage, 1999, Architecture and Building Research Institute, 1999 *http://www.abri.gov.tw/english/index.aspx*

Taiwanese Code, 2008, *Design and Construction of Timber Buildings*, Ministry of Interior, Taiwan (In Traditional Chinese)

Taiwanese Code, 2008, *Design of Buildings for Earthquake Resistance*, Ministry of Interior, Taiwan (In Traditional Chinese)

Thelin C. & **Olsson K.-G.**, 2005, Static Behavior of a Historic Roof Structure; *Journal of Architectural Engineering*, June 2005, pp 39-49

Tsai, Y.-L., 1997, "*Investigation on the Materials used for Timber Construction of Historical buildings*", Master dissertation, Department of Forestry, National Chung-Hsing University, Taiwan (In Traditional Chinese)

Tseng, Y.-J., 1997, "*The Preliminary Study of the Patterns for the Damages on Wooden Structural Components and the Non-destructive Examination of Taiwan's Listed Historical Buildings*" Master dissertation, National Cheng Kung University, Taiwan (In Traditional Chinese)

Tseng, Y.-J., 2007, "*Non-destructive Evaluation on Wooden Structural Frames of Historic Buildings in Taiwan*" PhD dissertation, National Cheng Kung University, Taiwan (In Traditional Chinese)

Venice Charter, 1964, ICOMOS, International Charter for the Conservation and Restoration of Monuments and Sites, www.international.icomos.org/charters.htm (accessed March 2009)

Wood Handbook,1999, *Wood as an engineering material*, US department of Agriculture, Forest Service, Forest Products Laboratory, Madison, WI, USA

Yang, S.-J., 2008, “Studies of dimensional system of tenons and mortise in traditional Dieh-Dou frame” Master dissertation, National Cheng Kung University, Taiwan, (In Traditional Chinese)

Yeomans, D., 2003, “*The Repair of Historic Structures*”, Thomas Telford, London

Appendix A

Results of step by step pushover analysis of Guan-Shi temple

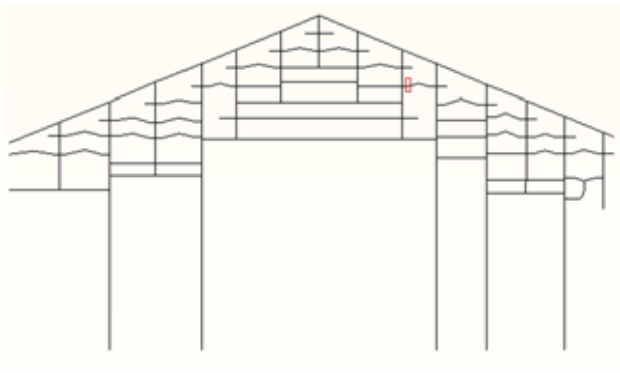	**Step 01: Failures up to this stage** Equivalent acceleration load:**0.033g** Roof Apex displacement: **1.039cm** Material failure: **None** Joint pull out failure at this step:**1** Joint rotational failure at this step: **None**
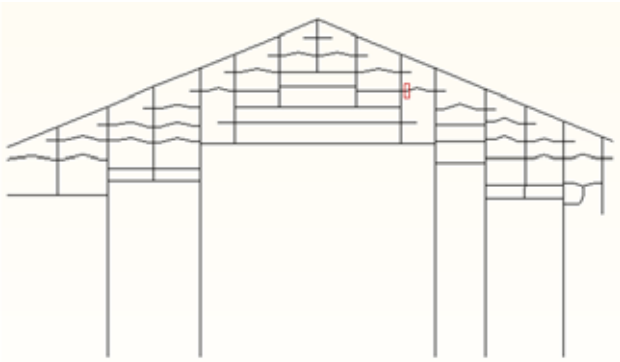	**Step 02: Failures up to this stage** Equivalent acceleration load: **0.033g** Roof Apex displacement: **1.065cm** Material failure: **None** Joint pull out failure at this step: **None** Joint rotational failure at this step: **None**
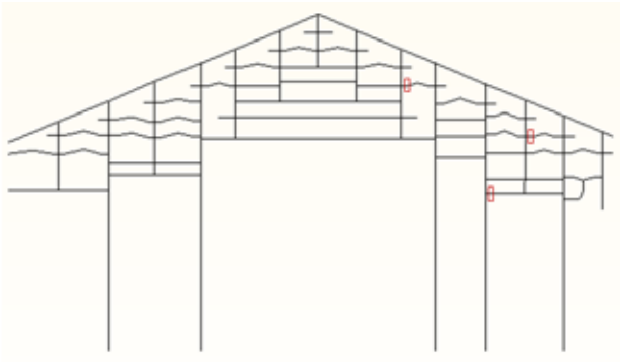	**Step 03: Failures up to this stage** Equivalent acceleration load: **0.066g** Roof Apex displacement: **2.002cm** Material failure: **None** Joint pull out failure at this step: **2** Joint rotational failure at this step: **None**
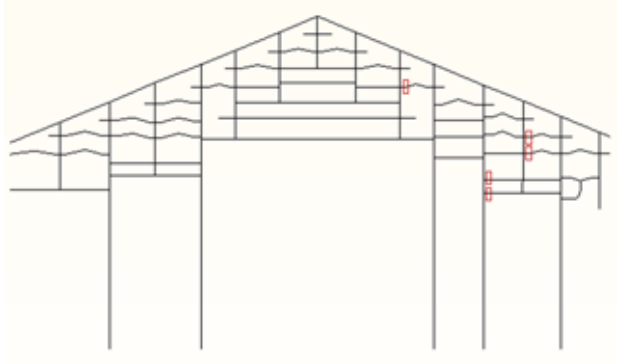	**Step 04: Failures up to this stage** Equivalent acceleration load: **0.066g** Roof Apex displacement: **2.145cm** Material failure: **None** Joint pull out failure at this step: **2** Joint rotational failure at this step: **None**

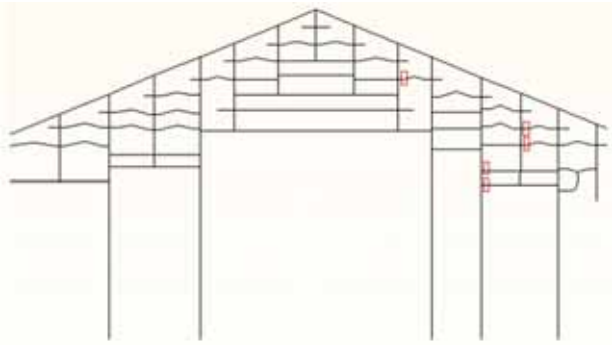	**Step 05: Failures up to this stage** Equivalent acceleration load: **0.066g** Roof Apex displacement: **2.314cm** Material failure: **None** Joint pull out failure at this step: **None** Joint rotational failure at this step: **None**
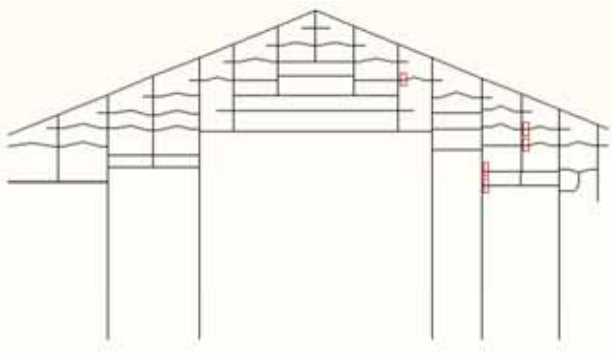	**Step 06: Failures up to this stage** Equivalent acceleration load: **0.099g** Roof Apex displacement: **3.383cm** Material failure: **None** Joint pull out failure at this step: **None** Joint rotational failure at this step: **None**
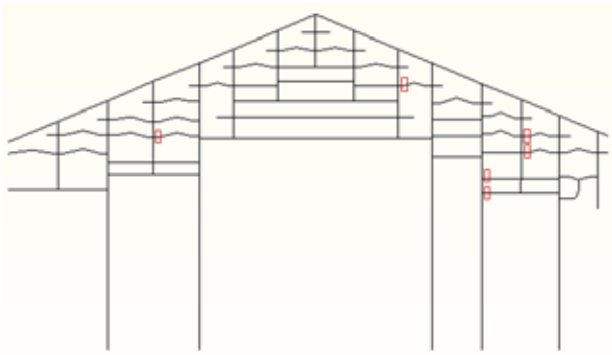	**Step 07: Failures up to this stage** Equivalent acceleration load: **0.132g** Roof Apex displacement: **4.452cm** Material failure: **None** Joint pull out failure at this step:**1** Joint rotational failure at this step: **None**
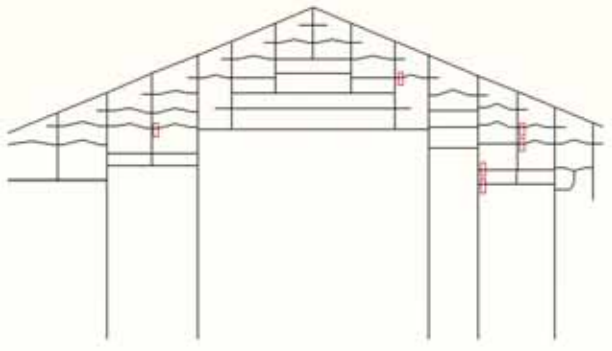	**Step 08: Failures up to this stage** Equivalent acceleration load: **0.132g** Roof Apex displacement: **4.5cm** Material failure: **None** Joint pull out failure at this step: **None** Joint rotational failure at this step: **None**

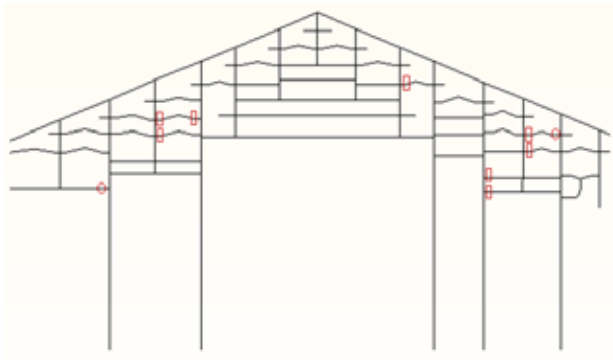

Step 09: Failures up to this stage
Equivalent acceleration load: **0.165g**
Roof Apex displacement: **5.58cm**
Material failure: **None**
Joint pull out failure at this step:**2**
Joint rotational failure at this step: **2**

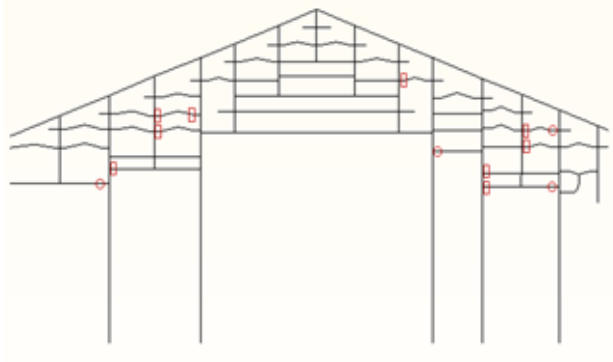

Step 10: Failures up to this stage
Equivalent acceleration load: **0.165g**
Roof Apex displacement: **5.886cm**
Material failure: **None**
Joint pull out failure at this step: **1**
Joint rotational failure at this step: **2**

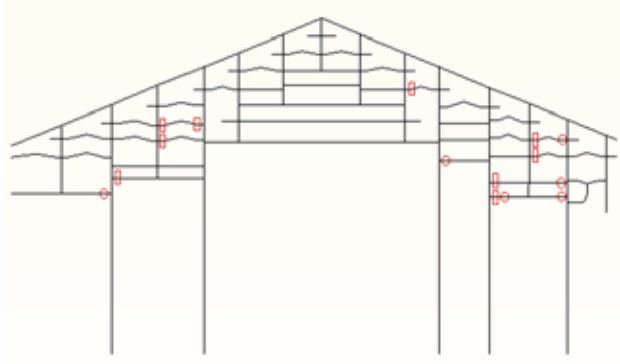

Step 11: Failures up to this stage
Equivalent acceleration load: **0.165g**
Roof Apex displacement: **6.2648cm**
Material failure: **None**
Joint pull out failure at this step: **0**
Joint rotational failure at this step: **2**

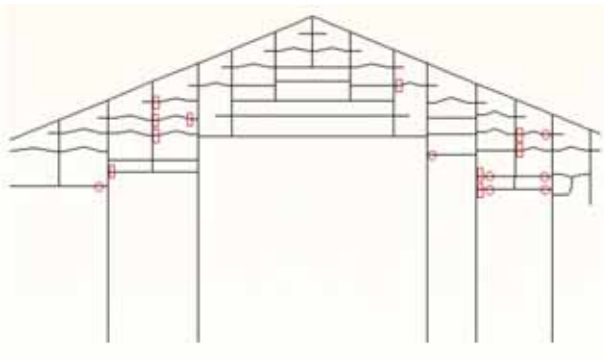

Step 12: Failures up to this stage
Equivalent acceleration load: **0.165g**
Roof Apex displacement: **6.6176cm**
Material failure: **None**
Joint pull out failure at this step: **1**
Joint rotational failure at this step: **1**

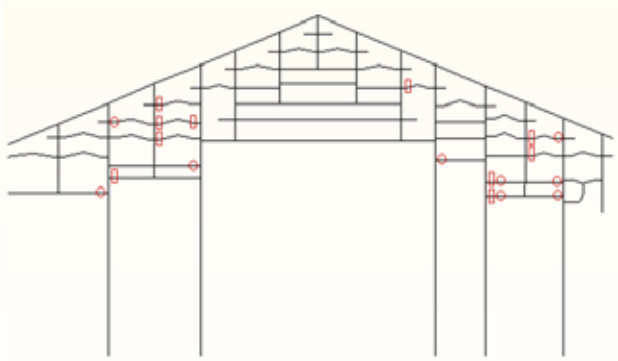	**Step 13: Failures up to this stage** Equivalent acceleration load: **0.165g** Roof Apex displacement: **6.831cm** Material failure: **None** Joint pull out failure at this step: **0** Joint rotational failure at this step: **2**
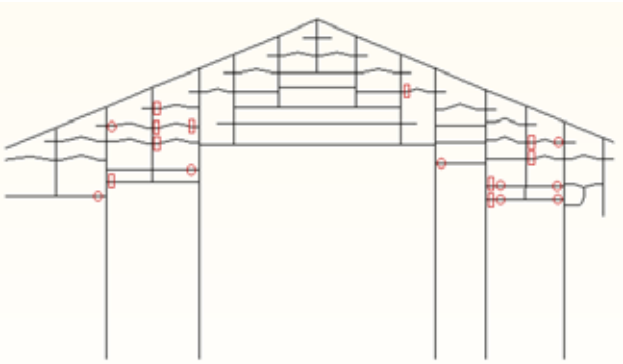	**Step 14: Failures up to this stage** Equivalent acceleration load: **0.165g** Roof Apex displacement: **7.06cm** Material failure: **None** Joint pull out failure at this step: **None** Joint rotational failure at this step: **None**
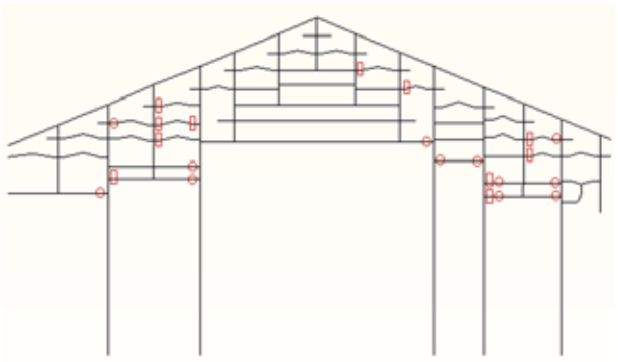	**Step 15: Failures up to this stage** Equivalent acceleration load: **0.198g** Roof Apex displacement: **8.422cm** Material failure: **None** Joint pull out failure at this step: **1** Joint rotational failure at this step: **3**
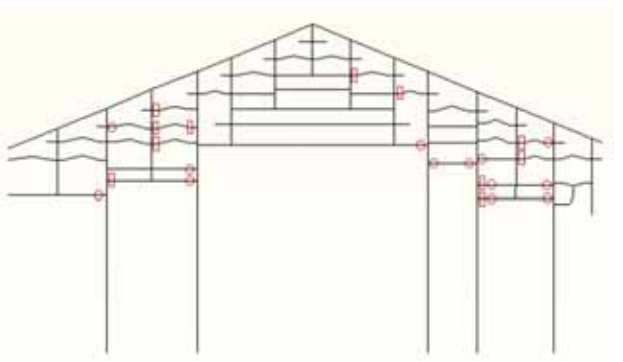	**Step 16: Failures up to this stage** Equivalent acceleration load: **0.198g** Roof Apex displacement: **9.00cm** Material failure: **None** Joint pull out failure at this step: **0** Joint rotational failure at this step: **1**

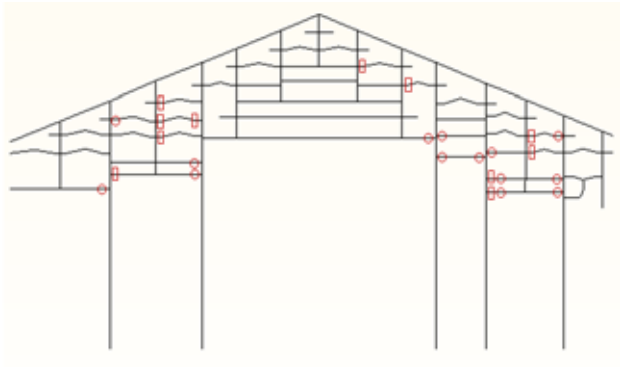	**Step 17: Failures up to this stage** Equivalent acceleration load: **0.198g** Roof Apex displacement: **9.157cm** Material failure: **None** Joint pull out failure at this step: **0** Joint rotational failure at this step: **1**
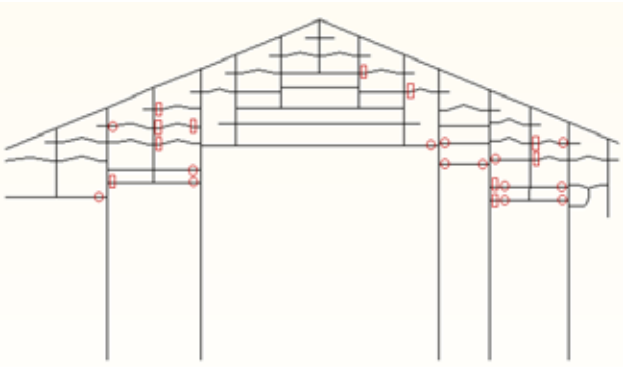	**Step 18: Failures up to this stage** Equivalent acceleration load: **0.198g** Roof Apex displacement: **9.306cm** Material failure: **None** Joint pull out failure at this step: **None** Joint rotational failure at this step: **None**
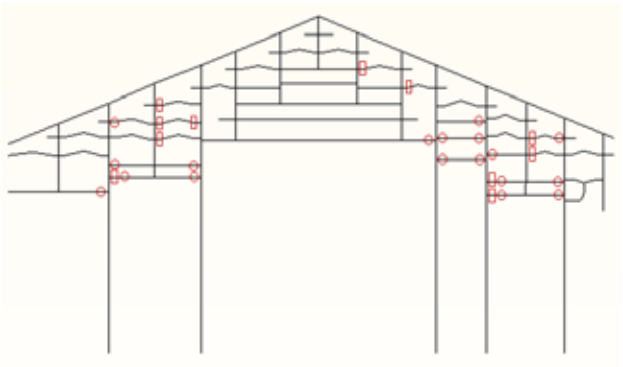	**Step 19: Failures up to this stage** Equivalent acceleration load: **0.231g** Roof Apex displacement: **10.8cm** Material failure: **None** Joint pull out failure at this step: **0** Joint rotational failure at this step: **4**
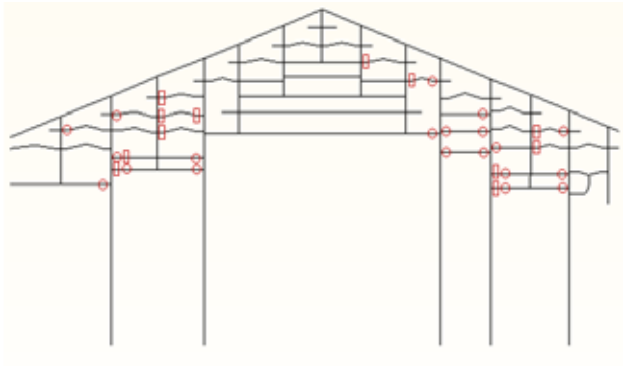	**Step 20: Failures up to this stage** Equivalent acceleration load: **0.231g** Roof Apex displacement: **11.435cm** Material failure: **None** Joint pull out failure at this step: **1** Joint rotational failure at this step: **2**

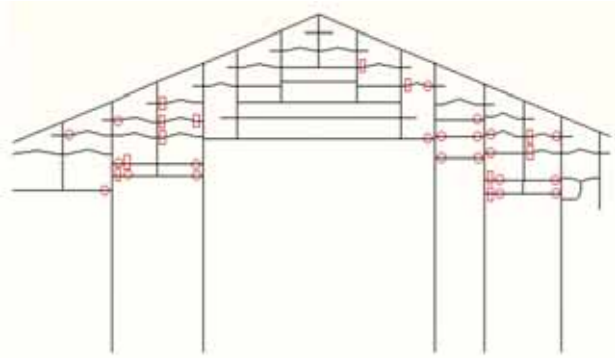	**Step 21: Failures up to this stage** Equivalent acceleration load: **0.231g** Roof Apex displacement: **11.6792cm** Material failure: **None** Joint pull out failure at this step: **0** Joint rotational failure at this step: **1**
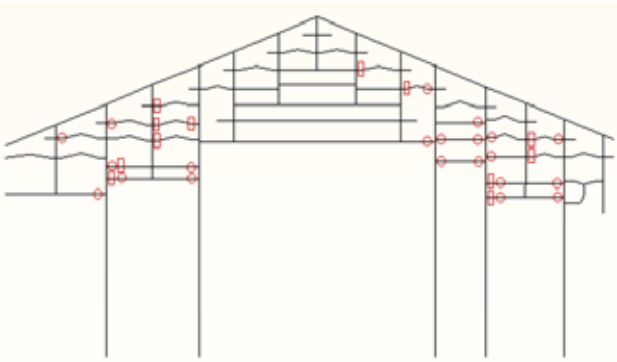	**Step 22: Failures up to this stage** Equivalent acceleration load: **0.231g** Roof Apex displacement: **11.835cm** Material failure: **None** Joint pull out failure at this step: **None** Joint rotational failure at this step: **None**
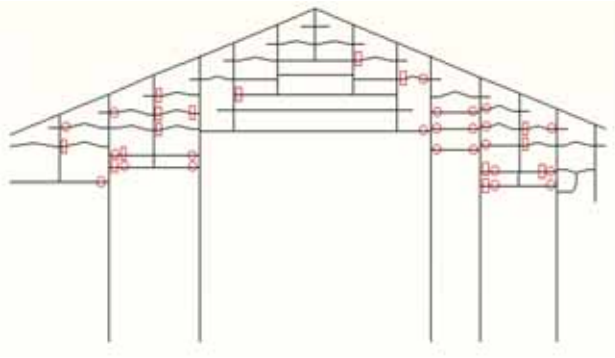	**Step 23: Failures up to this stage** Equivalent acceleration load: **0.264g** Roof Apex displacement: **13.474cm** Material failure: **None** Joint pull out failure at this step: **3** Joint rotational failure at this step: **2**
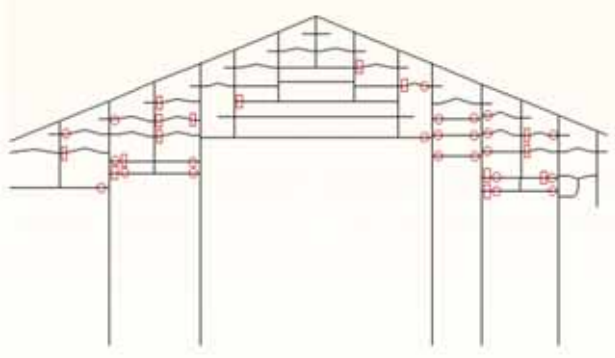	**Step 24: Failures up to this stage** Equivalent acceleration load: **0.264g** Roof Apex displacement: **13.834cm** Material failure: **None** Joint pull out failure at this step: **None** Joint rotational failure at this step: **None**

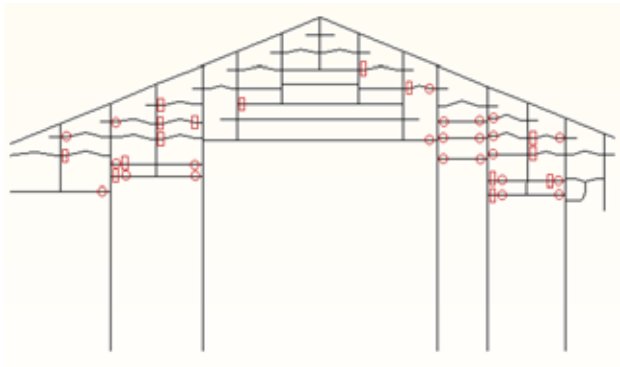	**Step 25: Failures up to this stage** Equivalent acceleration load: **0.297g** Roof Apex displacement: **15.519cm** Material failure: **None** Joint pull out failure at this step: **None** Joint rotational failure at this step: **None**
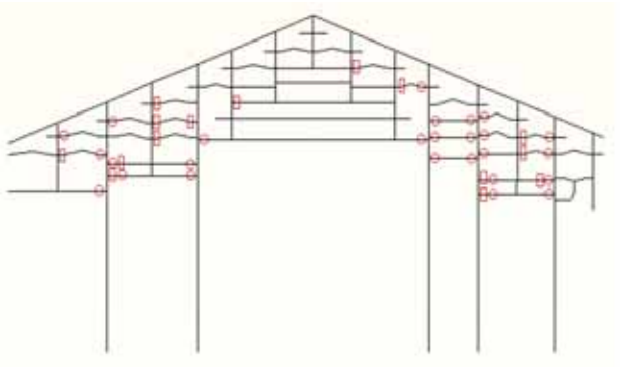	**Step 26: Failures up to this stage** Equivalent acceleration load: **0.33g** Roof Apex displacement: **17.203cm** Material failure: **None** Joint pull out failure at this step: **0** Joint rotational failure at this step: **3**
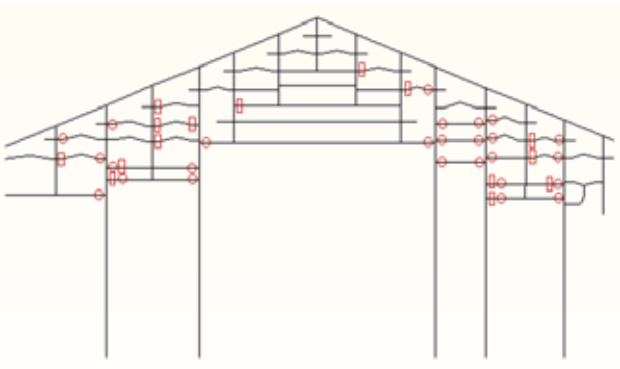	**Step 27: Failures up to this stage** Equivalent acceleration load: **0.33g** Roof Apex displacement: **17.556cm** Material failure: **None** Joint pull out failure at this step: **None** Joint rotational failure at this step: **None**

Appendix B

Results of step by step pushover analysis of Dou-Shan temple

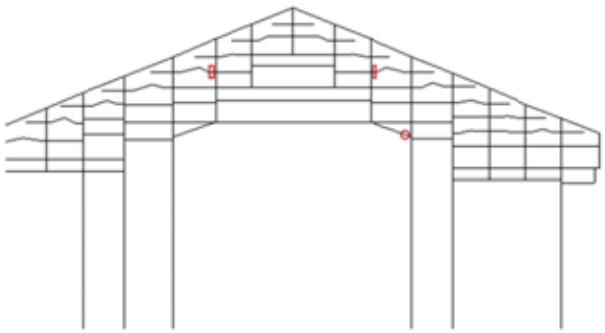	**Step 01: Failures up to this stage** Equivalent acceleration load: **0.033g** Roof Apex displacement: **0.667cm** Material failure: **None** Joint pull out failure at this step: **2** Joint rotational failure at this step:**1**
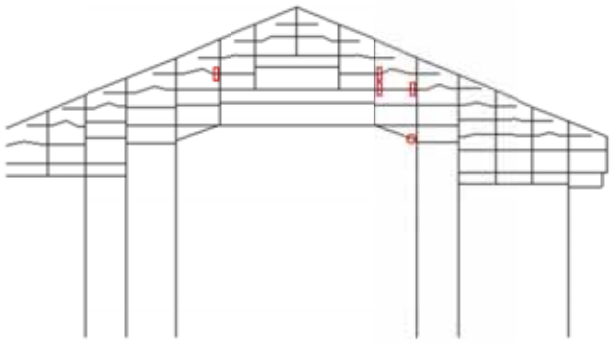	**Step 02: Failures up to this stage** Equivalent acceleration load: **0.033g** Roof Apex displacement: **0.790cm** Material failure: **None** Joint pull out failure at this step: **2** Joint rotational failure at this step: **None**
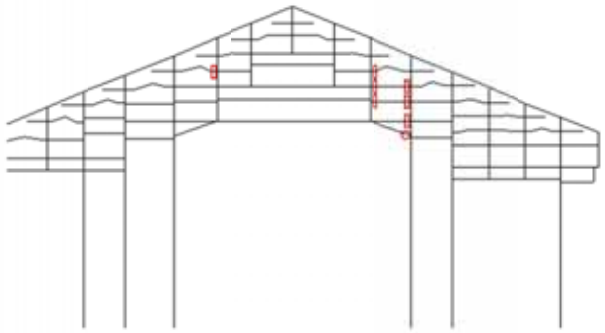	**Step 03: Failures up to this stage** Equivalent acceleration load: **0.033g** Roof Apex displacement: **0.812 cm** Material failure: **None** Joint pull out failure at this step: **3** Joint rotational failure at this step: **None**
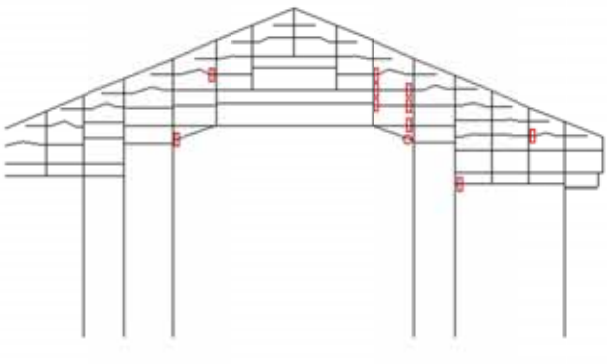	**Step 04: Failures up to this stage** Equivalent acceleration load: **0.033g** Roof Apex displacement: **0.866 cm** Material failure: **None** Joint pull out failure at this step: **3** Joint rotational failure at this step: **None**

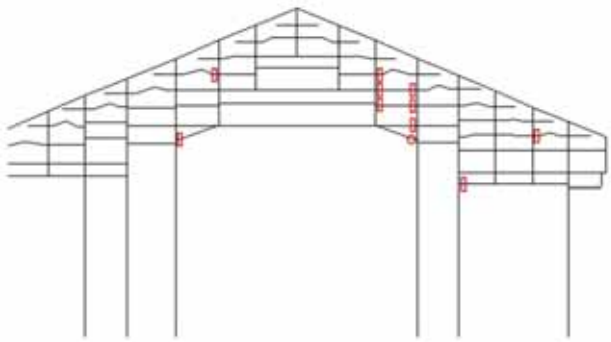	**Step 05: Failures up to this stage** Equivalent acceleration load: **0.066g** Roof Apex displacement: **1.570 cm** Material failure: **None** Joint pull out failure at this step: **None** Joint rotational failure at this step: **None**
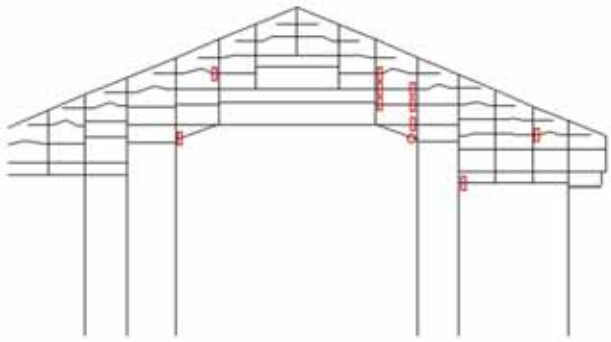	**Step 06: Failures up to this stage** Equivalent acceleration load: **0.099g** Roof Apex displacement: **2.273 cm** Material failure: **None** Joint pull out failure at this step: **None** Joint rotational failure at this step: **None**
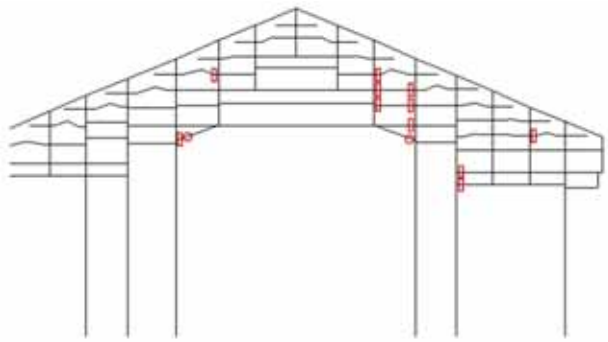	**Step 07: Failures up to this stage** Equivalent acceleration load: **0.099g** Roof Apex displacement: **2.390 cm** Material failure: **None** Joint pull out failure at this step: **1** Joint rotational failure at this step: **1**
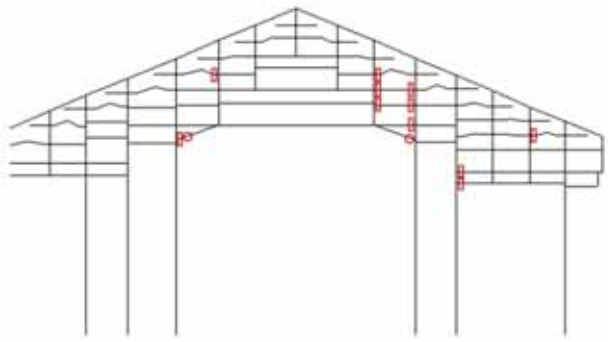	**Step 08: Failures up to this stage** Equivalent acceleration load: **0.099g** Roof Apex displacement: **3.137 cm** Material failure: **None** Joint pull out failure at this step: **None** Joint rotational failure at this step: **None**

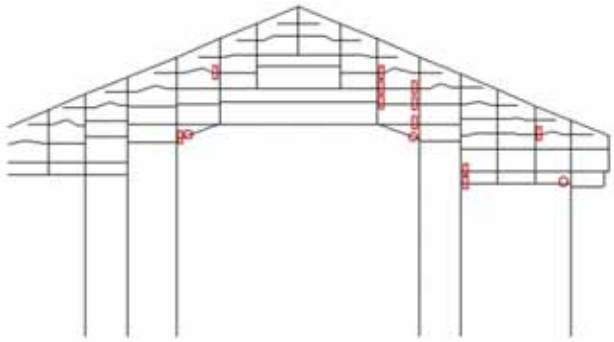	**Step 09: Failures up to this stage** Equivalent acceleration load: **0.132g** Roof Apex displacement: **3.269cm** Material failure: **None** Joint pull out failure at this step: **None** Joint rotational failure at this step: **1**
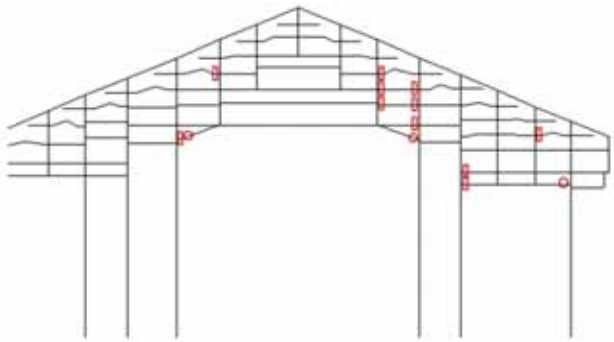	**Step 10: Failures up to this stage** Equivalent acceleration load: **0.165g** Roof Apex displacement: **4.069 cm** Material failure: **None** Joint pull out failure at this step: **None** Joint rotational failure at this step: **None**
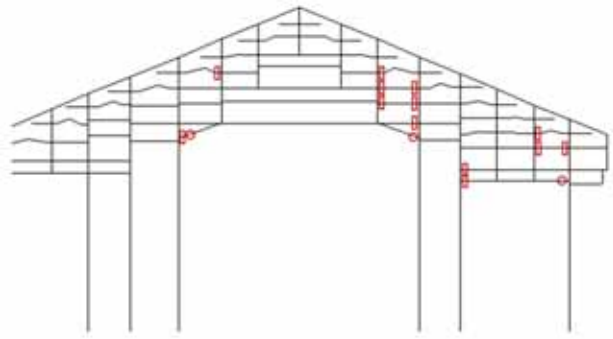	**Step 11: Failures up to this stage** Equivalent acceleration load: **0.165 g** Roof Apex displacement: **4.184cm** Material failure: **None** Joint pull out failure at this step: **2** Joint rotational failure at this step: **None**
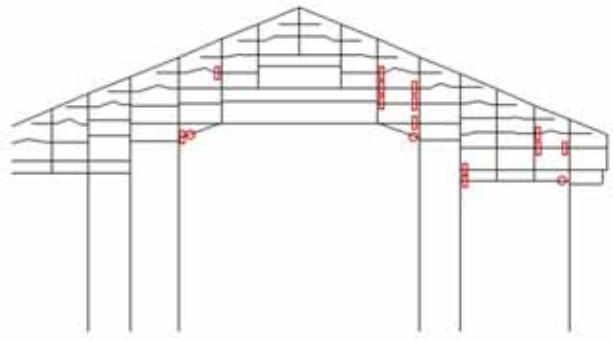	**Step 12: Failures up to this stage** Equivalent acceleration load: **0.165g** Roof Apex displacement: **4.214cm** Material failure: **None** Joint pull out failure at this step: **None** Joint rotational failure at this step: **None**

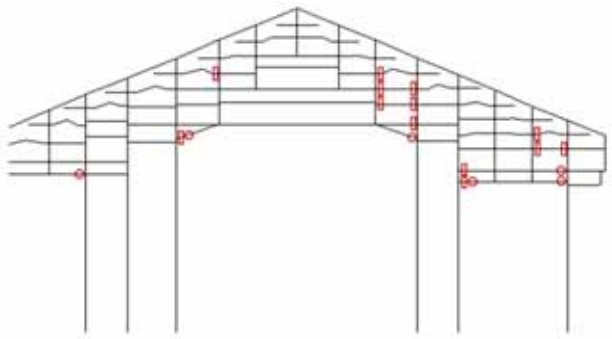	**Step 13: Failures up to this stage** Equivalent acceleration load: **0.198g** Roof Apex displacement: **5.039 cm** Material failure: **None** Joint pull out failure at this step: **None** Joint rotational failure at this step: **2**
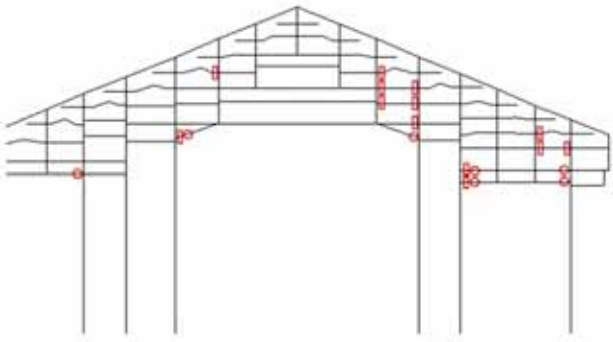	**Step 14: Failures up to this stage** Equivalent acceleration load: **0.198g** Roof Apex displacement: **5.425 cm** Material failure: **None** Joint pull out failure at this step: **None** Joint rotational failure at this step: **1**
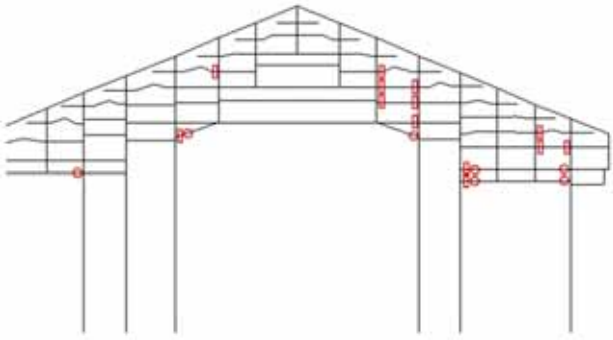	**Step 15: Failures up to this stage** Equivalent acceleration load: **0.198 g** Roof Apex displacement: **5.538cm** Material failure: **None** Joint pull out failure at this step: **None** Joint rotational failure at this step: **None**
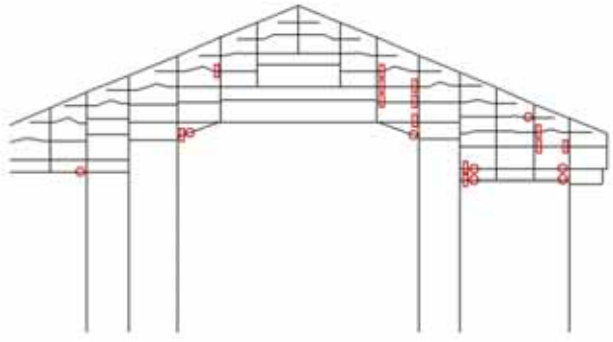	**Step 16: Failures up to this stage** Equivalent acceleration load: **0.231g** Roof Apex displacement: **6.444cm** Material failure: **None** Joint pull out failure at this step: **None** Joint rotational failure at this step: **1**

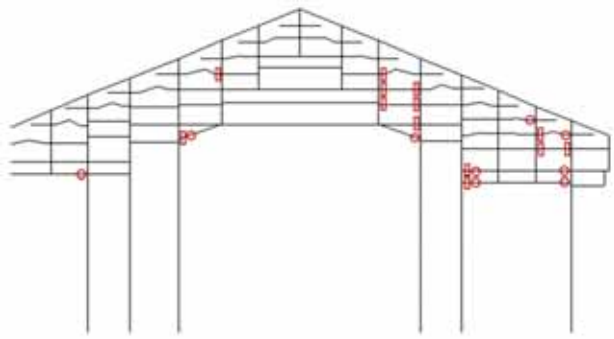	**Step 17: Failures up to this stage** Equivalent acceleration load: **0.231g** Roof Apex displacement: **6.536 cm** Material failure: **None** Joint pull out failure at this step: **None** Joint rotational failure at this step: **1**
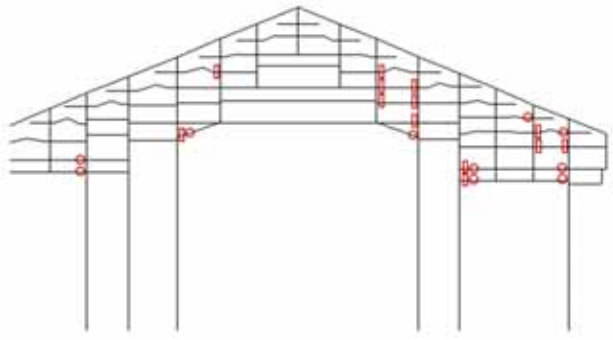	**Step 18: Failures up to this stage** Equivalent acceleration load: **0.231g** Roof Apex displacement: **6.587 cm** Material failure: **None** Joint pull out failure at this step: **None** Joint rotational failure at this step: **1**
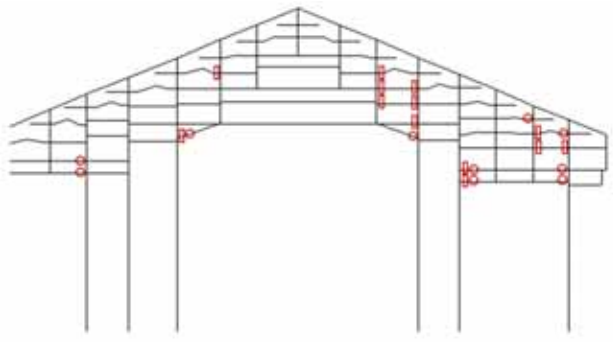	**Step 19: Failures up to this stage** Equivalent acceleration load: **0.231 g** Roof Apex displacement: **6.672cm** Material failure: **None** Joint pull out failure at this step: **None** Joint rotational failure at this step: **None**
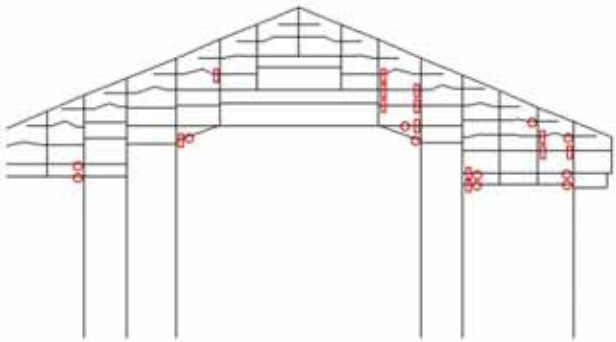	**Step 20: Failures up to this stage** Equivalent acceleration load: **0.264g** Roof Apex displacement: **7.607cm** Material failure: **None** Joint pull out failure at this step: **None** Joint rotational failure at this step: **1**

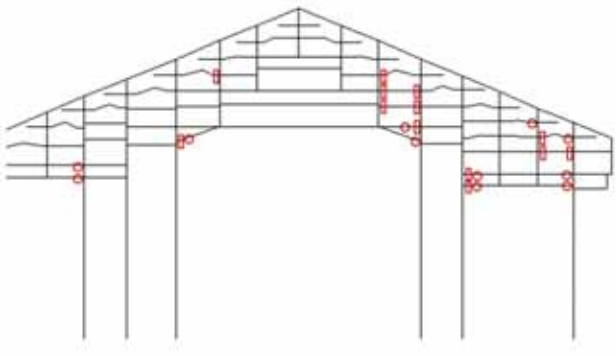	**Step 21: Failures up to this stage** Equivalent acceleration load: **0.264g** Roof Apex displacement: **7.657 cm** Material failure: **None** Joint pull out failure at this step: **None** Joint rotational failure at this step: **None**
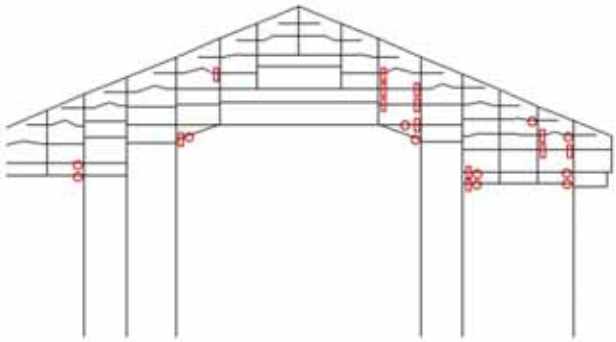	**Step 22: Failures up to this stage** Equivalent acceleration load: **0.297g** Roof Apex displacement: **8.59 cm** Material failure: **None** Joint pull out failure at this step: **None** Joint rotational failure at this step: **None**
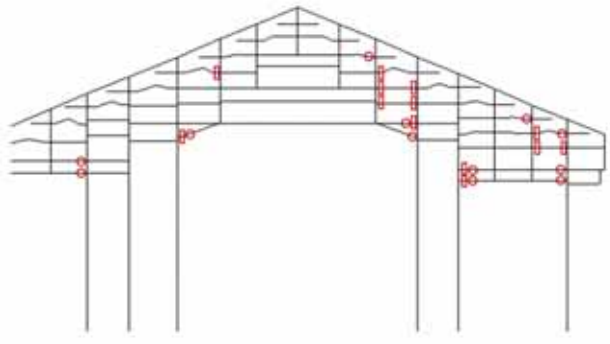	**Step 23: Failures up to this stage** Equivalent acceleration load: **0.33 g** Roof Apex displacement: **9.535 cm** Material failure: **None** Joint pull out failure at this step: **None** Joint rotational failure at this step: **1**
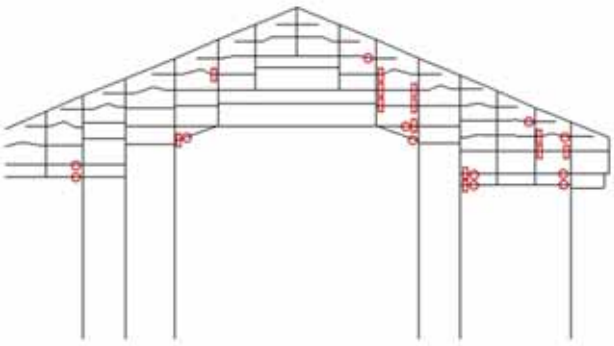	**Step 24: Failures up to this stage** Equivalent acceleration load: **0.33g** Roof Apex displacement: **9.56cm** Material failure: **None** Joint pull out failure at this step: **None** Joint rotational failure at this step: **None**